ŞTIINŢA ŞI INGINERIA MATERIALELOR

S U M A R

MATERIALS SCIENCE AND ENGINEERING

CONTENTS

DIFFRACTOMETER STUDY ON THE SHAPE MEMORY ALLOYS T YPE Cu$_{75.4}$Zn$_{18.6}$Al$_{5.85}$

BY

DRAGOŞ CRISTIAN ACHIŢEI[*1], PETRICĂ VIZUREANU[1], CRISTIAN PREDESCU[2] and ANDREI BERBECARU[2]

[1] "Gheorghe Asachi" Technical University of Iaşi,
The Faculty of Materials Science and Engineering
[2] University "Politehnica" Bucharest

Abstract. This paper presents some elements for obtaining of shape memory alloys the type Cu$_{75.4}$Zn$_{18.6}$Al$_{5.85}$ and diffractometer analysis performed during these phases.

Key words: shape memory alloys, diffractometer analysis.

1. Introduction

The metallic shape memory alloys from the construction of both facilities are subject to mechanical and thermal stresses, so that their enrollment in a calculus system to fatigue requires consideration of the function.

The shape memory alloys base copper studied are type Cu-Zn-Al and can be classified as, fundamentally speaking, the ternary alloys. Copper is the main component (base), and are zinc and aluminum alloy components.

---

[*] Corresponding author e-mail: dragos_adc@yahoo.com
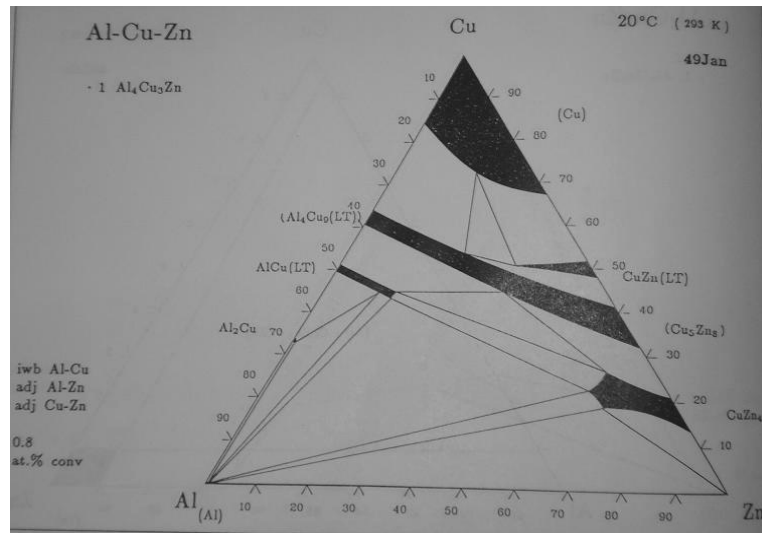
Fig. 1 – Ternary diagram Al-Cu-Zn at 20°C.

The steps for obtaining the type of shape memory alloys Cu-Zn-Al are the following:

• selecting the types of shape memory alloys, copper base (type Cu-Zn-Al)

• load calculation based on predetermined chemical composition

• ingot casting

• hot plastic deformation (forging)

• machining of specimens

• heat treatment: solution annealing commissioning

• shape memory effect induced by plastic deformation, elongation 3%.

If we exclude the residual elements, according to Fig. 2 shape memory alloy has a base structure with single phase.

It is possible that the actual conditions of development to form intermetallic compounds such as CuZn and Al_4Cu_9. Based on this observation seems appropriate to apply the technology of heat treatment effects in implementing the solution.

Development is the first step in the process of obtaining shape memory alloys. Making processes differ depending on the type of alloy and the same type of alloy, the properties sought.

The alloys used in experimental research on copper, such $Cu_{75.4}Zn_{18.6}Al_{5.85}$.

Development of alloys was carried out in an induction furnace with graphite crucible, using high-purity chemical elements Cu, Zn, Al and lack of moisture.

aluminum ingot, 99% purity   zinc ingot, 99.5% purity   copper electrolyte prepared, 99.95% purity
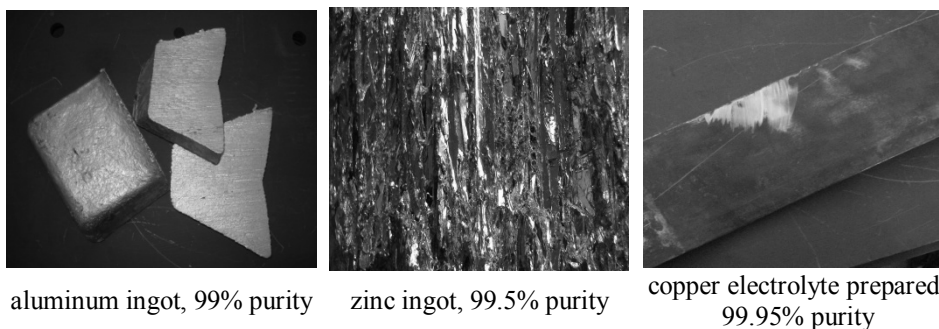
Fig. 2 – Components used in the making.

At the temperature of preparation, the interaction of the metal load with furnace atmosphere is oxidation reactions and dissolution of gas.

It has been observed to develop following recipe:
- copper is inserted into the crucible;
- after aluminum and copper smelting add a small amount of pre-alloy Cu - Al, to prevent overheating of the melt due to thermal reaction of aluminum and aluminum-oxygen;
- finally added zinc.

Fig. 3 – Induction furnace used for melting the alloy.

The melting temperature is limited to a maximum of 1200°C to reduce evaporation losses. There is a risk of burning zinc and dissolved gases, the metal bath. Protection against oxidation, metal bath is done with charcoal, borax ($Na_2B_4O_7$) or flux containing alkali metal halides.

After the homogenization of the alloy in high-frequency induction furnace (8000 Hz), the alloys are cast into a metal mold.

Analysis of chemical composition of cast samples was performed on a spectrometer Foundry Masters 01J0013 model, produced by WAS Worldwide Analytical Systems AG.

Table 1

Chemical Composition [%]

Cu	Zn	Al	Fe	Co	Si	Ni	As	Mn
75.4	18.6	5.85	0.02	0.01	0.02	0.005	0.008	0.007

To finish the structure, molded specimens are subjected to hot plastic deformation (forging free).

Heating temperature for forming CuZnAl alloys is 850 ± 50°C with duration of time the temperature regime of 0.5 hours per 25 mm thickness of material to ensure a single-phase structure (risk to maintain the structure CuZn type compounds).

Plastic deformation is done thermally in the range 850-800°C, which requires obtaining the degree of strain imposed by repeating the forming operation (10 to 20 cycles).

Fig. 4 – Heating furnace and forged specimen.

Fig. 5 – Forging cast specimens.

Fig. 6 – Hot-forged specimen (850 - 900°C).

The forged specimens will be machined to the dimensions set standards for experimental tests.

The specimens obtained by cutting, are subject to a hardening heat treatment.
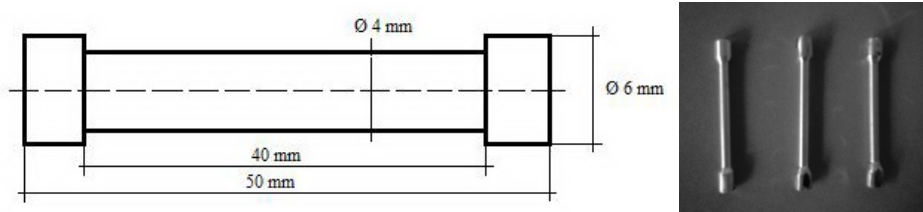
Fig. 7 – Machined specimens.

Heat treatment parameters are:

        - heating to 800°C;

        - maintain at temperature for uniform and complete structural changes, for 1 hour;

        - rapid cooling in water at room temperature.

     After treatment, the samples are subjected to an elongation machined with a degree of elongation of 3%. Controlled lengthening was performed on a tensile test machine Instron type 3382 USA.

     If the alloy has good properties of shape memory alloys, when heated around the transformation point values, the specimen and should suffer a sharp contraction, because of continuing to expand with temperature.

Specimen	Maximum strength F_{max} (N)	Young's modulus E (MPa)	Maximum tension σ_r (MPa)	Elongation at break A_u (%)
1	3576.16	20908.02	284.58	3
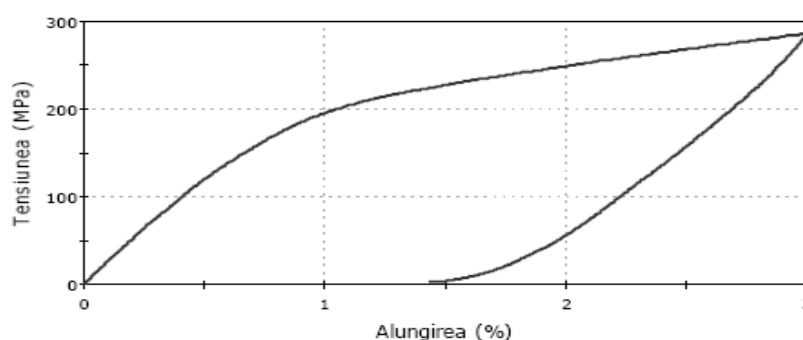
Fig. 8 – Tension – elongation diagram for $Cu_{75.4}Zn_{18.6}Al_{5.85}$ alloy, elongated 3%.

2. Diffractometric Studies

     The diffractometer analyses were performed using a X-ray diffractometer, type X-Pert Pro Philips Analytical.

a.Cast Specimens
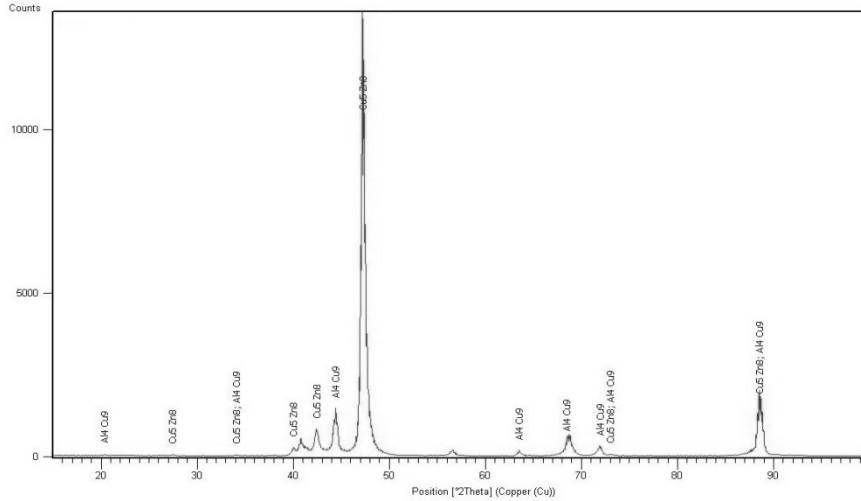
Fig. 9 – Distribution of compounds to $Cu_{75.4}Zn_{18.6}Al_{5.85}$ alloy, in able cast.

No.	Chemical compound	Chemical formula	Average quantity %
1	cooper-zinc	Cu_5Zn_8	53
2	aluminum - copper	Al_4Cu_9	47
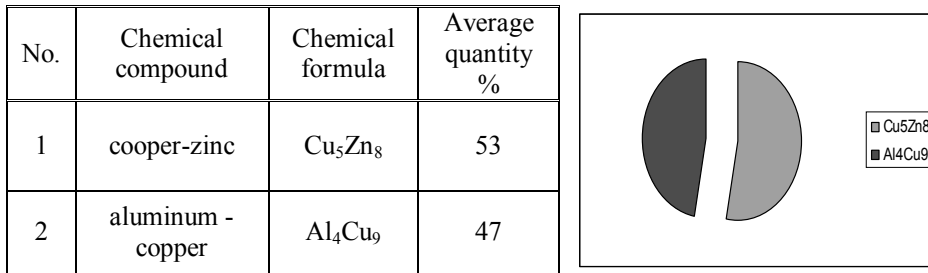
b. Forged Specimens
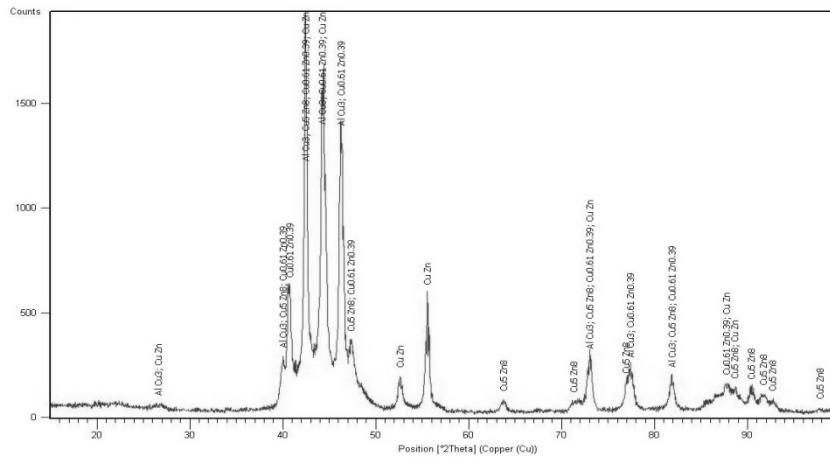
Fig. 10 – Distribution of compounds to $Cu_{75.4}Zn_{18.6}Al_{5.85}$ alloy, in able forged.

No.	Chemical compound	Chemical formula	Average quantity %
1	aluminum – copper	$AlCu_3$	20,5
2	copper-zinc	Cu_5Zn_8	33,3
3	α-$Cu_{0.61}Zn_{0.39}$	$Cu_{0.61}Zn_{0.39}$	25,6
4	copper –zinc	$CuZn$	20,6
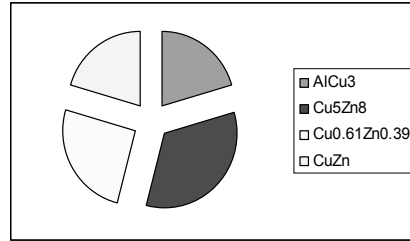
Cu-Zn-Al alloys behave as experienced in the structure of ternary alloys in the rough cast type intermetallic compounds are found Al_4Cu_9 and Cu_5Zn_8.

To finish the structure of Cu-Zn-Al alloys require processing by hot plastic deformation. After hot forming intermetallic compound Al_4Cu_9 not found, being replaced by $AlCu_3$ (20.5%).

Cu_5Zn_8 intermetallic compound is reduced from 53% to 33.3%.

It forms a new phase α - $Cu_{0.61}Zn_{0.39}$ in the amount of 25.6% and a new CuZn intermetallic compound at the rate of 20.6%.

After the annealing heat treatment for release in solution phase are amplified to 42.8% $AlCu_3$ and Cu_5Zn_8 reforming the average quantity of 51.2%.

c. Quenching Specimens
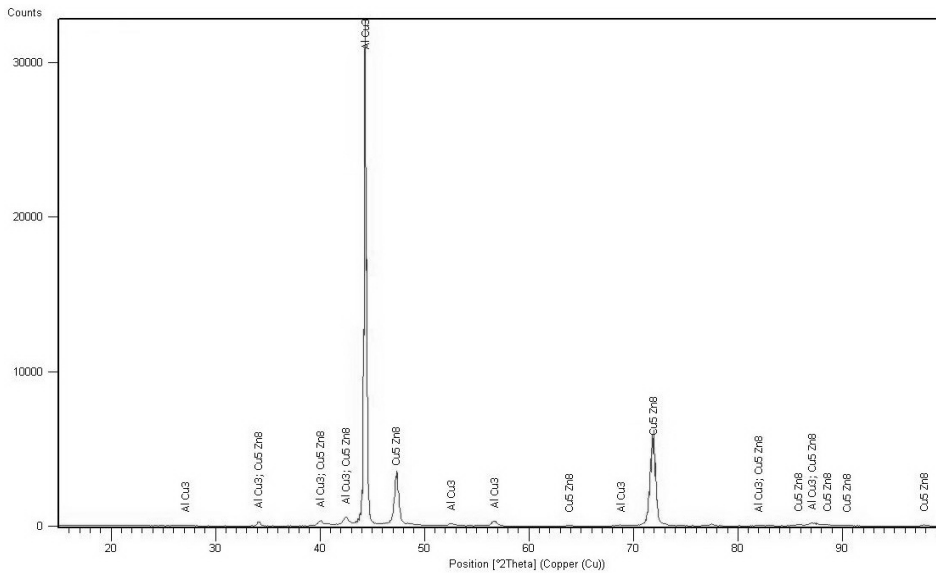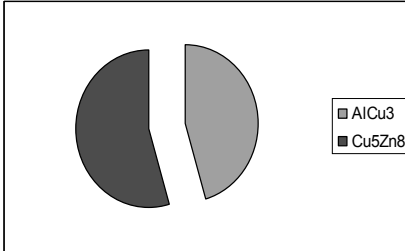
Fig. 11– Distribution of compounds to $Cu_{75.4}Zn_{18.6}Al_{5.85}$ alloy, in able quenching.

No.	Chemical compound	Chemical formula	Average quantity %
1	aluminum – copper	$AlCu_3$	42.8
2	copper – zinc	Cu_5Zn_8	51.2

3. Conclusion

The determination of the characteristics for a memory shape alloy allows components producers to assure a certain guarantee on these products.

Any influence in the development process, with changes calculated as a percentage of alloying elements, may result in a void shape memory alloy. A 1% variation in the percentage of Al and Zn can change or remove alloy temperatures characteristic of field usage.

The methods of investigation and testing of properties and behavior of these alloys while depending on the stresses they are subjected, can not fully characterize the influence of aspects of processing parameters and their default optimization.

REFERENCES

[1]. Bujoreanu L.G., ş.a., (2005), *Memoria mecanică şi termică a aliajelor pe bază de Cu-Zn-A*l, Editura Politehnium, Iaşi.
[2]. Stanciu S., (2009), *Materiale cu memoria formei. Metode şi aplicaţii in tehnică*, Editura Universitas XXI, Iaşi.
[3]. Planete AMF. Le portail des Alliages a Memoire de Forme: http://membres.lycos.fr/planeteamf/applications.htm
[4]. www.mnemoscience.com/?lang=eng&p=17
[5]. www.instron.us

STUDIUL DIFRACTOMETRIC ASUPRA ALIAJELOR CU MEMORIA FORMEI
DE TIPUL $Cu_{75.4}Zn_{18.6}Al_{5.85}$

(Rezumat)

Lucrarea prezintă elemente de obţinere a aliajelor cu memoria formei de tipul $Cu_{75.4}Zn_{18.6}Al_{5.85}$, precum şi analizele difractrometrice efectuate pe parcursul acestor etape.

ADAPTIVE HYDRAULIC TRANSMISSION FOR HORIZONTAL AXIS WIND TURBINES FOR LOW POWER

BY

MIHAI AFRĂSINEI[*], DORU CĂLĂRAŞU and ADRIAN OLARU

"Gheorghe Asachi" Technical University of Iaşi,
Department of of Machine Tools

Abstract. In order to convey energy to the ground a hydraulic transmission is used. The resulted hydraulic energy is then transmitted to the power unit on the ground, consists of an element, with adjusting unitary volume. The hydraulic gear must be of adaptive type related to the influence factors, achieving the automatic adaptive settlement of the system.

Key words: hydraulic transmission, adaptive, wind turbine.

1. Problem Statement

Worldwide, the hydraulic convey of wind energy on the ground represents a research line into the complex projects having the purpose of producing energy from unconventional sources (*160 kW Wind Turbine…*; *Low-wind Turbine…*; Patent *WO03098037*; Patent *WO2005103484*; Molenaar, 2003; Bansal *et al*., 2002).

---

[*] Corresponding author e-mail: automecanica_iasi@yahoo.com

The hydraulic conveying and settling in the wind station provide the following advantages:

- Easy accomplish of continuous variations, accurate and on a wide range, for forces, couples, speed and position, beside of a high and controllable level for energy;

- High power density, with good effects on the load of supporting and anchoring elements;

- Smooth running, without shocks or vibrations, with favourable effects on the wind station's kinematics.

In order to convey energy to the ground a hydraulic gear (transmission) is used. The resulted hydraulic energy is then transmitted (conveyed) to the power unit on the ground (Patent *WO03098037*; Molenaar, 2003).

In case of settle by pitch adjusting, the power unit consists of a single element, with adjusting unitary volume. At its power inlet a consumer of electrical generator type is connected. The hydraulic gear must be of adaptive type related to the influence factors, achieving the automatic adaptive settlement of the system (*Low-wind Turbine…*; Patent *WO03098037*).

The low power wind turbines with horizontal shaft and adaptive hydraulic gear can work with adjusting speed.

If the hydraulic gear is adaptive, the output may be fit to the user's needs (constant power or speed) without affecting the turbine performances, which will work at optimum regime until the limit power is achieved. Sometimes, the changing in wind orientation may be applied (*Low-wind Turbine…*). In this situation, the wind energy will be used for a large range of wind speed and a functioning with maximum power coefficient results.

2. Advantages and Disadvantages of the Hydrostatic Gear Solution beside the Usual Solutions for Low Power Wind Turbines

The solutions with mechanical speed multiplier or those with direct coupling between the turbine and a slow electrical generator are including very complex and expensive components: the slow generator, the gear drive and the frequency converters.

Replacing the mechanical speed multiplier with a hydraulic gear determines robustness and competitive costs. If the hydraulic gear assumes also the function of speed multiplier, the system may use as electrical generator usual capacity motors. Thereby, the redressing followed by the frequency inverter may be avoided. Advantages to the systems with turbines settled speed (optimum speed) could be achieved by adjusting the pump cylinder volume from the hydrostatic gear. If the plant is equipped with a

hydraulic cylinder, a possibility of settle the angle of turbine vane installation is possible, having two functions: turbine running-up at a convenient pitch and, by increasing of the installation angle the taking up of the brake function for plant protection. This way, the mechanical emergency brake from usual systems is no longer necessary.

The ranges of power and speed require for the hydraulic gear to use volume machines. Therefore, the gear will include a volume pump and a volume engine.

The gear efficiency at low power is near 0,6. Its improvement requires a complex technologic effort. Thereby, cca.40% of the power used by the wind turbine is dissipated through the gear, heating the liquid from the hydraulic circuit. A mechanical speed multiplier has efficiency over 0,9. This difficulty could be compensated by increasing the turbine dimensions. For the same useful power at the plant terminals, using the same location conditions, the turbine must assure a 50% larger swept area. The turbine diameter must be increased with approximately 25% beside the dimension of the usual structure. This disadvantage should be compensated by other advantages (robustness, safety, costs).

The optimal operating regime of the wind turbine: power between 0 and installation value, speed between 30 rpm and 100-150 rpm for 5kW power. The large range of power and speed values dictates the regime of the transmission pump: large variations for capacity and pumping static pressure.

If one avails the advantage of using an asynchrony electric generator connected to the electrical supply, eliminating this way the expensive components of the frequency converters, the volume motor of the gear will be used at the speed of electrical generator (according to the electrical slide). Therefore, the gear must use a pump with adjusting cylinder volume.

3. The Basic Diagram of the Hydraulic Adaptive Gear Visual Stand for Wind Turbines with Low Power and Horizontal Shaft

The basic diagram of the hydraulic adaptive gear visual stand for wind turbines with low power and horizontal shaft is illustrated in Fig. 1. The supply source is a double pump providing the system input, *i.e.* the supply of the consumers' circuits and the auxiliary operating circuits.

The motor loading is achieved hydraulically, using a pump loaded with the servo valve. The diagram includes devices for measuring the mechanical, hydraulic and electrical parameters.

To assess the behavior of the hydraulic gear into a wind system with variable wind speed and also the driving speed of the hydraulic generator, the electrical engine ME is fed from the frequency converter CF.

In the diagram closed-loop circuits are included, for monitoring the engine speed at the load and pump speed variations.
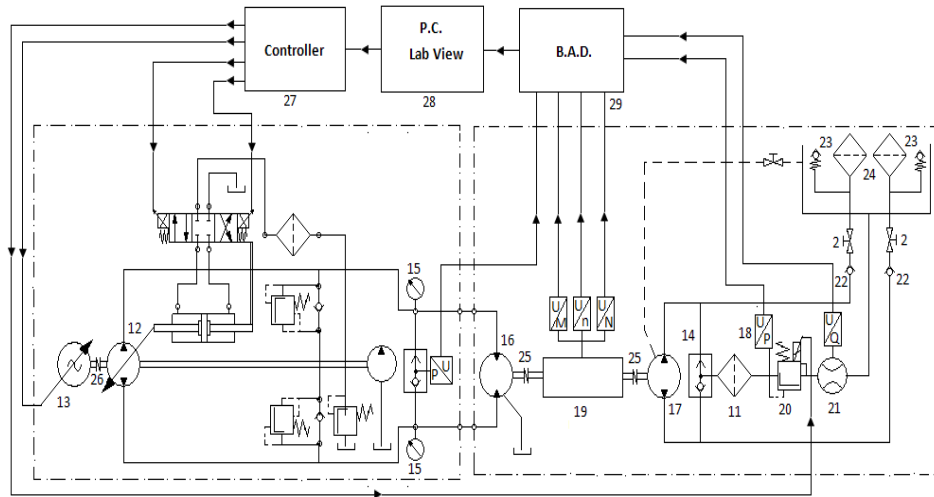
Fig. 1 – The basic diagram of the hydraulic adaptive gear visual stand for wind turbines with low power and horizontal shaft.

The stand represented in Fig. 1 allows the loading of the adaptive hydraulic gears for wind turbines with horizontal shaft. The stand is structured on three modules, the module with closed circuit having the following characteristics: power N = 20 kW, debit Q = (0…27) l/min, maximum pressure *p* = 300 bar.

Functioning of the wind turbine at different wind speed, *i.e.* variable speed is assimilated with the functioning of a capacity electrical engine *13*, fed through a frequency converter. The electrical engine drives with adjusting speed the pump *12*. This way the wind turbine is simulated, working with variable speed related to the wind speed.

The main pump *12* with unitary volume is designed for working in closed circuit. The oil rejected by the pump is getting back in the suction of the pump, after passing through the consumer.

The capacity adjusting is made with an electro-hydraulic servo control device, which receives a command signal of ± 0…10 V. The pump capacity is proportionally to the value of the command signal.

The pump *12* also includes a plate with all the necessary devices for a closed circuit, *i.e.* safety valves for both sides of the closed circuit and the safety valve for the filling circuit. The pressure at both energetic outlets A and B of the pump *12* are read at the manometers *15*, and the high pressure side is selected with the valve *14*. The high pressure achieved may be digitally displayed using the pressure transducer. The resulted hydraulic energy from pump *12* is converted in mechanical energy by the hydraulic cylinder *16*.

Fig. 2 – Adaptive hydraulic transmission for horizontal axis wind turbines for low power.

The shaft of the hydraulic engine *16* is connected through the transducer *19* to the pump's shaft *17*. The transducer *17* is displaying the speed, the couple and the mechanical power values conveyed by the engine *16* to the load pump *17*. The pump *17* is simulating the load represented by the electrical energy generator or by another consumer type.

The valve *14* is selecting the high pressure side of the pump and is conducting the working fluid to the proportional valve *20*, with the function of adjusting the charge with the load. The adjusting is made electrically. The pressure value is proportional with the electric signal value (0…10V or 4…20mA). The pressure filter *11* provides the resolution of 10 μm, imposed to the working fluid by the proportional valve.

The pressure and the debit transducers *18* and *21* from the load hydraulic circuit allow the digital display. The elements *22*, *2*, *23*, *24* are ensuring the proper functioning of the load module. The measurement conditions and choosing of the devices are specified by the standard STAS 9817-80. The Fig. 2 illustrates the achieved stand.

4. Conclusion

The hydraulic conveying and settling in the wind station provide the following advantages: easy accomplish of continuous variations, accurate and on a wide range, for forces, couples, speed and position, beside of a high and controllable level for energy; high power density, with good effects on the load of supporting and anchoring elements; smooth running, without shocks or vibrations, with favorable effects on the wind station's kinematics.

The accomplished stand allows the testing of the adaptive hydraulic gear from wind turbines with horizontal shaft and low power during stationary and dynamic running.

The wind turbines with horizontal shaft and low power equipped with adaptive hydraulic gears may run with variable speed.

The adaptive hydraulic gear allows adapting the output to the consumer's needs (constant power or speed).

The wind turbine may run on optimum regime until the limit power value is achieved.

REFERENCES

* * * *Water Current Turbine*. Patent Number *WO2005103484*.
* * * 160 *kW Wind Turbine with Hydraulic Transmission at Schiedam*. Ref: 16013 or 34127.
* * * *Low-wind Turbine with Hydraulic Blade Control. Measuring Program Included*. Ref: 8700106.
* * * *Wind Turbine with Hydraulic Transmission*. Patent number: *WO03098037*.
Bansal R. C., Bhatti T. S., Kothari D. P., *On Some of the Design Aspects of Wind Energy Conversion Systems*. Energy Conversion and Management, **43**, *16*, 2175-2187 (2002).
Molenaar D.P., *Cost-Effective Design and Operation of Variable Speed Wind Turbines*. Delft University Press, 2003.

TRANSMISIE HIDRAULICĂ ADAPTIVĂ DESTINATĂ
TURBINELOR EOLIENE CU AX ORIZONTAL DE MICĂ PUTERE

(Rezumat)

Pentru transmiterea energiei la sol se utilizează o transmisie hidraulică. Energia hidraulică astfel obţinută este transmisă la grupul motor aflat la sol, format dintr-o unitate, cu volum unitar reglabil. Transmisia hidraulică este de tip adaptiv în raport cu factorii perturbatori realizând reglarea automată a sistemului.

MECHANIC-HYDRAULIC CONTROL SYSTEM AND PROTECTION OF HORIZONTAL AXIS WIND TURBINE OF VERY LOW POWER

BY

MIHAI AFRĂSINEI[∗], DORU CĂLĂRAŞU and ADRIAN OLARU

"Gheorghe Asachi" Technical University of Iaşi,
Department of Machine Tools

Abstract. The paper presents an original adaptive mechanical-hydraulic system for the control and security of wind turbines with horizontal shaft of very little power, without adaptive hydraulic transmission.

Key words: wind turbines, adaptive, control.

1. Introduction

The orientation system represents the assembly for the support and orientation of the nacelle and of the rotor of the turbine on the direction of wind.

This wind orientation system is necessary for horizontal shaft wind turbines.

Wind turbines control with horizontal shaft assures the step change by blades command or the wind orientation of turbine shaft. Turbine security imposes to pull out by the shaft orientation change.

[∗] Corresponding author e-mail: automecanica_iasi@yahoo.com

The control and security principle of wind turbine by wind orientation change is presented in Fig. 1.

During the unit work the turbine must be all the time with the shaft parallel with the wind direction.

For the turbine positioning about the wind direction must be used, usually two drive modality: electrical drive, hydraulically drive.

Those drive modalities have the following advantages:

- obtaining of increasing forces and couples;

- obtaining of the correct control of the position of mobile assembly formed by nacelle of wind central unit on the wind direction;

- obtaining of a high value of the ratio between the values of the useful force and the inertial force and also between drive couple and inertial couple;

- obtaining of extra charges to the completely stop without danger.
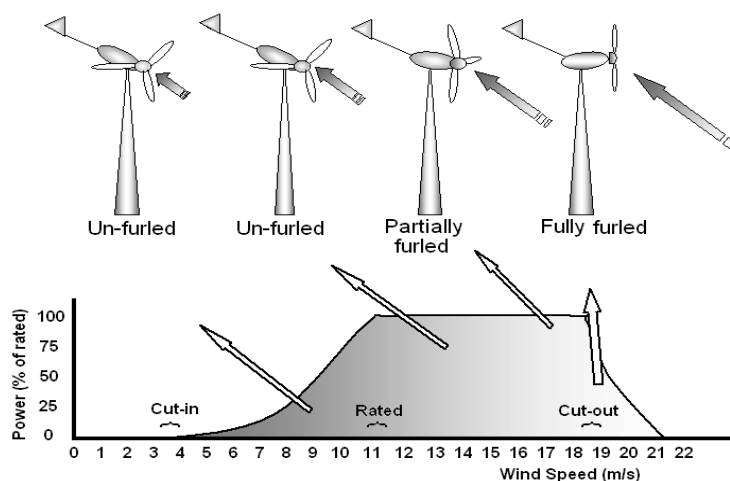
Fig. 1 – The control and security principle of wind
turbine by wind orientation change.

In those conditions energetically efficiency is greatest. Usually the servo drives assures also nacelle stopping on the wind direction by the brakes of those construction.

The control of the orientation is realized by the transducer of wind direction placed usually on the nacelle roof.

There are three security systems used for air electrical assembly: high wind speed security, acceleration security, vibrations security.

The mechanical-hydraulic system for security of wind turbine with small power, with horizontal shaft, assures the reduction of dynamical charges on the blade and to rise the turbine reliability and function security. For the

security system proposed the control is realized by the change of wind orientation.

The paper presents an original adaptive mechanical-hydraulic system for the control and security of wind turbines with horizontal shaft of very little power, without adaptive hydraulic transmission.

2. Construction and Functioning

The best constructive solution for wind turbines with horizontal of very small power, after the reference studies, is to bend of wind turbine in vertical plane when the wind speed exceeds the speed limit of turbine security.

The more important in system functioning are reliability, the absence of electrical device and the absence of hydraulic transmission.

The parts of wind central, with bend in vertical plane, are: rotor assembly, its support, transmission system, sustention pole.

The functioning of the rotor assembly and of his support is presented in the Figs. 2 and 3.
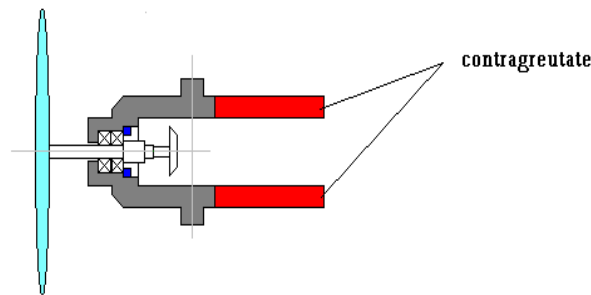
Fig. 2 – Rotor assembly.
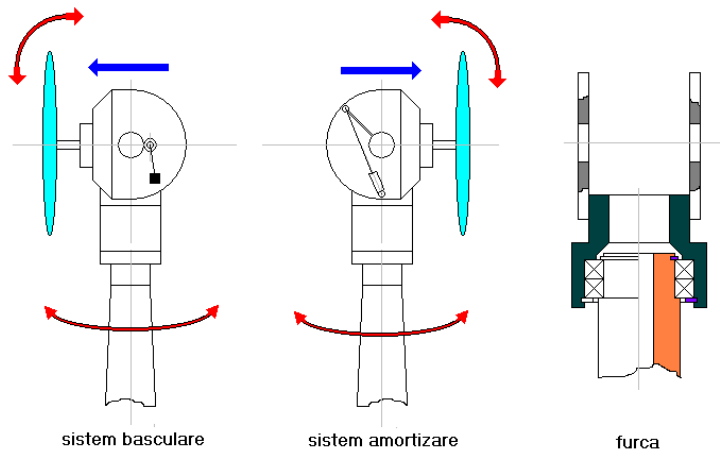
Fig. 3 – Support of rotor assembly.

The wind central is created to produce energy by changing of wind energy in mechanical energy with small values between 500 and 700 watts.

Central function manners:

• for small wind speeds, under 10 m/s, rotor assembly is not banded (the airscrew is turn in vertical plane);

• for equal or greater speeds then the choose one, the rotor assembly is bended (the airscrew is turn in horizontal plane);

• the orientating of rotor assembly in wind direction is possible with participation of upper bearing of sustention pole;

• the banded system protects the central because assure total air screw banded for establishing value of wind speed;

• damping system protects the central when is changed the wind speed, because the return of airscrew in initial position is in being late.

3. Results of Numerical Simulation of a Model of Adaptive Mechanical-Hydraulic for the Control and Security of Wind Turbine With Horizontal Shaft and Small Power

The numerical tests were achieved using MATLAB Simulink soft.

The model increases the turbine weight balance system, returning in initial position of turbine shaft, movement in both senses damping system, the limitation of shaft movement system to pull out of zero position and a signal set for wind speed simulation.

The Fig. 4 presents the surface variation in wind of the rotor in connection with the inclination angle of the turbine shaft. The increasing of rotor surface „in wind" is realized by inclination in vertical plane. The rise of inclinitation angle of turbine shaft assures the increasing of arm of the inclination couple, Fig. 5.
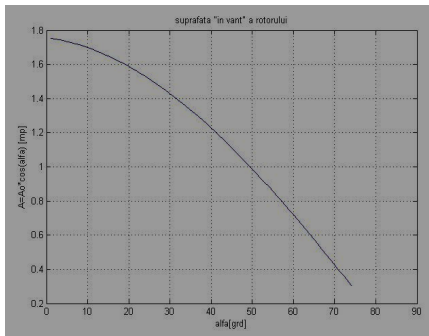
Fig. 4 – Surface variation in wind of the rotor in connection with inclination angle of the turbine shaft.
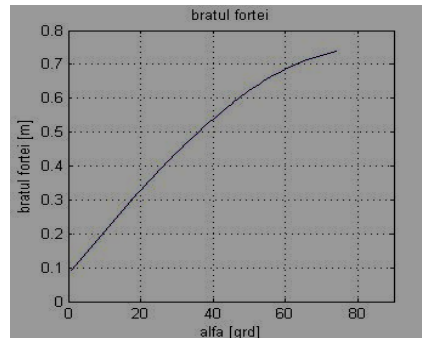
Fig. 5 – Evolution of the arm of rotor inclination force.

The Fig. 6 presents the signals of the system testing for the simulation of wind speed variation.
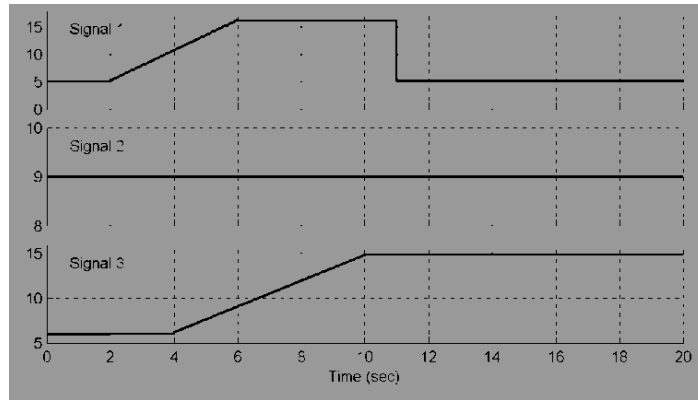
Fig. 6 – Model testing signals.

The signal 2 is used for static equilibration when the wind speed is equal with those of the beginning of the rotor inclination. The Fig. 7 presents the evolution of the inclination angle, having a constant value.

The signal 3 is used for testing the system's answer when the wind speed is greater than the limited value.

The Fig. 8 presents the evolution of the shaft inclination angle.
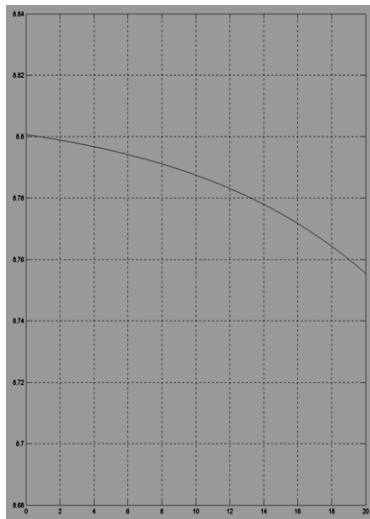
Fig. 7 – Inclination angle for constant wind speed.
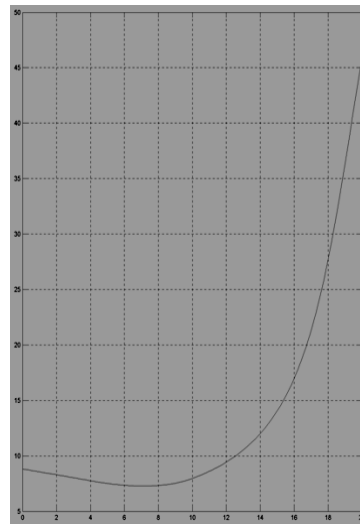
Fig. 8 – Inclination angle for wind speed rising.

4. Conclusion

The numeric simulation assures the change of some parameters for the construction and functioning of the system and also for the functioning testing signals.

The numerical model is used for simulation of some constructive parameters like weight of equilibration elements, axial dimensions of the rotor shaft, value of equilibration weight, amortization of the system performances.

REFERENCES

*∗ *160 kW Wind turbine with Hydraulic Transmission at Schiedam Ref: 16013 or 34127.*

*∗ *Low-Wind Turbine With Hydraulic Blade Control. Measuring Program Included Ref: 8700106.*

*∗ *Water current turbine*. Patent number *WO2005103484.*

*∗ *Wind Turbine with Hydraulic Transmission*, Patent number: *WO03098037.*

Bansal R.C., Bhatti T.S., Kothari D.P., *On Some of the Design Aspects of Wind Energy Conversion Systems*. Energy Conversion and Management, **43**, *16*, November 2002, 2175-2187.

Molenaar D.P., *Cost-Effective Design and Operation of Variable Speed Wind Turbines*. Delft University Press, 2003.

SISTEM MECANO-HIDRAULIC DE CONTROL ŞI PROTECŢIE A TURBINELOR EOLIENE CU AX ORIZONTAL DE FOARTE MICĂ PUTERE

(Rezumat)

Lucrarea prezintă un sistem mecano-hidraulic adaptiv de concepţie originală, pentru controlul şi protecţia turbinelor eoliene cu ax orizontal de foarte mică putere, fără transmisie hidraulică adaptivă.

SOME CONSIDERATIONS ABOUT THE ASSESSMENT OF WATER USAGE IN AN INDUSTRIAL FACILITY

BY

MIHAI ALEXANDRU*, DOINA HÎNCU and MIRCEA ASANDULUI

[1] Scholar Group "Stefan Procopiu" Iaşi,
[2]University "Al.I.Cuza" Iaşi

Abstract. The paper makes an approach on the water usage in industry and sketches the general management of it. Some guidelines on water usage assessment are also put into discussion.

Key words: durable development, industrial waste water assessment.

1. Introduction

The objective of this paper is to make some considerations about a sketch for the assessment of water usage in a facility, in such a manner, that opportunities for improvement can be detected.

Water is becoming a source of significant importance (Alzamora, 2010; http://www.wmo.int; Shimokura *et al*., 1998; http:// www.estis.net; http://www. google.ro) both from the perspective of an efficient use of natural resources and the management of operating expenses of operating facilities.

2. Material

Water is being used more and more in human activities, in all kind of facilities, taken from various sources, many of them requiring more and more a

---

* Corresponding author e-mail: malexandruis@yahoo.com

special attention about quality and quantity. Fig. 1 shows a diagram of water circuit specific for a general facility and various water categories.

Water usage includes the amount of water treated and taken into a facility from all sources: surface water (rivers, lakes and ponds), sea water, ground water and local utility company.

In a facility water is used for all kind of purposes: process, cooling, steam production, sanitary etc. and after, it has to be treated as waste water in treatment plants and discharged as effluent water.

As a category, process water, is all water - with the exception of cooling water - used in the process. Cooling water is water used exclusively in cooling water circuits: make-up for cooling towers, open circuits. Rain water in the precinct of a facility is not a source of fresh water but it could be contaminated and has to be assessed separately and sometimes also treated before discharging. Effluent water is water discharged to the receiving body from water treatment plants or directly from the process.

Having in mind the principles of durable development, and the fact that water, as a natural source is limited, water usage must be assessed in view of preserving environment and protecting all water sources (Alzamora, 2010; http: //www.wmo.int; Shimokura *et al.*, 1998; http://www.estis.net; http://www. google.ro). If one would like to make the assessment of water usage efficiently some steps have to be done. A first step should be the construction of the Development of Facility Block Flow Diagram, an example is shown in Fig. 1.

This diagram has to be build with detailed water mass balance around each process plant. This overall Facility Block Flow Diagram indicates location of all water and wastewater sources, flow-rates, pH, temperature, analysis of concentrations of important contaminants.
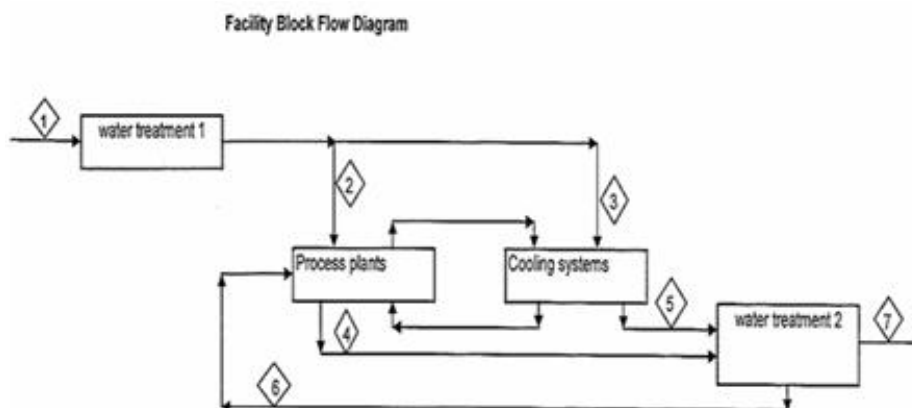
Fig. 1 – Water categories in a general facility (Alzamora C., 2010
1 – water input; *2* – process water first input; *3* – cooling water input; *4* – process water output; *5* cooling water output; *6* – process water second input; *7*– effluent water).

3. Discussions

Diagram values of parameters are very important to be measured as mentioned above and recorded to have in real time enough information for decision making at the management level of the facility, from the point of view of environmental and operational costs and also recycling opportunities.

Generally the recycling of treated wastewater „can be assessed by balancing the availability of good quality, low-cost make-up water and the treatment of wastewater for reuse. In areas where good quality raw water is not economically available, reuse of treated wastewater can be investigated. The cost of segregating the wastewater collection systems and treating for reuse can be justified on the basis of savings in raw water makeup costs, savings in energy use for pumping and decreased size of the central wastewater treatment system" (Alzamora , 2010).

Having these in mind it is easy to conceive a system for taking advantage of water parameters measurements and use water of certain quality without much cost only by redirecting at certain moments high quality waste water into „low sensitive water consuming systems". Alzamora uses the term of „cascading" for such an approach, even if poetry is less involved, by comparing to high automation and control needed.

Rain water, by Romanian rules of designing, must have a segregated water system and can be used, when available, to dilute water waste high concentrations into the effluent water. But there is also the possibility to not have rain for a long period of time and soil pollutants to be accumulated resulting in the necessity of after rain treating.

This is a matter that must be also handled: the surface runoff from the process and utility areas should be collected and conveyed through a dedicated sewer system to a contaminated storm water pond in the wastewater treatment unit prior to discharge/reuse.

The design of the contaminated storm water sewer piping system as well as the containment capacity of the contaminated storm water pond should take into consideration the design volumes of both rainfall and firewater.

The wastewater treatment system should have sufficient capacity to treat this volume of wastewater, added to its average flow, within a one-week period. Excess water from this is diverted to the clean wastewater sewer system (Alzamora, 2010; Shimokura *et al.*, 1998). Uncontaminated rainwater shall be discharged to the clean wastewater sewer.

Lack of segregation of rain waters can be a source of accidental pollution of receiving bodies.

4. Conclusions

On the basis of a correct construction of the Block Flow Facility Diagram, with proper sampling and monitoring wastewater apparatus, with the adequate information system economic decisions can be made in order to correctly asses waste water and comply to regulations in force.

Such an approach can lead to the solving of water pollution problem in the most economically efficient manner on short, average and long term situation.

REFERENCES

* * http://www.wmo.int/pages/prog/hwrp/wramanual.html
* * http://www.estis.net/sites/lcinit/default.asp?site=lcinit&page_id=2AAEA21D-4907-4E16-BF28-A63C072B6BF7
* * http://www.google.ro/#hl=ro&source=hp&biw=933&bih=495&q=assesment+of+water+usage&btnG=C%C4%83utare+Google&rlz=1W1RNRN_en&aq=f&aqi=&aql=&oq=&fp=1&cad=b
Alzamora C., *Guideline for the Assessment of Water Usage*. Arcellor Mittal, Addressed to Stelle Operating Facilities and Mining, AM ENV 5, 20/10/2010
Shimokura G.H., Savitz D.A., Symanski E., *Assessment of Water use for Estimating Exposure to Tap Water Contaminants*. Environ Health Perspect. 1998 Feb; 106(2):55-9.

UNELE CONSIDERAȚII PRIVIND EVALUAREA UTILIZĂRII APEI ÎNTR-O INSTALAȚIE INDUSTRIALĂ

(Rezumat)

Lucrarea abordează utilizarea apei în industrie și schițează managementul general al acesteia. Sunt puse în discuție unele linii directoare în domeniul evaluării apelor uzate.

MICROHARDENESS RESEARCHES ON DEPOSED HARD LAYERS 40Cr10 STEEL FOR MACHINE PARTS FRACTAL

BY

ADRIAN ALEXANDRU* and **GELU BARBU**

Technical University "Gheorghe Asachi" of Iaşi,
Department of of Materials Science

Abstract. The aim of this paper is to analyze the micro-hardness of hard layers deposed by electrical discharge in impulse on machine parts by 40Cr10 steel.

In order to establish the influence of alloying deposition by electrical discharge in impulse on machine parts, were made researches on 40Cr10 Romanian steel which was thermal treated before alloying deposition by electrical discharge in impulse by two variants : quenching and quenching +tempering.

Key words: micro-hardness, layer, electrode.

1. Introduction

Alloying and deposition by electrical discharge in impulse method uses the inverse polarity – the part which is processed is the cathode and the electrode is the anode- and in this case the deposition takes place in air or other gas, with or without a rotation movement.

---

* Corresponding author e-mail: axa72us@yahoo.com

By comparing with other methods, alloying and deposition by electrical discharge in impulse presents a series of advantages as: the deposed metallic layer presents a resistant connection with the basis material; the method makes possible the deposition of pure metals (Ni, Cr, Mo, W, Ti) or metallic alloys; it is not necessary a preliminary preparation of the deposition surface etc.

The demanded properties for the layer are different of those of the basic material and almost in contradiction with them. The efficient combination of alloying and deposition by electrical discharge in impulse with a superficial thermal treatment can make disappear many disadvantages of this method as: large roughness of the alloyed surface, residual stress in layers which decrease the wear resistance.

2. Basis Material, Electrodes and Technologies

In order to determining the influence of alloying and deposition by electrical discharge in impulse of layers wear resistant on machine parts were made researches on 40Cr10 steel used as support.

Chemical composition of 40 Cr10 steel is: 0,36 – 0,44%C; 0,5 – 0,8 % Mn; 0,17 – 0,37 % Si; 0,020 – 0,04 % S; 0,035 % P; 0,8 – 1,1 % Cr. In table 1 are presented the mechanical properties and thermal treatment parameters for the 40Cr10 steel.

Table 1
Mechanical Properties and Thermal Treatment Parameters

Steel	Mechanical properties					Thermal treatment parameters							
	$R_{p0,2}$ N/mm², min	R_m N/mm², min	A_5 % min	KCU J/cm² min	HB daN/ mm²	Annealing		Normalising		Quenching		Tempering	
						T, °C	Medium	T, °C	Medium	T, °C	Medium	T, °C	Medium
40Cr10	780	980	10	53	R217	680-720		845-875	c	845-875	a	450-550	a,u

Steels for this group of machine parts (rivets, screws, studs, pins, feathers, nuts, bushings grooved etc.) are common carbon steel, quality or allied to the nature and specific application requirements.

Thus, steels for the manufacture of assembly by cold plastic deformation (rivets, screws, studs, pins, feathers) are: OL34q; OL37q; RCB52q-thermal untreated; OLClOq; OLC15q; 15Cr9q; 18MnCrllq; 17MoCrNil4q; 21MoMnCrl2q –ag(e)ing of coal; 20MnB5q; OLC25q; OLC35q; OLC45q; 40Crl0q; 34MoCrllq; 40BCrl0q; 40CrNil2q; 42MoCrllq; 34MoCrNil6q; 30MoCrNi20q STAS 9382-82 improved. It delivers in rolled condition - L,

molding and annealing - LR, rolled and peeled LC, cold drawn - T, drawn and annealed TR, peeled, drawn and annealed – CTR.

The screws and studs are manufactured in three categories of performance (accurate, semi accurate and roughly) and 7 groups of mechanical characteristics: 4.6, 4.8, 5.6, 5.8, 8.8; 10.9 and 12.9, where the first number have 1/100 of tensile stress pull, the second figure represents the percentage 1/10 of the ratio of the nominal yield and tensile strength at break by nominal multiplying two numbers to get 1:10 of yield.

Nuts are manufactured in 2 grades of execution (accurate, semi accurate) and 4 groups of features: 5, 8, 10, 12. The numbers represent values of yields, offered by 1/100 screw's Rm or studs which is screwed.

As for screws, studs and nuts, each group of features ensures a certain category of steels. For example, 12.9 group is provided only of alloy steels and 4.6 group of ordinary steels. The first 4 groups of resistance of the bolts were secured without heat treatment characteristics and the last 3 treatment groups only with improvement.

The most important feature of these steels is the energy of breaking which has KV = 28 J between – 10 and -60˚C.

Tensile strength is 440 ... 780 N/mm^2, yield strength is 260 ... 590 N/mm^2, elongation is 20 ... 14%, resilience of 70 ... 120 J/cm^2, the state improved hardness HB = 220 ... 295 and creep resistance for 100 000 h operation at 500°C is 33.3 ... 240, it N/mm^2.

2.1. Variants of Thermal Treatment Applied Before Alloying and Deposition by Electrical Discharge in Impulse

It was found that the filing and processing of metal surfaces by electrical discharge in impulse gives clear advantages such as: obtaining a layer and substrate with high adhesion to the basic material, get a higher hardness and wear resistance of the deposited layer obtaining special features of superficial layers decreases their fatigue, to obtain a high surface roughness et al.

All the filing and alloying of the regions by electrical impulse filing can be totally or partially eliminated, combining effectively a thermochemical or thermal treatment with a processing of this kind.

Table 2
Variants of the Applied Heat Treatment.

Steel	Technological parameters
40 Cr10	a) Quenched at 860ºC/oil; b) Quenched at 860ºC/oil + tempered at 500 ºC/air

In Fig.1 are presented the applied heat treatment.
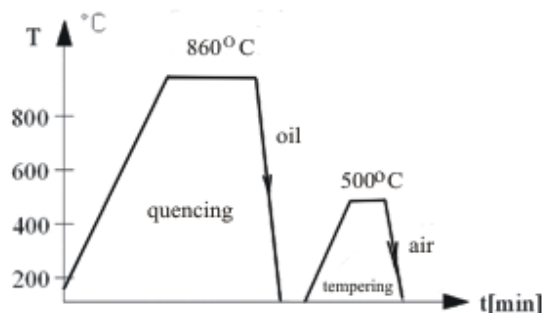
Fig. 1 – Applied heat treatment.

2.2. Electrodes (Deposed Materials)

It was established that the electrode material has a large influence on the depth and hardness of hardened layer. The best electrodes for hardening the machine parts in terms of obtaining maximum hardness depths are chromium-based electrodes, made from ferrochromium chrome - manganese and pure chrome. The same materials ensure the highest wear resistance of hardened parts in comparison to other materials.

Based on the investigations and practical tests it was concluded that the deposit materials as electrodes with Ø4 x 25 mm dimensions are as shown in Table 3.

Table 3
Electrode Materials

No.	Electrode materials	
	Name	Chemical composition
1	Stelite	56%Co; 32%Cr; 21%W; 2,8%C; rest Fe
2	WCo8	92%W; 8%Co
3	Fe – Mo	67,9% Mo; 0,73% Si; 0,09% C; 0,35% Cu; rest Fe
4	Fe - Cr	60%Cr; 0,82% Si; 0,08% C; 0,31% Cu; rest Fe
5	Mo	Mo 100%
6	40 Cr10	0,21% C; 1,1% Mn; 0,3% Si; 0,9% Cr
7	40Cr10	0,43% C; 0,7% Mn; 0,3% Si; 0,9% Cr
8	OLC 55	0,56% C; 0,7506% Mn; 0,32% Si

2.3. Deposition Technologies

The samples submitted to the depositing and processing of alloy by electrical impulse discharge has the areas adjusted to Ra = 5 to 10 micrometers cleaned of oxides and other impurities.

To make deposits it was used ELITRON 52 for manual installation in the flat electrode with circular cross section diameter of 4 mm and 25 mm, is presented in Fig. 2.
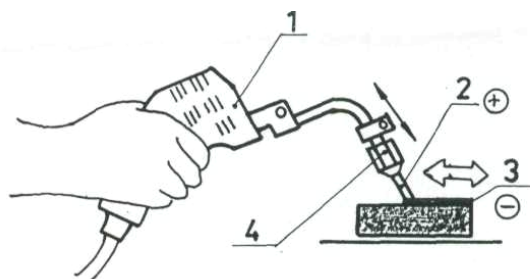
Fig. 2 – Scheme of work for manual deposit and alloy by electrical in pulse discharge; 1-shaker; 2-electrode; 3-deposited layer on the piece; 4-chuck clamping the electrode.

Working conditions of ELITRON facility is chosen according to the electrode material, machinery material to be treated and the characteristics that are desired to obtain.

The form and gauge of the machine parts treated by deposit and alloy by electrical in pulse discharge can be any, the areas processed can be external or internal. Power supply frequency is 50-60 Hz, and the roughness layer $2 \div 6$ microns.

Deposition parameters are given in Table 4.

Table 4
Deposition Parameters

Power consumed	1,12 kVA
Productivity	2 cm^2 / min
Voltage	220 V
Thickness of the deposited layer	$0,05 \div 0,2$ mm
Current Work	2,9 A
Surface roughness	$1 \div 6$ m
Discharge energy	2,1 J

3. Experimental Research and Results

Rectangular samples (10x10x30 mm), on which were deposited layers by impulse electrical discharge on ELITRON 52 B installation, with electrodes from materials given from Table 3, were subjected micro-hardness measurements, thickness of the deposed layer, thickness of alloyed layer, roughness and microscopic investigations.

3.1. Mechanical Characteristics and Geometric parameters of Layers

Measurements results are presented in Table 5.

Micro-hardness was measured on NAMICON 400DM/2006 microhardmeter with a force of 50 gf, a push time of 15 s and a thickness of 600:1. Roughness was measured on a SURTRONIC 3 + device.

Following implementation of experimental program is established that:

- High microhardness is obtained using for deposition stelite electrodes;

- Transition layer is alloy and very hard when it is used rich electrodes in alloying elements in descending order: WCO 8, stars, Fe - Mo - Fe - Cr - Mo;

- Filing of electrode layers of alloy steel and carbon (21MoMnCr12, 40Cr12, OLC 55) allows abtaining denser layers than suport steel, the cause is a very fine structure (nanocrystalline) and high internal tensions in these layers;

- One and the same electrode gives different microhardness depending of the nature of support stell and heat treatment condition (Q or Q + T);

- Transition layers are diffusion layers at using the rich electrodes in alloying elements Wco8, stelite, Fe-Mo, Fe-Cr and Mo and return layers on quenched steels;

- On transition layers microdensity is a lot higher than core samples, while microhardness in return layers is smaller than hardened core;

- Thickness of white layers is between 61 and 70 microns, because it was used on ELITRON 52 B device current intensities and discharge energies in pulse greater (16 A şi 2,1 J);

- The thickness of transition layer whether is difusion or tempered is smaller than white layers $30 \div 60$ m;

- Roughness Ra is higher when is using carbide electrodes (Wco8)and stelite ($4,02 \div 5,2$ μm) and low when is using construction steel electrodes ($1,12 \div 2,86$ μm).

Table 5
Measurements Results

Sample	Steel	Electrode	Heat treat-ment	Micro-hardness, HV_{50}			Thickness of the layers, m		Roughness R_a, m
				Deposed layer	Transition layer	core	deposed	transition	
1.a.1.		Stelit		1456	1111		65	56	4,17
1.a.2.		WCo8		1686	1211		64	51	4,21
1.a.3.		Fe-Mo		852	796		76	48	3,02
1.a.4.		Fe-Cr	Q	814	726	714	78	49	2,91
1.a.5.		Mo		780	755		72	51	2,80
1.a.6.		21MoMnCr12		721	687		77	56	2,08
1.a.7.	40Cr10	40Cr10		781	701		77	50	1,43
1.b.1.		Stelit		1390	998		79	50	4,14
1.b.2.		WCo8		1581	1018		74	46	4,02
1.b.3.		Fe-Mo		838	732		69	43	2,85
1.b.4.		Fe-Cr	Q+T	826	698	437	71	39	3,05
1.b.5.		Mo		818	667		66	38	3,02
1.b.6.		21MoMnCr12		714	500		74	46	2,59
1.b.7.		40Cr10		802	577		72	47	2,61

Obs. Q - quenching, T- tempering.
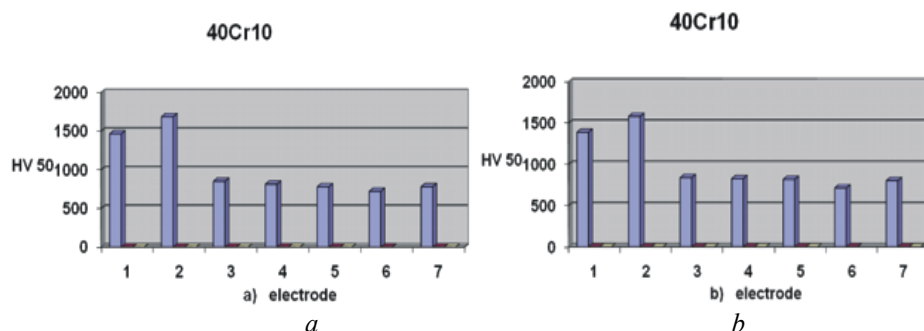
Fig. 3 – Micro-hardness values of the white layers (deposed) with different electrodes
on steels 40 Cr10; *a* – quenched; *b* – quenched and tempered.

Micro-hardness values of the deposited layers on the three steels in hardened, toughened and tempered condition are given in Fig. 3.
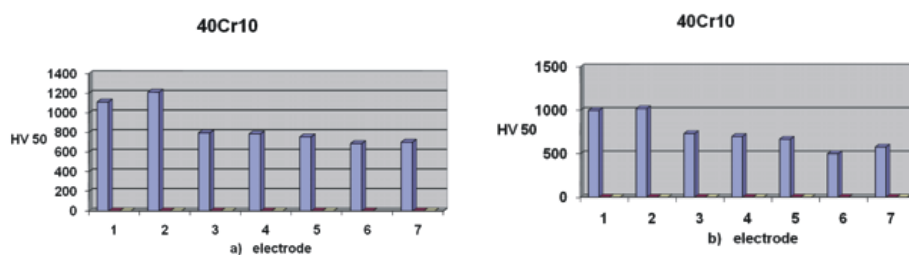
Fig. 4 – Micro-hardness values on transition values with different electrodes
on 40 Cr10 steel. *a* – quenched; *b* – quenched and tempered.

A transition micro-hardness value of this steel in hardened, toughened and tempered depending on the nature of the electrodes is given in Fig. 4.

4. Conclusion

– No matter of used electrode, the white layers are hard, even if the used electrode was from the same steel as the support.

– High micro-hardness values were obtained on the white layers deposed with WCo8 or stelite electrodes.

– On quenching steel, were obtained higher values of micro-hardness compared with quenched and tempering steel.

– Fe-Mo, Fe-Cr and Mo electrodes induced layers with high micro-hardness, and 40 Cr10 electrode induced smaller micro-hardness values, but higher than the case of the quenched or quenched + tempered steel.

REFERINTELE BIBLIOGRAFICE IN TEXT

REFERENCES

[1]. Alexandru A., Strugaru S.I., *Alierea şi depunerea superficială prin scânteie electrică-Influenţa tratamentelor termice asupra caracteristicilor straturilor*. Editura Tehnopress, Iaşi, 2008.

[2]. Alexandru A., Pop F., *Metalic Materials with Hardened Deposit Created by Electric Arc with Vibrating Electrode*. Lausane, Elveţia, Euromat Junior-94.

[3]. Alexandru I., Popovici R., Baciu C., Călin M., Cojocaru V., Bulancea V., Carcea I., Alexandru A., Paloşanu G., *Alegerea şi utilizarea materialelor metalice*. Editura Didactică şi Pedagogică, Bucureşti, 1997.

[4]. Anderson A.W., *Physical Chemistry of Surfaces*. Wiley-lnterscience, New-York, 1990.

[5]. Filip N., Abramciuc, Alex., *Studii şi cercetări experimentale privind formarea straturilor pe suprafeţele pieselor de maşini cu ajutorul metodei de aliere cu descărcări electrice în impuls*. In vol. Tehnologii avansate în secolul XXI, Chişinău, 68-69 (2000).

[6]. Vermeşan G., *et al.*, *Procedee speciale de tratamente termice*. Tipografia I.P. Cluj – Napoca, 1990.

CERCETĂRI DE MICRODURITATE PE STRATURI DURE DEPUSE PE OŢELUL 40Cr10 PENTRU ORGANE DE MAŞINI

(Rezumat)

Scopul acestei lucrări este analiza microdurităţii straturilor dure depuse prin descărcare electrică în impuls pe organe de maşini din oţel marca 40Cr10.

Pentru a stabili influenţa depunerii şi alierii prin descărcare electrică în impuls asupra organelor de maşini s-au făcut cercetări pe oţelul 40Cr10, care a fost tratat termic înainte de depunere şi aliere prin descărcare electrică în impuls în două variante: călire şi călire + revenire.

CUTTING TOOL MATERIALS: A REVIEW ON RECENT DEVELOPMENTS AND APPLICATIONS

BY

MIHAI APREUTESEI[1*], IONELA ROXANA ARVINTE[1] and EMILIA BLAJ[2]

[1]University Transilvania Braşov
[2]Polytechnic University of Bucureşti

Abstract. The purpose of this paper is to provide a brief overview of the recent developments in cutting tool materials and to indicate where future developments are likely to occur. Many types of tool materials, ranging from high carbon steel to ceramics and diamonds, are used as cutting tools in today's metalworking industry. It is important to be aware that differences do exist among tool materials, what these differences are, and the correct application for each type of material. The cutting tool materials must possess a number of important properties to avoid excessive wear, fracture failure and high temperatures in cutting, such as: hardness at elevated temperatures, toughness and wear resistance. Developments of ceramics, ceramic composites, sialons, PCBN and PCD tool materials and their applications are described. The engineering of the surface by coating and the improvement in fracture toughness and thermal shock resistance by material design will continue the evolution of improved cutting tool materials. Recent developments and applications of the main classes of tool materials will be described.

Key words: cutting tools materials, applications, development.

---

* Corresponding author e-mail: m.apreutesei@gmail.com

1. Introduction

Recent developments in machine tools, computerized control, automatisation, combined with the related unforeseen improvements in the cutting materials and their protective coatings with special geometrical shapes of the tools, make such a prognosis completely invalid. Moreover, the degree of use of the machining operations has even significantly increased (Ashby, 1992).

New cutting materials increase the tool efficiency costs of performing machining operations, and also highly increase the reliability of the cutting and the quality of the products. Machining of metals with a cutting tool harder than the work material is a common manufacturing operation in the production of a variety of parts. The unwanted material is removed from the work material in the form of chips, using geometrically defined, single- or multiple-point cutting tool on a machine tool. Various machining processes include turning, drilling, milling, boring, threading, tapping, and broaching. The process can be either continuous or intermittent. Each of them would operate under different set of machining conditions, namely, speed, feed and depth of cut. Consequently, the requirements of the tool material would differ from one operation to another. Materials used for grinding, polishing, lapping, *etc.*, that use abrasives whose cutting edges are not geometrically defined (*i.e.*, random geometry) and whose geometry changes continuously as the process progresses (also randomly) are outside the scope of this article.

Many types of tool materials, ranging from high carbon steel to ceramics and diamonds, are used as cutting tools in today's metalworking industry. It is important to be aware that differences do exist among tool materials, what these differences are, and the correct application for each type of material (Trent, 1991).

2. Requirements

A successful cutting tool material must resist these severe conditions and yet provide a sufficiently long tool life to justify its use economically.

The relative importance of each depends, however, upon the type of machining operation continuous versus intermittent cutting; roughing versus finishing; condition of the machine tool; volume of production (small batch versus mass production); chip handling and disposal; use of a cutting fluid whether permitted or not; geometry, finish, accuracy, and surface integrity requirements; tool-lifetime economics; other constraints such as delivery schedules and bottle-necks.

The cutting tool materials must possess a number of important properties to avoid excessive wear, fracture failure and high temperatures in cutting, The following characteristics are essencial for cutting materials to withstand the heavy conditions of the cutting process and to produce high quality and economical parts:

- *hardness* at elevated temperatures (so-called *hot hardness*) so that hardness and strength of the tool edge are maintained in high cutting temperatures.

- *toughness:* ability of the material to absorb energy without failing. Cutting if often accompanied by impact forces especially if cutting is interrupted, and cutting tool may fail very soon if it is not strong enough.

- *wear resistance:* although there is a strong correlation between hot hardness and wear resistance, later depends on more than just hot hardness. Other important characteristics include surface finish on the tool, chemical inertness of the tool material with respect to the work material, and thermal conductivity of the tool material, which affects the maximum value of the cutting temperature at tool-chip interface.
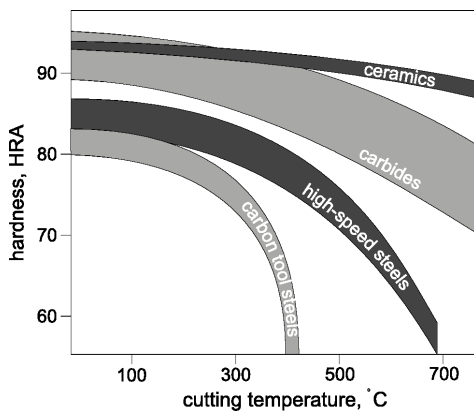
Fig. 1 – Hot hardness for different tool materials.

The materials from which cutting tools are made are all characteristically hard and strong. There is a wide range of tool materials available for machining operations, and the general classification and use of these materials are of interest here (Abrao *et al.*, 1993).

3. Cutting tool Materials

A simple classification of cutting tool materials can be made based on three groupings:
- High speed steels;
- Cemented carbides;
- Ceramic and super-hard materials including alumina based composites, sialons, diamond and cubic boron nitride.

The surface properties of these materials can also be modified by surface engineering using a range of coating or surface modification techniques (Bell, 1992). The performance of cutting tool materials is complex and depends on a number of factors including the machinability of the work piece which can

be modified by alloying (Mills & Redford, 1983). It has been shown (Mills, 1980) that the total level of residual elements present in otherwise similar leaded low carbon free machining steels has a significant influence on the V_{240} cutting speed (*i.e.* the speed to give a tool life of 240 minutes).

3.1. Carbon Steels

The carbon content is $0.6 \sim 1.5\%$ with small quantities of silicon, chromium, manganese, and vanadium to refine grain size. Maximum hardness is about HRC 62. This material has low wear resistance and low hot hardness. The use of these materials now is very limited.

Fig. 2 – Example of carbon steel tools.

3.2. High-Speed Steel (HSS)

They are highly alloyed with vanadium, cobalt, molybdenum, tungsten and chromium added to increase hot hardness and wear resistance. Can be hardened to various depths by appropriate heat treating up to cold hardness in the range of HRC 63-65. The cobalt component give the material a hot hardness value much greater than carbon steels. The high toughness and good wear resistance make HSS suitable for all type of cutting tools with complex shapes for relatively low to medium cutting speeds. The most widely used tool material today for taps, drills, reamers, gear tools, end cutters, slitting, broaches, etc. (Mills, 1996).
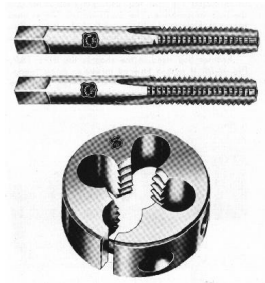
Fig. 3 – Thread tap and die made of high-speed steel.

3.3. Cemented Carbides

These are the most important tool materials today because of their high hot hardness and wear resistance. The main disadvantage of cemented carbides is their low toughness. These materials are produced by powder metallurgy methods, sintering grains of tungsten carbide (WC) in a cobalt (Co) matrix (it provides toughness). There may be other carbides in the mixture, such as titanium carbide (TiC) and/or tantalum carbide (TaC) in addition to WC.

Fig. 4 – Assortment of cemented carbide inserts for use by different cutting tools.

In spite of more traditional tool materials, cemented carbides are available as inserts produced by powder metalurgy process. Inserts are available in various shapes, and are usually mechanically attached by means of clamps to the tool holder, or brazed to the tool holder (see the figure in the next page). The clamping is preferred because after an cutting edge gets worn, the insert is indexed (rotated in the holder) for another cutting edge. When all cutting edges are worn, the insert is thrown away. The indexable carbide inserts are never reground. If the carbide insert is brazed to the tool holder, indexing is not available, and after reaching the wear criterion, the carbide insert is reground on a tool grinde (Schneider , 2009).
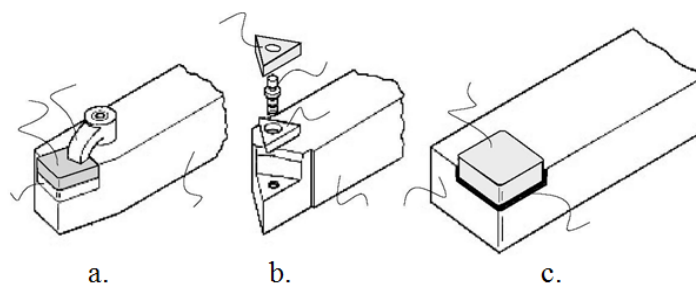
Fig. 5 – Methods of attaching carbide inserts to tool holder:
a – clamping; *b* – wing lockpins; *c* – brazing.

One advance in cutting tool materials involves the application of a very thin coating (~ 10 µm) to a K-grade substrate, which is the toughest of all carbide grades. Coating may consists of one or more thin layers of wear-resistant material, such as titanium carbide (TiC), titanium nitride (TiN), aluminum oxide (Al_2O_3) and/or other, more advanced materials. Coating allows to increase significantly the cutting speed for the same tool life.
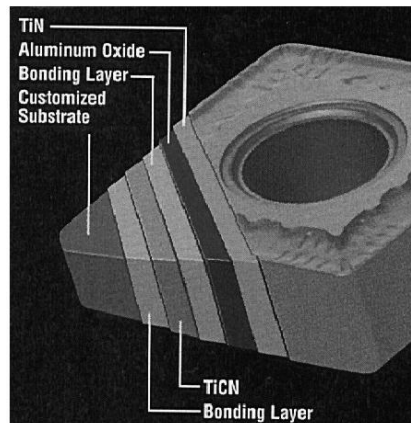
Fig. 6 – Structure of a multi-layer
coated carbide insert.

3.4. Ceramics

Ceramic materials are composed primarily of fine-grained, high-purity aluminum oxide (Al_2O_3), pressed and sintered with no binder. Two types are available:

- white, or cold -pressed ceramics, which consists of only Al_2O_3 cold pressed into inserts and sintered at high temperature.

- black, or hot-pressed ceramics, commonly known as cermet (from ceramics and metal).

This material consists of 70% Al_2O_3 and 30% TiC. Both materials have very high wear resistance but low toughness; therefore they are suitable only for continuous operations such as finishing turning of cast iron and steel at very high speeds. There is no occurrence of built-up edge, and coolants are not required (Stephenson & Agapiou, 1997).

3.5. Cubic Boron Nitride (CBN) and Synthetic Diamonds

Diamond is the hardest substance ever known of all materials. It is used as a coating material in its polycrystalline form, or as a single-crystal diamond tool for special applications, such as mirror finishing of non-ferrous materials.

Next to diamond, CBN is the hardest tool material. CBN is used mainly as coating material because it is very brittle. In spite of diamond, CBN is suitable for cutting ferrous materials.

Polycrystalline diamond (PCD) is widely used in machining aluminium silicon alloys because of its outstanding abrasion resistance; it is also widely used in machining non-metallic materials such as CFRP, silica filled resin and wood.
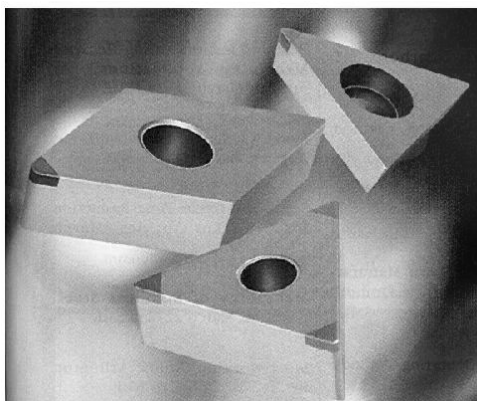
Fig. 7 – Polycrystalline CBN or synthetic diamond layer on a tungsten carbide insert.

Diamond is not recommended for machining ferrous materials, titanium alloys and high nickel alloys since diamond graphitises and wears rapidly (Juneja & Nitin, 2003). CBN in polycrystalline form (PCBN) is increasingly being used to machine hardened steels.

4. Conclusion

In this paper it was presented some cutting tool materials and recent developments together with their properties. For high speed steels the major recent development has been the deposition of hard wear resistant ceramic layers, such as titanium nitride layers by PVD techniques which have given significant improvements in tool performance.

Polycrystalline cubic boron nitride (PCBN) is finding increasing application in the machining of hardened steels such as ball bearing steels. Polycrystalline diamond is likely to find wider application in the machining of non-metallic materials such as wood and other composites.

The cemented carbides both CVD and PVD coating of tools with multilayers of different ceramics has led to improved performance. PVD coating would appear to offer a number of significant benefits in terms of improved coating adhesion and more favorable substrate compressive stresses.

REFERENCES

Abrao A.M., D.K. Aspinwall, M.L.H. Wise, *A Review of polycrystalline cubic boron nitride cutting tool developments and applications*. Proc. MATADOR Conference, UK, 169-180, (1993).

Ashby M.F., *Materials Selection in Mechanical Design*. Pergamon Press., Oxford.

Bell T., Surface Engineering. J Phys B. Appl. Phys. **25**, *A297-A306,* (1992).

Juneja B.L., Nitin Seth, *Fundamentals of metal cutting and machine tools*. New Age International, 2003.

Mills B., *Effect of residual elements on the machinability of leaded free machining steels*. Phil. Trans. Roy. Soc. Lond. *A295*, 87-8 (1980).

Mills B., Journal of Materials Processing Technology, *56*, 16-23, (1996).

Mills B., Redford A.H., *The Machinability of Engineering Materials*. Applied Science Publishers, London, 1983.

Schneider G., *Chapter 1 - Cutting Tool Materials*. American Machinist, October, 2009.

Stephenson David A., Agapiou John S., *Metal cutting theory and practic*, 1997.

Trent E.M., *Metal Cutting*. Third Edition. Butterworth-Heinemann. Oxford, 1991.

MATERIALELE DISPOZITIVELOR DE TĂIERE: O REVIZUIRE PRIVIND DEZVOLTĂRILE RECENTE ŞI APLICAŢIILE ACESTORA

(Rezumat)

Scopul acestei lucrări este de a oferi o scurtă prezentare a evoluţiilor recente a materialelor pentru dispozitivele de tăiere şi de a indica unde pot apărea dezvoltări viitoare. Multe tipuri de materiale pentru scule, variind de la oţel carbon rapid până la ceramică şi diamante, sunt folosite ca instrumente de tăiere în industria de astăzi pentru prelucrarea metalelor. Este important să se ţină cont de faptul că există diferenţe între materialele pentru scule, care sunt aceste diferenţe şi de aplicaţia corectă pentru fiecare tip de material. Materialele dispozitivelor de tăiere trebuie să aibă un număr de proprietăţi importante pentru a evita uzura excesivă, rezistenţa la rupere şi temperaturi ridicate în tăiere, cum ar fi: duritatea la temperaturi ridicate, tenacitate şi rezistenţa la uzură. Dezvoltarea ceramicii, compozitele ceramice, sialons, PCBN şi dispozitive din materiale PCD şi aplicaţiile lor sunt descrise. Ingineria suprafeţelor prin acoperiri şi îmbunătăţirea rezistenţei la rupere şi a rezistenţei la şoc termic prin proiectarea materialelor va continua prin îmbunătăţirea evoluţiei materialelor dispozitivelor de tăiere. Dezvoltările recente şi aplicaţiile principalelor clase de materiale ale dispozitivelor vor fi descrise.

POLARIZED GRID INFLUENCE ON HOLLOW CATHODE EFFECT IN PLASMA NITRIDING PROCESS

BY

MIHAI AXINTE*, **CARMEN NEJNERU, MANUELA CRISTINA PERJU, ION HOPULELE and ALEXANDRU ENACHE**

"Gheorghe Asachi" Technical University of Iaşi

Abstract. Hollow cathode effect occurs when the cathode glow drop discharge zone from the two surfaces of the part or two separate parts interfere with each other. To highlight their appearance parameters which have the effect we used a specimen with a V-shaped cutout, which has a variable opening, the effect of overheating occurring in the narrower channel. This paper presents an experimental study on variation U and I at hollow effect occurrence, when between the anode and cathode a negatively biased grid is interposed.

Key words: Grid, hollow cathode effect, cathode drop discharge zone.

1. Introduction

In general, for the plasma nitriding process, the components to be treated are subject to a high cathode potential and the grounded wall of the furnace forms the anode. The components are directly involved in the discharge process.

Many studies have indicated that the geometry, size and ratio of the surface to mass of the component have substantial effects on the temperature

---

* Corresponding author e-mail: mihai.axinte@gmail.com

distribution within the component and lead to inhomogeneous response to nitriding (Li *et al.*, 2010). Hollow cathode effect has the potential for electric arc occurrence that leads at destruction of part surface. Since the geometry is very wide range, on parts subject to nitriding process may appear hollow cathode effect.

Hollow cathode effect occurs when the cathode glow drop discharge zone from the two surfaces of the part or two separate parts interfere with each other (Axinte *et al.*, 2009). Under these conditions the electrons accelerated in the cathode potential drop zone, in front of an area are slowed down and reaccelerated in other area of the cathode drop region.

Because the repeated oscillation in space between the two surfaces, electrons runway length increases very much, so the default number of ionization. The flow of electrons originating from the collision of electrons by neutral atoms is very intense.
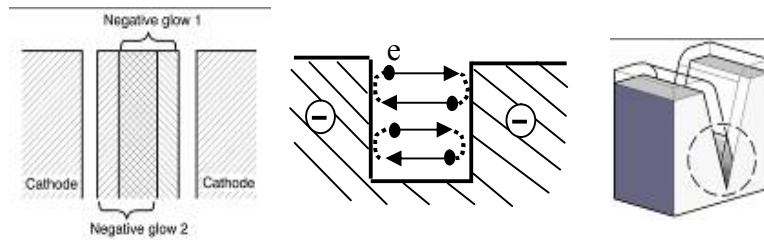
Fig. 1 – Graphical representation of the hollow cathode effect.

Increasing concentrations of ions causes an increase in ion bombardment (at cathode) which makes the cathode temperature to rise very much (a few hundred degrees).
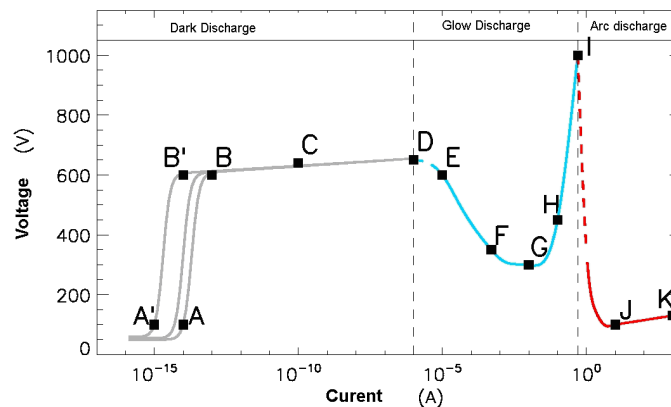
Fig. 2 – Voltage-current characteristics of electrical discharge in neon at 1 torr, with two planar electrodes separated by 50 cm.

The area is very bright due to emission of photons. Local current density increases, almost short-circuiting the rest of discharge. Discharging is so predominantly in the hollow cathode effect occurring here as well negative phenomena: delayed until melting and frequent switching under the electric arc (Alves *et al*., 2006).

Hollow cathode effect appears when the distance between cathode surfaces is in the range (2-3) d_{an}, when it crosses the cathode fall discharge zone – called negative lights.

The voltage-current characteristics of electrical discharge in neon at 1 torr, with two planar electrodes separated by 50 cm has different zones and their characteristics are: *A*: random pulses by cosmic radiation, *B*: saturation current *C*: avalanche Townsend discharge *D*: self-sustained Townsend discharge *E*: unstable region: corona discharge *F*: sub-normal glow discharge *G*: normal glow discharge *H*: abnormal glow discharge *I*: unstable region: glow-arc transition *J*: electric arc, *K*: electric arc

For the abnormal discharge, the length $d_c = d_{an}$ depends on discharge current according to the law of Aston.

$$d_c = d_{an} = a \cdot j^{\frac{-1}{2}} + b \cdot p^{-1}, \text{ in cm (HI zone)} \qquad (1)$$

Where: j = current density, p = pressure

In general, when the cathode emits a large number of electrons or the occurrence for favorable conditions through ionization processes appears, the cathode drop zone impedance decreases and switches to an electric arc glow discharge.

Giving the electric arc frequency occurrence in the process of ion nitriding and its destructive effects on the burden and source of electricity supply, the conditions of its occurrence should be avoided (Axinte *et al*., 2009).

Switching to the electric arc occurs when the cathode by bombardment of ions and fast neutral atoms reach the termoemision energetic state. In general, the electric rectifier supplies electrical energy to the discharge from a ion nitriding recipient and maintains the temperature of cathode part at values much lower than the thermo emission temperature. Because during the degassing process, in front of the cathode occurs high density areas fill with charge carriers, which favors the appearance of "channels" with very low impedance, practically the whole power is concentrated in these areas.

2. Experimental Results:

For this experiment the 38CrMoAl09 steel samples were used with chemical composition shown in Table 1:

Table 1
Chemical Composition for 38CrMoAl09 Steel

Element	Fe	C	Cr	S	Cr	Mo	Ni	Al	Cu	W	Ti
Procent	95.4	0.50	1.49	0.29	1.49	0.12	0.12	1.17	0.12	0.06	0.01

For the experiment we used a plasma nitriding facility build in the heat and thermochemical treatments laboratory from Faculty of Materials Science and Engineering, Iaşi. In Fig. 3 the plasma nitriding facility chamber is presented. Also, to highlight the emergence of double cathode effect and its dependence on process parameters (voltage, current, pressure), we used a wedge-type specimen, and its dimensions are represented in Fig. 4.

Fig. 3 – Plasma nitriding chamber with cathode grid.
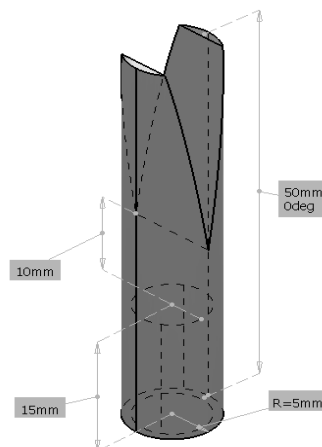
Fig. 4 – The sample sketch to highlight the influence of the grid to hollow cathode effect in wedge-type sample.

Table 2 and Table 3 shows the experimental data. Table 2 summarizes the data obtained at the discharge on facility with the cathode grid. In Table 3 are presented data obtained at discharge without cathode grid.

Table 2
Cylindrical Sample + Grid

Image	Pressure	Cathode voltage	Anode intensity	Temperature	Grid intensity
	torr	V	A	˚C	mA
4a	0.5	500	0.04	500	10
4b	1	467	0.11	500	10
4c	2	407	0.16	500	10

a   *b*   *c*
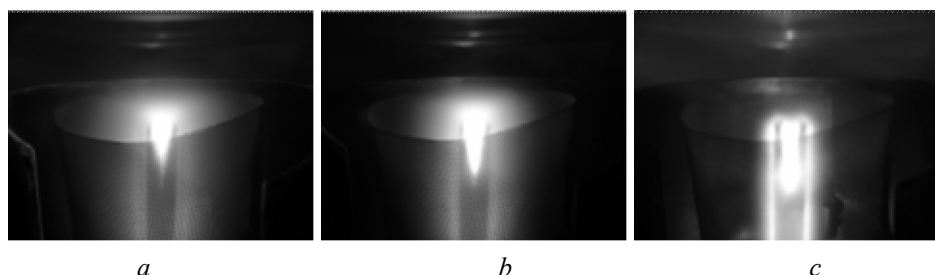
Fig. 4 − Grid discharge images.

Table 3
Cylindrical Sample Without Grid

Image	Pressure	Cathode voltage	Anode intensity	Temperature	Grid intensity
	torr	V	A	˚C	mA
5a	0.5	505	0.02	500	-
5b	1	472	0.12	500	-
5c	1.8	409	0.17	500	-

a   *b*   *c*
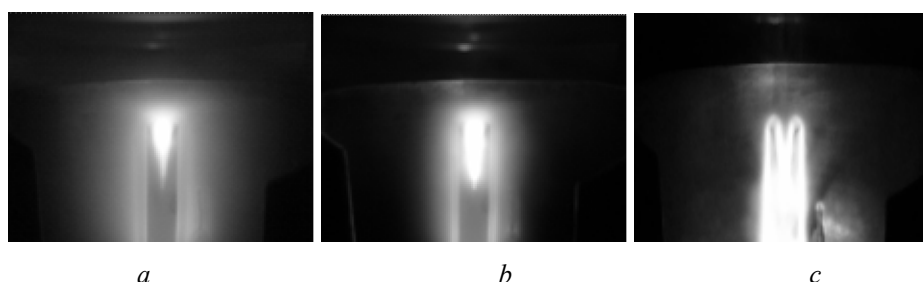
Fig. 5 − Without grid discharge images.

3. Results and Debates

Voltage, intensity and pressure during discharge are dependent on and their dependence is shown in Paschen curve (Fig. 2). Ion nitriding thermochemical treatment uses the HI zone from Paschen curve (the abnormal discharge luminescence), which is quite narrow that there is danger of electrical arc discharge.

Biased grid has the effect of changing the shape of the anode and cathode voltage drop, which normally would have a very high value near the cathode and insignificant in the rest of the enclosure. Thus an important part of the discharge occurs on the grid so that the cathode sputtering is modified, also the intensity discharge is modified.

Hollow cathode effect is slightly diminished, fact showed by photographs of Figs. 4 *a,...,c*. As seen from experimental data, in the grid case the discharge is earlier interrupted, and can occur at maximum 1.8 torr.

4. Conclusion

1. The biased grid changes the cathode voltage drop shape between anode and cathode, introducing an intermediate step, fact that generates a less intense cathode sputtering.

2. Hollow cathode effect changes its parameters in the presence of cathode grid meaning a slower discharge ignition (increasing discharge ignition intensity for hollow cathode effect) from 0.02 to 0.04 A. It also drops 10% from discharge pressure for hollow cathode effect occurrence.

3. Effect of the grid on the hollow cathode discharge is beneficial to part temperature, avoiding excessive growth for electric arc danger.

REFERENCES

Alves Jr. C. *et al.*, *Use of Cathodic Cage in Plasma Nitriding.* Surface & Coatings Technology, *201*, 2450–2454 (2006).
Axinte M. *et. al.*, *Facility for Study Heating and Diffusion Process, Using a Ionic Triode in a Plasma Nitriding Installation.* Tehnomus XV, Suceava (2009).
Li Y. *et al.*, *Plasma Nitriding of 42CrMo Low Alloy Steels at Anodic or Cathodic Potentials.* Surface & Coatings Technology, *204*, 2337–2342 (2010).

INFLUENŢA GRILEI POLARIZATE ASUPRA EFECTULUI DE CATOD DUBLU
LA NITRURARE

(Rezumat)

Efectul de catod dublu apare atunci când se întâlnesc luminile de cădere catodică a două suprafeţe ale piesei aflate faţă în faţă. Pentru evidenţierea parametrilor la care are loc apariţia efectului s-a folosit o epruvetă cu un decupaj în formă de V, care prezintă o deschidere variabilă, efectul de supraîncălzire apărând în zona mai îngustă a canalului. Lucrarea prezintă un studiu experimental asupra variaţiei U şi I la apariţia efectului de catod dublu, când între anod şi catod este interpusă o grilă polarizată negativ.

PROPOSAL FOR A CONTEXTUAL THEORETICAL APPROACH IN ACCIDENT PREVENTION

BY

GABRIEL BUJOR BĂBUȚ[*] **and ROLAND IOSIF MORARU**

University of Petroşani,
Mining Engineering and Industrial Safety Department

Abstract. In action-oriented, preventive accident research, the enterprise's internal conditions are traditionally in focus, resulting in numerous methods and much advice on how to reduce and avoid occupational accidents. The influence of the context on the enterprise's accident prevention activities has only rarely been included in prescriptive accident research. The recently issued ISO 31000: 2009 standard, concerning the risk management principles and guidelines for implementation requests to include the external and internal contexts of enterprises the risk management process and into models to prevent accidents at work. This paper presents different contextual theories in order to analyze whether this type of theory could be a way to elaborate our understanding of context. A differentiation is made between theories of understanding relations between enterprises and regulatory agencies and theories to perceive the relation between enterprise and the broader context. The last group of theories has its point of departure in an organizational understanding diverging from the classical, rational understanding of organizations and organizational processes. The conclusion is that contextual theories open for an elaborated understanding of the role of contextual relations in accident prevention, but also that an investigation of the potentials for making the theories action-orientated is needed.

Key words: accident, prevention, contextual theory, regulatory approaches.

---

[*] Corresponding author e-mail: gabriel_babut@yahoo.com

1. Introduction

In action-oriented, preventive accident research, the enterprise's internal conditions are traditionally in focus, resulting in numerous methods and much advice on how to reduce and avoid occupational accidents. The influence of the context on the enterprise's accident prevention activities has only rarely been included in accident research. This conforms to Rasmussen's request for models that include the context on equal terms with internal conditions (Rasmussen & Svedung, 2000). Rasmussen and Svedung present a model - shown in Fig. 1 - that includes the impact on risk caused by the decisions made by regulators, associations, and the government (Rasmussen & Svedung, 2000). This model opens for an awareness that includes the context in understanding and affecting local activities concerning accident prevention.
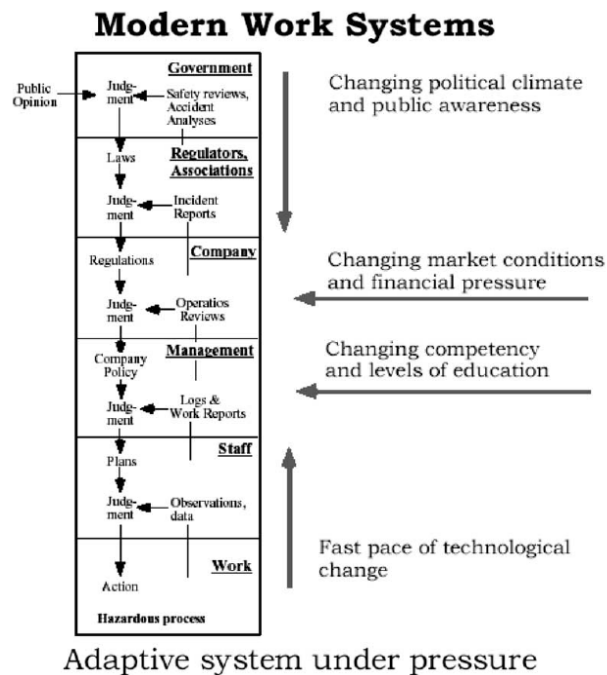
Fig. 1 – Levels of nested decision making involved
in risk management (Rasmussen & Svedung, 2000).

We can label this new theoretical approach a contextual approach that aims to emphasize an understanding of the relation between external agencies and local action when enterprises prevent accidents. A central concept within contextual theory is „strategizing" instead of strategy. In this context, the focus

is on actions concerning accident prevention. The theories of relevance for accident prevention will be discussed here.

As a basis, a presentation of several contextual theories is done, within two domains:

- ***regulatory approaches*** focusing on the relation between enterprises and regulatory agencies, typically a labor inspectorate, and
- ***approaches focusing on relations*** between enterprises and other external actors.

Since especially the latter approaches are based on understandings of organizations which diverge from the classical model of understanding organizations and organizational decision making, these other models of enterprises' internal decision making are also presented. It is not the intention here to evaluate the different theories but to introduce different approaches in the field.

The focus in this paper is on *„normal accidents"*. This implies a focus on understanding preventive actions related to accidents occurring with higher frequency and with limited consequences in comparison to major accidents.

2. Regulatory Approaches

The expectation is that legislative demands give a clear signal of what actions are expected. Within the last 40-50 years, regulatory approaches have developed from primarily emphasizing detailed specifications of demands towards a more differentiated approach that complements detailed specifications with specification of general goals to be accomplished and procedures to be followed locally.

The development in regulation is an ambiguous process. While Romanian national regulation is moving towards the principles of reflexive regulation, regulation of machinery within EU through standardization is still primarily based on detailed specifications, just as more departmental orders follow the same principles. In any case, these ambiguities must be included in the understanding of how legislative initiatives affect enterprise behavior (Băbuţ & Moraru 2009; Moraru *et a*l., 2009).

Here, a more analytical model by Winter can be applied. This model combines the *„... most promising theoretical elements that really have contributed to our understanding of implementation"* (Winter, 1990). His model - shown in Fig. 2 - emphasizes the social aspects of implementing regulation. First, Winter states that to understand the implementation process, knowledge of the policy-formation process is necessary.

The following issues are of importance for the subsequent implementation process. The level of conflict among the group of people (the legislators) making the policy, their specific knowledge of the causal mechanisms within the field they want to regulate, the seriousness of their

actions (where symbolic actions denote low degree of seriousness), and the attention given to the policy-formulation process.

Secondly, the general policy has to be specified. The specification is not a simple rational process. It is influenced by both the organizational processes within the agency (labeled organizational implementation) and the relations with the external organizations affecting this process (labeled inter-organizational implementation). Thirdly, the street-level bureaucrats (e.g. the labor inspectors) play a key role in delivering „*the specified message of the policy"* to the target group (employers but also all groups of employees). Finally, the behavior of the target groups both towards the street-level bureaucrats and concerning the issue in general has to be included to understand the results of the policy and implementation process.
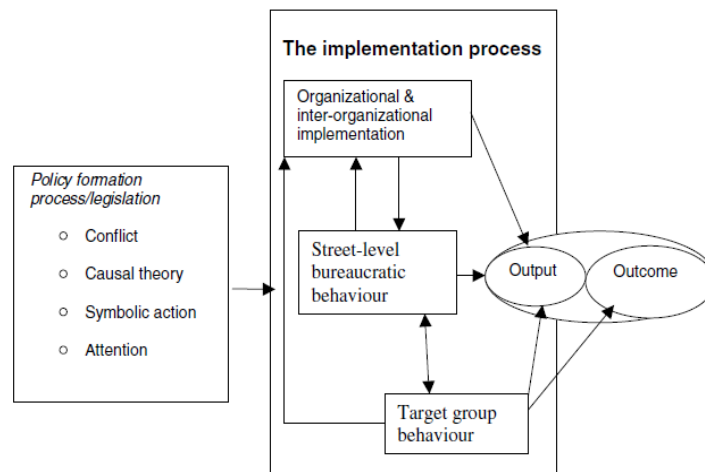
Fig. 2 – The implementation process and determinants of the implementation result (Winter, 1990).

3. Understanding Decision Making

Before addressing the contextual relations, the theoretical understanding of decision-making processes in organizations must be addressed. Here, two major theoretical positions can be outlined: a behavioral understanding of organizations and evolutionary theory. These are both formulated as alternatives to the rational model of organizational decision making dominating most recommendations on accident prevention (Hale & Glendon, 1987). The rational understanding of organizational decision making is often implicitly linked to the legalistic understanding in the traditional approach.

In decision making, the process of establishing a coalition between individuals and groups around a specific goal is of central importance. Goals

and coalitions are constantly changing over time. However, they can also be seen as a set of arguments that make it possible for safety representatives, safety managers etc. to widen and strengthen their coalition by incorporating stronger actors arguing for a focus on minimizing costs. This opens for a supplementary model for understanding decision making: *„garbage can decision making"* (Cohen *et al.*, 1972).

This model presents a more anarchic image of an organization. The model operates with ambiguous and constantly shifting goals; unclear and complex relations exist between goals and means; and many decision makers are often involved only part-time in decision making on specific issues. Decision making in organizations can be understood as: (1) a flow of choice opportunities, *i.e.* situations or occasions when it is expected that something that can be labeled a decision is produced; (2) a flow of issues and problems searching for a situation or an arena in which to be expressed; (3) a flow of solutions and actions; and (4) a flow of participants primarily characterized by the amount of energy (*i.e.* time, knowledge etc.) they can afford at a given time. The coupling of the four flows is dependent on: (a) the decision structure determining which participants participate or are expected to participate in specific choice opportunities; (b) the access structure determining the coupling between problems and issues on the one hand and choice opportunities on the other; (c) the total energy (time and money) available; and (d) the distribution of energy among the participants. The name *„garbage can"* is the image used to illustrate the theory. The flow of choice opportunities can be pictured as garbage cans flowing through the enterprise. The participants can throw problems and solutions into each garbage can by using a certain amount of energy. When the garbage can leaves the arena some problems and solutions have been linked in a decision.

Broberg has used this model - or derivatives thereof - to explain the difficulties in accomplishing an integration of health and safety issues (including accident prevention) into the planning of production systems (Broberg, 1997). The groups in an organization concerned with health and safety have their own arena (in Romania, the two-partite joint safety committee) for coupling problems and solutions. According to the theory, an amelioration of this situation demands a focus on the decision-making structure, the access structure, and the energy available for the actors maintaining accident prevention.

4. Proposal for a Contextual Approach

Many theories deal with the relation between external actors and agencies and individuals and groups in enterprises. The theories to be presented here are divided into two groups. The first focuses directly on these relations, while the second is based on a systemic perspective on the context.

The first group comprises agency theory, stakeholder theory, resource dependence theory, and network theories, while the second group is represented by institutional theory.

4.1. Understanding Relations

In the agency theory the discussion of power is embedded in a contract. As described by Ravn *et al*. (2001), agency theory is used to analyze the relations between two individuals: a principal and an agent. The principal (a person or an organization) is characterized by wanting a task to be carried out without being able to manage it alone. The agent (again a person or an organization) takes on the assignment. In some cases, a shift to behavioral contracts has occurred, demanding audits at regular intervals or maybe even demanding the use of formalized risk-management systems, like the DuPont system and OHSAS 18001.

In stakeholder theory, more relations are taken up. The focus is on the relation between the organization and external individuals, groups of people, or organizations. All actors having an interest in the organization are stakeholders. By analyzing the stakeholders' interests, the theory arrives at recommendations on how to strategize towards fulfilling the stakeholders' different interests so they do not withdraw or even actively oppose the interests of the organization. According to stakeholder theory, the organization can pursue four types of strategizing: collaboration, defense, monitoring, and involvement. The type of strategizing is selected according to a description of the stakeholders based on the answers to four questions: (1) Who are the stakeholders? (2) What kind of claim can they put on the organization by virtue of their interest? (3) What kind of challenges and scope do the stakeholders give the organization? (4) What kind of responsibility does the organization have towards the stakeholders? The answers lead to a characterization of the stakeholders, focusing on their potential to threaten and cooperate with the organization.

Pfeffer and Salancik present a further development of understanding contextual relations by introducing the resource dependence perspective (Pfeffer & Salancik, 1978). The main issue within this theory is therefore to analyze the organization's dependency on resources and provide recommendations for reducing this dependency. Secondly, the objective for the organization is to be an attractive partner by controlling resources that are critical for other organizations.

A fourth approach for understanding the contextual relation of an enterprise is network theory. This approach expands the understanding presented in principal agent theory. In a network analysis, these relationships are in focus because they are ascribed to have great influence on organizations' strategizing. The structure of a network can be characterized

along the following dimensions: (1) degree of continuity, (2) degree of complexity (concerns the number of people from different organizational levels involved in the relation), (3) degree of symmetry (concerns a comparison of resources invested), and (4) degree of formalization. The processes in the network can be characterized along dimensions concerning: (a) degree of mutual adaptation, (b) degree of cooperation, (c) the type of foundation (personal trust) and (d) the degree of routine.

4.2. Systemic Contextual Theory

In line with stakeholder theory and resource dependency theory, institutional theory argues that it is important for an organization to gain acceptability and legitimacy in the eyes of the stakeholders. Organizations cannot only rely on economic performance; they must also adapt to the rules, code of conduct, and norms in their institutional environment. The theory operates with three ways of affecting behavior: (1) through regulative structures (*i.e.* forcing individuals and groups to follow established rules), (2) through normative structures (*i.e.* common norms and values guiding behavior), and (3) cognitive structures (*i.e.* interpretative schemes and worldviews determining choice).

Using the institutional approach to organizations, four institutions are especially relevant to include. The first is the state and other political institutions that can control the organization through legislation. Second, professions can influence strategizing through the profession's ethical rules. The same may apply to other organizations, *e.g.* industrial organizations and research institutes. Finally, culture (*i.e.* basic, generally accepted norms and values) generally has to be respected and followed. DiMaggio and Powell have reflected on the institutional approach and described the terms organizational fields and isomorphism (DiMaggio & Powell, 1991). The structure of the organizational field has to be defined on the basis of empirical investigation and cannot be determined a priori. DiMaggio and Powell (1991) describe isomorphism as *„a constraining process that forces one unit in a population to resemble other units that face the same set of environment conditions"* (DiMaggio & Powell, 1991).

There are two different driving forces for isomorphism. The first is competition and profit maximization; the other is the striving for legitimacy in the organizational field. The cited authors identify three types of institutional isomorphism: coercive isomorphism, mimetic isomorphism, and normative isomorphism. Coercive isomorphism partly results from other organizations' formal or informal use of their political power, and partly from organizations' need for legitimacy through observing the legitimate demands existing in society. Mimetic isomorphism is seen as a standard response to uncertainty where organizations imitate other organizations in solving problems in order

to minimize the cost of finding a usable solution. Finally, normative isomorphism stems from professionalization and is understood as a collective effort by members of an occupation to establish a cognitive base for the conditions and method of their work. If a strategy of adaptation is difficult due to a discrepancy between profit maximization and legitimacy, this could be handled through decoupling what is said and what is actually done.

In a study of the Romanian implementation of the demand for risk assessment in the European Framework directive, we found out that coercive isomorphism offers a strong theoretical position for explaining the present results (Băbuţ & Moraru, 2009). Most enterprises do not internalize the basic content and idea behind risk assessment. They do what they are told to do in official guidelines and do not take a position on the actual demands formulated in the law, *i.e.* coercive isomorphism.

Consequently, only limited effects of preventive activities can be reported. Presently, in large and medium-sized companies in Romania, there is a weak tendency toward professionalization of the working environment field (Moraru & Băbuţ, 2009; Moraru & Băbuţ, 2010). The employment of professional safety personnel has become a normal procedure for larger companies. In cooperation with universities, labor market organizations, and The Labor Inspectorate, safety personnel may be able to develop a mutually recognized practice whereby a normative isomorphism could be established. Over time, this could lead to another outcome of the preventive activities, depending on the competencies among safety professionals for organizational manoeuvring.

5. Conclusion

The contextual theories offer an understanding of how the judgment made according to Rasmussen and Svedung (2000) can be understood. Table 1 gives an overview.

The use of the theories that a theoretical substantiation of well-known, every-day experiences can enlarge ones understanding of such experiences by pinpointing common features and distinctive differences at a more generalized level. Therefore, the approach has to be developed in more directions. First, the theoretical field has to be searched for supplementary theories; and secondly, the possibilities of combining these rather fragmented theories into a shared conceptual framework have to be investigated. But the primary task is to investigate the potentials for developing this theoretical approach from a post-ante, descriptive, analytical tool to a conceptual framework for the strategizing of actors and agencies concerned with accident prevention. The authors are presently pursuing these aims by analyzing present Romanian activities in accident prevention.

Table 1

A Framework of Theories Presented to Understand Accident
Prevention in Enterprises Contextually

Level		Traditional approach		New approach	
		Name	Characteristics	Name	Characteristics
Understanding contextual relations	Relational theories — Systemic			Institutional Theory	Legitimacy through isomorphism
				Network Theory	Developing trust-based relations with organizations in the network
				Stakeholder theory	Handling the relations to many different stakeholders to assure continuous support
				Principal-agent theory	Contract as primary regulatory mechanism
	Regulatory theory	Detailed specification	Specified demands towards structural arrangements	Reflexive regulation	Specified goals and procedures on a more general level
		Legalistic implementation	A series of phases to pass to implement a political program	Winters' model of implementation	Social factors affecting the implementation of a political program
Understanding processes in enterprises		Rational models of decision making	Optimizing goals by fully informed evaluation of alternatives	Enterprises as loosely coupled subsystems	Coalitions between individuals and groups
		Bounded rationality	Satisfying expectations by searching for an acceptable solution	Garbage can decision making	Anarchistic linkage between problems and solutions dependent on access and resources
				Evolutionary theory	Embedded routines determines outcome
Enterprise activities concerning accident prevention					

REFERENCES

Băbuţ G.B., Moraru R.I., *Risk Assessment - The Transposition of the 89/391/EEC Directive Requirements Into European Union State Member's Legislations* (transl. from Romanian), Universitas Publishing House, Petroşani, 2009.

Broberg O., *Integrating Ergonomics Into the Product Development Process*. Internat. J. of Industrial Ergonomics, *19*, 317-327 (1997).

Cohen M.D., March J.G., Olsen J.P., *A Garbage Can Model of Organizational Choice*. Administrative Science Quarterly **17** (*1*), 1-26 (1972).

DiMaggio P.J., Powell W.W., *The Iron Cage Revisited: Institutional Isomorphism and Collective Rationality in Organizational Fields.* In: Powell, W.W., DiMaggio, P.J. (Eds.), The New Instit. Org. Analysis, The Univ. of Chicago Press, 63-82 (1991).

Hale A.R., Glendon A.I., *Individual Behaviour in the Control of Danger.* Elsevier Science Publisher BV, Amsterdam, 1987.

Moraru R.I, Băbuţ G.B., *Risk Management: Global Approach - Concepts, Principles and Structure.* Universitas Publishing House, Petroşani, 2009.

Moraru R.I., Băbuţ G.B, Cioca L.I., *Risk Interpretation and Decision Making in Occupational Risk Management.* Annals of the University of Petroşani - Mining Engng, Univ. Publishing House, Petroşani, **10** (**XXXVII**), 223-230 (2009).

Moraru R.I., Băbuţ G.B, *Participatory Risk Assessment and Management: A Practical Guide.* (transl. from Romanian)*,* Focus Publishing House, Petroşani, 2010.

Pfeffer J., Salancik, G.R., *The External Control of Organizations: A Resource Dependence Perspective.* Harper & Row, New York, 1978.

Rasmussen J., *Risk management in a dynamic society: A modeling problem.* Safety Science, **27**, *2-3*, 183-213 (1997).

Rasmussen J., Svedung I., *Proactive Risk Management in a Dynamic Society.* Readdningsverket, Karlstad, 11, 2000.

Ravn J., Nygaard C., Kristensen P.H., *Strategen Tegner Kontrakter-Agentteori (The Strategist Draws up Contracts-Agency Theory).* In: Nygaard C. (Ed.), Strategizing - Kontekstuel Virksomhedsteori. Samfundslitteratur, Copenhagen, 80-99 (2001).

Winter S., *Integrating Implementation Research.*In: Palumbo, D.J., Calista, D.J. (Eds.), Implement. and the Policy Process, Greenwood Press, New York, 19-39 (1990).

PROPUNERE PRIVIND O ABORDARE TEORETICĂ CONTEXTUALĂ A PREVENIRII ACCIDENTELOR

(Rezumat)

În cercetarea preventivă, orientată spre acţiune, a accidentelor de muncă, condiţiile interne ale întreprinderii sunt de obicei în centrul atenţiei, rezultând numeroase metode şi recomandări privind evitarea sau reducerea numărului de evenimente nedorite. Influenţa contextului asupra activităţilor de prevenire derulate într-o întreprindere sunt rareori incluse în cercetarea apriori riscurilor profesionale. Recentul standard ISO 31000:2009, privind principiile şi liniile directoare de implementare a managementului riscurilor, impune includerea contextului extern şi a celui intern în procesul de management şi în modelele de prevenire a accidentelor de muncă. Lucrarea de faţă prezintă anumite teorii contextuale, atent selectate, în scopul stabilirii oportunităţii aplicării acestei categorii de teorii la elaborarea şi înţelegerea contextului. Lucrarea realizează o diferenţiere a teoriilor aplicabile pentru înţelegerea corectă a relaţiilor dintre întreprindere şi instituţiile de reglementare legislativă şi control pe de o parte, şi teoriile care facilitează percepţia relaţiei dintre întreprindere şi contextul extern, pe de altă parte. Ultima grupă de teorii prezentate îşi găseşte punctul de pornire într-o înţelegere organizaţională diferită de înţelegerea clasică, raţionalistă, a proceselor organizaţionale. Se concluzionează că teoriile contextuale deschid noi căi de înţelegere

a rolului relaţiilor contextuale în prevenirea accidentelor de muncă, dar şi că este necesară o investigare mai detaliată a potenţialului de a transpune asemenea teorii în modele şi soluţii cu caracter practic, orientate spre acţiune.

EXPERIMENTAL RESEARCHES REGARDING THE WEAR BEHAVIOR OF DIFFERENT LAYERS OF NANOFILL COMPOSITE MATERIAL USED IN DIRECT DENTAL RESTORATIONS

BY

RALUCA ELENA BACIU[1]*, IRINA GRĂDINARU[1], DANIELA CALAMAZ[1] and MARIA BACIU[2]

[1] “Gr.T.Popa” University of Medicine and Pharmacy of Iaşi,
Department of Dental Materials
[2] “Gheorghe Asachi” Technical University of Iaşi,
Faculty of Material Science and Engineering

Abstract. Nanofill composite diacrylic resins have been promoted in recent years to improve the esthetic and mechanical resistance characteristics. This study aimed at evaluating the biomechanical behavior in case of Premise nanofill composite material (Kerr, Orange, CA, USA). The experimental researches followed the abrasive wear behavior for the photopolymerisable composite resins Premise enamel, Premise dentine, Premise translucent and Premise packable. From the analysis of the experimental data, one may notice that Premise enamel material exhibits the smallest values of mass loss being the material with the best behavior to abrasive wear.

Key words: nanofill composite material, wear resistance, mass loss.

---

* Corresponding author e-mail: maria_baciu2004@yahoo.co.uk

1. Introduction

The patients' esthetic exigencies from the last decades have led to the increase of the demands for nonmetal restorations, both direct and indirect. In parallel, the intense efforts of the companies producing composite restorative materials have led to the elaboration of a new generation more and more capable to meet the esthetic and structural resistance requirements (Terry, 2004; http://kerrdental.com.).

The nanofill composite diacrylic resins have been launched in recent years with the intention and pretention to satisfy the universal use requirements for all types of cavities and a series of direct esthetic rehabilitations. Their particularity consists in the presence of some nanofill particles between 0.005-0.01 m (Venhoven *et al*., 1996) that are below the wave length of visible light (0.02-2 m), and do not produce the dispersion or absorption of light (Mitra *et al*., 2003). The filling nanoparticles will physically behave more like a liquid than as a solid allowing for the significant increase of the filling levels in the organic matrix, without the unwanted modification of the maneuverability characteristics. Besides the improvement of the mechanical properties, we obtained the accurate colour and translucidity for the dentine, enamel and incisal layers, a remarkable chameleonic effect and surface polish comparable to the natural enamel and stable in time (Terry, 2004; http://kerrdental.com.).

This study aimed at evaluating the biomechanical behavior in case of Premise nanofill composite material.

2. Material and Method

The experimental researches followed the abrasive wear behavior for Premise (Kerr, Orange, CA, USA) photopolymerisable composite resin available in the variants: enamel, dentine, translucent and packable (amalgam replacer) (Table 1).

Table 1
Photopolymerisable Composite Resins Under Study

Dental material	Producer	Representative class	Form f presentation	Code	Indications
Premise	Kerr, Orange, CA, USA	photopolymerisable RDC	Premise packable	PP	-restoration of cavities from class I, II, III, IV, V, and the atypical ones; -dental veneers; -closing diaereses and diastemata.
			Premise enamel	PE	
			Premise dentine	PD	
			Premise translucent	PT	

The Ø=7 mm specimens were made in the Dental Material lab from the Faculty of Medicine and Pharmacy, "Gr. T. Popa" UMF of Iaşi, in accordance with producers' recommendations.

The photopolymerisable composites were put into test tubes in 2 mm successive layers, each layer being polymerized according to the producer's indications by means of a Demetron LC photopolymerisation lamp from Kerr (Table 2).

To obtain the precise diameter of specimens, it was necessary to reduce their size by means of a shaping machine and a mill (Fig.1).

Table 2
Polymerisaiton Times

Code	Material under study	Polymerization time
PP	Premise packable	40 sec.
PE	Premise enamel	20 sec.
PD	Premise dentine	40sec.
PT	Premise translucent	20 sec.

Fig. 1 – Processing the specimens by means
of the shaping machine and mill.

The wear tests were run at the Department for Material Engineering and Industrial Security from the Faculty of Material Science and Engineering, "Gheorghe Asachi" Technical University of Iaşi.

The wear behavior was studied in the specific conditions of a dry friction situation at the level of the frontal surfaces of specimens.

The experimental researches were carried out during a slipping rotation movement having a continuous character, the surfaces in contact being plane (Fig. 3) and having a cover coefficient: $0 < K_{ac} = 0.232 < 0.5$.

Measurements aimed at determining the mass wear, namely the absolute variation (Δm_a) and relative variation (Δm_r) of specimens' mass, sizes that may be found in the calculations of the two specific indicators of the wear resistance. Determinations were made for 4 different time intervals to which different friction lengths correspond (Table 3).

Table 3
Time – Length of the Friction Layout Length Correspondence

Test time t, [min]	15	30	45	60
Friction length L_f, [m]	1500	3000	4500	6000

Mass wear was determined by weighing the specimens by means of an analytic balance before and after every determination, and so we evaluated the mass loss.

3. Results and Discussions

The first stage of experimental tests regarding the abrasive wear behavior consisted in the determination of the evolution of absolute mass losses (Δm_a) and relative mass losses (Δm_r), corresponding to different values of the friction layout length and the 30 N press force. The values of masses determined after every 1500 m of the friction layout length are given in Table 4.

Table 4
Mass Wear for Force F = 30 N

Friction layout length, m	Specimen mass, m [g] for F = 30 N			
	PP	PE	PD	PT
$L_0 = 0$	1.9078	1.8635	2.7459	2.6960
$L_1 = 1500$	1.8945	1.8410	2.7103	2.6600
$L_2 = 3000$	1.8355	1.7838	2.6081	2.5620
$L_3 = 4500$	1.6706	1.6557	2.4138	2.3846
$L_4 = 6000$	1.5422	1.5287	2.1692	2.1345

Based on these results, we calculated the absolute mass losses Δm_a (Table 5, Fig. 2) and relative mass losses Δm_r (Table 6, Fig. 3).
The absolute mass losses were calculated by means of the regard:

$$\Delta m_a = \left(m_{L_0} - m_{Li} \right), \; i = \overline{0,4} \tag{1}$$

Table 5
Absolute Mass Losses for F = 30 N

Friction layout length, m	Absolute mass losses, Δm_a [g] for F = 30 N			
	PP	PE	PD	PT
$L_1 = 1500$	0.0133	0.0225	0.0356	0.036
$L_2 = 3000$	0.0723	0.0797	0.1378	0.134
$L_3 = 4500$	0.2372	0.2078	0.3321	0.3114
$L_4 = 6000$	0.3656	0.3348	0.5767	0.5615
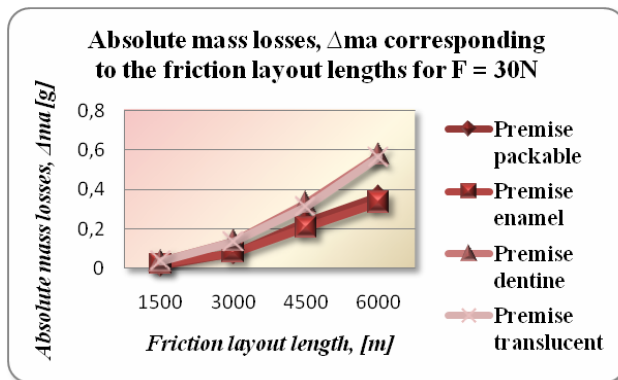
Fig. 2 − Comparative presentation of the absolute mass losses
corresponding to the friction layout length F=30 N.

The relative mass losses were calculated by means of the regard:

$$\Delta m_r = \frac{\Delta m}{m_{L0}} * 100 \,, [\%] \qquad (2)$$

Table 6
Relative Mass Losses for F = 30 N

Friction layout length, [m]	Relative mass losses, Δm_r [g] for F = 30 N			
	PP	PE	PD	PT
L_1 = 1500	0.6971	1.2074	1.2964	1.3353
L_2 = 3000	3.7897	4.2768	5.0183	4.9703
L_3 = 4500	12.4331	11.1510	12.0943	11.5504
L_4 = 6000	19.1634	17.9661	21.0022	20.8271
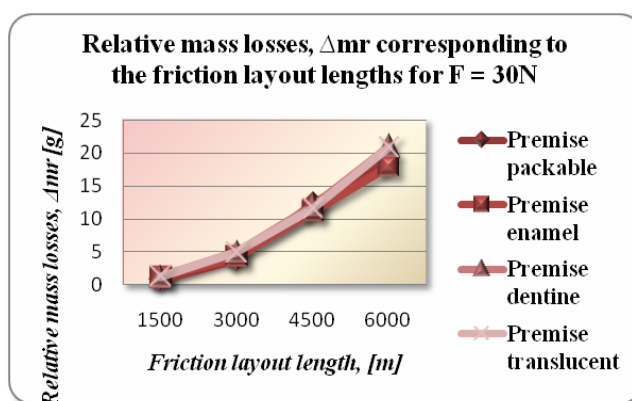
Fig. 3 − Comparative presentation of the relative mass
losses corresponding to the friction layout length F=30 N.

An indicator for the evaluation of the abrasive wear behavior was represented by the mass wear intensity I_m.

The regard for this value is:

$$I_m = \frac{\Delta m}{A_f * L_f}, \; [g/m^3] \tag{3}$$

where: A_f represents the area of the friction surface; for the specimens with 7 mm diameter it is $A_f = 3.848 * 10^{-5}$, $[g/m^3]$.

Knowing the values of mass losses Δm and friction layout length L_f, we determined the evolution of mass wear intensity for every dental material under analysis (Table 7, Fig. 4).

Table 7
Mass Wear Intensity for F = 30 N

Friction layout length, [m]	Mass wear intensity, I_m [g/m³] for F = 30 N			
	PP	PE	PD	PT
$L_1 = 1500$	0.23	0.38	0.61	0.62
$L_2 = 3000$	0.62	0.69	1.19	1.16
$L_3 = 4500$	1.36	1.2	1.91	1.79
$L_4 = 6000$	1.58	1.45	2.49	2.43
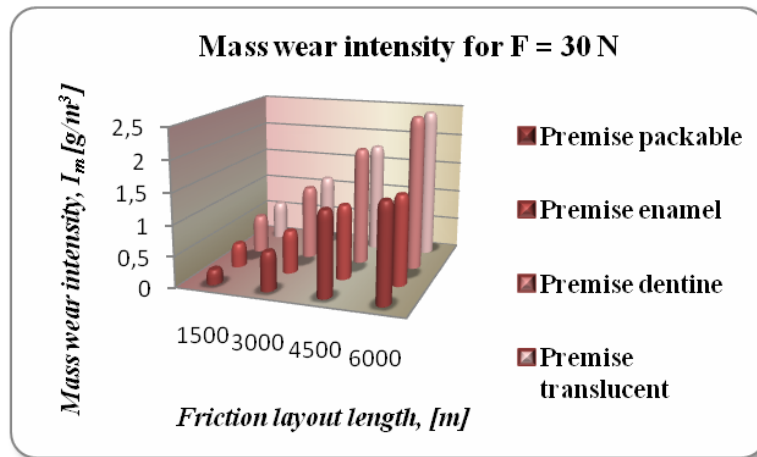
Fig. 4 – Comparative presentation of mass wear intensity for F = 30 N.

The mass wear speed was calculated by the formula: $V = \Delta_m / t$ (g/h), where t is the operation period, t=0.5 hours for $L_f = 3000$ m (Table 8, Fig. 5).

Table 8

Mass Wear Speed for F = 30 N

Lf, F=30N Material	1500	3000	4500	6000
Premise packable	0.0532	0.1446	0.3162	0.3656
Premise enamel	0.09	0.1594	0.277	0.3348
Premise dentine	0.1424	0.2756	0.4428	0.5767
Premise translucent	0.144	0.268	0.4152	0.5615
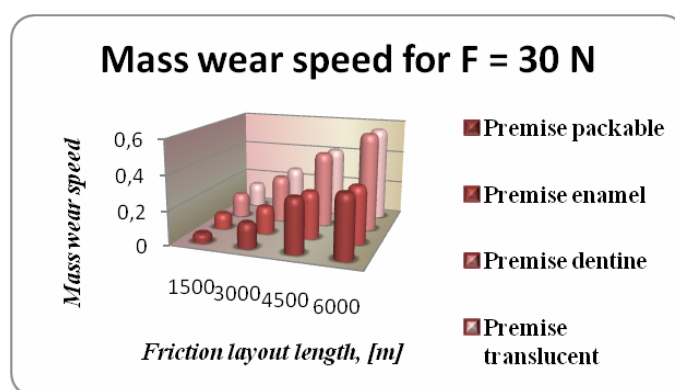
Fig. 5 – Comparative presentation of mass wear speed for F = 30 N.

4. Conclusion

From the analysis of the experimental data we notice that *Premise enamel* exhibits the lowest values of absolute mass loss when using the force of 30 N, values that are close to those of *Premise packable* composite. The behavior of *Premise packable* may be explained through the much higher concentration of inorganic filling that allows for an efficient condensation of the material in the prepared cavity.

The photopolymerisable composite *Premise dentine* has intermediate results in this test with higher values of mass losses than in the case of the other two materials discussed before, but also lower values as compared to the photopolymerisable composite *Premise translucent*. The latter exhibits the highest values of mass losses that are significantly higher as compared to all the others materials under study. That is why, the nanofill composites *Premise dentine* and *Premise translucent* are used as layers at the level of dentine and incisal area.

Following the study of mass wear intensity and speed, composites *Premise enamel* and *Premise packable* exhibit the lowest values, a fact proving their superior resistance.

For all the composite materials analysed, the substance loss increases with the getting over of the friction layout and the intensity of the force applied.

REFERENCES

[1]. Terry D.A., *Applications of Nanotechnology*. PPAD, **16**, *3*, 220-2222004.
[2]. ∗ ∗ http://kerrdental.com.
[3]. Venhoven B.A.M., de Gee A.J., Werner A., Davidson C.L., *Influence of Filler Parameters on the Mechanical Coherence of Dental Restorative Resin Composites*. Biomaterials, *17*, 735 – 740 (1996).
[4]. Mitra S.B., Wu D., Holmes B.N, *An Application of Nanotechnology in Advanced Dental Materials*. J. Am Dent Assoc, *134*, 1382–1390 (2003).

NU SE REGASESTE RESTUL BIBLIOGRAFIEI IN TEXT

[5]. Bratu D., *Materiale dentare în cabinetul stomatologic*. Editura Helicon, Timişoara, 1994.
[6]. Bratu D., *Materiale dentare: bazele fizico-chimice*. Editura Helicon, Timişoara, 1994.
[7]. Craig G.R., Powers M.J., *Restorative Dental Materials*. Ediţia a XIa, Editura Mosby, Inc, 212-215, 232-248, 249-251 (2002).
[8]. Pătraşcu I., *Materiale Dentare*. Editura Horanda Press, Bucureşti, 2002.

CERCETĂRI EXPERIMENTALE PRIVIND COMPORTAMENTUL LA UZARE AL DIFERITELOR STRATURI DE MATERIAL COMPOZIT CU NANOUMPLUTURĂ UTILIZATE ÎN RESTAURĂRILE DENTARE DIRECTE

(Rezumat)

Răşinile diacrilice compozite cu nanoumplutură au fost promovate în ultimii ani în scopul îmbunătăţirii caracteristicilor estetice şi de rezistenţă mecanică. Prezentul studiu a avut ca scop evaluarea comportamentului biomecanic în cazul materialului compozit cu nanoumplutură Premise (Kerr, Orange, CA, USA). Cercetările experimentale au urmărit comportamentul la uzare abrazivă în situaţia răşinilor compozite fotopolimerizabile *Premise enamel*, *Premise dentine*, *Premise translucent* şi *Premise packable*. Din analiza datelor experimentale se constată că materialul Premise enamel prezintă cele mai mici valori ale pierderii de masă, fiind materialul cu cea mai bună comportare la uzarea abrazivă.

QUALITY IMPROVEMENT OF CAST IRON BY DYNAMIC SOLIDIFICATION

BY

GELU BARBU[*] and ADRIAN ALEXANDRU

"Gheorghe Asachi" Technical University of Iaşi,
Department of Materials Science

Abstract. This work approaches the field of dynamically solidified cast iron, regarding the procurement of materials with improved structure, as well as its rupture particularities. They have moulded cast iron samples with nodular and lamellar graphite, under static and dynamic conditions. The vibration was performed on an installation performing horizontal circular vibrations. Polished samples and break sample were studied by electronic microscope. They have noticed the finishing of the granulation, the more uniform distribution of chemical elements as well as of graphite, as well as the alteration of the rupture mechanism. At non-vibrated samples the rupture dominantly takes place intercrystalline with time while for vibrated samples, it is transcrystalline. The vibration applied for the solidification of cast parts leads to a good cohesion between the grains in their structure.

Key words: vibrations, lamellar cast iron, nodular cast iron, SEM.

1. Overview

At the use of vibrations for obtaining parts made of different materials one can notice improvements of the properties, presented as well in

---

[*] Corresponding author e-mail: axa72us@yahoo.com

various specialty works.

There appear at vibration a series of physical processes like the action of impulse forces, cavitation phenomena, increase of undercooling degree, mass macroscopic transfer and change of the solid-liquid balance conditions.

The mechanisms of vibration on vibrated alloys are multiple. Nevertheless, the power of vibrations needs to be proper, as there is as well the possibility to appear, at large amplitudes of the vibratory movement, holes in the casted material as well as drops at the outside surface.

Vibrations have the effect to diminish the viscosity and the superficial pressure, but also by the dynamic effects it generates, there is a fluidity growth, albeit under vibration conditions the heat transfer is intensified, the total solidification time of the alloy diminishes.

One knows a series of technological effects of the vibration application to solidification: homogenisation and finishing of solidification structure, increase of cast material capacity, degassing the alloy, diminish internal pressure, reducing segregations, removing non-metal inclusions and increase of alloy flowing capacity, (Zhao *et al.*, 2004).

Vibration during solidification finishes the structure of non-metal materials, by finishing, obtaining as well the improvement of physical-mechanical features, being used in various fields: continuous casting, casting in mixture moulds and metallic moulds etc.

The research directions in the field of casting under the influence of vibration regards the procurement of the wanted effects under the conditions of optimally setting the parameters of the vibration process - frequency, amplitude, vibration time, vibration method and for setting the mechanisms of this influence.

2. Experimentations

They have analyzed the influence of vibrations on the structures obtained at grey cast iron solidification with lamellar and nodular graphite and elements distribution.

In order to perform vibrations they have used a device, which produces mechanical vibrations, through the agency of an eccentric driven by an electric engine. The vibrations are transmitted to a work bench rigidly fastened to the engine.

The vibratory bench supports on a frame bed through the agency of balls. The vibratory bench is fastened with elastic cables, allowing the performance of horizontal rotation movements.

Other installations, similar as working method, use a bench fastened

on metallic pillars, but takes a part of the energy of the system for the deformation of the pillars. The advantage of the used installation consists of using flexible cables.

The elaboration aggregate is furnace with black-lead crucible, with average frequency (8,000 Hz), capacity of which is of approx. 30 kg alloy.

They have elaborated two grey cast irons, one with lamellar graphite, another with nodular graphite, with the following chemical composition: 3.8% C; 2.9% Si; 0.6% Mn; 0.15%P; 0.04% S.

The load needed for elaborating the cast iron consisted of high purity cast iron (HCA) with the following chemical composition: 3.6...4.2% C; 1.75% Si; 0.75% Mg; 0.03 % P; 0.02% S.

After weighting, the load was introduced in the furnace and melted. 25 kg, high purity cast iron was introduced, a quantity restricted by the capacity of the crucible. In order to obtain the wanted chemical composition, they needed to improve the percentage of Si, for reaching a new concentration of 2.9% Si in the obtained cast iron, compared to 1.75% Si in the metal load.

Therefore, they used a hardening alloy of ferrosilicon - FeSi75, chemical composition of which is the following: 70...79% Si; 0.70% Mn; 0.4% Cr; 0.05% P; 0.04% S; 0.1% C; 2.5% Al. It was introduced in the metal bath in the moment of cast iron overheating, at a temperature of 1450°C.

In order to obtain the nodular graphite cast iron they have weighted a quantity of 1.5% modifier which was laid in the casting ladle.

They have used as modifier NODULIN 10 - 4, a ferroalloy with Mg and Mischmetall content (rare earths), with the following chemical composition: 10% Mg; 1.5% Mischmetall (FeSiCaMgCe); 42 % Si; 1.5%Al. At the evacuation in the ladle of the liquid metal which is at the temperature of 1450°C, it reacted with the modifier. The two mould parts were made of mixture of core, obtained according to the following recipes: dry sand with water-glass in proportion of 6%.

They have moulded, gravitationally, samples in shapes on the vibrating device and statically solidified.

3. Results

The shape and rupture distribution of metal grains can explain the method the vibrations applied to solidification influence the mechanism of the structure forming.

Figs. 1 and 2 present the distribution of silicon and manganese on the section of moulded samples of nodular and lamellar graphite cast iron.

vibrating nodular cast iron   non-vibrating nodular cast iron
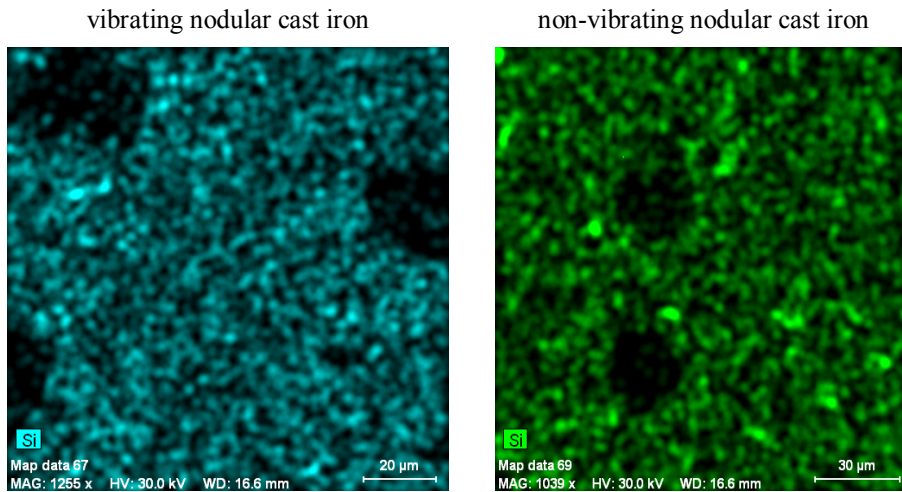
Fig. 1 – Distribution of silicon on the section of nodular graphite cast iron samples,
electronic microscopy.

vibrating lamellar cast iron   non-vibrating lamellar cast iron
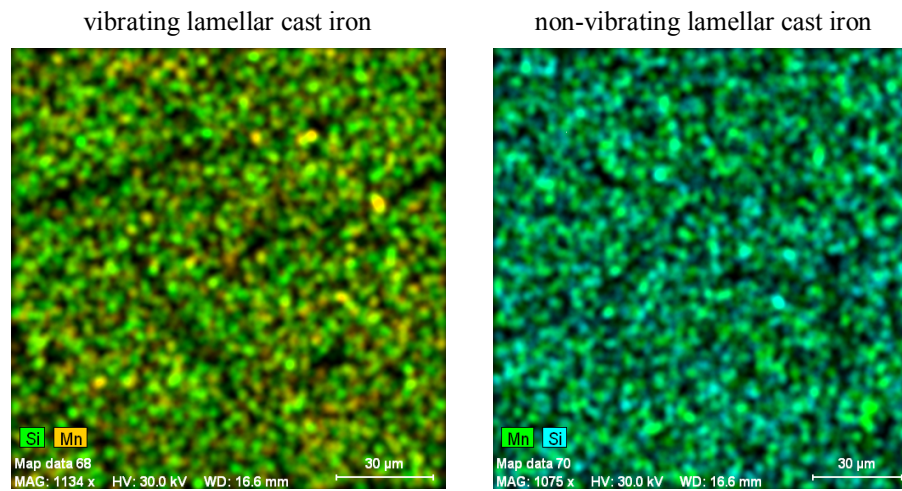
Fig. 2 – Distribution of silicon on the section of lamellar graphite cast iron samples,
electronic microscopy.

Fig. 3 presents the distribution of nodular graphite on the polished
surfaces of the samples, and Fig. 4 presents the distribution of lamellar
graphite.

Fig. 6 presents the distribution of nodular graphite on polished
surfaces of samples and Fig. 7 presents the distribution of graphite at lamellar
graphite samples.
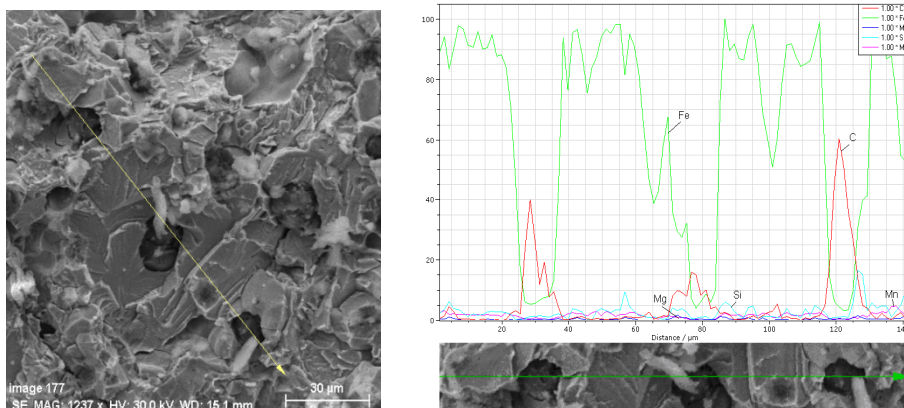
a − vibrating nodular cast iron
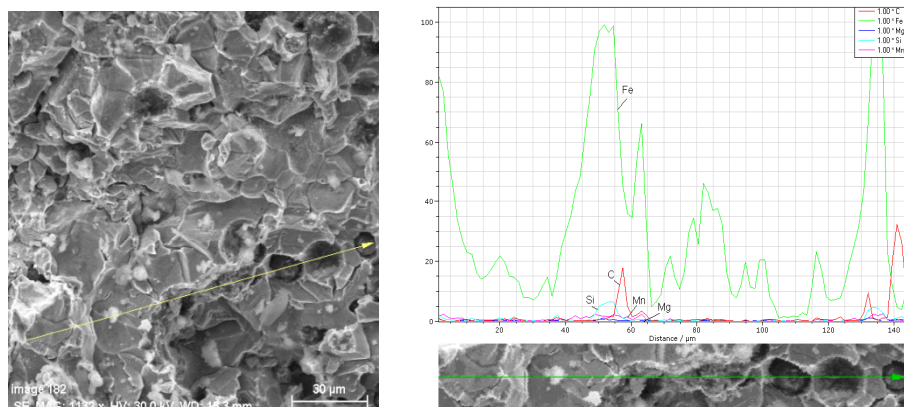
b − non-vibrating nodular cast iron

Fig. 3 − Rupture microstructure of nodular graphite cast iron, electronic microscopy.
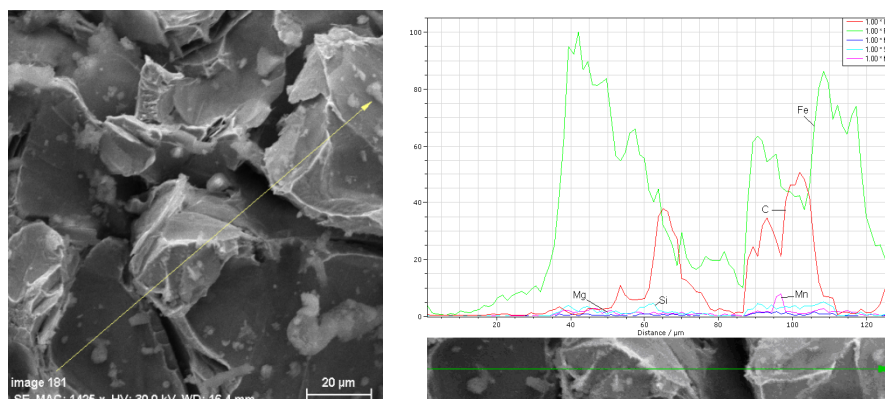
a − vibrating lamellar cast iron
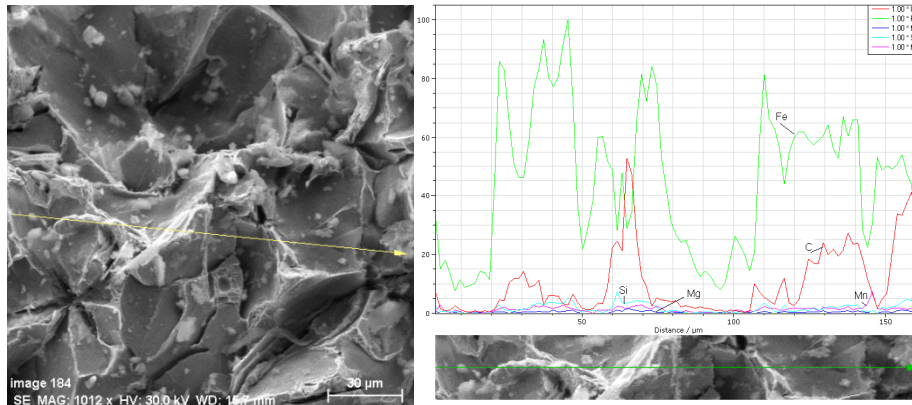
b – non-vibrating lamellar cast iron

Fig. 4 – Rupture microstructure of gray cast iron with lamellar graphite, electronic microscopy.

The study of microstructures leads to a series of observations:

- structure of cast irons has a higher finishing degree in case of vibrated cast irons compared to non-vibrated cast iron;

- the graphite is distributed more uniformly in case of cast iron under vibration than in case of static cast iron;

- for the nodular graphite cast iron we notice that the graphite nodules are of smaller size and with a shape close to sphere.
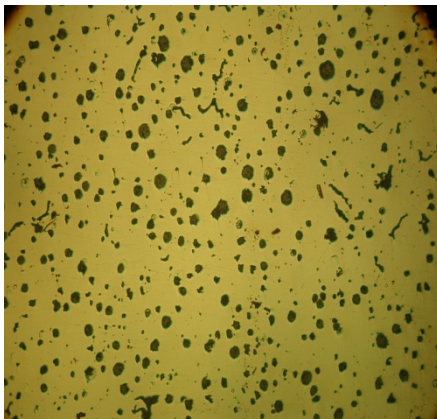
vibrating nodular cast iron   non-vibrating nodular cast iron
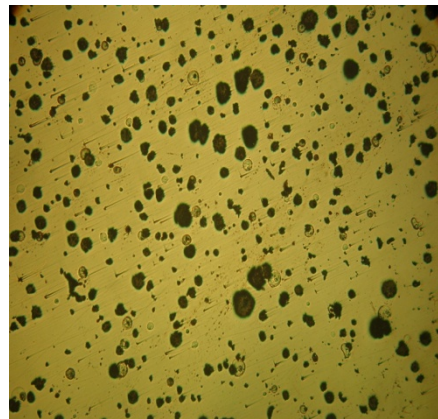
Fig. 6 – Distribution of nodular graphite on the polished surfaces of samples, optical microscopy, x 70.

vibrating lamellar cast iron   non-vibrating lamellar cast iron
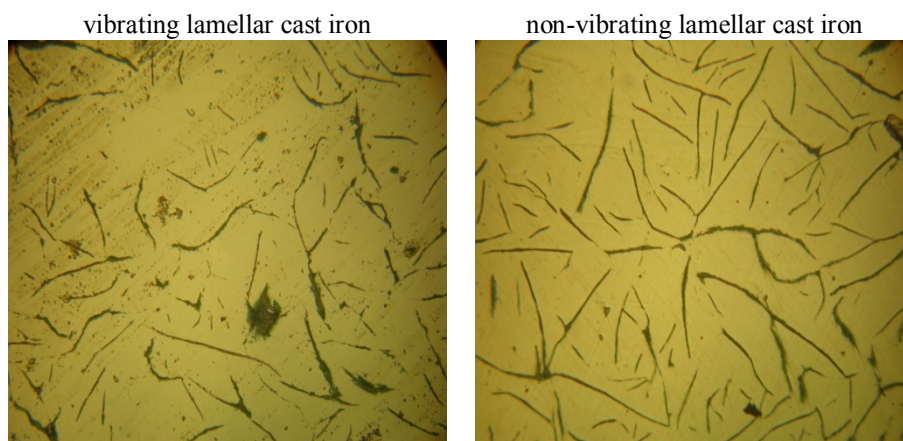
Fig. 7 − Distribution of lamellar graphite on the polished surfaces of samples, optical microscopy, x120.

Considering the rupture shape and aspect of samples we notice a change of the rupture mechanism, passing from intercrystalline rupture to transcrystalline rupture in case of vibrated samples. As well, the size of the rupture plans is different in case of the two types of cast iron: at vibrated cast iron, the cleavage surfaces are smaller, due to a finer graining.

4. Conclusion

The size of grains differs at the two types of cast iron, as one can notice that for vibrated cast iron they are finer and more uniformly dispersed;

Solidified cast irons under the influence of vibrations have mechanical properties superior to statically solidified cast irons, due to the homogenous structure and to uniform distribution of the graphite in the metal matrix.

The lamellar graphite is better contoured at the vibrated cast iron with lamellar graphite;

One can notice the change of the rupture mechanism from the intercrystalline rupture to transcrystalline rupture.

NU SE REGASESC IN TEXT
REFERENCES

[1]. Barbu G., *Solidificarea aliajelor sub influenta vibratiilor*. Ed. Vasiliana'98, Iaşi 2003.
[2]. Barbu G., Cojocaru V., Carcea I., *Instalaţie de turnare cu vibrare*. Brevet invenţie România, nr. 108.934 Bl, 1994.

[3]. Zhao Y.G., Liang Y.H., Qin W., Jiang Q.C., *Effect of mechanical Vibration on the Microstructure, Impact Toughness and Thermal Fatigue Behavior of Cast Hot Working Die Steel*. ISIJ International, **44**, *7*, 1167-1172 (2004).

ÎMBUNĂTĂŢIREA CALITĂŢII FONTEI PRIN SOLIDIFICARE DINAMICĂ

(Rezumat)

Această lucrare abordează domeniul fontelor solidificate dinamic, referindu-se la obţinerea unor materiale cu structura îmbunătăţită, cât şi particularităţile ce apar la rupere. S-au turnat epruvete din fontă cu grafit nodular şi lamelar, în condiţii statice şi dinamice. Vibrarea s-a realizat pe o instalaţie ce realizează vibraţii circular orizontale. Probe lustruite cât şi probe în ruptură au fost studiate cu microscopul electronic. S-a observat finisarea granulaţiei, repartizarea mai uniformă a elementelor chimice cât şi a grafitului, precum şi modificarea mecanismului ruperii. La epruvetele nevibrate ruperea are loc preponderent intercristalin în timp ce la probele vibrate este transcristalină. Vibrarea aplicată la solidificarea pieselor turnate conduce la o bună coeziune între grăunţii din structura acestora.

MECHANICAL PROPERTIES OF SOME Ti-HA BASED FUNCTIONALY GRADED MATERIALS

BY

**GABRIEL BATIN[∗], CĂTĂLIN POPA, LIVIU BRÂNDUŞAN
and IOAN VIDA-SIMITI**

Technical University of Cluj-Napoca,
Faculty of Materials and Environmental Engineering

Abstract. Functionally graded materials based on titanium and hydroxyapatites were produced via a powder metallurgy route. Samples with the following composition were produced: Ti+10% HA, (Ti+5% HA)+(Ti+10% HA) and Ti+(Ti+5% HA)+(Ti+10% HA). Vickers microhardness was tested on polish surfaces under a load of 196 N. Elastic modulus and compresive strength were determined using a Galdabini Sun5 universal testing machine. The Vickers microhardness increases with the content of hydroxyapatite.

Key words: biomaterials, titanium, hydroxyapatite, functionally graded materials, microhardness, Young modulus.

1. Introduction

To create a biomaterial simulating the structure and biological characters of natural bone is a priority for biomaterials researchers (Aho *et al*., 2004; Babini & Tampieri, 2004). The materials for hard tissue replacement need to satisfy in the same time some conditions: biocompatibility,

---

[∗] Corresponding author e-mail: Gabriel.Batin@stm.utcluj.ro

osteoconductivity, adequate strength and corrosion resistance. A bulk material with a single composition and a uniform structure does not complete all these requirements simultaneously this is why functionally graded materials based on titanium and hydroxyapatite are proposed for use in this study.

Hydroxyapatite (HA) is the main mineral constituent of the bone. Synthetic HA shows an excellent biocompatibility with hard tissue and muscle tissue. It seems to be the most suitable material for bone replacement, but it can't be used for heavy load-bearing applications due to its low mechanical properties (Aho *et al.*, 2004; Cheling *et al.*, 1999).

Titanium represents an attractive material for endosseus implants because of the high resistance against corrosion and high resistance/weight ratio with biocompatibility (Thieme *et al.*, 2001; Watari *et al.*, 2004; Oliveira *et al.*, 2002).

The Young's moduli of metallic materials used for bone replacement range from ~110 GPa to ~210 GPa, and is much higher than the modulus of human cancellous bone or compact bone (see Table 1). This large stiffness mismatch between bulk metallic implant and the surrounding human bone produce stress-shielding and can induce implant loosening) (Thieme *et al.*, 2001; Greiner *et al.*, 2005).

Table 1
Values of Young Modulus for Human Bone and Other Materials used for Implants
(*Thieme et al., 2001; Chu Chengling et al.,1999*)

Material	Human bone		Stainless steel	Co alloys	Ti and Ti based alloys	Hydroxyapatite
	cortical	cancellous				
E [GPa]	12-17	< 3	~ 190	~ 210	~ 110	~ 117

The decreasing of stiffness and thus the stress-shielding effect can be achieved by creating porous implants. An open pore, fully interconnected geometry in a highly porous structure will allow bone in-growth and an accurate cell distribution throughout the porous structure. This will facilitate the neurovascularization of the structure from the surrounding tissue (Salgado *et al.*, 2004).

2. Materials and Methods

The raw materials were high purity titanium powder obtained through hydriding - milling - dehydriding and hydroxyapatite powder. The hydroxyapatite powder was obtained through a sol-gel method using $Ca(NO_3)_2$ and $(NH_4)_2HPO_4$ as precursor reagents. Its Ca/P ratio was 1,67. Samples with the following composition were produced: Ti + (Ti + 10% HA),

(Ti + 5% HA) + (Ti + 10% HA) and Ti + (Ti + 5% HA) + (Ti + 10% HA). After mixing and die-compaction (400 MPa), samples were sintered in vacuum (0,01 Pa) at 1160°C for two hours.

Compression and microhardness tests were performed to determine the mechanical properties of the samples.

3. Results and Discussions

Compression is one of the most important stresses that occur in bones. Compressive strength was determined using a Galdabini Sun5 universal testing machine.

a

b

c
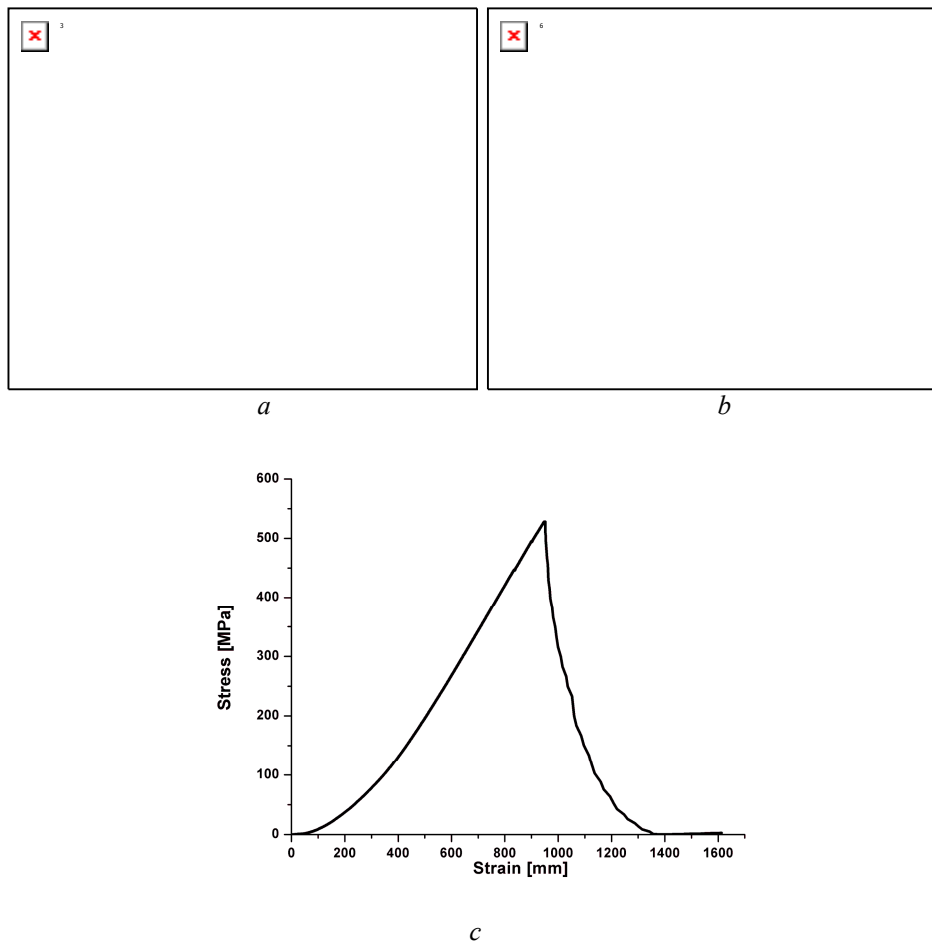
Fig. 1 − Compression test results: *a*) Ti+(Ti+10%HA),
b) (Ti+5%HA)+(Ti+10%HA), *c*) Ti+(Ti+5%HA)+(Ti+10%HA).

It can be observed that while the content of hydroxyapatite increases, the compression strength decreases. Poor mechanical strength of hydroxyapatite explain this behavior. Best results were obtained for 3 layer samples, about 528 MPa. The sample with the composition (Ti+5%HA)+(Ti+10%HA) presents an inflexion point around 132 MPa. We consider the failure of sample at this point, even the complete destruction had place at a higher value. At 132 MPa appears the first crack, but under the load a rearregement of material occure.

Values obtained are higher then in the human bones – about 170 MPa (Zioupos *et al*., 2000). Young modulus was assessed from the tangent to the linear region of the compression curve.

As the content of active phase (hydroxyaptite) increases, the Young modulus decreases. This can be explained by the partial decomposition of hydroxyapatite and the formation of some compounds based on calcium, as we shown in our previous study (Popa *et al*., 2005).

Table 2
Young Modulus

Sample	E [GPa]
Ti+(Ti+10%HA)	57
(Ti+5%HA)+(Ti+10%HA)	48
Ti+(Ti+5%HA)+(Ti+10%HA)	63

Layer's thickness of samples was too small to determine the macrohardness, so we decided to evaluate the microharness. Vickers microhardness was determinate on polish surfaces under a load of 196 N, using Neophot 2. Nine values were measured on each sample (Fig. 2).
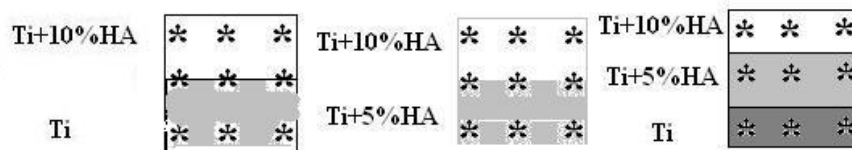
Fig. 2 – Places of measurements for Vickers microhardness test.

The results of the test are shown in Table 3.

A higher content of active phase (HA) leads to a high value of microhardness. There are some differences between the values for the same content of hydroxyapatite because of the inhomogeneities of the layers (being a two phases layer, the same content of one phase can be different distributed) and by the diffusion of hydroxyapatite.

Table 3

Vickers Microhardness Results

Sample	Layer	$MH_{0,02}$
Ti+(Ti+10%HA)	Ti+10%HA	1788
	Inteface between layers	1547
	Ti	1295
(Ti+5%HA)+(Ti+10%HA)	Ti+10%HA	110 0
	Inteface between layers	963
	Ti+5%HA	756
Ti+(Ti+5%HA)+(Ti+10%HA)	Ti+10%HA	1323
	Ti+5%HA	929
	Ti	795

Values obtained are higher than reported in literature for human bone (~478 MPa) (Wesley *et al.*, 2007).

4. Conclusion

Functionally graded materials based on titanium and hydroxyapatite were obtained via a powder metallurgy route.

Values obtained are higher than of human bone, but much lower that of bulk materials.

As the content of hidroxyapatite increases, the young modulus and the compression strength decrease.

A higher content of hydroxyapatite leads to the increase of Vickers microhardness.

REFERENCES

Aho A.J., Hautamäki M*.,* Mattila R., Alander P., Strandberg N., Rekola J., Gunn J., Lasila L.V.J., Vallittu P.K., *Surface Porous Fiber-Reinforced Composite Bulk Bone Substitute. In Vitro Studies and Vivo Evaluation in Segment Defect.* Cell and Tissue Banking, *5*, 213-221 (2004).

Babini G.N., Tampieri A., *Towards Biologically Inspired Materials.* British Ceramics Transactions*, 103*, *3*, 101-109 (2004).

Cheling C., Jingchuan C., Zhongda Y., Shidong W., *Hydroxyapatite-Ti Functionally Graded Biomaterials Fabricated by Powder Metallurgy.* Materials Science and Engineering A*, 271*, 95-100 (1999).

Thieme M., Wieters K.-P., Bergner F., Schrnweber D., Worch H., Ndop J., Kim T.J., Grill W., *Titanium Powder Sintering for Preparation of a Porous Functionally Graded Material Destined for Orthopaedic Implants.* Journal of Materials Science: Materials in Medicine, **12**, 225-231 (2001).

Watari F., Yokoyama A., Omori M., Hirai T., Kondo H., Uo M., Kawasaki T., *Biocompatibility of Materials and Development to Functionally Graded Implant for Bio-Medical Application.* Composite Science and technology, **64**, 893-908 (2004).

Oliveira M.V., Pereira L.C., Cairo C.A.A., *Porous Structure Characterization in Titanium Coatings for Implants.* Materials Research, **5**, *3*, 269-273 (2002).

Greiner C., Oppenheimer S.M., Dunand D.C., *High Strength, Low Stiffness, Porous NiTi with Superelastic Properties*, Acta Biomaterialia, **1**, 705-716 (2005).

Chu Chengling, Zhu Jingchuan, Yin Zhongda, *Wang Shidong, Hydroxyapatite-Ti Functionally Graded Biomaterial Fabricated by Powder Metallurgy.* Materials Science & Engineering **A**, *271*, 95-100 (1999).

Salgado A.J., Coutinho Olga P., Reis R.L., *Bone Tissue Engineering: State of the Art and Future Trends.* Macromolecular Bioscience, **4**, 743-765 (2004).

Zioupos P., Cris W. Smith, Yuehuei H. An, Factors *Affecting Mechanical Properties of Bone, in Mechanical Testing of Bone and the Bone-Implant Interface Editred* by Yuehuei H. An and Robert A. Draughn, CRC Press, 65-87 (2000).

Popa C., Şimon V., Vida-Simiti I., Batin G., Cândea V., Şimon S., *Titanium – Hydroxyapatite Porous Structures for Endosseous Applications*, J. of Materials Science: Materials in Medicine **16**, 1165 – 1171 (2005).

Wesley M. Johnson, Andrew J. Rapoff, Microidentation in bone: *Hardness Variation with Five Independent Variables.* J. of Materials Science: Materials in Medicine, **18**, 591-597 (2007).

PROPRIETĂŢILE MECANICE ALE UNOR MATERIALE CU GRADIENT
FUNCŢIONAL PE BAZĂ DE Ti-HA

(Rezumat)

Au fost realizate probe cu gradient funcţional pe bază de titan şi hidroxiapatită. Au fost determinate rezistenţa mecanică la compresiune – fiind una din principalele solicitări la care sunt supuse oasele, microduritatea Vickers şi modulul de elasticitate la compresiune. Rezistenţa mecanică la compresuine scade odată cu creşterea conţinutului de hidoxiapatită; acest lucru fiind pus pe seama rezistenţei mecanice scăzute a acesteia. Acelaşi comportament este observat şi în cazul modulului de elasticitate la compresiune. Creşterea conţinutului de hidroxiapatită duce la valori ridicate ale microdurităţii.

PREPARATION OF IRON OXIDE POWDERS FROM CHEMICAL SOLUTION

BY

MEDINA – NATALIA BATIN* and VIOLETA POPESCU

Technical University of Cluj - Napoca,

Abstract. The obtaing of hematite from precursor powders dissolved in aqueous solution is reported in the present work. FeOOH powders obtained from $FeCl_2$ in presence of urea, were treated in an oven at $500^{\circ}C$, for 4 hours. After the thermal treatment a reddish brown powder containig α-Fe_2O_3 has been obtained. X-ray diffraction (XRD) and UV-VIS spectrometry analysis were performed in order to study the structural and optical properties of the powders.

Key words: α-Fe_2O_3, hematite, XRD, optical properties, thermal treatment.

1. Introduction

Iron oxide particles of different shapes and dimensions have attracted the interest of the researchers from different fields. Due to their physico-chemical, optical, magnetic and electrical properties, iron oxide can be used in a wide range of applications like magnetic storage media (Sarangi *et al*., 2009), sensors (Sarangi *et al*., 2009; Zhang *et al*., 2009; Jin *et al*., 2010), catalysts (Liu *et al*., 2007; Guo *et al*., 2010), clinical diagnosis and treatment (Sarangi *et al*., 2008; Zhong *et al*., 2006). Iron oxide can also be successfully used as a pigment (Pailhé *et al*., 2008), in lithium ion batteries (Li *et al*., 2008) or for photoelectrochemical generation of hydrogen (Satsangi *et* al., 2008).

---

* Corresponding author e-mail: medina.batin@yahoo.com

Due to its band gap (Eg ~ 2.2 eV) iron oxide is a promising material for photocatalytic application, collecting up to 40% of the solar spectrum energy (Zhang *et al.*, 2010).

The preparation of iron oxide attracted a lot of interest, so various methods (chemical and physical) have been developed.

Dar and collaborators obtained α-FeOOH and α-Fe$_2$O$_3$ particles by sol-gel method (Dar *et al.*, 2005) starting from Fe(NO$_3$)$_3$·9H$_2$O precursor. Iron oxide nanoparticles were obtained by Karami using solid state chemical reaction method (Karami, 2009) of a mixed powders containing FeCl$_2$·4H$_2$O, FeCl$_3$·6H$_2$O and KCl. Sarangi *et al.*, (2009) obtained α-Fe$_2$O$_3$ nanopowders by reacting aqueous solutions of ferric nitrate and PVA and sucrose (method 1) and EDTA (method 2). Liu *et al.* reported the preparation of uniform nanocrystalline α-FeOOH and α-Fe$_2$O$_3$ using hydrothermal synthesis (Liu *et al.* 2007). Qiu *et al.* described the obtaining of porous ultrafine iron oxide particles by homogenous precipitation method (Qiu *et al.*, 2005). Nasar and Husein prepared iron oxide nanoparticles by microemulsion process (Nassar & Husein, "2006). In order to obtain iron oxide nanoparticles used in health field, Guo and Kenedy used the gas-phase flame synthesis (Guo & Kennedy, 2007). Using the thermal decomposition of Fe(IO$_3$)$_3$, Ristić and Musić (2006) obtained porous α-Fe$_2$O$_3$.

In this paper we report two synthesis methods for preparation of α-Fe$_2$O$_3$ powders from β-FeOOH by thermal treatment.

2. Experimental

The chemical precursors used were iron chloride II tetrahydrate and urea, without further purification. Distilled water was used as solvent. Precursor powders were prepared by the methods, described in the next chapter.

2.1. Preparation of Iron Oxide Powders

Method 1. An aqueous solution of iron chloride was prepared by dissolving 9.93g FeCl$_2$·4H$_2$O in distilled water. 1.5 g of urea (NH$_2$CONH$_2$) was dissolved in 25 ml of distilled water. The two solutions were vigorously mixed in a beaker. The as-prepared solution was maintained in a thermostated bath (TRADE Raypa) at 90°C, for 2 hours. The precipitate thus obtained was allowed to settle until the next day. On the second day the solution was ultrasonicated for several minutes and maintained again in a thermostated bath for two hours at 90°C. This cycle was also repeated in the third day, on the same conditions. We consider that the solution was totally maintained in the thermostated bath for 6 hours. At the end of the three cycles the obtained precipitate was ultrasonicated, washed, and filtered with a vacuum pump (VACUUM PUMP 707). The product obtained after filtration was treated in an oven at 500°C for 4 hours.

Method 2. An aqueous solution consisting of 9.93 g of $FeCl_2$, 1.5 g NH_2CONH_2 and 50 ml of distilled water was heated in a thermostated bath for two hours at 90°C. The obtained solution was ultrasonicated for several minutes. After ultrasonication the product was washed and filtered with a vacuum pump. The powder obtained after filtration was treated 4 hours at 500°C.

2.2. Samples Characterization

The obtained powders were characterized using various techniques. X-ray powder diffraction patterns were obtained on a Shimadzu XRD 6000 diffractometer with CuKα (λ = 1.5405 Å) radiation. The operation voltage and current were kept at 40 kV and 30 mA, respectively. Diffraction data were collected in a 2θ range of 10 – 60° at a scan speed of 2.0000 (deg/min). The samples were also characterized by UV – VIS spectrometry.

3. Results and Discussion

3.1. X-Ray Analysis

α-Fe_2O_3 (hematite) is obtained by thermal treatment of the obtained powder. The diffraction peaks in XRD spectra (Fig. 1) at 2θ = 24.08°, 33.1°, 35.6°, 40.8°, 49.4° and 54.0° were in good agreement with the corresponding (012), (104), (110), (113), (024), and (116) diffraction planes of α-Fe_2O_3, confirming the formation of α-Fe_2O_3 phase. Similar results were obtained by P. Sarangi *et al.* (2009) and X. Liu and co-workers (2007).
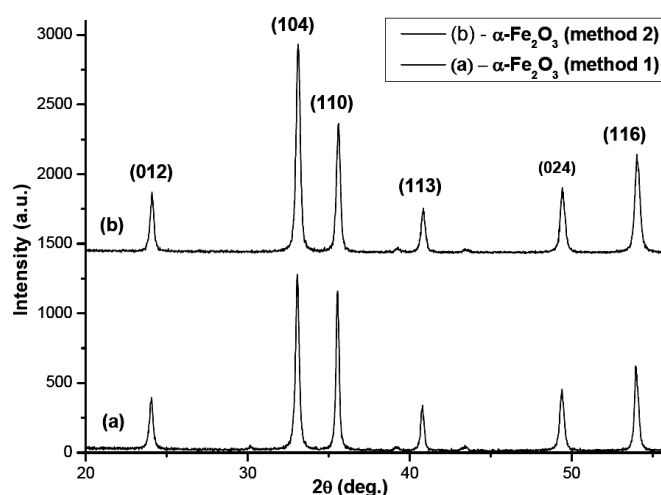
Fig. 1 − Diffraction patterns of the (a) α-Fe_2O_3 − thermal treated powders at 500ºC (method 1), (b) α-Fe_2O_3 thermal treated powders at T = 500ºC (method 2).

Crystallite size of the α-Fe$_2$O$_3$ powders was calculated using the Scherrer's equation (Ray *et al.*, 2008):

$$D = \frac{0.9\lambda}{\beta \cos\theta} \tag{1}$$

where D - is the average crystallite size, λ - the X-ray wavelength, β - the width of the diffraction peak at half maximum for the diffraction angle, cos θ - the Bragg diffraction angle.

One can see that the crystallite sizes have been influenced by the obtaining method. The crystallite sizes were smaller for α-Fe$_2$O$_3$ powder obtained using the second method (2 hours instead of 6 hours) as can be seen in Table 1.

Table 1

Crystallite Size of the α-Fe$_2$O$_3$ Powders

Crystallite size (nm)	
Method 1 α-Fe$_2$O$_3$ powder	173
Method 2 α-Fe$_2$O$_3$ powder	152

3.2. Optical Investigation

Optical studies of iron oxide powders were performed using a Perkin Elmer Lambda 35 spectrophotometer.

The optical absorption spectrum of the treated powders - α-Fe$_2$O$_3$ was recorded over the wavelengths ranged from 300-1100 nm. In Fig. 2 are presented the absorption spectra of the iron oxide powders.
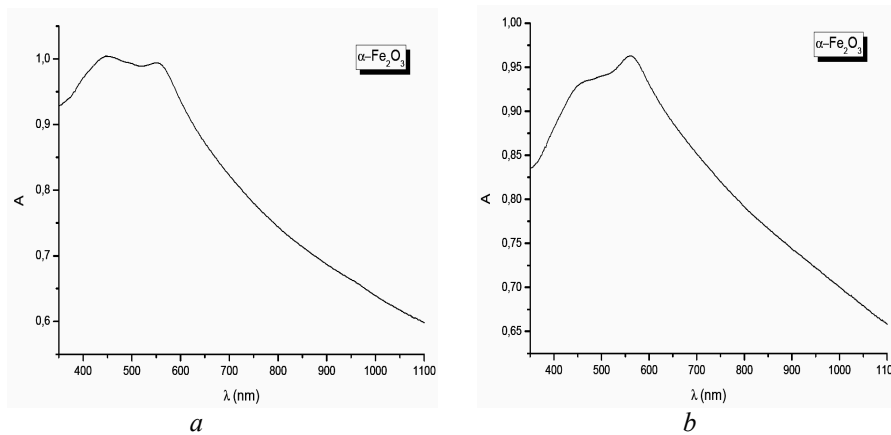
Fig. 2 – Absorption spectra of the treated powders at T= 500 ºC: *a* - treated powders prepared by method 1, *b*- treated powders prepared by method 2.

It can be seen that for hematite the absorption decrease with the increase of the wavelength, for wavelength higher than 555 nm (sample 1) and 564 nm (sample 2) As is shown in Fig. 2a the α-Fe_2O_3 powders obtained by method 1 presents 2 maximum absorption at 555 nm and respectively at 450. The maximum absorption for the α-Fe_2O_3 powders obtained by method 2 is at 564 nm (Fig. 2 b). The results are in good agreement with the literature data which confirm that hematite has an absorption band in visible at about 600 nm (Chiriţă & Grozescu, 2009). The maximum absorption has been displaced from 555 to 564 when the formation time was reduced from 6 to 2 hours.

The optical band gap of the hematite (α-Fe_2O_3) was determined by extrapolation of the plot $(\alpha h \upsilon)^2$ versus $h \upsilon$.

a

b
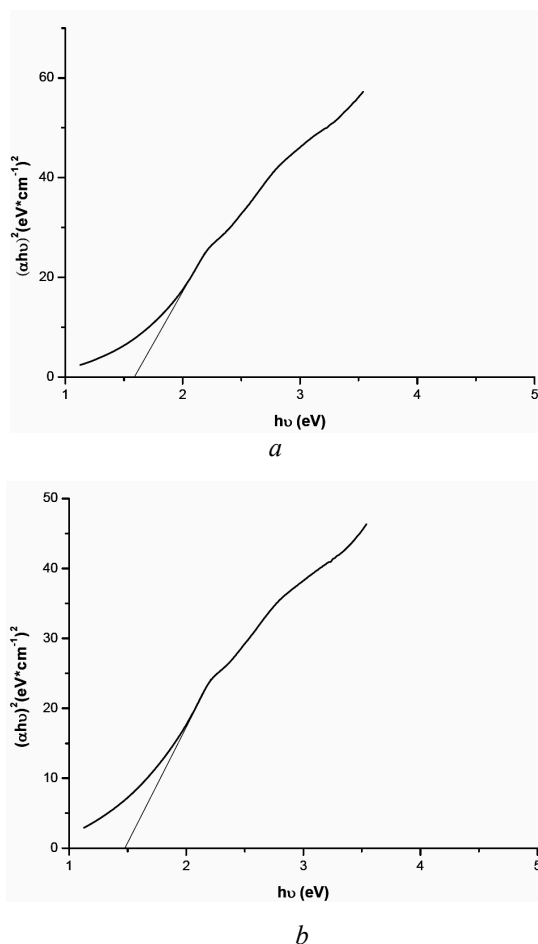
Fig. 3 – The plot of $(\alpha h \nu)^2$ vs. $h \upsilon$ of: *a*) α-Fe_2O_3 phase obtained by method 1; *b*) α-Fe_2O_3 phase obtained by method 2.

In Fig. 3 it is represented the determination of optical band gaps for the α-Fe$_2$O$_3$ powders. The band gap value for the α-Fe$_2$O$_3$ powders obtained by method 1 was 1.59 eV (Fig. 3 *a*), respectively 1.47eV for the α-Fe$_2$O$_3$ powders obtained by method 2 (Fig. 3 *b*), values which are lower compared to the band gap value of bulk α-Fe$_2$O$_3$ - 2.2 eV (Zeng & Tang, 2007). This may be possible due to another phase or impurity imbedded in Fe$_2$O$_3$ at a very low concentration that was not detected by XRD. Other analyses are necessary in order to establish the cause for the lowering of the energy band gap of hematite powder.

4. Conclusion

A simple chemical method for the preparation of iron oxyhydroxide and iron oxide (hematite) was described. Thermal treatment of the obtained powders (FeOOH) leads to α-Fe$_2$O$_3$ phase conversion. In the case of hematite the absorption decrease with the increase of the wavelength, for wavelength higher than 555 nm (sample 1) and 564 (sample 2) nm. The optical band gap of the hematite (α-Fe$_2$O$_3$) containing powder was determined by extrapolation of the plot $(\alpha h\upsilon)^2$ versus $h\upsilon$. The band gap value for the α-Fe$_2$O$_3$ powders obtained by method 1 was 1.59 eV, respectively 1.47eV for the α-Fe$_2$O$_3$ powders obtained by method 2.

REFERENCES

Chiriţă M., Grozescu I., *Fe$_2$O$_3$ – Nanoparticles, Physical Properties a Their Photochemical and Photoelectorchemical Applications*. Chem. Bull. "POLITEHNICA" Univ., *54*, 2009.

Dar M.A., Kulkarni S.K., Ansari Z.A, Ansari S.G., Shin H.-S., *Preparation and Characterization of α-FeOOH and α-Fe$_2$O$_3$ by Sol-Gel Method*. Journal of Materials Science, **40**, 3031-3034 (2005).

Guo B., Kennedy I.M., *Gas-Phase Flame Synthesis and Characterization of Iron Oxide Nanoparticles for Use in a Health Effects Study*. Aerosol Science Technology 41:10 (2007 first publication) 944-951.

Guo L., Chen F., Fan X., Cai W., Zhang J., *S-doped α-Fe$_2$O$_3$ as a Highly Active Heterogeneous Fenton-Like Catalyst Towerds the Degradation of Acid*

Orange 7 and Phenol. Applied Catalysts B: Environmental, **96**, 162-168 (2010).

Jin W., Dong B., Zhao C., Mai L., Day Y., *Synthesis and Gas Sensing Properties of Fe₂O₃ Nanoparticles Activated V₂O₅ Nanotubes*. Sensors and Actuators, **B 145**, 211-215 (2010).

Karami H., *Synthesis and Characterization of Iron Oxide Nanoparticles by Solid State Chemical Reaction Method*. J. Clust. Sci., **21**, 11-20 (2009).

Li Y.N., Zhang P., Guo Z., Munroe P., Liu H., *Preparation of α-Fe₂O₃ Submicro-Flowers by a Hydrothermal Approach and Their Electrochemical Performance in Lithium-Ion Batteries*. Electrochimica Acta, **53**, 4213-4218,(2008).

Liu X., Qiu G., Yan A., Wang, Li X., *Hydrothermal Synthesis and Characterization of α-FeOOH and α Z.-Fe₂O₃ Uniform Nanocrystallines*. J. of Alloys and Compounds, **433**, 216-220 (2007).

Nassar N., Husein M., Preparation of Iron Oxide Nanoparticles from FeCl₃ Solid Powder Using Microemulsions. Phys. Stat. Sol. **(a) 203**, *6*, 1324-1328 (2006).

Pailhé N., Wattiaux A., Gaudon M., Demourges A., *Impact of Structural Features on Pigment Properties of α-Fe₂O₃ Haematite*. Journal of Solid State Chemistry, **181**, 2697-2704 (2008).

Qiu J., Yang R., Li M., Jiang N., *Preparation and Characterization of Porous Ultrafine Fe₂O₃ Particles*. Materials Research Bulletin, **40**, 1968-1975 (2005).

Ray I., Chakraborty S., Chowdhury A., Majumdar S., Prakash A., Pyare Ram, Sen A., *Room Temperature Synthesis of γ-Fe₂O₃ by Sonochemical Route and its Response Towards Butane*. Sensors and Actuators, **B 130**, 882-888 (2008).

Ristić M., Musić S., *Formation of Porous α-Fe₂O₃ Microstructure by thermal Decomposition of Fe(IO₃)₃*. J. of Alloys and Compounds, **425**, 384-389 (2006).

Sarangi P.P., Naik B., Ghosh N.N., *Low Temperature Synthesis of Single-Phase α-Fe₂O₃ Nano-Powders by Using Simple But Novel Chemical Methods*. Powder Technology, *192*, 245-249 (2009).

Sarangi P.P., Naik B., Ghosh N.N., *Synthesis of Single α-Fe₂O₃ Nanopowders by Using A Novel Low Temperature Chemical Synthesis Route*. J. Am. Ceram. Soc., **91**, *12*, 4145-4147 (2008).

Satsangi V.R., Kumari S., Singh A.P., Shrivastav R., Dass S., *Nanostructured hematite for photoelectrochemical generation of hydrogen*. International Journal of Hydrogen Energy, **33**, 312-318 (2008).

Zeng S., Tang K., Li T., *Controlled Synthesis of α-Fe₂O₃ Nanorods and its Size-Dependent Optical Absorption, Electrochemical, and Magnetic Properties*. Journal of Colloid and Interface Science, **312**, 513-521 (2007).

Zhang F., Yang H., Xie X., Li L., Zhang L., Yu J., Zhao H., Liu B., *Controlled Synthesis Nd Gas-Sensing Properties of Hollow Sea Urchin-Like α-Fe₂O₃ Nanostructures and α-Fe₂O₃ Nanocubes*. Sensors and Actuators, **B 141**, 381-389 (2009).

Zhang Z., Hossain Md. F., Takahashi T., *Fabrication of Shape-Controlled α-Fe₂O₃ Nanostructures by Sonochemical Anodization for visibile Light Photocatalytic Application.* Materials Letters, **64**, 435-438 (2010).

Zhong L.-S., Hu J.-S., Liang H.-P., Cao A.-M., Song W.-G., Wan L.-J., *Self-Assembled 3D Flowerlike Iron Oxide Nanostructures and Their Application in Water Treatment*. Advanced Material, **18**, 2426-2431(2006).

OBŢINEREA PULBERILOR DE OXID DE FIER DIN SOLUŢIE CHIMICĂ

(Rezumat)

Lucrarea de fată prezintă obţinerea unor pulberi de oxid de fier utilizând ca şi precursori pe bază de soluţii de clorură de fier în prezenţă de uree. Pulberile de FeOOH obţinute au fost tratate termic in cuptor la temperatura de 500°C timp de 4 ore. În urma tratamentului termic s-a obţinut pulbere de oxid de fier de culoare roşu-maroniu - faza α-Fe₂O₃. Proprietăţile optice şi structurale ale pulberii obţinute au fost determinate cu ajutorul analizelor UV-VIS şi XRD.

EXPERIMENTAL RESEARCH ON THE EXTRACTION OF HEAVY METALS FROM POLLUTED SOILS DUE TO THE METALLURGIC INDUSTRY

BY

IOANA MONICA BERAR (SUR)[*]**, VALER MICLE, SIMONA AVRAM
and CAMELIA SIMONA COCIORHAN**

"Gheorghe Asachi" Technical University of Iaşi,
Faculty of Materials Science and Engineering

Abstract. The paper is based on preliminary studies concerning the utilization of heavy metals extraction solutions from polluted soil, the decontamination being the purpose of these analyses. The experiments were conducted on soil assays, sampled from a heavily polluted area due to the metallurgic industry. Preliminary leaching tests (with different amounts of sulphuric acid) were carried out to extract the heavy metals from soil samples. The experiments led to the conclusion that heavy metals present in this polluted soils were extracted considerably using this method, a high level of treatment was achieved.

Key words: heavy metals extraction, metallurgic industry, soil pollution, sulphuric acid.

1. Introduction

The heavy metal pollution of soils presents a cumulative character, which means the slow accumulation rate of pollutants in soils. Permanent and

---

[*]Corresponding author e-mail: Ioana.BERAR@im.utcluj.ro

long-term exposure of soil to the action of these pollutants, without their removal or decaying, denotes the residual character of those pollutants. Once contaminated, the soil regenerates itself very difficult. Therefore, the soil fertility is adversely affected, (Berar *et al*., 2011).

The environmental pollution is delineated, more clearly, as one of the main problems of the contemporary world. Awareness of the major risks involved in the pollution of both the geospheres and the human health, as well as the adoption of stringent and aggressive both environmental policies and strategies in the pollution reduction, vary from state to state. The phenomenon of environmental pollution no longer has a locally or regionally character, but a global one, with great implications on the whole geosystem, (Berar *et al*., 2010b).

The accumulation of metals (Zn, Pb, Cr, Mn, Fe, Cu, Cd, As) in soil has special ecological implications, not only because of these metals toxicity and of the compounds formed up by them, but also due to the soil minerals which bind metals. All these influence the soil reaction. The pollution of soil with heavy metals can increase its response. Thus there is a danger that the new formed compounds, leached from soil by the infiltration waters, to reach into groundwater or they can be assimilated by plants and thereby to enter the food chain. Ensuring the protection of soil quality is not only a means to enhance soil resources, but also a way to protect the environment. These measures include among others the utilization of remediation methods and technologies designed to neutralize or block the flow of pollutants. The measures taken to this end must ensure the desired efficiency in accordance with the laws on protection of soil quality. The soil pollution by heavy metals in the Baia Mare area is recognized today as a significant problem, representing a serious risk to human health and the environment, (Coman *et al*., 2010). The presence of high concentrations of heavy metals in soils is due to the metallurgic industry.

The concentration of heavy metals in soils around Baia Mare is significant because of the high amounts of Cu, Zn, Cd that are present in them. The preliminary results obtained through the acidic leaching of some soil samples polluted with heavy metals taken from inside Romplumb Baia Mare are presented in this paper. The presence of heavy metals in high concentrations gives a relevant historical pollution of the studied area. Excessive quantities of heavy metals in soil inhibit plant growth and adversely affect nitrogen fixation by microorganisms, (Berar *et al*., 2010b).

2. Materials and Methods

The extraction of heavy metals was carried out on polluted soil samples from the Baia Mare area, taken from depth interval of 55 – 75 cm. The two soil samples were prepared in accordance with ISO 11464 standard methods for the extraction of soil elements in aqua regia. The determined concentration was

reported to the alert and intervention thresholds established by Order no 756/1997, regarding soils with less sensible utilization. The concentrations of these elements (Cu, Zn, Cr) exceed the alert and intervention limit thresholds, (Berar *et al*., 2010 a). 3 g of soil were weighed from the soil samples chosen for the experiment. The metals extraction was performed with 96% sulphuric acid in different amounts using the following extraction solutions: 30 mL water +1 mL H_2SO_4 (solution A); 20 mL water +10 mL H_2SO_4 (solution B).

The leaching of soil samples was done with the acidic solutions at a ratio of 1: 10. Samples thus prepared were placed in a magnetic stirrer at 200 rpm, at constant temperature of 28 ± 2ºC. The leaching time was set at 2, 4, 8, 12, 24, 48, 72 hours respectively. At the end of this time set up for the leaching of soil samples, 10 ml of solution were collected from each sample and were subjected to metals determination by atomic spectrometry.

3. Results and Discussions

The histograms analysis regarding the amount of chromium (Fig. 1) and copper (Fig. 2) extracted, a sharp increase of the metals extraction was identified, especially in the first 12 hours from the beginning of the experiment. After that, a slower extraction rate was marked out. The extraction of chromium was approximately identical to the copper extraction, being independent on the amount of sulphuric acid used.
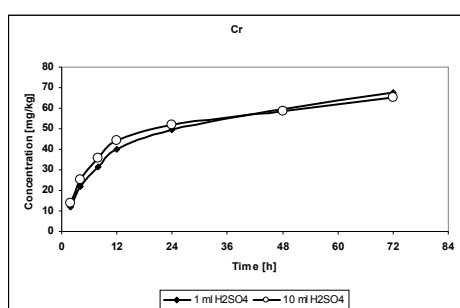
Fig. 1 – Variations of Cr concentration function of time.
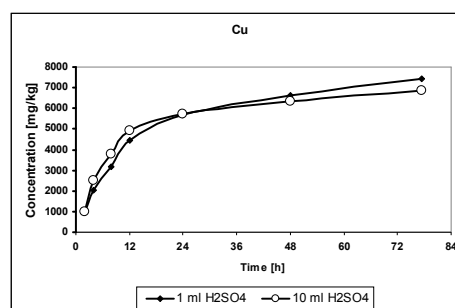
Fig. 2 – Variations of Cu concentration function of time.

The concentration of extracted pollutant was higher in the first 24 hours when the solution B was used, but when the solution A was used the extraction of Cr and Cu was more thoroughly performed after 24 hours. The chart analysis of the Zn extraction revealed a sharp increase of Zn extracted concentration in the first 12 hours. After that, a slow linear increase was obtained in both cases of extraction solutions. In the Zn case a better result was obtained when 1 mL H2SO4 was used (Fig. 3).
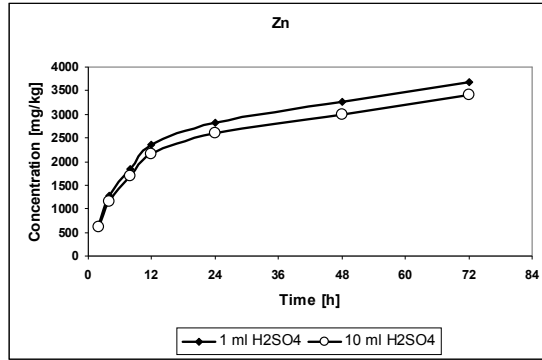
Fig. 3 – Variations of Zn concentration
function of time.

The effectiveness of the extraction process was evaluated by determining the final remediation efficiency, with the following formula:

$$\eta = \frac{m_e}{m_i} \cdot 100 \ [\%] \tag{1}$$

where: m_e - the concentration of extracted pollutant [mg/kg]; m_i - the initial concentration of existent pollutant (extractable in royal water), [mg/kg].
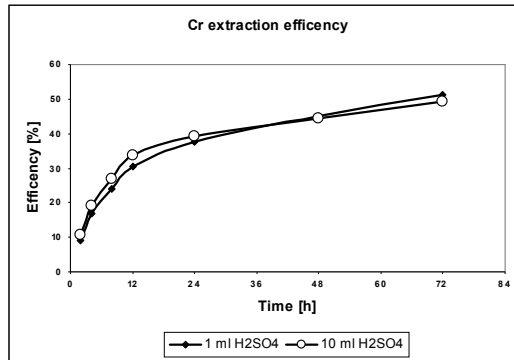
Fig. 4 – The effectiveness of the remediation
process of Cr.

The obtained experimental results were plotted; the charts that show the effectiveness variation of the leaching process as a function of time are presented in Figs. 4,...,6. The analyses of these graphs showed that the extraction solutions used presented an extraction effectiveness of the studied metals, as followed: Cu: 99%, Cr: 52% and Zn: 48%.
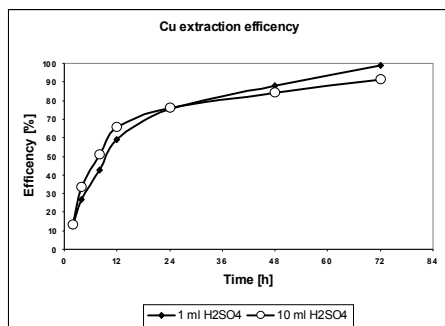
Fig. 5 – The effectiveness of the
remediation   process of Cu.
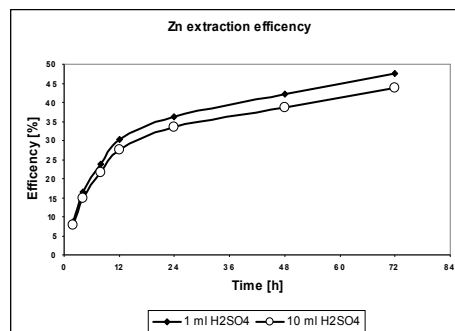
Fig. 6 – The effectiveness of the
remediation process of Zn.

4. Conclusion

The pollution by Cr, Cu and Zn of soil sampled from the studied area was confirmed by this research. The concentrations exceed the alert and the limits of the intervention thresholds. The extraction variations of the heavy metals concentration from the soil samples records a noticeable increase up to 12 hours, then a linear slightly tempered growth for all studied elements (Cr, Cu, Zn). The results indicate that the extraction solutions used have good extraction effectiveness for Cu (99%) and medium extraction effectiveness for Cr and Zn (50%). There are no significant differences regarding the extraction effectiveness as a function of different amounts of sulphuric acid used in the preparation of extraction solutions. The experiments carried led to the conclusion that heavy metals from polluted soils can be extracted by acidic leaching process. But, the risk of soil acidification appears when the sulphuric acid is used in leaching processes.

REFERENCES

* * ORDIN nr. 756/1997 al MAPPM, *Pentru aprobarea Reglementării privind evaluarea poluării mediului.* 1997.
Berar (Sur) I.M., Cociorhan C.S., Oros V., Micle V., Coman M., Juhas J., Taro G., Falaus B., Pop R. *Research Regarding Metal Contents of Soil from Romplumb*

Baia Mare, in Order to Establish the Remedial Techniques. Buletinul Ştiinţific al Universităţii de Nord din Baia Mare, **24**, 33 – 38 (2010 b).

Berar (Sur) I.M., Micle V., Cociorhan C., *Investigations for Remediation of Soils Polluted with Heavy Metal*. The 7th Edition of the Carpathian Basin Conference on Environmental Science, Cluj Napoca, **2**, 578 – 582 (2011).

Berar (Sur) I.M., Micle V., Oros V., Cociorhan C.S., Urs (Nedelcu) A.M. *Studies and Research on Soil Quality Evaluation in S.C. Romplumb S.A. Baia Mare to Address Remediation of Polluted Sites*. ProEnvironment/ProMediu, **3**, 292 – 296 (2010 a).

Brusturean G.A., Perju D.M., *Extracţia sub presiune redusă sau prin ventilare in situ – studiu comparativ al performanţelor de depoluare a solurilor poluate cu compuşi organici volatile*. Buletinul AGIR, *1-2*, 224-229 (2008).

Coman M., Fălăuş B., Pop R., *Soil Pollution with Heavy Metals - Specific Issues for Baia Mare Area*. ProEnvironment, Cluj-Napoca, 29-32 (2010).

CERCETĂRI EXPERIMENTALE PRIVIND EXTRACŢIA METALELOR GRELE DIN SOLUL POLUAT PRIN ACTIVITĂŢILE SPECIFICE INDUSTRIEI METALURGICE

(Rezumat)

În această lucrare se prezintă studii preliminare privind utilizarea unor soluţii de extracţie a metalelor grele din solurile contaminate, scopul fiind depoluarea. Experimentările s-au efectuat pe probe de sol prelevate dintr-o zonă puternic poluată prin activităţile specifice industriei metalurgice. În vederea extracţiei metalelor grele din probele de sol, s-a utilizat pentru spălare acid sulfuric în cantităţi diferite. În urma acestor experimentări se poate concluziona că metale grele prezente în solurile poluate s-au extras în mod considerabil, obţinându-se un nivel de tratare ridicat.

RESEARCHES REGARDING THE CAUSES OF DEGRADATION OF THE *SEN'S* FROM THE CONTINOUS CASTING OF STEELS

BY

A. BERBECARU[∗], A.PREDESCU, C. PREDESCU and A. NICOLAE

University Politehnica of Bucharest,
Faculty of Engineering and Materials Scinece

Abstract. This paper presents the research performed to establish the causes that lead to premature deterioration of the SEN's from the continuous casting of steel.

Were used as methods of analysis: - **X - ray diffraction (XRD)** - to analyze the existing phases in the material; - **SEM - EDAX** - to highlight the micro aspect of the material and to determine the distributions of elements in the material.

Key words: XRD, SEM.

1. Introduction

In the context of technology development and winning of a lot more selling markets, in metallurgical domain exists programs of costs optimization, of development and discovering new advantageous methods of production, butt in the same time of obtaining an increase quality which has to assure a better position on market.

In the case of factories that elaborate and process steel it was adopted a aggresive politics of optimization for resources and production process, together with decreasing of production costs and increasing of quality.

[∗] Corresponding author e-mail: andrei_berbecaru@ecomet.pub.ro

During the continous casting of steel, the submerged entry nozzle (SEN) plays a very important role as it is the last refractory in contact with the liquid steel. If SEN cannot withstand thermal shock or corrosion attack from the liquid steel and molten flux, the quality of the steel products will be deteriorated or the casting process may fail. While the use of stabilized ZrO_2 – graphite at the SEN provides better corrosion resistance, it is also attacked by the mold flux and liquid steel. This sometimes results in the formations of ZrO_2 – based inclusions, which have a deletrious effect on the steel quality.

Attack of refractories is a complex phenomenon involving not only chemical wear (corrosion) but also physical/mechanical wear (such as erosion/abrasion) processes which may act synergistically.

The most important properties of these refractories during the casting are thermal shock resistance, erosion resistance to molten steel and slag, and clogging resistance by Al_2O_3 and metal.

The chemical compositions of the SENs are basically based on Al_2O_3 – graphite, with MgO, ZrO_2 or others materials in some areas in contact with liquid steel and slag.

The chemical wear mechanism in the mould powder slagline of the SEN used in the continuous casting of the steels is very important to be known because in the time of this process graphite is dissolved in steel while the ZrO_2 grains are destroyed due the destabilizing effect of the slag.

The wear mechanism of the refractories containing oxide and graphite due to contact with steel and slag is as follows:

a) Refractory material is initially covered with slag film which wets oxide material and dissolves it in favor of graphite. This produces a graphite rich layer at the surface;

b) Molten metal wets and dissolves graphite in favor of oxides which results in the disappearance of the graphite layer and the surface of the refractory is again covered with the slag and so the process is repeated. In other words, the oxide material is attacked by the slag whereas the graphite is attacked by the steel melt.

2. Experimental Researches

The purpose of the analyses was to determinate the causes that lead to premature deterioration of the SENs used in the process of continuous casting of steel, together with determination of causes that produce the corrosion of this SENs.

2.1. Crack in SEN: Particular Case

On the samples analyzed were made the next investigations:
1. Macroscopic examination;

2. Chemical analyses (Chemical composition, elements distribution - EDX + phase analyses - XRD);

Before to start the analyze the sample was numbered as it follows:

- **Sample 1 – SEN 1**

The SEN 1 who was in service for 110 min and had appeared in his wall a hole. The hole was propagated from the outside to inside of the wall. The correspondent Fig.

Fig. 2 shows the sample 1 with the two compounds from which the wall is made (on the inside the compound - Al_2O_3 predominant 82.05%, and on the outside compound – ZrO_2 predominant 84.41% according to product certificate).

Direction of hole propagation
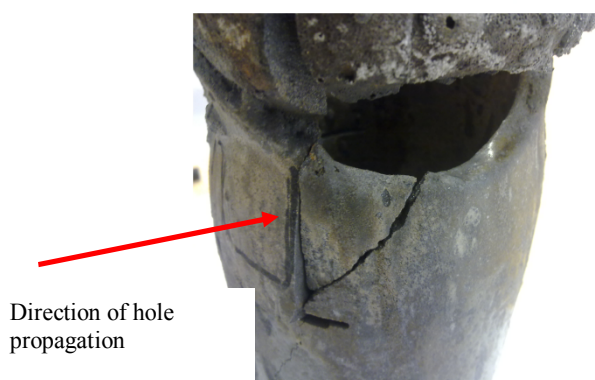
Fig. 1 – Aspect of sample 1- SEN 1 after use.

ZrO_2

Al_2O_3
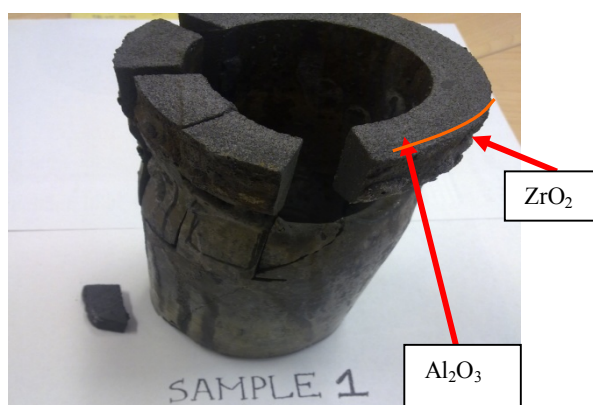
Fig. 2 – The compounds zone from the sample 1.

2.2. XRD – Phase Analyses of the SENs

The SEN was analyzed with the X-ray diffraction method. Through this analyze where determinate the chemical compounds that exist in this sample.

The experimental measurements were made with an X-ray diffractometer, model PANalytical X'pert PRO MPD, with X-ray tube of Co (K-alpha1 = 1.78901Å), in gonio geometry, with a proportional detector.

In the next figure is presented the X-ray diffractogram for this sample with presentation of the main compounds that were found in them.

➢ **Sample 1 (SEN 1)**

Analyze was made on a small sample which was cut from the broken wall near to the crack hole. Normally the material from this sample should be form from 2 types of material, but it was found jus one type of material.

In this type of material were founded the next compounds: Al_2O_3, C (graphite), ZrC, ZrO_2. The main compound of this SEN which corresponds to 100% of intensity (2theta = 30.8404°) is C. In the sample were founds also a second main compounds which is Al_2O_3.

In the Fig. 3 are presented the compounds founded in the sample 1.

Nr.	Sichtba	PDF-Nr.	Verbindungsn...	Chemische Formel	Score	Skale...	Halbqu...
1	☐	00-043-1484	Corundum, syn	Al2 O3	74	0,193	33
2	☐	01-089-7213	Graphite 2H	C	42	0,884	65
3	☐	01-074-1221	Zirconium Carb	Zr C	26	0,033	1
4	☐	01-074-0815	Zirconium O...	Zr O2	6	0,023	1

Fig. 3 – List of compounds founded in sample 1 (SEN 1).

In the Fig. 4 is presented the diffractogram for the sample no1.
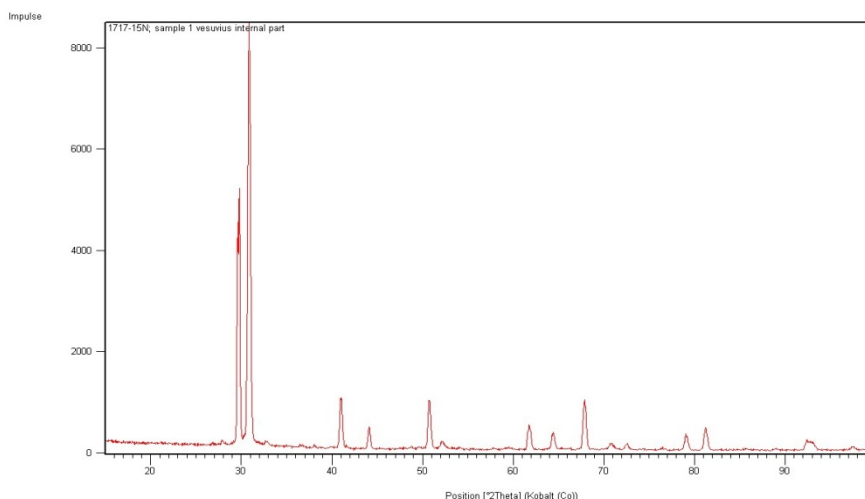
Fig. 4 – Diffractogram of sample 1 (SEN 1).

2.3. SEM – EDX Analyses

On the sample on which was made the XRD analyze, has been made also *Scanning electron microscopy (SEM)* analyze and *Energy disperse X-ray (EDX)* analyze. These types of analyses were made for determinations of surface aspect, material homogeneity and elements distribution in material.

The analyses were made with a *scanning electron microscopy* Zeiss EVO 60 equipped with field emission gun and EDAX *energy disperse X-ray* detector. To make the surface electrical conductivity, samples were glued on the sample holder with carbon and aluminum band.

The next figure present the SEM-EDX machine use to analyses.
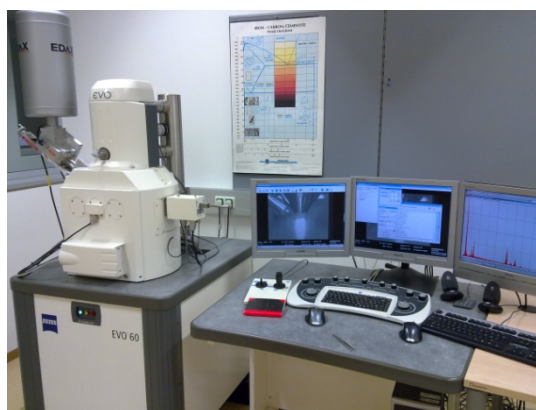
Fig. 5 – Image of SEM-EDX machine used on analyses.

✓ **Sample 1 (SEN 1)**

For this sample was made a SEM image on an area with specific aspect of the material, this image was made in BSE mode, on a magnification of 1000x. Also for this sample was made with EDX the maps of elements for analyzed area.

In the Fig. 6 is presented the BSE image of the analyzed area.
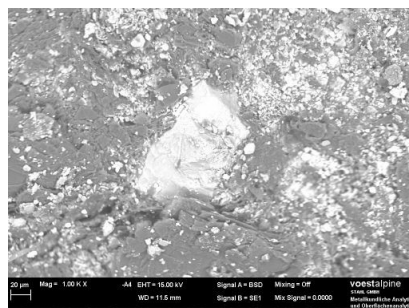
Fig. 6 – BSE image of analyzed area for S1.
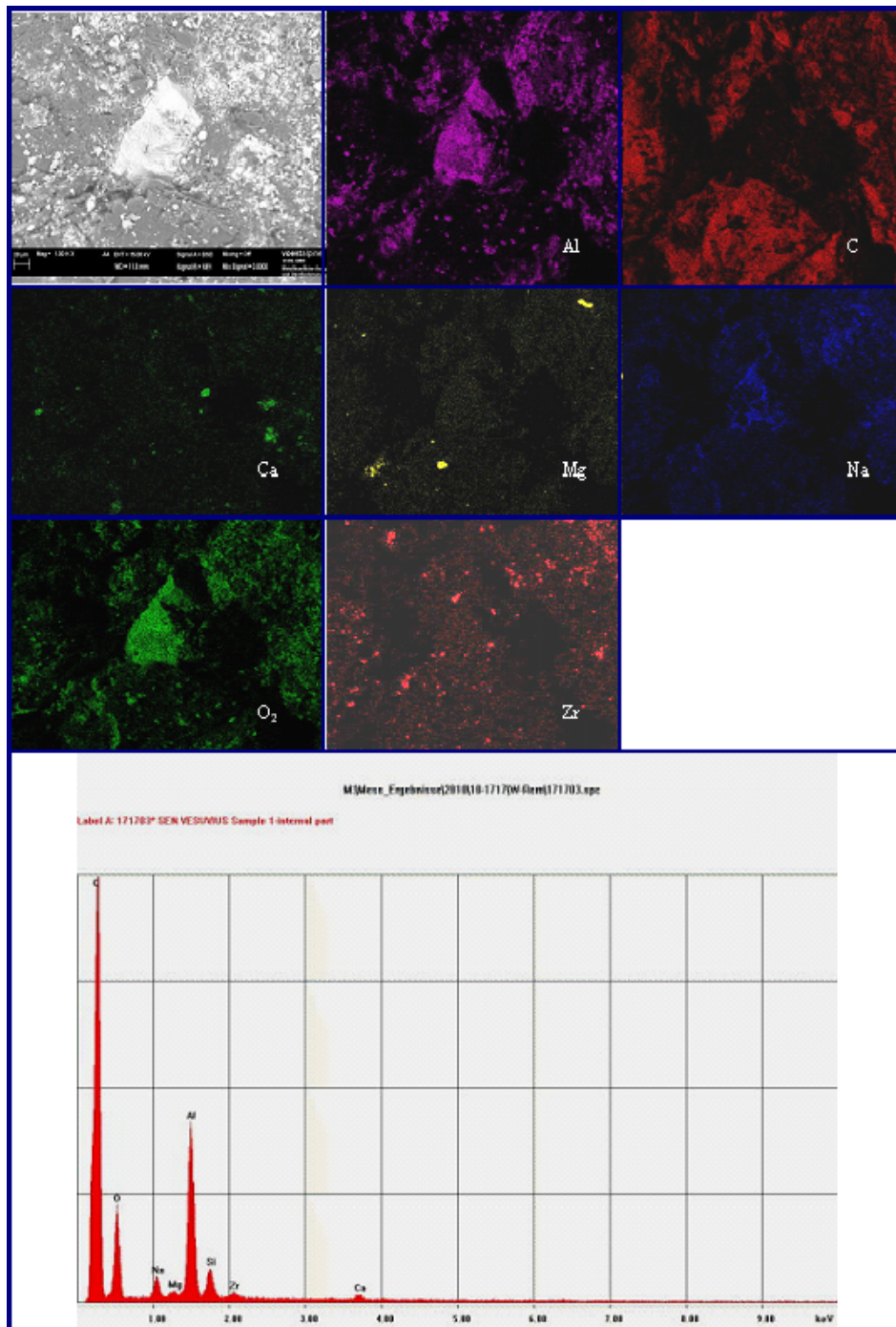
Fig. 7 – EDX maps of elements, EDX spectrum of elements for S1.

In Fig. 7 is presented the EDX map of the elements with the EDX elements spectrum founded in analyzed area.

3. Conclusion

- It can be observed that between the both type of material had appread a diffusion.
- The slag and the preheating process has a big influence on the SEN material.
- From the both type of analyses (XRD and SEM+EDX) we can conclude that the compounds found in the sample are: Al_2O_3, C (graphite), ZrC, ZrO_2.

NU SE REGASESC IN TEXT TRIMITERILE LA BIBLIOGRAFIE

REFERENCES

[1]. Ito Satoru, Inuzuka Takayuki, *Technical Development of Refractories for Steelmaking Processes*. Nippon Steel Technical Report, *98*, 2008.
[2]. Brandaleze E., Walter G., Bentancour M., Madias J., *Behavior During Preheating of Stopper Rod and SEN*. Steelmaking Conference Proceedings, 2002.
[3]. Heikkinen E.-P., Mattila R.A., Kokkonen Tommi M.T., Harkki J.J., *The Chemical Wear of the SEN-SLAGLINE in the Continuous Casting of Stainless Steels*. Steelmaking Conference Proceedings, 2002.
[4]. Bui A.-H., Park S.-C., Chung In-Sang, Lee H.-G., *Dissolution Behavior of Zirconia-Refractories during Continuous Casting of Steel*. Metals and Materials International, *12*, *5*, 435-440 (2006).
[5]. Zhang S.,. Lee W.E, *Use of Phase Diagrams in Studies of Refractories Corrosion*. IoM Communications Ltd and ASM International, 2000.
[6]. Lee W.E., ZHANG S., *Melt Corrosion of Oxide and Oxide-Carbon Refractories*. IoM Communications Ltd and ASM International, 1999.

CERCETĂRI PRIVIND CAUZELE DEGRADĂRII TUBURILOR DE IMERSIE DE
LA TURNAREA CONTINUĂ A OŢELURILOR

(Rezumat)

Lucrarea prezintă cercetările efectuate în vederea stabilirii cauzelor care duc

la deteriorarea prematură a tuburilor de imersie de la turnarea continuă a oţelului.

Au fost utilizate ca metode de analiză:- **X - ray diffraction (XRD)** – pentru analiza de faze existente în material; - **SEM – EDAX** – pentru a evidenţia aspectul microstructural al materialului, precum şi pentru determinarea distibuţiei elementelor în material.

DETERMINATION OF STRATEGIES FOR MANAGERIAL-TECHNICAL DEVELOPMENT OF PRODUCTIVE SYSTEMS OF THE MOTOR TRANSPORT

BY

V. BILICHENKO[*]

Vinnitsa National Technical University

Abstract. There had been determined the terms of the productive system and managerial-technical development of the productive systems. It is suggested to use the rate of management quality as an index for credibility of the enterprises. It is possible to see the positions of enterprises according to their liable areas and in response to them the most rational strategies of the development.

Key words: strategy, productive systems, managerial-technical development, motor transport enterprise.

1. Introduction

Quick formation of the market for transport services in Ukraine, changes in competitive environment and creations stipulate for the great degree of uncertainty in the operation of auto transport enterprises and firms as well as their dependency upon fluctuation of market situation which predetermines the impossibility in using traditional approaches and methods for their further development (Афанасьев *et al*., 2003).

---

[*] Corresponding author e-mail: bilichenko_v@mail.ru

Under contemporary market conditions the auto transport enterprises especially small-sized auto transport enterprises are forced to look for the ways of their development under conditions of pretty dynamic environment, respond to its change to be competitive and self-efficient in its sate and development. Under such complicated, dynamic and uncertain economic conditions, the auto transport enterprises considered as complex selforganizing and selfdeveloping manufacturing systems.

2. Main Part

The manufacturing system may be determined as an aggregate of active elements, presented by groups of people united, equipped and cooperate with the frameworks of manufacturing process on the base of agreed upon interests with incessant improvement of manufacturing possibilities.

Such an increase stipulates for the top priority in the development of the two sub-systems: organizational and technical.

The availability of these subsystems allow to determine the organizational and technical development as the complex of active, irrevocable, directed, natural changes which imply for the development and realization of the development projects (strategies), causing the qualitative changes in technical characteristics of the equipment, technological and organizational processes and improvement of manufacturing possibilities system with its ability to ensure the competitive output (services) in the necessary quantity and assortment, optimizing the expenditures, counteracting negative influences of an environment which constantly changes.

Proceeding from the above allows asserting that the organizational and technical development of transport manufacturing systems is not the simple equipping with new machinery and its improvement.

This is the form of the reproduction of manufacturing approaches, which is its complex transformation, aimed at change and support of the rolling stock, manufacturing and technical base of an enterprise within the specific time which is requires for providing a range of highly competitive services at the optimal level of expenditures.

The main objective of strategic development of manufacturing system implies for ensuring its activity for all functions and success on basic direction of activity, which may be achieved by regulating the structure and strategic management, active creating of favorable environment.

Proceeding from the above allows asserting that strategic management is the necessary component in strategic development.

The famous specialist in strategic management I. Ansoff determines such a management as complex of both, strategic managerial decisions, which determine the long-term development of the organization, as well as specific activities, which ensure quick response of manufacturing system to change of

external market situation, which may cause the necessity in strategic maneuvers, revision of goals and improvement of the general way for development (Ансофф, 2006). Strategic management as a sphere of science and practice of management is assigned for ensuring the strategic development of the organization.

The main content of the strategic management is a choice and realization of the strategy. Strategy is the main instrument for management and a base for methodology in strategic management. I. Ansoff determines a strategy as "... detailed and comprehensive complex plan assigned to ensure the fulfillment of organization's mission and achievement of its goals" (Ансофф, 2006).

There are many other determinations of strategies (Майкл, 2006), but all of them are united in consideration of strategy as the conscious and thoughtful aggregate of norms and rules which are in the background of the development and making strategic decisions, influencing the future state of manufacturing system as the way for connection with external environment.

Considering the development of manufacturing system, the strategy shall be considered as the dynamic system of interconnected rules, methods and principles, ensuring the coordination in development of internal potential and the desired to change the external environment, for the creation of maximum realization of all capabilities of the manufacturing system.

The possibilities for further development of manufacturing system of automobile transport greatly depend upon their financial state. If the financial and organizational state is not stable, there is no way one can consider its development.

But when, following all principle factors of enterprise's activity there is more or less stable situation, it is possible to develop and realize the strategies for further development.

This is required and sufficient condition for development and strategic approach to management in general. In this case talking about stability we mean combination of goal-oriented acts of certain elements and a system in general. Elements in turn, are of this origin only because each of them, relating to enterprise executes a separate function, therefore their action is functional and goal-oriented.

Using a structural and financial approach to the determination of automobile transport stability, we use general indicator such as a factor of organization which looks as:

$$K_{op\varepsilon} = \sum_{i=1}^{n} a_i \cdot \alpha_i \to 1, \tag{1}$$

Where $K_{op\varepsilon}$ – factor of organization ; a_i –f actor of significance of the i-th function; α_i factor of sufficiency in execution of the i-th function; n – number of functions in structure.

A system, which functions on proper level and maximally fulfills its

goals, has the factor of organization close to 1.

Each function as a property in the system of the set of functions which are in divisions and on an enterprise, in general has characteristics which determine the significance of each of the i-th function and sufficiency in its realization relating to the ideal (plan).

Values of characteristics a_i and a_i is possible to calculate directly by mathematical processing of the set of indices changes - P_i which are the criteria for the realization of the set of functions.

During the calculation of the significance factor a_i it is necessary follow some rules:

- research of the strategic complex of variable factors of all the functions of the manufacturing system has to be conducted within pretty-long period of time;

- it is usually determined by sampling of statistic data;
- for each factor it is necessary to determine the ideal (planned) value- $P_i^{n\pi}$;

- for each function their shall be determined the factors of sufficiency in execution of a_i which create a set:

$$\alpha_i = \frac{P_i^{\phi}}{P_i^{n\pi}}, \tag{2}$$

where P_i^{ϕ} – real value of a certain function; $P_i^{n\pi}$ – ideal (planned) value of a certain function.

If $P_i^{\phi} < P_i^{n\pi}$ - this testifies to partial execution of the i-th function and if $P_i^{\phi} \geq P_i^{n\pi}$ - it considered to be the full execution of the i-th function.

The level of the organization depends on how fully urgent and precise are the functions of the elements of this system, *i.e.* components of the manufacturing system. In the process of its functioning, an enterprise as a system under influence of managerial activities approaches the stable state.

The external environment may not be stable within the whole enterprise's period. Therefore the enterprise must constantly adapt to the changes in the environment.

Such response of a system, if these changes do not cause the catastrophe, is called labialization, which means the possibility of the function to change without the significant change in its structure. In this case the labiality of the enterprise is determined as its ability to sustain deviations of external factors within a certain range which is the condition of enterprise's vitality.

A principle of labiality is a separate case of sustainability and is used as a factor of enterprise's stability in external environment in correspondence to its stabilizing factors.

It's necessary to note, that the range of labiality of the enterprise depends on both, force and direction of external factors and on personal potential and business activity.

The aggregate of ranges of deviations from the stable state relating to each of the external factor creates a field of labialization.

There had been determined the following positions of the enterprises relating to the field of labiality:

- position of normal state- an enterprise is organized quite well;

- position of a tense state (organized);

- position of the not stable sate (not well organized), when the external factors exceed the margin of labiality range;

- position of the extreme state (weakly organized enterprise) when an impact of destabilizing factors is very high.

Following the statistical research and expert evaluations, there had been suggested method for the determination of the margin of the range of enterprise's labiality. It is backgrounded on the force of influence of destabilizing external factors and potential of the enterprise.

Table 1

Margins of Labialization of Automobile Transport Enterprise

	General characteristic of situation	Margin of enterprise labiality	Possible strategies
+5+10	Well organized enterprises. Negative influence of external factors is minimal; the speed of regeneration processes exceeds rate of negative factor change	Stable position. Factor of organization. $K_{opg} = 0,88 - 0,90$	Expansion, creation of different kinds of associations
0+5	Organized enterprises, but influence of external factors exists. Potential of enterprise is equal to or exceeds destabilizing factors, rate of change of destabilizing factors does not exceed the rate of regeneration of an enterprise.	May achieve a point of bifurcation, has the possibility to return to field of labialization, the state homeostasis is preserved $K_{opg} = 0,85 - 0,87$	Diversification, specialization.
0-5	Insufficiently organized enterprises. The force of destabilizing external factors greatly exceeds potential of an enterprise. The rate of change of destabilizing factors exceeds the rate of regeneration processes.	Unstable state, often gets in the point of bifurcation $K_{opg} = 0,82 - 0,85$	Restructuring, merger.
-5-10	Weakly structured enterprises. The force of destabilizing external factors is greatly significant, functioning conditions are usually extreme. Other changes of destabilizing factors greatly exceed the rate of regeneration processes.	Total loss of state of homeostasis. The state is close to crisis. $K_{opg} = 0,80 - 0,82$	Restructuring

The labiality is understood as the ability of manufacturing system withstands the influence of external factors without significant structural changes. In the result of processing of expert data there had been determined the level of enterprises' stability according o the great scale (Table 1).

Each level of stability of enterprise is characterized by a certain force of influence of destabilizing factors of external environment, correlation of ways of their changes and regenerative processes on automobile transport enterprise. The destabilizing factors are: change of cargo type to transport; change of transportation technology; unexpected change in cargo volume declared for transportation; unexpected rejection of clients from transportation services, rendered by company; road accidents and etc.

The formation of strategic factors which ensure long-term success of the automobile transport enterprise may be executed by realization of the following functions: determination of strategic factors of success in the activity of an enterprise; creation of strategic potential for success of an enterprise; transformation of strategic potential into strategic factors of success. Transformation of strategic potential into strategic factors of success is possible only on condition of efficient marketing activity.

As is seen from Table 1, the level of stability of enterprise, which is located in the range [+5 +10] testifies to the economic stability on the market of transportation services.

Under such conditions the enterprise has the possibility to use the development strategies such as: expansion, creation of different types of associations, diversification and specialization etc. (Біліченко & Цимбал, 2004).

The state of enterprises which are within the interval of labiality [-5 -10] is characterized as the margin of stability, such conditions require extreme actions overcome the state.

Management of an enterprise in this case takes place under non-standard or extreme conditions and must be directed to overcoming of negative phenomena, trying to overcome the state of crisis.

3. Conclusion

The development of the manufacturing system may be achieved only on condition of stable organizational and financial state.

It had been determined that the stability in functioning and development of automobile transport enterprises, as the manufacturing system is characterized by the level of organization and labiality.

The organization is understood to be the stage of realization of functions of separate elements of manufacturing system, and labiality – the

ability withstands the influence of external factors without the significant structural changes.

There had been determined the relative fields of labiality and possible positions of enterprises: position of normal state, position of a tense state, and position of an unbalanced state.

There had been introduced grade scale system for evaluation of stability as well as determined the factor of organization. Using these factors allows us to suggest this or the other strategy for the development of the specific automobile transport enterprise.

REFERENCES

Афанасьев Н.В., *Управление развитием предприятия: монография.* Афанасьев Н.В., Рогожин В.Д., Рудыка В.И. – Х.: Издательский Дом "ИНЖЭК", 184 с, 2003.

Ансофф И., *Стратегическое управление.* И. Ансофф. – М.: Экономика, 358с, 2006.

Майкл Портер. *Конкурентная стратегия. Методика анализа отраслей и конкурентов.* – 2-е изд. / Майкл Портер. – М.: АльпинаБизнесБукс, 454 с, 2006.

Біліченко В.В., Цимбал С.В. *Стратегії розвитку підприємств автомобільного транспорту в умовах ринкових відносин // Вісник Східноукраїнського національного університету ім. Волод. Даля.*, 7 (77), част. 1, С. 97-102 (2004).

STABILIREA STRATEGIILOR PENTRU DEZVOLTAREA MANAGERIAL-TEHNICĂ A SISTEMELOR DE PRODUCTIE ÎN TRANSPORTUL AUTO

(Rezumat)

S-au determinat termenii sistemului de producţie şi ai dezvoltării managerial-tehnic ai sistemului de producţie. S-a sugerat folosirea managementului calităţii ca şi index al credibilităţii întreprinderilor. Este posibil se evidenţieze poziţiile întreprinderilor în funcţie de domeniile lor de răspundere şi ca răspuns la acestea strategiile cele mai raţionale de dezvoltare.

A CONTRIBUTION TO THE RECOVERY OF POLIMETALLIC CONCENTRATES FROM COMPONENTS OF ELECTRONIC WASTE

BY

IONELA POENIȚA BÎRLOAGĂ* and **TRAIAN BUZATU**

University Politehnica of Bucharest,
Department of Engineering and Management
for Elaboration of Metallic Materials

Abstract. Waste microprocessors disassembled from obsolete computers were used for the experiments. In this work, a fundamental study has been carried out on the mechanical pre-treatment that is necessary to recover metallic concentrates from electronic waste. The objective is to recover precious metals, especially gold, from the waste electrical and electronic equipment (microprocessors) by technological flows which consist in: sorting microprocessors, milling and magnetic separation. Sorted microprocessors were crushed with a hummer and after that were milled in to type of mill: the plastic microprocessor was milled in a cutting mill and the ceramic microprocessors in a vibratory disc mill. The milled concentrates were separated into magnetic and non-magnetic fractions by means magnetic laboratory separator. After these technical methods, the concentrates were analyzed by X-ray fluorescence XEPOS spectrometer.

Key words: microprocessors, sorting, magnetic separation, concentrates.

---

* Corresponding author e-mail: ionelabirloaga@yahoo.com

1. Introduction

In the last decades the treatment of electronic and electric waste represents a priority field as their role in modern life is increasing.

Have been performed studies for recycling of waste electric and electronic equipment by techniques such as mechanical, thermal and chemical processes (Zhang *et al*., 1998; Hall & Williams, 2007; Oishi *et al*., 2007), but most of them dealt with the recovery of one or two specified materials of all WEEE compositions.

In this paper are present the first preliminary stages of recovering precious metals to form used microprocessor by physical processes such as: sorting, milling and magnetic separation. This study is expected to continue obtaining data useful for next steps into the recovery of precious metals used in manufacturing of microprocessors.

2. Experimental

Waste microprocessors disassembled from obsolete computers were used for the experiments. The microprocessors used for the experiment were two types: embedded microprocessors in plastics materials and embedded microprocessors in ceramics materials.

The microprocessors were sorted and was resulted a quantity of 173.05g microprocessors embedded in plastic material and a quantity of 171.68g microprocessors embedded in ceramic material and then were milled. Plastic microprocessors have been milled in heavy-duty cutting mill and the ceramics in vibratory disc mill.

The concentrates resulted by milling of plastic microprocessors were then volumetrically separated using a sieve with a mesh size of 0.8 mm.

From this physical processes were resulted three samples with different dimensions and aspects. The milled samples were then separated magnetic to performed separation of the magnetic and non-magnetic fractions.

This process was done whit a high-intensity induced-roll magnetic laboratory separator. The distribution of the major elements in all six fractions is present in Table 1.

Copper is the most abundant metallic element in the plastic microprocessors, while aluminum is the metal with the highest content in ceramic microprocessors.

By the magnetic separation, iron and nickel, which are the typical ferromagnetic metallic elements, were largely separated into the magnetic fraction.

In the non-magnetic fraction the mostly distributed were the paramagnetic or diamagnetic elements, such as aluminum, tin, copper, and lead.

Beside this metals others elements appear, but in low concentrations.

At the end of preparation technology the precious metal distribution for each fraction of plastic microprocessor embedded in plastic materials was as the following: gold wasn't present in the first sample because, after magnetic separation, it was distributed more in the magnetic fraction, fractions with a size greater than 0.8 mm, while in those with sizes smaller than 0.8 mm, this precious metal was proportionately distributed in the fractions with nonmagnetic and magnetic particles.

In the magnetic fraction of milled plastic microprocessor with a particle size smaller than 0.8 mm in addition to gold silver appears with a concentration of 0.24%. It results that gold is well separated by magnetic separation from larger particles while silver is good separated from a smaller size.

Table 1
Distribution of the Major Elements in Mass Samples

Sample / Element%	M. Plastic A				M. Ceramic B	
	1 Fr. non-mag. >0,8	2 Fr. mag. >0,8	3 Fr. non-mag.<0,8	4 Fr. mag. <0,8	5 Fr. non-mag.	6 Fr. mag.
Al	0.00	0.96	3.10	3.38	37.10	25.50
Si	17,80	5.25	17.40	17.40	6.29	5.13
Fe	0.25	5.87	0.40	3.21	0.34	0.85
Ni	0.12	10.90	0.12	1.86	0.15	0.66
Cu	25.50	23.40	16.40	15.60	0.14	0.30
Zn	0.16	0.00	0.31	0.27	0.00	0.00
Au	0.00	1.56	0.21	0.49	0.19	0.00
Ag	0.00	0.00	0.00	0.24	0.38	1.31

Fractions resulting from magnetic separation of ceramic microprocessors exhibited the following precious metals distribution: gold remained in the magnetic fraction in a concentration of 0.19%, while silver was distributed in both samples, with concentrations of 0, 38% in the non-magnetic fraction and 1.31% in the magnetic fraction.

3. Results and Discussion

Samples of 8g of each fraction were analyzed to determine the elements and their distribution in concentrates obtained after milling and magnetic separation. These samples were analyzed by X-ray fluorescence using an X-ray fluorescence XEPOS spectrometer.

Fig. 1,..., 3 shows the X-ray fluorescence for fraction with the highest content of precious metals obtained after milling and magnetic separation of used microprocessors.
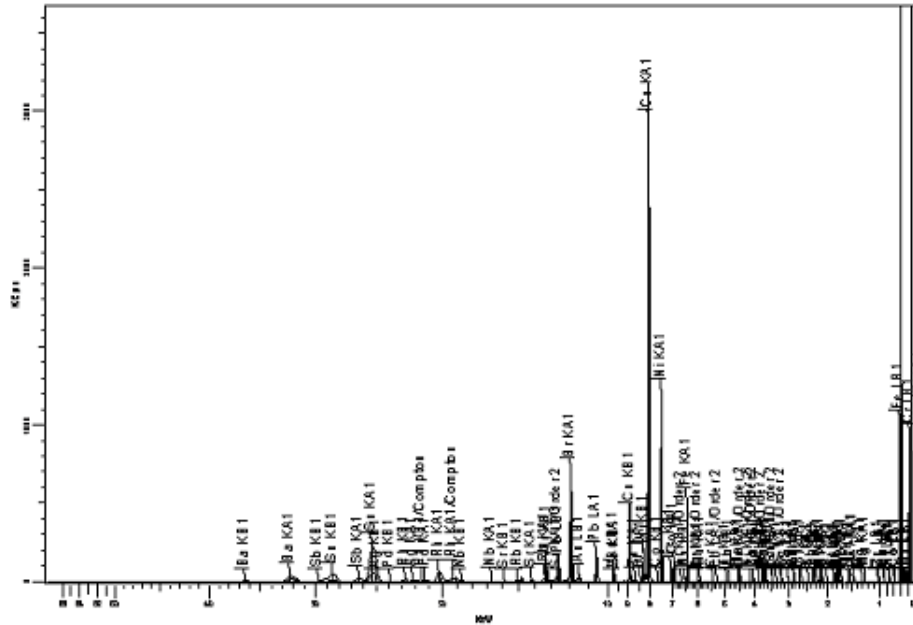
Fig. 1 – XRF analysis of plastic microprocessors, size> 0.8 mm, magnetic fraction.
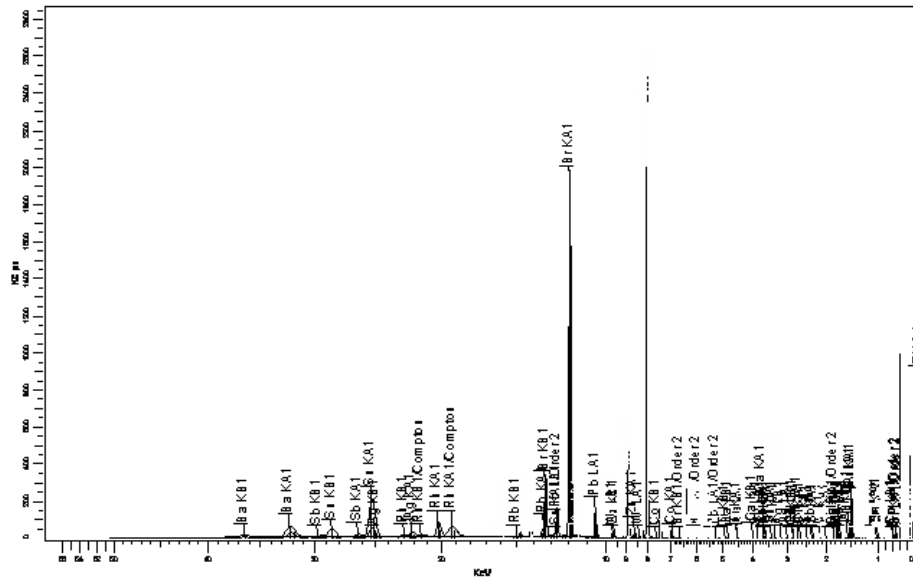
Fig. 2 – XRF analysis of plastic microprocessors, size < 0.8 mm, magnetic fraction.
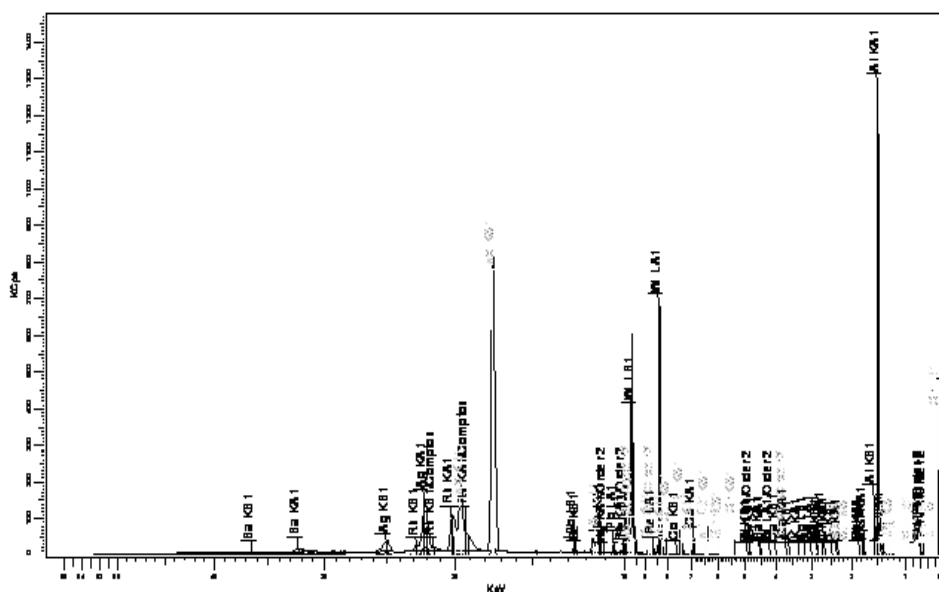
Fig. 3 - XRF analysis of ceramic microprocessors, size < 0.8 mm,
non magnetic fraction.

4. Conclusion

From the results obtained, the following may be concluded: Following the milling process, which was performed in two types of mills, due to different embedding materials for microprocessors, two types of concentrates resulted, one of microprocessors embedded in plastic, with particles of different sizes, and the other of microprocessors embedded in ceramic materials, in powder form.

It can be said that gold was separated best in the magnetic fraction of plastic microprocessors concentrates with size dimensions greater than 0.8 mm and had a much higher concentration than those with smaller size. After magnetic separation, in was noticed that in the concentrates from microprocessors with ceramics gold was left in the non-magnetic fraction, while silver was distributed in both fractions, but with a higher concentration in the magnetic fraction.

REFERENCES

Bîrloagă I., Buzatu T., Matei E.*, Physical Methods for Processing Electronic and Electrical Equipment Waste (WEEE) for Nonferrous Metals Recovery.*

Hall W.J., Williams P.T., *Separation and Recovery of Materials from Scrap Printed Circuit Boards.* Resources, Conservation and Recycling, **51**, *3*, September 2007, 691-709.

Oishi T., Koyama K., Konishi H., Tanaka M., Lee J.C., *Influence of Ammonium Salt on Electrowinning of Copper from Ammoniacal Alkaline Solutions.* In Electrochimica Acta, **53**, *1*, 20 November 2007, 127-132.

Zhang S., Forssberg E., Arvidson B., Moss W., *Aluminum Recovery from Electronic Scrap by high-Force Eddy-Current Separators.* In Resources, Conservation and Recycling, **23**, *4*, September 1998, 225-241.

O CONTRIBUŢIE PRIVIND RECUPERAREA COCENTRALELOR POLIMETALICE DIN COMPONENTELE DEŞEURILOR ELECTRONICE

(Rezumat)

Pentru experiment au fost folosite deşeuri din echipamentele electrice şi electronice. În acestă lucrare un studiu fundamental s-a efectuat asupra pretratamentului mecanic care este necesar recuperării concentratelor metalice din deşeurile electronice. Obiectivul este recuperarea metalelor preţioase, în special aur, din deşeurile echipamentelor electrice şi electronice (microprocesoare) printr-un flux tehnologic care a constat în: sortarea microprocesoarelor, măcinarea şi separarea magnetică. Microprocesoarele sortate au fost mărunţite cu un ciocan şi apoi măcinate în două mori: microprocesoarele din plastic în moara cu cuţite tăietoare, iar cele din ceramică în moara cu discuri oscilante. Concentratele măcinate au fost apoi separate în fracţii magnetice şi nemagnetice cu ajutorul unui separator magnetic de laborator. După aceste metode tehnice, concentratele au fost analizate cu un spectrometru de fluorescenţă XPOS de raze X.

ABOUT THE POSITIONING OF THE ULTRASONIC ENERGY REFLECTORS DURING THE PROCESS OF THE THIN AND VERY THIN WIRES DRAWING

BY

FRANCISC BIRO[3]*, MIHAI SUSAN[1], VIOREL ILIESCU[2], BOGDAN GAVRILĂ[1], ORESTE CRISTODULO[1] and BOGDAN APREUTESEI[2]

[1]Technical University "Gheorghe Asachi" of Iaşi,
The Faculty of Materials Science and Engineering
[2]S.C. Cablero S.R.L.
[3]S.C. CORD S.A. Buzău

Abstract. The paper presents a calculation method for the determining of the positioning distances of the ultrasonic energy reflectors, during the drawing process of the thin and very thin wires in ultrasound field, when the die is placed in the antinodes of the wave oscillation and it is activated along the drawing direction.

Key words: ultrasounds, ultrasound field, oscillator system, ultrasonic energy reflector, positioning distance of the reflector.

1. Introduction

The technologies of the metals drawing in ultrasound field are modernized technologies/MT, in comparison with the classic technologies/CT, and their aim is to obtain "softening effects" or "surface effects" of the ultrasounds. The ultrasounds are a variety of elastic waves which have the values of the frequency between 16000Hz and 10^{10}Hz. The area of the elastic

---

* Corresponding author e-mail: bgdnlcn@yahoo.com

medium which is in a vibratory state and it is the place of the ultrasound waves is called ultrasound field.

During the wires drawing processes, ultrasound activated, there are used special oscillator systems presented in Fig.1, (Severdenko *et al.*, 1990; Susan, 2008). The oscillator system presented in Fig.1*a* is recommended in the drawing process of the thin, very thin and medium thickness wires; for the drawing process of the thick wires, the recommended oscillator systems are presented in Fig.1*b*,…, *d*.

During the wires drawing process with the die placed in the antinodes of the wave oscillation and activated along the drawing direction, it takes place "the ultrasound surface effect", an effect which is explained based on "the reversion mechanism of the mean friction"; the die is placed in the maximum point of the stress, however its activated way is. It also takes place a strong "volume effect" based on the mechanism of the superposition of the ultrasound stresses on the deformation static once, (Severdenko *et al.*, 1990; Susan, 2008). So, the expected effect of the ultrasound energy action in the plastic deformation drawing will be obtained when there are used high energy ultrasounds – longitudinal ultrasound waves as standing waves with antinodes and vertexes (maximums and minimums) of the oscillation, Fig.2.
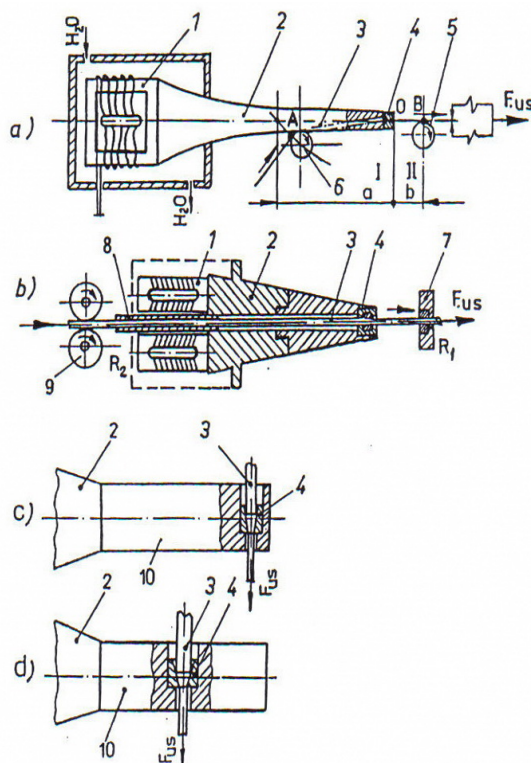
Fig. 1 – Specific oscillator systems used for the wires drawing, (Severdenko *et al.*, 1990): *a*) and *b*) the die is placed in the antinodes of the wave oscillation and it is activated along the drawing direction; *c*) the die is placed in the antinodes of the wave oscillation and it is activated normally on the drawing direction; *d*) the die is placed in the maximum of the waves stress and it is activated normally on the drawing direction; *1* – magnetostrictor transducer; *2* – energy concentrator; *3* – semi-finished wire; *4* – die; *5*, *6* – ultrasound energy reflectors (pressure rolls); *7* – additional die; *8* – guiding tube for the semi-finished wire; *9* – pressure rolls (R_2); *10* – waveguide.

As a matter of fact, depending on the displacement of the deforming focus/the drawing tool – minimum or maximum of the wave oscillation – it will obtain "the softening effect" or "the reduction of the metal – tool contact friction effect" – also called "the ultrasound surface effect" because it takes place at the metal – tool contact surface, (Grant CNCSIS – tip A / Gr. 80, 2007).
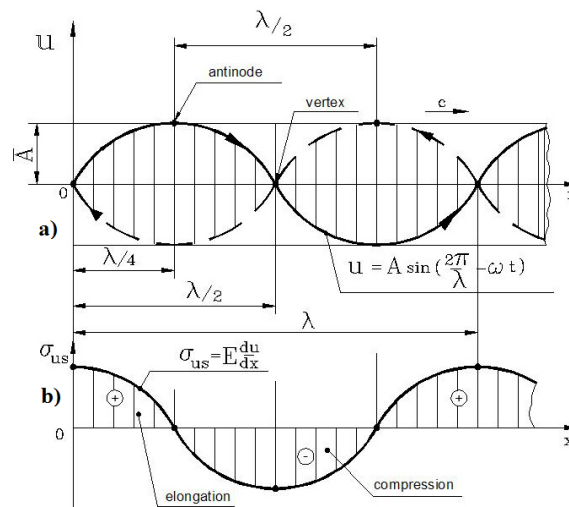
Fig. 2 – Standing waves system (Grant CNCSIS – tip A / Gr. 80, 2007): a) motion of the wave (u); c-ultrasounds wave velocity; λ-wavelength (λ = c/f, f – frequency resonance); Ā-oscillation amplitude of the wave / maximum value: ――― running wave; – – – – regressive wave.

The paper makes an analyze of the ultrasound drawing process of the thin and very thin wires, $\Phi \in (1,5…0,01\text{mm})$, made from metallic materials, hardened by cold plastic deformation; the die is placed in the antinodes of the wave oscillation and it is activated along the drawing direction. There was used a variety of oscillator systems, as Fig.1*a* shows. The using of this kind of oscillator system in the ultrasonic drawing process implied the using of the ultrasonic energy reflectors (pressure rolls) which were placed at well defined distances, at the oscillator system level (distances a and b).

2. Positioning of the Ultrasonic Energy Reflectors During the Process of thin and Very thin Wires Drawing

The plastic deformation by drawing in ultrasound field, "ultrasonic vibration drawing"/ UVD System or UVD Technology, became very interesting to study in the case with the die placed in the antinodes of the wave oscillation

and activated along the drawing direction. The using of this kind of oscillator system goes to the using of the ultrasonic energy reflectors (the using of the ultrasound energy along well defined distances, a and b), Fig.3.

In the case of the ultrasound drawing / UVD Technology of the thin and very thin wires, according to Fig.1*a*) and the technological elements presented in Fig.2, the displacement of the reflectors must always be in the vertexes (minimum) of the wave motion, (Severdenko *et al.*, 1990; Susan, 2008).
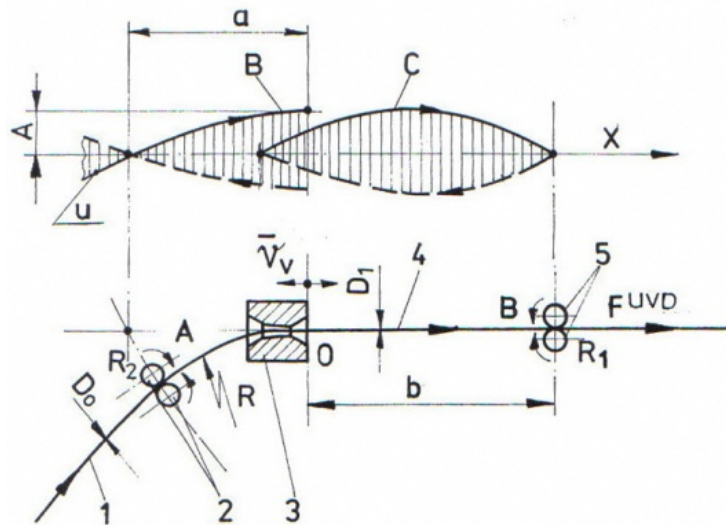
Fig. 3 – Ultrasonic activation of the die along the drawing direction: 1 – semi finished wire; 2, 5 – ultrasound energy reflectors, (R_1, R_2 / pressure rolls); 3 – die; 4 – drawn wire; A –maximum amplitude of the wave oscillation; B – wave oscillation at the oscillator system level; C – wave oscillation of the processed wire; D_0, D_1 – wire diameters (semi-finished and, respectively, processed wire); $\overline{v_v}$ - vibratory rate of the die; a, b – positioning distances of the ultrasound energy reflectors: ——— running wave; – – – – regressive wave.

It considers O, the point of application of the drawing force varying according to the displacement law given by the relation (1), (Severdenko *et al.*, 1990; Susan, 2008):

$$F^{UVD} = A_0 \cdot \sin \omega t \qquad (1)$$

where: A_0 – oscillation amplitude; ω – angular frequency, ($\omega = 2\pi f$); t – time.

The variation of the particles transfer function on the distances a and b is given, respectively, by the relations (2) and (3):

$$U_1 = A_1 \sin\frac{\omega}{c}(x+a)\sin\omega t \tag{2}$$

$$U_2 = A_2 \sin\frac{\omega}{c}(x-b)\sin\omega t \tag{3}$$

where: A_1, A_2 – oscillation amplitudes; a, b – distances from the die to the ultrasound energy reflectors; x – current coordinate.

Due to the fixing of the wire at its contact point with the energy reflectors, it results $U_1(a, t) = 0$ and $U_2(b, t) = 0$.

In point O, the continuity conditions must be obey, $U_1(o) = U_2(o)$, so, it results the relation (4):

$$A_1 \sin\frac{\omega}{c}a + A_2 \sin\frac{\omega}{c}b = 0 \tag{4}$$

The forces which action in point O must be in a phase concordance, meaning that the relation (5) may be written:

$$E \cdot S \cdot \left[\frac{\partial U_1}{\partial x}(o) - \frac{\partial U_2}{\partial x}(o)\right] = F^{UVD} \tag{5}$$

where: E – elastic modulus; S – wire section.

Replacing the partial derivative of the functions U_1 and U_2 in the relation (4), it will obtain the relations (6) and (7):

$$A_0 = E \cdot S\frac{\omega}{c}A_1\cos\frac{\omega}{c}a - E \cdot S\frac{\omega}{c}A_2\cos\frac{\omega}{c}b \tag{6}$$

$$A_1\cos\frac{\omega}{c}a - A_2\cos\frac{\omega}{c}b = \frac{A_0}{E \cdot S}\cdot\frac{c}{\omega} = B_0\frac{c}{\omega} \tag{7}$$

Resolving, in the same time, the relation (4) and (7), it will determine the amplitudes A_1 and A_2 as functions of a and b. So, it results the equations (8) and (9):

$$A_1 = B_0\frac{c}{\omega}\cdot\frac{\sin\frac{\omega}{c}b}{\sin\frac{\omega}{c}(a+b)} \tag{8}$$

$$A_2 = B_0 \frac{c}{\omega} \cdot \frac{\sin \frac{\omega}{c} b}{\sin \frac{\omega}{c}(a - b)} \tag{9'}$$

Respectively, the corresponding deformations are given by the relations (10) and (11):

$$\varepsilon_1 = \frac{\partial U_1}{\partial x} = B_0 \frac{\sin \frac{\omega}{c} b}{\sin \frac{\omega}{c}(a + b)} \cos \frac{\omega}{c}(x + a) \tag{10}$$

$$\varepsilon_2 = \frac{\partial U_2}{\partial x} = B_0 \frac{\sin \frac{\omega}{c} b}{\sin \frac{\omega}{c}(a - b)} \cos \frac{\omega}{c}(x - b) \tag{11}$$

If the values of a and b will be choose as the conditions $\sin \frac{\omega}{c} a = 0$ and $\sin \frac{\omega}{c} b = 1$ to be satisfied, the output deformation ε_2 will be equal to 0 and the input deformation will be given by the relation (12):

$$\varepsilon_1 = B_0 \cos \frac{\omega}{c}(x + a) \tag{12}$$

This means that the wire deformation will have a maximum value, so, the heat emission in points A and B will be maximum. In this situation, the wire output from the die will not rise its temperature as an ultrasound effect.

From relations $\sin \frac{\omega}{c} a = 0$ and $\sin \frac{\omega}{c} b = 1$, it results the values of the distances a and b, relations (13) and (14):

$$a = \pi \frac{c}{\omega} \tag{13}$$

$$b = \pi \frac{c}{2\omega} \tag{14}$$

where: c – ultrasound wave velocity into the metallic material

In Table 1, there are represented the values of the distances a and b during the drawing of the thin and very thin wires made from various metallic materials.

Table 1

Values of the Distances a and b During the Drawing of thin and Very thin Wires, Made from Various Metallic Materials

No.	Metallic material	Ultrasound wave velocity, c [m/s]	Resonant frequency, f [Hz]	a [mm]	b [mm]
1	Steel	5050	18000	140	70
			20000	126	63
			22000	114	57
2	Gold	2030	18000	56	28
			20000	50	25
			22000	46	23
3	Silver	2640	18000	72	36
			20000	66	33
			22000	60	30
4	Molibdenum	5170	18000	142	71
			20000	128	64
			22000	116	58
5	Nickel	4760	18000	132	66
			20000	118	59
			22000	108	54
7	Titanium	4260	18000	118	59
			20000	106	53
			22000	96	48

3. Conclusion

The paper presents oscillator systems specifically for the thin and very thin wires drawing in ultrasound field, when the die is placed in the antinodes of the wave oscillations and it is activated along the drawing direction. In this case, the process of plastic deformation goes to "the ultrasound surface effect" or "the reduction of the metal – tool contact friction effect". A better usage of the ultrasound energy, on well defined lengths of the wire, will take place using the ultrasound energy reflectors which, from a technological point of view, "close" the oscillator system.

For the determining of the positioning distances of the ultrasound energy reflectors, a calculation method was presented; the method takes into account the sinusoidal variation of the wave oscillation.

REFERENCES

∗ ∗ Grant CNCSIS – tip A / Gr. 80, 2007.

Severdenko V.P., Klubovici V.V., Stepanenko A.V., *Prokatkia i volocenie c ulitrazvukom*. NAUKA I TEHNICA, Minsk, 1990.

Susan M., *Tragerea metalelor cu vibraţii ultrasonice*. Editura CERMI , Iaşi, 2008.

DESPRE POZIŢIONAREA REFLECTORILOR DE ENERGIE ULTRASONICĂ LA TREFILAREA SÂRMELOR SUBŢIRI ŞI FOARTE SUBŢIRI

(Rezumat)

Lucrarea prezintă o metodă de calcul pentru stabilirea distanţelor de poziţionare a reflectorilor de energie ultrasonică la trefilarea sârmelor subţiri şi foarte subţiri în câmp ultrasonor, atunci când filiera este poziţionată în maximul oscilaţiei undelor şi activată pe direcţia tragerii.

DISMOUNTABLE TYPE D LAMELLAR HEAT EXCHANGERS

BY

CONSTANTIN BORIS[*]

"Gheorghe Asachi" Technical University of Iaşi

Abstract. In the case of this type of exchanger the intermediary (inter-lamellar) channels have the shape of a flux network. The lamellae are dollied from steel in sheets of various marks. The gofferings of the lamellae have in their sections the profile of an isosceles triangle with a base of 36 mm and the height of 4.5 mm. The technical feature of the lamella: Measurements (length, width, thickness), mm: 960 x 460 x 1; Area of the surface of the heat exchange in square meters: 0.2; Weight, Kg: 2.5.

Key words: heat exchangers on consollic frame, Heat exchanger on frame with double support

1. Introduction

1.1. Type 0,2 Lamellar Heat Exchangers

In the case of this type of exchanger the intermediary (inter-lamellar) channels have the shape of a flux network. The lamellae are dollied from steel in sheets of various marks. The gofferings of the lamellae have in their sections

---

[*] Corresponding author e-mail: borisconstantin@yahoo.com

the profile of an isosceles triangle with a base of 36 mm and the height of 4.5 mm. The technical feature of the lamella: - Measurements (length, width, thickness), mm: 960 x 460 x 1; - Area of the surface of the heat exchange in square meters: 0.2; - Weight, Kg: 2.5.

The machines are meant for the work with liquids, as well as for the condensation in the exchanger of the steams between gas and liquid fluxes. They work at a certain pressure of up to 1 Mpa (up to 10 kgf/sq.cm.) and the temperature of the working media ranges from 253° to 423° K (*i.e.* from - 20° to + 150°C).

The machines have small hydraulic resistance (see Table 1). On the contour of the lamellae one may notice channels for the rubber fittings. The passing holes in the lamella are placed diagonally.

The lamellae are assembled on the rods of the frame (with no suspension mechanism). Each lamella is positioned at 180° from the other lamella. Depending on the construction of the support frames, the type 0,2 heat exchangers can be manufactured in three ways: 1 – on consollic frame, 2 – on frame with double support and 3 – on frame with triple support.

1.2. Heat Exchangers on Consollic Frame

Example: the conventional notation of the dismountable heat exchanger with lamellae of the type 0,2, the area of the surface of the heat exchange of 5 square meters, on consollic frame, lamellae with a thickness of 1 m; of steel 10 H 17 N 12 m 2 T, with rubber fittings, with a composition scheme Sc $\frac{13}{14}$; Heat exchanger D 0,2 -5-1K-0 SF.001.96 Sc $\frac{13}{14}$; steel lamellae 10 H 17 N 13 M 2 T; rubber fittings.

Table 1
Measurements (mm) and Weight of Machines (kg)

Type of the lamella	Code	Nominal area of the surface of the heat exchange in square meters	Number of lamellae from the machine	L	L₁	L₂	L₃	Weight	
								General weight	Weight of the parts made of anti-corrosive steel
0,2	36 1251 3089	1	8	0	190	190	340	546	12
	36 1251 3104	2	12	0	215	220	375	562	24,5
	36 1251 3119	5	28	53	315	340	500	622	172,5
	36 1251 3134	6,3	34	85	350	385	550	645	130,7

1.3. Heat Exchanger on Frame With Double Support

Example: conventional notation of the dismountable heat exchanger with lamellae of the type 0,2, the area of the surface of the heat exchange of 10 square meters, on double support frame, steel lamellae 10 H 17 M 13 M2T, with rubber fittings, with the composition scheme Sc $\frac{25}{26}$; Heat exchanger D 0,2 - 10 - 2K - 0,6, SF.001-96 Sc $\frac{25}{26}$; steel lamellae 10 H 17 N 13 M2T; rubber fittings.

Table 2

Measurements (*mm*) *and Weight of Machines* (*kg*)

Type of the lamella	Code	Nominal area of the surface of the heat exchange in square meters	Number of lamellae from the machine	L	L_1	L_2	L_3	Weight	
								General weight	Weight of the parts made of anti-corrosive steel
0,2	36 1251 3149 36 1251 3164	10 12,5	52 66	78 51	495 545	770 880	847 957	24 771	131,5 166,9

1.4. Heat Exchangers on Frame with Triple Support

These are recommended in case of frequent dismounting and mounting for the cleaning of the machine.

Table 3

Measurements (*mm*) *and Weight of Machines* (*kg*)

Type of the lamella	Code	Nominal area of the surface of the heat exchange in square meters	Number of lamellae from the machine	L	L_1	L_2	L_3	Weight	
								General weight	Weight of the parts made of anti-corrosive
0,2	36 1251 3179 36 1251 3194 36 1251 3209 36 1251 3224	16 25 31,5 40	84 128 160 204	20 40 23 37	895 1040 1255 1480	85 65 90 160	615 975 225 565	222 371 485 636	208 324 401 511

Fig. 1 – General view of the heat exchanger with measurements
and coupling parameters.

Example: conventional notation of the dismountable heat exchanger
with lamellae of the type 0,2, the area of the surface of the heat exchange of 16
square meters, on the frame with triple support, of steel 12 H 18 N 10T, with
rubber fittings with a composition scheme Sc $\dfrac{10+10}{11+10}$ ‖ $\dfrac{10+10}{11+10}$:

Heat exchanger D 0,2 – 16 3k – 12 SF. 001-96 Sc $\dfrac{10+10}{11+10}$ ‖ $\dfrac{10+10}{11+10}$;

Steel lamellae 12 H 18 N 10T; rubber fittings.

1.5. Type 0,3 D Lamellar Heat Exchanger

These are meant to function in liquid and vapor media and refer to a
small number of surfaces of the heat exchanger. They work on a theoretical
pressure of up to 1 MPa (up to 10 Kkf/sq.cm.), the temperature of the working
media ranging from 253 up to 423 K (from -20 to + 150°C) (according to the
brand of the fittings).

The heat exchangers are manufactured according to SF.001 - 96 for
industrial use. The lamellae with a 60° inclination angle of the gofferings in
relation to the longitudinal axis of the lamella are much more efficient for the
working media whose viscosity is closer to the viscosity of the water.

The lamellae are made of steel in sheets, the thickness of the lamella
(depending on the beneficiary's will) being 0.8 mm or 1 mm. On the contour of
the lamella one has a channel for rubber fittings. Strengthening the fittings on
the channel is done with the help of keys.

The lamellae in the machine are thus assembled so that all the fittings are oriented in the direction of the mobile plate. The lamellae are done from all brands of steel given in Table 5. The lamellae of the type 0,3 d are not to be dollied.

The technical feature of the lamella

The area of the surface of the heat exchange in square meters: 0,3

The measurements (length x width x thickness): 1370 x 300 x 1 mm

Weight, Kg : 3,2

The heat exchangers that have a thickness higher than 1 mm are used in aggressive media, with a speed of metal corrosion of 0.05 mm per year.

Angular passing holes of the working media have a complicated shape, which ensures the decrease of the local hydraulic resistance and a great part of the area of the surface of the heat exchange of the lamella is used for heat transfer.

The lamellae on the upper rail of the consollic frame or with double support are attached vertically by means of clamps. Each lamella may be easily taken out of the package and then fitted up in it. Depending on the construction of the support frames, the 0,3 d type heat exchangers are made in two variants: 1 – on consollic frame, 2 – on double support frame.

1.6. The Heat Exchangers on Double Support Frame
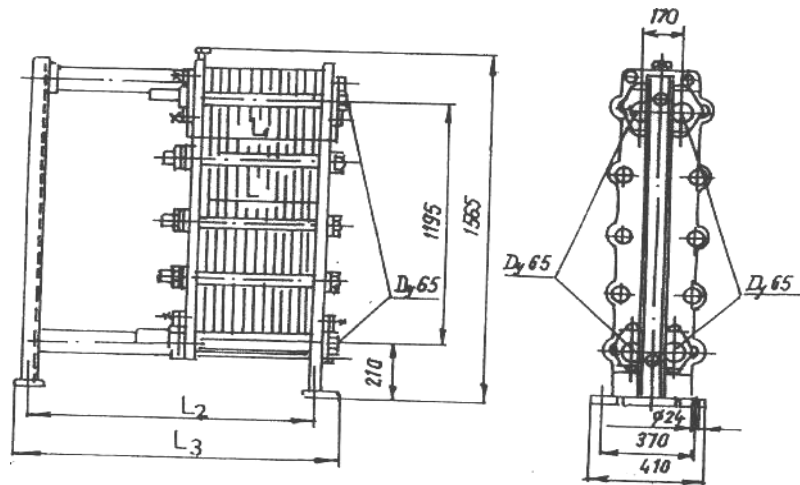
Fig. 2 – General view of the heat exchanger with measurements and coupling parameters.

Example: conventional notation of the dismountable heat exchanger with type 0,3d lamellae, 0.8 thickness, with the area of the surface of the heat exchange of 16 square meters on double support frame, steel lamellae 12 H 18 N 10T, with rubber fittings with a composition scheme Sc $\dfrac{9+9+9}{10+9+9}$;

Heat exchanger D 0,3 - 0,8 - 16 - 2 K - 0,3. SF.001-96. Sc $\dfrac{9+9+9}{10+9+9}$; steel lamellae of steel 12 H 18 N 10T; rubber fittings.

Table 4
Measurements (*mm*) *and Weight of Machines* (*kg*)

Type of the lamella	Code	Lamella Thickness mm	Nominal area of the surface of the heat exchange in square meters	Number of lamellae from the machine	L	L₁	L₂	L₃	Weight	
									General weight	Weight of the parts made of anti-corrosive
0,3d	36 1251 3446	0,8	12,5	44	205	295	740	800	397	112
		1		56	215	305	740	800	425	141
	36 1251 3018	0,8	16		260	350	840	900	436	143
		1		70	270	360	840	900	472	179
	36 1251 3445	0,8	20		320	410	950	1100	481	179
		1		86	335	425	950	1010	526	224
	36 1251 3019	0,8	25		390	480	1065	1130	525	220
		1			410	500	1065	1130	587	275
	36 1251 3019									
	36 1251 3019									
	36 1251 3019									
	36 1251 3019									

1.7. Type 0,6 d Lamellar Heat Exchangers
(inclination angle of the gofferings in relation to the longitudinal axis of the lamella of 60°)

They are meant for work with liquid and vapor media, with a temperature ranging from 253° up until 453°K (from -20° to 180°C) (depending on the brand of the rubber of the fittings). They work at a theoretical pressure of up to 1 HPa (up until 10 kgf/cm²), the working media according to Table 1. The heat exchangers are manufactured according to SF.OO1 for industrial purpose. The heat exchangers with lamellae of the type 0,6 d work more efficiently with liquid working media, which have properties (caloric indices) close to the properties of water. In this case the consumption of the working media in the

machine may be of 1200 - 3000 (m^2 x K) and the hydraulic resistance of up to 0.1 MPa (up to 1 Kgf/cm^2).

1.8. Technical Feature of the Lamella

- Area of the surface of the heat exchange in square meters: 0,6
- Measurements (length x width x thickness),mm: 1375x600x1
- Weight (of the 1 mm sheet), Kg :   5,8

The heat exchanger with the lamella of the thickness of 1 mm is used in aggressive media with the speed of corrosion of the metal of maximum 0.05 mm per year. The lamellae are dollied from steel in sheets (see Table 5). On the contour of the lamella there is a channel for the rubber fitting.

The angular holes for the passage of the working media have a complicated shape.

This allows the decrease of the hydraulic resistance on the entrance of the channel and the exit of it, also allowing the decrease of the separation speed of salts on these portions and ensure a more rational use of the whole surface of the lamella for the heat exchange.

The undulated lamellae are gathered in a pack so that the inclination of the gofferings on the neighboring lamellae is oriented in the opposite direction. The lower rail of the frame is not loaded from the weights of the lamellae destined for fixing them in a given position. Each lamella may be taken out of the pack or introduced in the pack without dismounting the mobile plate and the remaining lamellae. In each pair of lamellae there appears a channel, through which the working media flow.

The channels are in flux, in reticular form. In these the liquid has a sinuous, spatial and tridimensional movement and is thus turbulated.

The total value of the surface of the transversal section of the intermediary channels is constant on all perpendicular sections of the flux of the working medium. The placement of the collecting holes for the entrance and exit of the working medium is only on one side (left or right). The heat exchangers are assembled directly on the floor with hydro-insulating floor, also calculated for the corresponding weight of the machine, and strengthened with truss bolts (screws).

The life of the main parts made of materials subject to work in neutralized media is the following: at least 10 years in the case of lamellae and at least 2 years in the case of the fittings.

Depending on the construction of the support frames, the heat exchangers with 0,6 d type lamellae are manufactured in three variants: 1 – on consollic frame, 2 – on double support frame, 3 – on triple support frame.

1.9. Heat Exchangers on Consollic Frame

The example of the dismountable heat exchanger (conventional notation) with 0,6 d type lamellae, thickness of 0.8 mm, area of the surface of the heat exchange of 16 square meters, on consollic frame, steel lamellae 12 H 18 N 10T, with rubber fittings, with a composition scheme Sc $\dfrac{14}{15}$;

Heat exchanger D 0,6d - 0,8 -16 1K - 01. SF.001 –96. Sc $\dfrac{14}{15}$; steel lamellae 12 H 18 N 10 T, rubber fittings type 359.
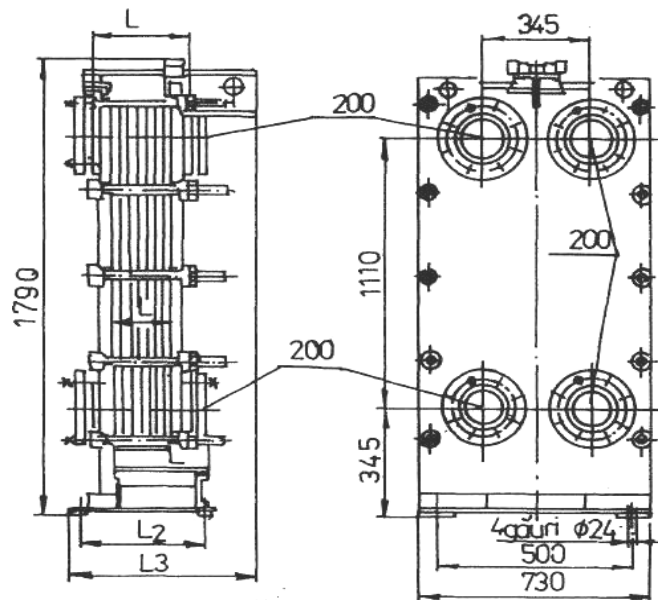
Fig. 3 – General view of the exchange heater with
Measurements and coupling parameters.

The example of the dismountable heat exchanger (conventional notation) with type 0,6 d lamellae, thickness 1 mm, area of the surface of the heat exchange of 80 square meters, on double support frame, steel lamellae 10 H 17 N 13M2T, with rubber fittings, with composition scheme Sc $\dfrac{67}{68}$;

Heat exchanger D 0,6d - 1 - 80 - 2K - 02. SF.001 –96. Sc $\dfrac{67}{68}$; steel lamellae 10 H 17 N 13 M2T, rubber fittings.
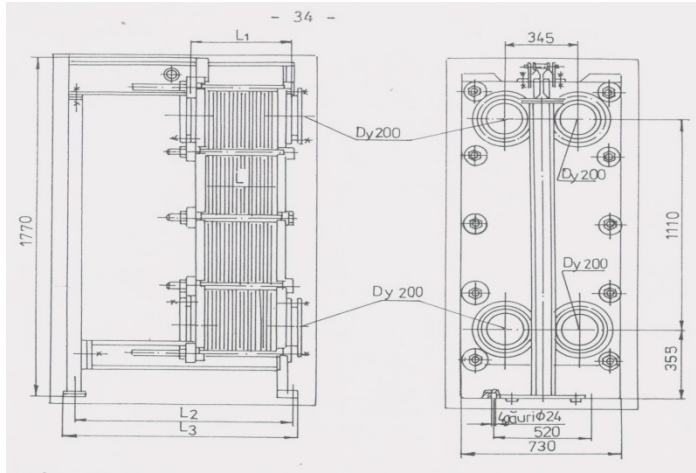
Fig. 4 – General view of the heat exchanger with measurements and coupling (connection) parameters.

Table 5
Measurements (mm) and Weight of Machines (kg)

Type of the lamella	Code	Lamella Thickness mm	Nominal area of the surface of the heat exchange in square meters	Number of lamellae from the machine	L	L_1	L_2	L_3	Weight	
									General weight	Weight of the parts made of anti-corrosive
0,3d	36 1251 3462	0,8 1	10	20	95 100	215 220	290	425	944 976	93 116
	36 1251 3022	0,8 1	16	30	140 145	260 265	365	495	1006 1041	139 174
	36 1251 3461	0,8 1	25	44	205 215	325 335	470	605	1095 1146	205 255
	36 1251 3024									
	36 1251 3463									
	36 1251 3026									

1.10. Heat Exchanger on Triple Support Frame

Example: the conventional notation of the dismountable heat exchanger with 0.6 d type lamellae, thickness 1 mm, the area of the surface of the heat exchange of 200 square meters, on triple support frame, steel lamellae 12 H 18 N 10T, with rubber fittings type 4321-1, with compositions scheme Sc $\frac{84}{85}$ ‖ $\frac{84}{85}$;

Heat exchanger D 0,6 d - 1,0 - 200 - 34 - 03.SF.001-96 Sc $\frac{84}{85}$ $\parallel$ $\frac{84}{85}$; steel lamellae 12 H 18 N 10T, rubber fittings.

Fig. 5 – General view of the heat exchanger with measurements and coupling parameters.

Table 6

Measurements (*mm*) *and Weight of Machines* (*kg*)

Type of the lamella	Code	Lamella Thickness mm	Nominal area of the surface of the heat exchange in square meters	Number of lamellae from the machine	L	L_1	L_2	L_3	Weight	
									General weight	Weight of the parts made of anti-corrosive
0,6d	36 1251 3024	0,8 1	31,5	56	310	390 455	980 1080	1100	1207 1270	26 32
	36 1251 3460	0,8 1	40	70	385	539	1180	1200	1291 1371	32 40
	36 1251 3459	0,8 1	50	86	475 590	635	1340	1300	1385 1483	40 49
	36 1251 3028	0,8 1	63	108	745	765	1540	1460	1510 1636	50 62
	36 1251 3458	0,8 1	80	136	925	945	1780	1660	1676 1834	63 78
	36 1251 3029	0,8 1	100	170	1135	1155 1690	2290 2530	1900	1880 2076	78 98
	36 1251 3457	0,8 1	140	236	1385			2360	2265 2538	110 137
	36 1251 3030	0,8 1	160	270				2600	2463 2774	117 146
	36 1251 3456									
	36 1251 3031									
	36 1251 3455									
	36 1251 3032									
	36 1251 3454									
	36 1251 3033									

	36 1251 3453 36 1251 3037									

Table 7

Measurements (mm) and Weight of Machines (kg)

Type of the lamella	Code	Lamella Thickness mm	Nominal area of the surface of the heat exchange in square meters	Number of lamellae from the machine	L	L_1	L_2	L_3	Weight	
									General weight	Weight of the parts made of anti-corrosive
0,6d	36 1251 3452 36 1251 3042 36 1251 3451 36 1251 3014 36 1251 3464 36 1251 3046	0,8 1 0,8 1 0,8 1	200 250 300	340 420 404	310 385 475	926 385 1142 1095 1368 1310	2115 2550 3020	3810 4370 4980	3535 4027 4108 4594 4700 5192	1810 2172 2100 2520 2470 2964

LIPSA BIBLIOGRAFIA IN TEXT

REFERENCES

[1]. Boris C., *Multitube Heat Exchangers*. Buletinul Institutului Politehnic din Iasi, **LIII (LVII)**, *3*, 2007.

[2]. Boris C., *Schimbătoare de căldură*. Editura Tehnopress, Iaşi, 2005.

[3]. Curievici I., Simionescu A., Dinulescu H., *Experimental Study of a wire Heat Exchanger*. Preprints of Papers Presented at the "First Heat Transfer Conference", Iaşi, **II**, 581-593 (1973).

[4]. Fraas A.P., Heat Exchangers Design, John Wiley Inc., New York, ediţia a-II-a, 1989.

[5]. Gardner K., Taborek J., *Mean temperature difference: A reappraisal*. AIChE Journal., *23*, *6*, 770-786 (1977).

[6]. Hewitt G.F. Heat Exchanger Design Handbook, Begell House, New York, 1998.

[7]. Hennecke D.K., Sparrow E.M., *Local Heat Sink on a Convectively Cooled Surface – Application to Temperature Measurement Error*. Int.J.Heat Mass Transfer, **13**, 287-304 (1970).

[8]. Incropera F.P., DeWitt D.P., *Fundamentals of Heat and Mass Transfer*. 4th Edition Wiley, USA, 1996.

[9]. Larry Wall, Tom Christiansen, Randal Schwartz Programming Perl, O'REILLY U.S.A., 1996.

[10]. Mukherjee R., *Effectively Design Shell and Tube Heat Exchangers*. Chemical Eng. Progress, Febr.1998, 112-123.

[11]. Tubular Exchanger Manufacturers Association, *Standards of the Tubular Exchanger Manifacturers Association*, 7th ed., TEMA, New York, 1988.

SCHIMBĂTOARE DE CĂLDURĂ LAMELARE DEMONTABILE DE TIP D

(Rezumat)

Pentru acest tip de schimbător, canalele (interlamelare) intermediare sunt în formă de reţea în flux. Lamelele se ştanţează din oţel în coli de mărci diferite. Gofrajele lamelelor au în secţiune profilul unui triunghi isoscel cu baza de 36 mm şi înălţimea de 4,5 mm. Caracteristica tehnică a lamelei: Dimensiuni gabaritice (lungime, lăţime, grosime), mm: 960 x 460 x 1; Aria suprafeţei schimbătorului de căldură, m2: 0,2; Masa, Kg: 2,5.

ALGORITHMS USED FOR THE GENERATION OF RANDOM NUMBERS

BY

CONSTANTIN BORIS[*]

"Gheorghe Asachi" Technical University of Iaşi
The Faculty of Materials Science and Engineering

Abstract. In many practical applications one encounters the issue of generating some selections of n random numbers having a certain distribution of probability. For this, n random numbers with a uniform distribution of probability U(0,1) are generated. With these one may actually generate random numbers that correspond to any distribution calculating n values of the inversed distribution function. In other words here one has two types of generations: generation of uniform random numbers followed by the generation of random numbers that correspond to some types of distribution. In this paper we intend to present the way in which the distributions used in statistics may be obtained by the generation of random numbers with a given distribution with the help of the uniform distribution.

Key words: random numbers, congruent methods, congruential generators, distribution of probability.

1. Introduction

In many practical applications one encounters the issue of generating some selections of n random numbers having a certain distribution of

---

[*] Corresponding author e-mail: borisconstantin@yahoo.com

probability. For this, n random numbers with a uniform distribution of probability U(0,1) are generated. With these one may actually generate random numbers that correspond to any distribution calculating n values of the inversed distribution function. In other words here one has two types of generations: generation of uniform random numbers followed by the generation of random numbers that correspond to some types of distribution. In this paper we intend to present the way in which the distributions used in statistics may be obtained by the generation of random numbers with a given distribution with the help of the uniform distribution.

Uniform distribution between zero and one is given by the following relation:

$$\mathbf{f(x)} = \begin{cases} 1, & \text{pentru } 0 < x < 1, \\ 0, & \text{altfel} \end{cases} \tag{1}$$

Since $\mathbf{f(x)} \geq 0$ for $-\infty < \mathbf{x} < \infty$ and $\int_{-\infty}^{+\infty} \mathbf{f(x)dx} = \int_{0}^{1}\mathbf{f(x)dx} = [\mathbf{x}]_{0}^{1} = 1$ it results that the function above has the properties of a probability density function.

Uniform random numbers are generated on the computer using algorithms that implement congruent methods. Two numbers m and k are congruent after module n, m = k(mod n), then there is an integer p, so that m − k = p n, which means that the difference m − k is divided exactly to n and the numbers m and k generate the same remainders when dividing them by number n.

There are several congruent methods to generate uniform random numbers: multiplicative methods, additive methods, mixed methods. The congruent multiplicative method uses the following formula:

$$\mathbf{x_i} = (\mathbf{ax_{i-1}} + \mathbf{c})\bmod \mathbf{n} \tag{2}$$

where: The numbers a and c are positive integers, known as multiplicator and increment, respectively. According to this method one should pick the last random number xi-1 and multiply it by a constant coefficient a , to which one should also add the value of the increment and then we should take the module of the number obtained after n, *i.e.* divide (ax i-1 + c) to n and consider the remainder of the division being xi. In order to generate a series of numbers x i-1 one needs an initial value x0 known as seed, a multiplicator, an increment and the module n. The value ui = xi / n is regarded as a uniform random number ranging between zero and one and is known as linear congruent generator.

When c = 0, it is known as multiplicative linear congruent generator. Any number generator based on this method may only provide a finite number of random numbers, after which the series of numbers starts to repeat itself. If n,

a and c are well chosen, the period of the generator is n. This period however depends a lot also on the length of the word of the computer one works on.

The period should be as big as possible and the correlation between the generated numbers should be as small as possible. This thing depends a lot on the selection of the values a and c.

In fact, using the twin computer we generate a series of pseudo-random numbers which, even though they comply with all randomness statistical tests, remain entirely determinate. This means that if each working cycle of the generator of random numbers starts with the same seed, on the exit we obtain series of identical random numbers. Further on we intend to present two generators of uniform random numbers, one for the 16 bits computer and one for the 32 bits computer.

1.1. Wichmann-Hill Generator,

which is in fact a combination of three congruential generators, has the following form:

$$
\begin{aligned}
\mathbf{x_i} &= 171\mathbf{x_{i-1}} \bmod 30269 \\
\mathbf{y_i} &= 172\mathbf{y_{i-1}} \bmod 30307 \\
\mathbf{z_i} &= 170\mathbf{z_{i-1}} \bmod 30323
\end{aligned}
\tag{3}
$$

and

$$
\mathbf{u_i} = \left(\frac{\mathbf{x_i}}{30269} + \frac{\mathbf{y_i}}{30307} + \frac{\mathbf{z_i}}{30323} \right) \bmod 1
$$

For this generator one should set the value of three seeds: x0, y0 and z0. The value ui is regarded as a uniform random representation ranging between zero and one. The period of this generator is of 6.95 x 1012. The source code for this generator is provided in the subroutine urnd16(ix,iy,iz,r n), where ix, iy and iz are the seeds and r n is the uniform random number ranging between zero and one. The subroutine is used by a main program (main), named in our case urnd1. If one wants to generate more uniform random numbers, we use the subroutine urnd16 several times (in our case n 3 times), thus generating n3 uniform random numbers. Further on we shall present the urnd1 program which uses the subroutine urnd16.

```
    program urnd1
        write(*,20)
 20   format(' ','introdu valorile pentru ix, iy, iz, n')
      read(*,*) ix, iy, iz, n
        do 100 i =1, n
                ix = ix + i
                do 200 j =1, n
```

```
                            iy = iy + j
                            do 300 k =1, n
                                    iz = iz + k
                                    call urnd16(ix,iy,iz,rn)
                                    write(*,*) ix, iy, iz, rn
 300                        Continue
 200                 Continue
 100  Continue
      end
        subroutine urnd16(ix,iy,iz,rn)
    1 ix = mod(171*ix,30269)
      iy = mod(172*iy,30307)
        iz = mod(170*iz,30323)
        rn = ix/30269. + iy/30307. + iz/30323.
        rn = rn - int(rn)
        if(rn .le. 0) go to 1
        return
                end
```

1.2. L'Ecuyer Generator

This is in fact a combination of k congruential generators that have prime nj modules, so that all the values of $(n j – 1) / 2$ are relatively prime, with the multiplicators that lead to complete (full) periods. Let x j,1,   x j,2, x j,3 … be a sequence resulting from the j generator. We take into consideration the case in which each individual generator j is a multiplicative linear congruential generator with a maximum period, having the module nj and the multiplicator aj, *i.e.*:

$$\mathbf{x}_{j,i} \equiv \mathbf{a}_j \mathbf{x}_{j,i-1} \bmod \mathbf{n}_j$$

Assuming that the first generator is a good one and that n1 is big enough, we make up the i integer from the sequence in the following way:

$$\mathbf{x}_i = \sum_{j=1}^{k} (-1)^{j-1} \mathbf{x}_{j,i} \bmod (\mathbf{n}_j - 1)$$

where the other modules nj, j = 2, 3, …, k need not be big. In order to be sure that in this sequence we have no zeros, we proceed to the following normalization:

$$
\mathbf{u}_i = \begin{cases} \dfrac{\mathbf{x}_i}{\mathbf{n}_1} & \text{daca } \mathbf{x}_i > 0 \\[2ex] \dfrac{\mathbf{n}_1 - 1}{\mathbf{n}_1} & \text{daca } \mathbf{x}_i = 0 \end{cases}
$$

The following statements apply for each individual generator j in part. Let us define q = [n / a] and r n mod a, i.e. n is reduced to n = aq + r, where r < a. In this case, for 0 < x < n, we have:

$$
\mathbf{ax} \bmod \mathbf{n} = \left(\mathbf{ax} - [\mathbf{x}/\mathbf{q}]\,n\right)\bmod \mathbf{n} = \left(\mathbf{ax} - [\mathbf{x}/\mathbf{q}](aq + r)\right)\bmod \mathbf{n} =
$$
$$
\left(\mathbf{a}(\mathbf{x} - [\mathbf{x}/\mathbf{q}]q) - [\mathbf{x}/\mathbf{q}]r\right)\bmod \mathbf{n} = \left(\mathbf{a}(\mathbf{x} \bmod \mathbf{q}) - [\mathbf{x}/\mathbf{q}]r\right)\bmod \mathbf{n}
$$

In fact one suggests here the combination of two congruential generators, for which k = 2, (a1, n1, q1, r1) = (40014, 2147483563, 53668, 12211) and (a2, n2, q2, r2) = (40692, 2147483399, 52774, 3791).

For the implementation of the generator one needs two seeds. The period of this generator is of 2.31 x 1018 i.e. a period long enough. The source code for this generator is given in the subroutine urnd(ix,iy, rn), where ix and iy are the seeds and r n the uniform random number ranging between zero and one. The subroutine is used by a main program (main), called in our case urnd2. If one wants to generate more uniform random numbers, we use the subroutine urnd several times (in our case n 2 times) thus generating n 2 uniform random numbers. Further on we shall present the urnd2 program that uses the subroutine urnd.

```
      program urnd2
         write(*,20)
  20   format(' ','introdu valorile pentru ix, iy, n')
         read(*,*) ix, iy, n
           do 100 i = 1, n
                   ix = ix + i
                   do 200 j =1, n
                         iy = iy + j
                                call urnd(ix,iy,rn)
                                write(*,*) ix, iy, rn
  200                Continue
  100 Continue
          end
         subroutine urnd(ix,iy,rn)
    1   kx = ix/53668
         ix = 40014*(ix - kx*53668) - kx*12211
         if(ix .lt. 0) ix = ix + 2147483563
c
```

```
ky = iy/52774
iy = 40692*(iy - ky*52774) - ky*3791
if(iy .lt. 0) iy = iy + 2147483399
  rn = ix-iy
  if(rn .lt. 1.) rn = rn + 2147483562
  rn = rn*4.656613e-10
  if(rn .le. 0.) go to 1
  return
          end
```

Further on allow us to focus on some continuous distributions extensively used in statistics, for which the density functions are obtained starting from the uniform distribution U(0,1) by the transformation of the variables.

1.2.1. *The Normal Distribution N(0,1).* The normal distribution with zero average and one variant, i.e. the standard normal distribution, is represented by the function:

$$\mathbf{f}(\mathbf{x}) = \frac{1}{\sqrt{2\pi}} \exp\left(-\frac{\mathbf{x}^2}{2}\right)$$

for $-\infty < \mathbf{x} < +\infty$. Obviously we have f(x) ≥ 0 for all values of x. This function is a probability density function since $I = \int_{-\infty}^{+\infty} \mathbf{f(x)dx} = 1$. The normal random variable is built by using two independent uniform random variables. The two variables X1 and X2 are mutually independently distributed as normal random variables with zero average and one variant.

The source code for this generator is given in the subroutine snrnd (ix,iy, rn), where ix and iy are the seeds and r n the standard random number ranging between zero and one. The subroutine is used by a main program (main), called in our case urnd3. If one wants to generate more uniform random numbers, one uses the subroutine snrnd several times (in our case n2 times) thus generating n2 uniform random numbers. Further on we present the urnd3 program that uses the snrnd subroutine.

```
    program urnd3
      write(*,20)
 20  format(' ','introdu valorile pentru ix, iy, n')
    read(*,*) ix, iy, n
      do 100 i =1, n
            ix = ix + i
            do 200 j =1, n
                  iy = iy + j
                        call snrnd(ix,iy,rn)
```

```
                              write(*,*) ix, iy, rn
200              Continue
100  Continue
     end
       subroutine snrnd(ix,iy,rn)
       pi = 3.1415926535897932385
       call urnd(ix,iy,rn1)
       call urnd(ix,iy,rn2)
       rn = sqrt(-2.0*log(rn1))*sin(2.0*pi*rn2)
       return
               end
```

The value r n from snrnd(ix,iy,rn) corresponds to X2. Totally in a conventional manner we use as random number either X1 or X2. Generally speaking one wants algorithms that avoid the evaluation of the sine and cosine functions, since these evaluations require a lot of time. Further on we present an alternative generator that complies with this goal.

```
     program urnd4
       write(*,20)
 20  format(' ','introdu valorile pentru ix, iy, n')
     read(*,*) ix, iy, n
       do 100 i = 1, n
               ix = ix + i
               do 200 j = 1, n
                       iy = iy + j
                               call snrnd2(ix,iy,rn)
                               write(*,*) ix, iy, rn
200              Continue
100  Continue
     end
       subroutine snrnd2(ix,iy,rn)
 1     call urnd(ix,iy,rn1)
       call urnd(ix,iy,rn2)
       s = ((2.*rn1-1.)**2) + ((2.*rn2-1.)**2)
       if(s .gt. 1) go to 1
       rn = sqrt(-2.0*log(s)/s)*(2.0*rn2-1.)
       return
               end
```

The standard normal probabilities. When $X \approx N(0,1)$, the following problem appears: finding for a given x the probability p, so that $p = F(x)$, where:

$$\mathbf{F(x)} = \int_{-\infty}^{x} \mathbf{f(t)\,dt} = \mathbf{P(X < x)}$$

In other words one should find the probability for X to be smaller than a given x value. This probability is known as standard normal probability. The subroutine that implements this approximation, known as snprob(x,p) is used by a main program (main), called in our case probsn.

```
      program probsn
       write(*,20)
  20  format(' ','introdu valoarea pentru x:N(0,1) si n')
      read(*,*) x, n
        do 100 i = 1, n
             x = x + (0.1)*i
                   call snprob(x,p)
                   write(*,*) x, p
 100  Continue
      end
       subroutine snprob (x,p)
       pi = 3.14159265358979932385
       a0 = 0.2316419
       b1 = 0.319381530
       b2 = -0.356563782
       b3 = 1.781477937
       b4 = -1.821255978
       b5 = 1.330274429
c
       z = abs(x)
       t = 1.0/(1.0 + a0*z)
       pr = exp(-.5*z*z)/sqrt(2.0*pi)
       p = pr*t*(b1*t*(b2*t*(b3*t*(b4 + b5*t))))
       if(x .gt. 0.0) p = 1.0 - p
c
       return
       end
```

1.2.2. *The standard normal percentage points.* When $X \approx N(0,1)$, one may approximate for a given value of the probability p, on x, which is actually the percentage point, so that $p = F(x)$, where $F(x)$ is the standard normal cumulated distribution function.

The subroutine that implements this approximation, known as snperpt(p,x) is used by a main program (main), called in our case ptsnper.

```
      program ptsnper
       write(*,20)
```

```
 20  format(' ','introdu valoarea pentru p si n')
     read(*,*) p, n
       do 100 i = 1, n
             p = p + (0.1)*i
             call snperpt (p,x)
             write(*,*) p, x
100 Continue
     end
     subroutine snperpt(p,x)
c    Input: p - probabilitatea (err < p <1 - err cu err = 1e -20)
c    Output: x: N(0,1) - punctul procentual corespunzator lui p
     p0 = - 0.322232431088
      p1 = -1.0
      p2 = - 0.342242088547
      p3 = - 0.204231210245e-1
      p4 = - 0.453642210148e-4
      q0 = 0.993484626060e-1
      q1 = 0.588581570495
      q2 = 0.531103462366
      q3 = 0.103537752850
      q4 = 0.385607006340e-2
      ps = p
      if(ps .gt. 0.5) ps = 1.0 - ps
      if(ps .eq. 0.5) x = 0.0
      y = sqrt(-2.0*log(ps))
      x = y + ((((y*p4 + p3)*y + p2)*y + p1)*y + p0)
  @      /((((y*q4 + q3)*y + q2)*y + q1)*y + q0)
     if(p .lt. 0.5) x = -x
     return
          end
```

The normal distribution: $N(\mu, \sigma^2)$

The normal distribution written down as $N(\mu, \sigma^2)$ is represented in the following way:

$$f(x) = \frac{1}{\sqrt{2\pi\sigma^2}} \exp\left(-(x-\mu)^2 / 2\sigma^2\right)$$

for $-\infty < x < \infty$. The value μ is called location parameter whereas the value σ^2 is called scale parameter. We may generalize the normal distribution $N(\mu, \sigma^2)$ starting from the generators of the distribution $N(0,1)$ and using the fact that $X = \mu + \sigma Z$. In other words a value r n for $X: N(\mu, \sigma^2)$ may be obtained by

adding the average value μ and the value r n1 for Z: N(0,1) multiplied by the radical of the variant. The algorithm implementing this method is the following:

```
      program dnrn
         write(*,20)
  20  format(' ','introdu valorile pentru ix, iy, mean, variance, n')
      read(*,*) ix, iy, ave, var, n
         do 100 i = 1, n
                ix = ix + i
                do 200 j = 1, n
                     iy = iy + j
                          call nrnd(ix,iy,ave,var,rn)
                          write(*,*) ix, iy, rn
 200              Continue
 100 Continue
      end
         subroutine nrnd(ix,iy,ave,var,rn)
c    Input: ix, iy - seminte
c         ave: media; var: varianta
c    Output: rn: N(ave,var)
      call snrnd(ix,iy,rn1)
        rn = ave + sqrt(var)*rn1
        return
                end
```

1.2.3. *The normal logarithmic distribution.* The normal logarithmic distribution with the parameters μ and σ^2 is represented in the following way:

$$f(x) = \begin{cases} \dfrac{1}{x\sqrt{2\pi\sigma^2}}\exp\left(-\dfrac{1}{2\sigma^2}\left(\log x - \mu^2\right)\right), & \text{pentru } 0 < x < \infty \\ 0, & \text{altfel} \end{cases}$$

The generation of the normal logarithmic distribution is based on normal distribution. The algorithm implementing this method is the following:

```
      program nrndlog
         write(*,20)
  20  format(' ','introdu valorile pentru ix, iy, mean, variance, n')
      read(*,*) ix, iy, ave, var, n
         do 100 i = 1, n
                ix = ix + i
                do 200 j = 1, n
                     iy = iy + j
                          call lognrnd(ix,iy,ave,var,rn)
```

```
                         write(*,*) ix, iy, rn
 200            Continue
 100 Continue
      end
      subroutine lognrnd(ix,iy,ave,var,rn)
c   Input: ix, iy - seminte
c        ave: media; var: varianta
c   Output: rn: exponentiala lui N(ave,var)
      call snrnd(ix,iy,rn1)
      rn = exp(ave + sqrt(var)*rn1)
      return
      end
```

1.2.4. *The exponential distribution.* The exponential distribution with the parameter is represented in the following way:

$$f(x) = \begin{cases} \dfrac{1}{\beta}\exp\left(-\dfrac{x}{\beta}\right), & \text{pentru} \quad 0 < x < \infty \\ 0, & \text{altfel} \end{cases}$$

for $\beta > 0$. The parameter β shows a scale parameter. The exponential distribution with the parameter β may be generated starting from the uniform random distribution between zero and one. The algorithm implementing this method in the following:

```
      program prndex
       write(*,20)
 20   format(' ','introdu valorile pentru ix, iy, beta, n')
      read(*,*) ix, iy, beta, n
        do 100 i = 1, n
              ix = ix + i
              do 200 j = 1, n
                  iy = iy + j
                        call exprnd(ix,iy,beta,rn)
                        write(*,*) ix, iy, rn
 200            Continue
 100 Continue
      end
      subroutine exprnd(ix,iy,beta,rn)
c   Input: ix, iy - seminte
c          beta: parametru
c   Output: rn
```

```
      call urnd(ix,iy,rn1)
        rn = -beta*log(rn1)
        return
        end
```

1.2.5. *The gamma distribution: G(α, β)*. The gamma distribution with the parameters α and β has the following form:

$$f(x) = \begin{cases} \dfrac{1}{\beta^{\alpha}\Gamma(\alpha)}\, x^{\alpha-1} \exp\left(-x/\beta\right), & \text{pentru} \quad 0 < x < \infty \\ 0, & \text{altfel} \end{cases}$$

for $\alpha > 0$ and $\beta > 0$, where the value β is called form parameter and the value is a scale parameter. $\Gamma(\cdot)$ is known as gamma function, which is defined in the following way:

$$\Gamma(\alpha) = \int_0^{\infty} x^{\alpha-1} e^{-x}\, dx$$

In order to obtain the gamma distribution with the parameters α and β, we use the uniform random variables since the sum of α exponential random variables leads to a gamma random variable with the parameters α and β. In this case, the source code generating the gamma random numbers is the following:

```
      program rndgama
        write(*,20)
  20   format(' ','introdu valorile pentru ix, iy, alpha, beta, n')
        read(*,*) ix, iy, alpha, beta, n
          do 100 i = 1, n
                ix = ix + i
                do 200 j = 1, n
                    iy = iy + j
                      call gammarnd(ix,iy,alpha,beta,rn)
                      write(*,*) ix, iy, rn
  200             Continue
  100 Continue
        end
        subroutine gammarnd(ix,iy,alpha,beta,rn)
c    Input: ix, iy - seminte
c        alpha : parametru de forma
c        beta : parametru de scala
c    Output:rn
        rn = 0.0
```

```
        Do 1 i = 1,nint(alpha)
           call exprnd(ix,iy,beta,rn1)
   1       rn = rn + rn1
           return
                end
```

1.2.6. *The inverse gamma distribution: IG*(α, β).The inverse gamma distribution with the parameters α and β is represented in the following way:

$$
f(x) = \begin{cases} \dfrac{2}{\Gamma(\alpha)\beta^{\alpha} x^{2\alpha+1}} \exp\left(-\dfrac{1}{\beta x^2}\right), & \text{pentru} \quad 0 < x < \infty \\ 0, & \text{altfel} \end{cases}
$$

for α >0 [i β > 0. The inverse gamma distribution derives from the gamma distribution. The source code for the generation of the inverse gamma distribution is then the following:

```
        program irndgama
          write(*,20)
   20   format(' ','introdu valorile pentru ix, iy, alpha, beta, n')
        read(*,*) ix, iy, alpha, beta, n
           do 100 i = 1, n
                 ix = ix + i
                 do 200 j = 1, n
                      iy = iy + j
                         call igammarnd(ix,iy,alpha,beta,rn)
                         write(*,*) ix, iy, rn
   200               Continue
   100 Continue
        end
        subroutine igammarnd(ix,iy,alpha,beta,rn)
c    Input: ix, iy - seminte
c        alpha : parametru de forma
c        beta : parametru de scala
c    Output:rn
        call gammarnd(ix,iy,alpha,beta,rn1)
        rn = 1./sqrt(rn1)
        return
        end
```

1.2.7. *The beta distribution.* The beta distribution with the parameters α and β is represented in the following way:

$$
\mathbf{f(x)} = \begin{cases} \dfrac{1}{\mathbf{B(\alpha,\beta)}} \mathbf{x}^{\alpha-1}(1-\mathbf{x})^{\beta-1}, & \text{pentru} \quad 0 < x < 1 \\[2mm] 0, & \text{altfel} \end{cases}
$$

for $\alpha > 0$ [i $\beta > 0$. B(.,.) is called beta function and is defined by the following relation:

$$
\mathbf{B}(\alpha,\beta) = \int_0^1 \mathbf{x}^{\alpha-1}(1-\mathbf{x})^{\beta-1}\,\mathbf{dx} = \frac{\Gamma(\alpha)\Gamma(\beta)}{\Gamma(\alpha+\beta)}
$$

Using two independent generations for the random variables with gamma distribution we may obtain a generation for a random variable with beta distribution, as one may observe in the source code al the program implementing this generation way.

```
      program rndbeta
         write(*,20)
  20   format(' ','introdu valorile pentru ix, iy, alpha, beta, n')
      read(*,*) ix, iy, alpha, beta, n
         do 100 i = 1, n
                 ix = ix + i
                 do 200 j = 1, n
                      iy = iy + j
                          call betarnd (ix,iy,alpha,beta,rn)
                          write(*,*) ix, iy, rn
 200               Continue
 100 Continue
       end
         subroutine betarnd(ix,iy,alpha,beta,rn)
c    Input: ix, iy - seminte
c         alpha : parametru de forma
c         beta : parametru de scala
c    Output: rn
     call gammarnd(ix,iy,alpha,1.0,rn1)
     call gammarnd(ix,iy,beta ,1.0,rn2)
     rn = rn1/(rn1+rn2)
     return
     end
```

1.2.8. *The chi-square distribution:* $\chi^2(\mathbf{k})$. The chi-square distribution with k degrees of freedom is represented in the following way:

$$f(x) = \begin{cases} \dfrac{1}{2^{k/2}\Gamma(k/2)}\, x^{(k/2)-1}e^{-x/2}, & \text{pentru} \quad 0 < x < \infty \\ 0, & \text{altfel} \end{cases}$$

where k is a positive integer. One may generate a chi-square distribution starting from the sum of the squares of some standard normal random distributions. The source code implementing this algorithm is the following:

```
      program rndchi2
        write(*,20)
  20  format(' ','introdu valorile pentru ix, iy, k, n')
      read(*,*) ix, iy, k, n
        do 100 i = 1, n
             ix = ix + i
             do 200 j = 1, n
                  iy = iy + j
                       call chi2rnd(ix,iy,k,rn)
                       write(*,*) ix, iy, rn
 200               Continue
 100 Continue
      end
        subroutine chi2rnd(ix,iy,k,rn)
c    Input: ix, iy - seminte
c         k : gradele de libertate
c    Output: rn
        rn = 0.0
        do 1 i = 1,k
                call snrnd(ix,iy,rn1)
     1 rn = rn + rn1*rn1
        return
        end
```

In order to use the chi2nrd subroutine, one needs to generate k standard normal random representations. Such a representation is comprised of two uniform random representations (see the snrnd subroutine). Therefore, a chi-square random representation with k degrees of freedom requires 2k uniform random representations. Thus the chi2rnd subroutine is from a strictly computational point of view a rather inefficient generator of random numbers. That is why one invented all sort of other types of generators. Such a generator starts from the fact that the exponential distribution with $\beta = 2$ is equivalent to the chi-square distribution with two degrees of freedom, as results from the comparison of the generating functions of the moments for the two distributions. When k is even, one needs to generate k/2 independent

exponential random representations, and when k is odd, one generates [k/2] independent exponential random representations and a standard normal random representation, [k/2] representing the maximum integer than is not higher than k/2. The generator of random numbers based on this approximation is given in the source code of the chi2rnd2 subroutine. This requires k standard normal random representations (or 2k uniform random representations).

```
      program rnd2chi2
        write(*,20)
 20   format(' ','introdu valorile pentru ix, iy, k, n')
      read(*,*) ix, iy, k, n
        do 100 i = 1, n
              ix = ix + i
              do 200 j = 1, n
                    iy = iy + j
                        call chi2rnd2(ix,iy,k,rn)
                        write(*,*) ix, iy, rn
 200              Continue
 100 Continue
      end
        subroutine chi2rnd2(ix,iy,k,rn)
c    Input: ix, iy - seminte
c        k : gradele de libertate
c    Output: rn
              if (k- (k/2)*2 .eq. 1) then
call snrnd(ix,iy,rn1)
rn = rn1*rn1
else
rn = 0.0
endif
do 1 i = 1,k/2
call exprnd(ix,iy,2.0,rn1)
   1            rn = rn + rn1
      return
      end
```

1.2.9. *The chi-square probabilities*. Let Q(x; k) be the probability P(X > x), where X. The source code estimating the chi-square probabilities is the following:

```
      program probchi2
      write(*,20)
 20   format(' ','introdu valoarea pentru x:hi2(k), k si n')
      read(*,*) x, k, n
        do 100 i = 1, n
```

```
                    x = x + (0.1)*i
                              call chi2prob(x,k,p)
                              write(*,*) x, p
  100  Continue
       end
         subroutine chi2prob (x,k,p)
         dimension f(1000), q(1000)
c    input
c        x : punctul procentual in care se doreste probabilitatea
c        k : numarul gradelor de libertate (.le. 1000)
c    output
c        p : probabilitatea calculata in punctul x
         pi = 3.1415926535897932385
         f(1) = exp(-.5*x) / sqrt(2.*pi*x)
         f(2) = exp(-.5*x) / 2
         call snprob(sqrt(x),pr)
         q(1) = 2.*(1.-pr)
         q(2) = exp(-.5*x)
         do 1 i = 3,k
         f(i) = x*f(i -2) / float(i -2)
    1 q(i) = q(i-2) + 2.*f(i)
      p = 1.- q(k)
         return
         end
```

1.2.10. *The chi-square percentage points.*In order to find the percentage points x when one knows the probabilities p in these points, one starts from the Cornish-Fisher series expansion. The source code of the algorithm proposed by us according to this expansion, is the following:

```
      program perptchi2
         write(*,20)
   20  format(' ','introdu valorile pentru p si k')
      read(*,*) p, k
         call chi2perpt(p,k,x)
         write(*,*) p, x
       end
         subroutine chi2perpt(p,k,x)
c    input:
c        p : probabilitatea
c        k : numarul gradelor de libertate
c    output
c        x : punctul procentual corespunzator probabilitatii p
      p = 1. - p
```

```
call snperpt(p,z)
g1 = z*sqrt(2.*k)
g2 = (2./3.)*(z*z-1.)
g3 = z*(z*z-7.) / (9.*sqrt(2.*k))
g4 = -2.*(3.*z*z*z*z + 7.*z*z-16.) / (405.*k)
x = float(k) + g1 + g2 + g3 + g4
return
        end
```

1.2.11. The F distribution: F(m,n). The F distribution with m and n degrees of freedom is represented in the following way:

$$f(x) = \begin{cases} \dfrac{\Gamma((m+n)/2)}{\Gamma(m/2)\Gamma(n/2)} \left(\dfrac{m}{n}\right)^{m/2} x^{(m/2)-1} \left(1 + \dfrac{m}{n} x\right)^{-(m+n)/2}, & \text{pentru } 0 < x < \infty \\ 0, & \text{altfel} \end{cases}$$

where m and n are positive integers. A random variable with a distribution F can be obtained starting from two random variables characterized by a chi-square distribution. The source code implementing this method to generate a F distribution with m and n degrees of freedom is the following:

```
      program rndf
            write(*,20)
 20   format(' ','introdu valorile pentru ix, iy, m, n, nn')
      read(*,*) ix, iy, m, n, nn
            do 100 i = 1, nn
            ix = ix + i
            do 200 j = 1, nn
            iy = iy + j
            call frnd(ix,iy,m,n,rn)
            write(*,*) ix, iy, rn
 200        Continue
 100        Continue
      end
              subroutine frnd(ix,iy,m,n,rn)
c    input
c        ix, iy : seminte
c        m,  n : grade de libertate
c    output
c        rn : reprezentarea aleatoare a lui F
      call chi2rnd(ix,iy,m,rn1)
              call chi2rnd(ix,iy,n,rn2)
              rn = (rn1 / float(m)) / (rn2 / float(n))
```

```
    return
     end
```

*1.2.12. The t distribution: t(k).*The t distribution or Student distribution with k degrees of freedom is represented in the following way:

$$
f(x) = \frac{\Gamma\left(\dfrac{k+1}{2}\right)}{\Gamma\left(\dfrac{k}{2}\right)} \frac{1}{\sqrt{k\pi}} \left(1 + \frac{x^2}{k}\right)^{-(k+1)/2}
$$

for $-\infty < x < \infty$. A random variable with a distribution t may be obtained starting from two random variables – one with chi-square distribution and the other with a standard normal random distribution. The source code implementing this method of generating a t distribution with k degrees of freedom is the following:

```
     program rndt
                         write(*,20)
 20   format(' ','introdu valorile pentru ix, iy, k, n')
     read(*,*) ix, iy, k, n
                         do 100 i = 1, n
                         ix = ix + i
                         do 200 j = 1, n
                             iy = iy + j
                                 call trnd(ix,iy,k,rn)
                                 write(*,*) ix, iy, rn
 200                     Continue
 100  Continue
     end
                         subroutine trnd(ix,iy,k,rn)
c    input
c        ix, iy : seminte
c            k : grade de libertate
c    output
c        rn : reprezentarea aleatoare a lui t
     call snrnd(ix,iy,rn1)
                         call chi2rnd(ix,iy,k,rn2)
                         rn = rn1 / sqrt(rn2/k)
                         return
                         end
```

The t probabilities. Let $Q(\theta; k)$ be the probability $P(X < x)$, where $X \approx$ t(k) and $\theta = x/\sqrt{k}$. The source code that in this approximation estimates the t probabilities is the following:

```
      program probt
                              write(*,20)
  20  format(' ','introdu valoarea pentru x:t(k), k si n')
      read(*,*) x, k, n
                        do 100 i = 1, n
                        x = x + (0.1)*i
                                      call tprob(x,k,p)
                                      write(*,*) x, p
 100  Continue
      end
                          subroutine tprob (x,k,p)
                          dimension f(1000), q(1000)
c     input
c         x : punctul procentual in care se doreste probabilitatea
c         k : numarul gradelor de libertate (.le. 1000)
c     output
c         p : probabilitatea calculata in punctul x
                          pi = 3.1415926535897932385
                          theta = atan(x/sqrt(float(k)))
                          f(1) = cos(theta)*sin(theta) / pi
                          f(2) = cos(theta)*cos(theta)*sin(theta) / 2.
                          q(1) = .5 + theta / pi
                          q(2) = .5 + sin(theta) / 2.
                          do 1 i = 3,k
                          f(i) = (float(i-1) / float(i-2))*(cos(theta)**2)*f(i-
2)
   1  q(i) = q(i-2) + f(i-2) / float(i-2)
      p = q(k)
                          return
                              end
```

The t percentage points. In order to find the percentage points x when one knows the probabilities p in these points, one starts from the series expansion. The source code of the algorithm proposed by us according to this expansion is the following:

```
      program perptt
                              write(*,20)
  20  format(' ','introdu valorile pentru p si k')
      read(*,*) p, k
                          call tperpt(p,k,x)
```

```
                          write(*,*) p, x
      end
                       subroutine tperpt(p,k,x)
c    input:
c        p : probabilitatea
c        k : numarul gradelor de libertate
c    output
c        x : punctul procentual corespunzator probabilitatii p
                    g1(z) = z*(    (z**2) +   1.) / 4.
                    g2(z) = z*( 5.*(z**4) +  16.*(z**2) + 3.) / 96.
                    g3(z) = z*( 3.*(z**6) +  19.*(z**4)
  @        +   17.*(z**2)  -  15.) / 384.
    g4(z) = z*(79.*(z**8)  +  776.*(z**6) + 1482.*(z**4)
  @        -  1920.*(z**2)  -  945.) / 92160.
    g5(z) = z*(27.*(z**10) +  339.*(z**8)
  @        +   930.*(z**6)  - 1782.*(z**4)
  @        -   765.*(z**2) - 17955.) / 368640.
                      call snperpt(p,z)
                      x = z + g1(z) /  float(k)
  @        + g2(z) / (float(k)**2)
  @        + g3(z) / (float(k)**3)
  @        + g4(z) / (float(k)**4)
  @        + g5(z) / (float(k)**5)
                          return
                           end
```

NU SUNT TRIMITERILE BIBLIOGRAFICE IN TEXT

REFERENCES

[1]. Bassett E.E., Bremner J.M., Morgan B.J.T., Jolliffe J.T., Jones B., North P.M. – *Statistics. Problems and Solutions*. World Scientific Publishing Co. Pte. Ltd., P.O.Box 128, Farrer Road, Singapore 912805, Singapore, 2000.

[2]. Boris C., *Analiză numeric*. Tehnopress, Iaşi, **1**, 2007.

[3]. Boris C., *Analiză regresională*. Tehnopress, Iaşi, **1**, 2006.

[4]. Boris C., *Certificat de autor al bibliotecii de programe FIZMAT*. ICCI Bucureşti, 1986.

[5]. Boris C., *Metode numerice şi implementarea lor pe calculator; Principiile calculului numeric, Rezolvarea ecuaţiilor algebrice, Sisteme de ecuaţii neliniare*. Tehnopress, Iaşi, **1**, 2005.

[6]. Boris C., *Metode numerice şi implementarea lor pe calculator; Concepte de bază în estimarea erorilor, Integrare şi derivare numerică, Integrare adaptivă*. Tehnopress, Iaşi, **2**, 2005.

[7]. Cox D.R., Snell E.J., *Applied Statistics. Principles and Examples*, Chapman and Hall Ltd., 11 New Fetter Lane, London EC4P 4EE, 1981.

[8]. Cox D.R., Reid N., *The Theory of the Design of Experiments*. Chapman & Hall/Crc, Library of Congress Cataloging-in-Publication Data, USA, 2000.

[9]. Douglas C. Montgomery, George C. Runger – *Applied Statistics and Probability for Engineers*. Third Edition, John Wiley & Sons, Inc., New York, USA, 2003.

[10]. Dominique M. Hanssens, Leonard J. Parsons, Randall L. Schultz, *Market Response Models. Econometric and Time Series Analysis*. ISQM International Series in Quantitative Marketing, Kluwer Academic Publishers, USA, 2007.

[11]. Roussas G., *Introduction to Probability and Statistical Inference*. Academic Press, An imprint of Elsevier Science, 525 B Street, Suite 1900, San Diego, California 92101-4495, USA, 2003.

[12]. Roussas G. George, *A Course in Mathematical Statistics*. Second Edition, Academic Press, 525 B Street, Suite 1900, San Diego, CA 92101-4495, USA, 1997.

[13]. Herman J. Bierens, *Introduction to the Mathematical and Statistical Foundations of Econometrics*. Cambridge University Press, The Edinburgh Building, Cambridge CB2 2RU, UK, 2005.

[14]. Hisashi Tanizaki – *Computational Methods in Statistics and Econometrics*. Marcel Dekker, Inc.,270 Madison Avenue, New York, NY 10016, USA, 2004.

[15]. John S. Oakland, *Statistical Process Control, Butterwrth – Heinemann*. An imprint of Elsevier Science, Linacre House, Jordan Hill, Oxford OX2 8DP, 200 Wheeler Road, Burlington MA 01803, UK, 2003.

[16]. Jerome L. Myers, Arnold D. Well – *Research Design and Statistical Analysis*. Lawrence Erlbaum Associates, Publishers, Mahwah, New Jersey, London, 2003.

[17]. Jeanmarc Aeschlimann, Christian Bonjour, Elisabeth Stocker – *Methodologies et Techniques de Plans D'experiences*. 28e Cours de perfectionnement de l'Association Vaudoise des Chercheurs en Physique, Saas – Fee, 2 – 8 mars, Lausanne, 1996.

[18]. Johnston R.L.. *Numerical Methods: A Software Approach*. John Wiley&Sons, New York, 1999.

[19]. Kincaid D., Cheney W., *Numerical Analysis Mathematics of Scientific Computing*, Brooks/Cole Publishing Company, Pacific Grove, California, 1999.

[20]. Murray R. Spiegel, Larry J. Stephens – *Theory and Problems of Statistics*. Third Edition, Schaum's Outline Series, McGraw-Hill, QA 276.2.S65, USA, 1998.

[21]. Petruş O., *Probabilităţi şi statistică matematică. Computer Applications*. Tehnopress, Iaşi, 2006.

[22]. Petruş O., FORTRAN 90/95. *Limbaj şi tehnici de programare*. Universitatea "Gh.Asachi", Iaşi, 2001.

[23]. Radhakrishna Rao C., Toutenburg Helge, *Linear Models: Least Squares and Alternatives*. Second Edition, Springer-Verlag, New York, SPIN 10726080, USA, 1999.

[24]. Rudolf J. Freund, William J. Wilson, *Statistical Methods*. Academic Press, An imprint of Elsevier Science, 525 B Street, Suite 1900, San Diego, California 92101-4495, USA, 2003.

[25]. Robert L. Mason, Richard F. Gunst, James L. Hess – *Statistical Design and Analysis of Experiments*. With Applications to Engineering and Science, Wiley Series in Probability and Statistics, J. Wiley, New York, USA, 2007.

[26]. Salvatore D., Reagle Derrick, *Theory and Problems of Statistics and Econometrics*. Schaum's Outline Series, McGraw-Hill, USA, 2002.

ALGORITMI UTILIZAŢI PENTRU GENERAREA NUMERELOR ALEATOARE

(Rezumat)

În multe aplicaţii practice se pune problema generării unor selecţii de n numere aleatoare cu o anumită distribuţie de probabilitate. Pentru aceasta se generează n numere aleatoare ce posedă o distribuţie de probabilitate uniformă U(0,1). Cu acestea se pot genera numere aleatoare ce corespund unei distribuţii oarecare calculând n valori ale funcţiei de distribuţie inverse. Cu alte cuvinte avem două tipuri de generări: generarea numerelor aleatoare uniforme urmată de generarea numerelor aleatoare ce corespund unor anumite tipuri de distribuţii. În această lucrare prezentăm modul în care distribuţiile folosite în statistică pot fi obţinute prin generarea numerelor aleatoare cu o distribuţie dată cu ajutorul distribuţiei uniforme.

RESEARCH REGARDING THE BEHAVIOR OF WASTE FOUNDRY SANDS WITH ORGANIC BINDERS IN THE THERMAL REGENERATION

BY

MARIA BORLA (GOIA)* and GHEORGHE ZIRBO

Technical University of Cluj-Napoca
Faculty of Materials and Environmental Engineering

Abstract. In the last years, the imposition of disposal foundry waste into a particular type of landfills and closing those that don't comply the safety regulation for environment is imperative. The best way to reduce these wastes is thermal regeneration. In this paper, are determined the temperatures of ignition – destruction (versus time), of two of the most used mixed with organic binders from Romania. Also, are described the physical characteristics of sand resulted.

Key words: waste foundry sands, thermal regeneration, chemical bonded sand.

1. Introduction

Due to the pollutant character of synthetic resins which linger in foundry sands waste, the optimum recovery of this waste is regeneration (Wright, 2001; Băcanu *et al*., 2007). Currently, the most used systems of regeneration are mechanical. In these systems, the recovery degree of sand is 65-80% (Wright, 2001). Applying this method of regeneration can't be ensure complete removal of the binder on the grains of sand, so that after a number of uses appear ecological and technological problems. Environmental issues relate to emissions of sulfur

---

* Corresponding author e-mail: borla_mara@yahoo.com

oxides, nitrogen oxides, nitrides and hydrocarbons. The technological issues affects the quality of castings, due to an accumulation of sulfur and nitrogen mixture formation, causing diffusion of these elements in the surface layer of the casting (Dumitru *et al.*, 2006). Through thermal sand regeneration of those wastes, are eliminated the tehnological problems and are reduced the environmental issues. Regarding the temperature required for destruction of organic binders from foundry sands waste, the opinions of the experts are divided, the temperature variates from 250°C to 1000°C (Rhee Seung-Whee, 2007). In this paper, are determined the temperatures of ignition – distruction (versus time) of two of the most used mixture with organic binders from Romania.

2. Materials and Methods

Laboratory investigations were conducted on two types of waste foundry sands. These tow type of waste containing at least 96% quartz silica. The first type contains a binder based on furfuryl alcohol, phenol, formaldehyde and hardener-sulfonic acid and the other is based on furan containing furfuryl alcohol, formaldehyde, ethanol and p- toluene-sulfonic acid hardener. Both type of waste were used for the casting of cast iron. To determinate the temperatures of ignition -destruction binder from the grains sand was used an oven-type chamber. The temperature range chosen for the study was 200-1000°C.

3. Discussion

In Fig. 1 are presented the temperatures chart of ignition-destruction the binder for two types of foundry sands.
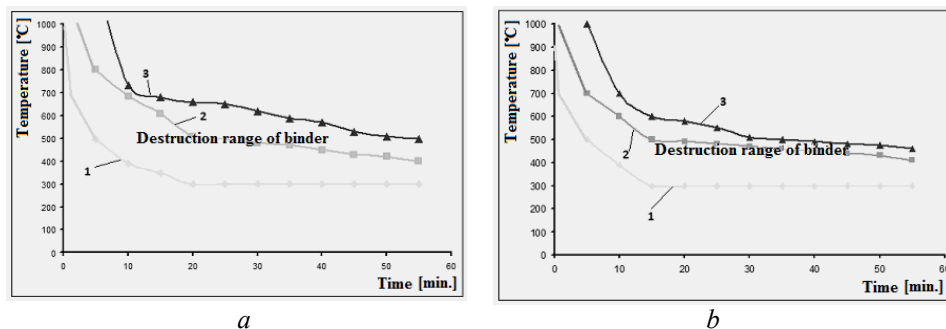
Fig. 1 – The temperatures chart of ignition-destruction the binder (Borla , 2010):
a – Phenolic/acid sands; *b* – Furan/ethanol sands.

The first curve represents the start of burning binder, the second cuve represents the destruction of the binder from surface and the third curve represents the complete destruction temperature of the binder. Between the first and second curve is the temperature range where takes place binder destruction.

It was observed that for both types of waste mixture, until 250 °C take place only drying and removal of volatile organic compounds from this waste (the mixture does not change its appearance). After the 300°C the binder on the grains from the surface starts to burn. It was found that at a temperature of 400°C binder begins to burn on the sand grains after 10 minutes. If the spent mixture is maintained at a temperature of 500°C for 5 min binder begins to burn on the sand grains, and if it kept at that temperature for 20 minutes binder is completely destroyed. Following the research that carried out has been observed that the temperature suitable for destruction binder of this waste is 650°C.

| a | b |
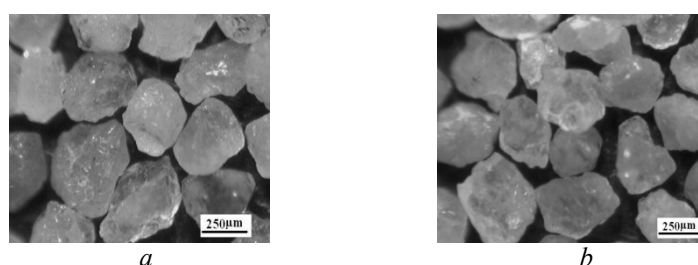
Fig. 2 – Grains of sand form
a − Phenolic/acid sands; *b* − Furan/ethanol sands.

Figure two shows the aspect of sand grains resulted from thermal regeneration at 650°C of the waste mixture with organic binders. As shown in these figure the sand doesn't contains binder to the grains surface. In table one are shown the characteristics of sand which was thermal regenerated at a temperature of 650°C.

Table 1
Characteristics of Sand Thermal Reclaimed to 650°C

No.	Mean grain M(50) mm	Uniformity degree %	Leachate parts %	Vitrification temperatu °C	pH
Phenolic/acid sands					
1.	0,23	64	0,50	1480	6,30
2.	0,25	67,5	0,56	1470	6,5
3.	0,24	66	0,54	1480	6,32
Furan/ethanol sands					
1.	0,2	63	0,52	1400	6,33
2.	0,2	63	0,51	1400	6,30
3.	0,23	64	0,52	1450	6,34

As can be seen from Table 1, the sand resulted from thermal regeneration of the waste mixture has a medium grain which is comprised between 0,2 to 0,25 [mm] and a high uniformity, which is comprised between 63 – 67,5%. In terms of leachate parties, these two types of sands have values

close to those of the new sand of Aghireş (0.5%). The pH values resulted from both waste mixtures has a less acidic character, the use of a binder in this case would adversely affect the basic properties of molding sand. So, for pH value < 7, is indicated to work with binders which has chemical acid character.

4. Conclusion

From the investigations carried out it was observed that the burning of the binder from the grain sand is achieved in a shorter time for furan/ethanol mixtures compared with phenolic/acid mixtures. The main reason for this is due to the grain of sand used in the mixture with those types of binder. The temperature of 650°C is sufficient to destroy the binder from the grains sand. The superiority of regenerated sand, the low loss material, the calorific power of the mixture (Borla & Zirbo, 2010) and the possibility of using heat results, makes thermal regeneration the best method to regenerated those types of mixtures.

REFERENCES

Băcanu I.A., *et al.*, *Regenerarea amestecurilor liate chimic, o necesitate ecologică, tehnică, dar mai ales economică, pentru turnătoriile din România.* Revista de turnătorie, *3, 4,* 2007.

Borla M., *Cercetări privitoare la comportarea deşeurilor din amestecurile de formare cu lianţi organici în procesul de regenerare termică.* Raport ştiinţific, **2**, 2010.

Borla M., Zirbo Gh., *Unele cercetări privitoare la determinarea puterii calorifice a amestecurilor de formare cu lianţi organici.* Revista de turnătorie, *1-2,* 2010.

Dumitru C., *et al.*, *Sistem ecologic de regenerare destinat reciclării deşeurilor de amestec de formare liat chimic în industria de turnătorie.* Contract CEEX, *164,* 2006.

Rhee Seung-Whee, *A Study on Thermal Stabilization of Spent Foundry Sand.* Material Science Forums, Switzerland, **544-545**, 507-510 (2007).

Wright J.R., *Take a New Look at Sand Reclamation.* Foundry Management &Technology, 2001.

CERCETĂRI PRIVITOARE LA COMPORTAREA DEŞEURILOR DIN AMESTECURILE DE FORMARE CU LIANŢI ORGANICI ÎN PROCESUL DE REGENERARE TERMICĂ

(Rezumat)

În ultimii ani, impunerea depozitării deşeurilor din turnătorii în halde special amenajate şi închiderea celor care nu îndeplinesc condiţiile de siguranţă pentru mediu este imperativa. Cea mai bună metodă de reducerea a acestor deşeuri este regenerarea termică. În această lucrare sunt determinate temperaturile de aprindere – distrugere (funcţie de timp) a două dintre cele mai utilizate amestecuri cu lianţi organici din România. Sunt prezentate deasemenea caracteristicile fizice ale nisipului rezultat.

STUDIES ON BREAKING PROCESS OF SINTERED MATERIALS

BY

LIVIU BRÂNDUŞAN[∗], GABRIEL BATIN and RADU MUREŞAN

Technical University of Cluj-Napoca,
Faculty of Materials and Environmental Engineering

Abstract. The breaking of sintered materials requested static and dynamic is different, in many aspects, in comparison with compact materials break. This different is determined of specific structure of sintered materials and the stress situation from inter-granular necks level. This presence of the pores in the material structure make effective section of the breaking to be smaller and irregular shape of pores introduces tension concentrators responsible, for most cases, the static and dynamic breaking of materials. Breaking of the sintering materials occurs through the pores. The propagate cracks will be from one pore to another until the entire material will be sectioned.

The researches effected on many sintered materials from iron powder base category, with the tensile testing and fatigue by plane bending, showed that deformation and breaking mechanism of them is more complex. The work wants to show the phenomenon which precede sintered materials break process request static and dynamic and the break mechanism of them. It show the causes which lead at sintered materials breaking difference in comparison with compact ones.

Key words: Powder Metallurgy, Sintering, Mechanical Properties.

1. Introduction

Sintered materials, especially those made from iron powder, have a large applicability domain. But, there are some domains like variable loadings,

---

[∗] Corresponding author e-mail: liviu.brandusan@staff.utcluj.ro

were the use of this sintered materials is still limited. This is due to the fact that sintered materials are more sensitive to variable loadings than to static ones. The fracture of sintered materials has a specific characteristic. This specific characteristic is determined by the pores existence in structure, pore characterized by shape, size and localization. Pores are considered to be defects and also they are the first responsible for materials failure. So, we can say that the pores act not only in reduction of mechanical properties, but also they influence the fracture process.

This paper wants to identify the way the deformation and the breaking mechanism take place, especially the fatigue fracture for sintered materials. It also characterized the influence of chemistry and pores upon the deformation and fracture process of these parts. This, due to the fact that the presence of pores in their structure create a new and complex stress in the materials structure, stress that make the deformation and fracture process different from the one that take place in the compact materials.

2. Base Materials

To investigate the deforming, fracture and plan bending fatigue processes the materials that were used was a mixture of iron powder, DWP 200.28, produced by S.C. Ductil Iron Powder Romania and cooper, W150. This mixture was then homogenized for 15 minutes, after that, the mixtures were pressed at 600MPa. The samples were sintered at 1120°C for 30 minutes in endogaz. The characteristics and the chemistry of iron powder are presented in Table 1.

Table 1
The Characteristics of DWP 200.28 Iron Powder

Granulometric distribution	%
>160 m	2
160-100 m	20-40
100-63 m	20-40
<63 m	10-15
Apparent density [g/cm^3]	2,7-2,9
Flow time [sec/50g]	≤33
Chemical composition	%
C	≤0,02
Si	≤0,05
Mn	≤0,20
P	≤0,015
S	≤0,02
O$_2$	≤0,20
Compresibility	
P=6Tf/cm^2 [g/cm^3]	≥6,90

The tensile test was done on a computerized machine GALDABINI which also allow the investigation of the way that deformation before fracture takes place. The same type of samples were used for plan bending fatigue test, using a symmetric alternative cycle and normal frequency until it breaks, to determine the maximum number of cycles until fracture and also to identify the way the fracture take place.

3. Tensile test Analysis

Tensile strength and ductility are very much depended on the presence of pores in the materials. Deformation leads to fracture. Pores shape and sintering parameters have the major influence on the deforming and tensile fracture of iron base materials. It's very important to know the intergranular bridges effective loading. This because pores acts as micro stress and deforming accumulators. The effect of pores on the stress induced in materials structure is more complicated than that of metallic inclusions, due to their shape, size and localization in respect to the loading direction.

The stress is concentrated in the intergranular bridges area between the particles. It distributes randomly and depends on the loading direction. We can see that the deforming process is also localized at the intergranular level in material structure. The different state of stress that appears at each intergranular level makes that, on some intergranular bridges, properly orientated, the stress will produce plastic deformation and in the same time, in another areas that are not so well orientated, will appear elastic and elasto-plastic deformations (Dudrova *et al.*, 1987). The stress concentrated at the intergranular bridges level reaches the maximum yield strength sooner and easier that in the case of all material and so, a slight increase of the applied tension will determine a plastic flow. Still, even if the strain stress associated to the yield strength for sintered iron powder base material is not that high (Fig 1, point A), the intergranular tension is high and will produce a locally plastic deformation, which influence the material structure. The A point in Fig. 1 stand for the first appearance of sliding planes in the structure, which will continue until in point B, were the material breaks. Local sliding is limited and depends on intergarnular bridges (Danninger *et al.*, 1990).

In the case of materials with low porosity, the elongation depends on the volume that in deformed, which depend on pores geometry. For sharp pores, the deformation is small and concentrated on these sharp points, while for the round pores, the deformation takes place in the volume of intergranular bridges and it grows as the pores are smaller and the distance between them is bigger. The deformed volume for each intergranular bridge depends on the intergranular bridge diameter and on the pore diameter. As this ratio is smaller, deformation and elongation smaller too (Danninger *et al.*, 1990).
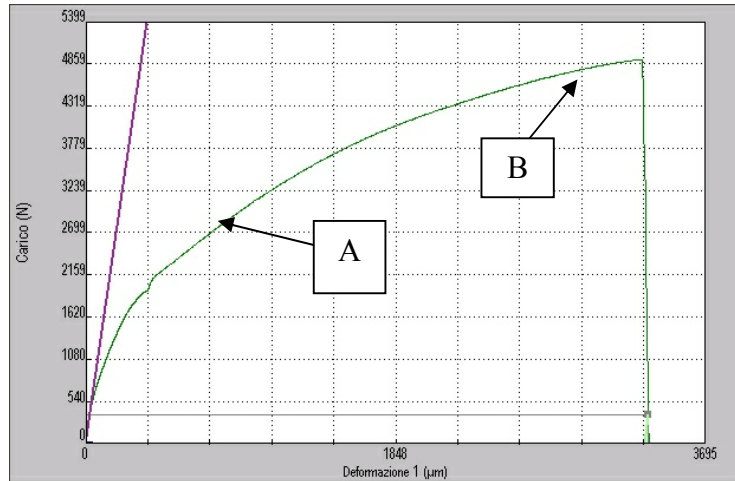
Fig. 1 – Tensile test curve of a material obtained of DWP 200.28 iron powder.

Sintered material plastic deformation that takes place in tensile test appears as sliding strips in the intergranular bridges. This sliding strips begin in pores sharp angles, pores orientated perpendicular to the loading direction. The increase in loading determine the sliding strips to become grow and so, to interact with individual pores and initiate the crack. The crack that take place at pore levels, in sharp angles area, will reduce their cross section and will lead to material final failure. At the beginning of failure process, the number of crack near that area is bigger, and as the process goes on, this number drops.

Failure process, characterized by crack initiation and propagation through sliding slips is dependent on material total porosity. For materials with high porosity, the sliding strips grow more easily. That's way, the failure of these materials is not accompanied by visible deformations, and the deformation takes place at intergranular level. For low porosity materials, the deformation process takes place in all metallic matrix, leading to an increase of ductility and strength, due to the fact that particles core also contribute to plastic deformation and failure process.

Iron powder base materials breaking surface shows a ductile failure for intergranular bridges. In the fracture area we can identify the points, the lines and the breaking areas. The points and the lines are the result of a final breaking that has taken place through contraction of intergranular bridges before their final breaking, especially for those with a small cross section. The breaking areas are the result of intergranular breaking, their cross section being and are dominant upon the breaking area. Usually, small pores, that are the effect of the surface asperity, can be identifying in the inside of this breaking surface.

By adding cooper we'll have a liquid phase sintering. As the liquid phase forms, the cooper diffuses in iron matrix, especially at the intergranular

bridges, leading to a cooper-alloyed ferrite. More over, cooper is responsible for the apparition of secondary large pores in the iron matrix (Danninger, 1987; Cambronero *et al.*, 1990). So, cooper addition leads to a hardening of materials structure and to a reduce plasticity. As the cooper content increases, the elongation decreases. The tensile resistance characteristic curve for sintered iron powder base material has no apparent yield strength (Fig. 2).

But, the curve has two distinct deformation areas. The first one, which stands for plastic deformation, starts with point A, when the first sliding strips appear.
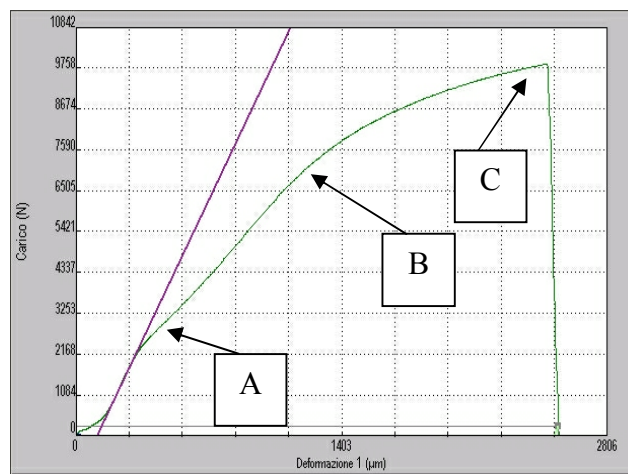
Fig. 2 – Tensile test curve of a material obtained of
DWP 200.28 and 2.4% copper powder.

Due to the lower ferrite plastic properties, a higher loading is necessary in order to realize the material deformation. This ferrite is located at iron powder grain surface and in the intergranular bridges. Once the crack passed the rich cooper area, deformation will take place as the loading increase slowly. This phase is marquee on the characteristic curve with point C. Material failure starts in point B.

4. Fatigue Failure Analisys

Sintered powder materials fatigue strength is very much depending to their porosity. In this case, the medium pore radius and the distance between them have a very important role. Fatigue strength is determined not only by the porosity but also by the pores, characterized by shape, size and localization. Pores stand for crack initiation and propagation through material structure. Due to the roughness of material, its micro irregularities represent an important source of crack initiation. As a consequence, fatigue strength depends also on the pore surface roughness. Fig. 3 reveals the way that the crack extends

through material, beginning from one side (A), it grows bigger (B) and goes on and extends to a big pore (C) near the material surface. As we go on we can see more cracks like this, which determine the appearance of secondary cracks. In fatigue fracture there are many cracks that amours themselves, but only one of them will lead to final failure. For the time being, the secondary crack is consuming all the energy that is necessary for first crack to be able to propagate, slowing down its track. In Fig. 4 we can see the first cracks, A, developed from material side to central area and the secondary ones, B, near the first ones.
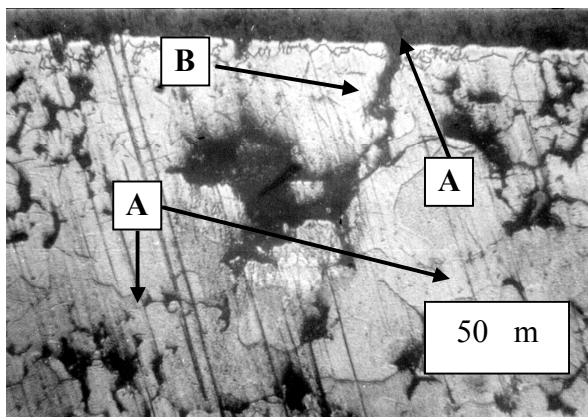
Fig. 3 – Fissure forming and propagating in a sintered material of base iron powder.
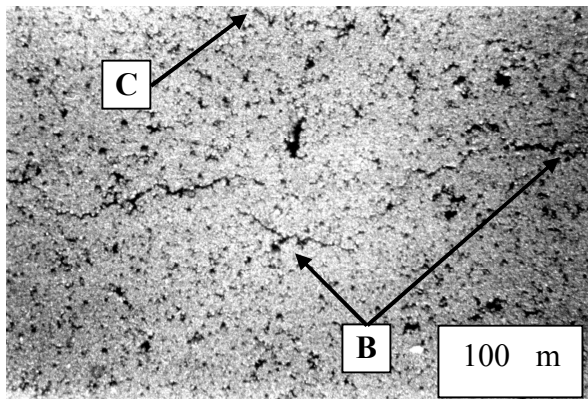
Fig. 4 – Fissure propagating through material subjected to fatigue.

It has been noticed that the crack track is from one pore to another, through intergranular bridges that interconnect the pores, for every kind of material structure. Fine round pores increase the fatigue strength. This because the fatigue cracks initiates from pore surface or from materials sides were the density is lower and pores are more round and big. Due to the sharper angle sides and to the pores surface roughness, the pores are considered to be strong stress concentrators and possible souses for cracks growth. It has been demonstrated that pores doesn't influence the intergranular fatigue fracture mechanism. They are considered to be the connected places for the cracks to propagate.

Analyzing the sketched from Fig. 5, we can see that if the material is tested for 60-70 min using a symmetric discontinuous cycle and normal frequency there appear no important cracks that will reduce the material cross section. During this time, we have only cracks initiation at intergranular stages that are strongly solicited. Starting from point A, we can observe slight crack propagation. It seems that the crack slow propagating rate is due to the presence of some pores that produce secondary cracks that consume all the necessary energy needed for the first cracks to propagate. This slow rate crack propagation corresponds to point B in the characteristic curve, Fig. 5. C area corresponds to the accelerated rate crack propagation and leads to a quick fatigue fracture for material.
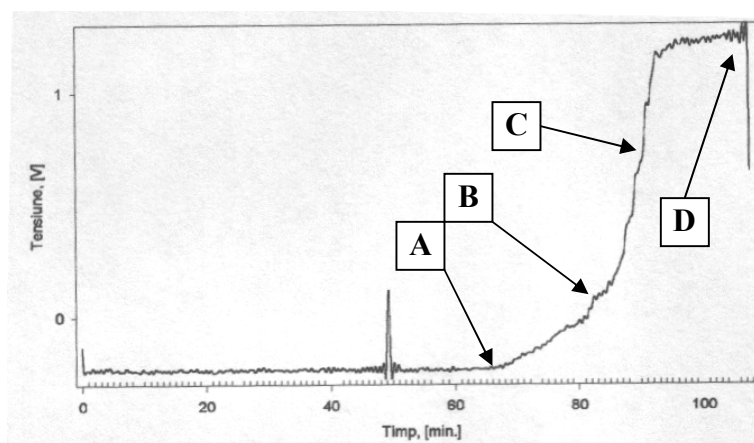
Fig. 5 – Fissure starting and propagating graph in a sintered
material on the iron base powder.

This is due to the fact that the material cross section has been greatly reduced in the previous area and to the increasing of the intergranular stress, which leads to an acceleration of crack propagation. D area corresponds to the material fatigue failure. The rate of crack increasing in the material depends upon its plastic deformed area. Pore structures reflect especially the crack propagation rate in fatigue testing. A lower porosity associated with fine and round pores, with a small distance between them, increase the fatigue strength.

5. Conclusion

The deformation and fracture mechanisms of sintered materials subjected to static and dynamic loadings depend very much upon the presence of pores in their structure. These pores are considered to be stress concentrators inside the material, determining its deformation and also generating the crack initiation and propagation. The crack propagates in material from one pore to another through the intergranular bridges until the material is entirely sectioned.

The process of crack initiation and propagation related to fatigue behaviour consists three stages. The first stage stands for cracks initiation. The second one for slow propagation of cracks and the final one for the accelerated propagation of crack leading to material failure.

REFERENCES

Brânduşan L., *The Study of the Correlation Between the Elasticity Modulus and the Fatigue of the Sintered Steels*. Powder Metallurgy Progress Journal of Science and Technology of Particle Materials., **3**, *3*, 135-139 (2003).

Cambronero L.E.G., Torralba J.M., Ruiz-Prieto J.M., *Microstructure and Properties of P/M Cu-P-Steels*. Powder Metallurgy International, **22**, *2*, 26-28 (1990).

Christian K.D., German R.M., *Relation Between Pore Structure and Fatigue Behaviour in Sintered Iron-Copper-Carbon*. The Internat. J. of Powder Metallurgy, **31**, *1*, 51-60 (1995).

Danninger H., Jangg G., Weiss B., Stickler R., *The Influence of Porosity on Static and Dynamic Properties of P/M Iron*. World Conference on Powder Metallurgy, **1**, 433-439 (1990).

Danninger H., *Pore Formation During Sintering of Fe-Cu and Its Effects on Mechanical Properties*. Reprint from Powder Metallurgy Internat., **19**, *1*, 1-5 (1987).

Dudrova E., Parilak L., Rudayova E., Pelikan K., *Heterogeneity of Deformation Processes in the Bulk of Porous Iron During Static Tensile Testing*. Powder Metallurgu International, **19**, *3*, 23-26 (1987).

STUDII ASUPRA PROCESULUI DE RUPERE A MATERIALELOR SINTERIZATE

(Rezumat)

Ruperea materialelor sinterizate solicitate static şi dinamic este diferită, în multe privinţe, faţă de materialele compacte clasice. Acest lucru este determinat de structura specifică a materialelor sinterizate şi a stării de tensiune de la nivelul punţilor inter-granulare. Această prezenţă a porilor în structura materialului face ca secţiunea efectivă de rupere să fie mai mică, iar forma neregulată a porilor să introducă concentratori de tensiune responsabili, în cele mai multe cazuri, de ruperea statică şi dinamică a materialelor sinterizate. Ruperea materialelor sinterizare are loc prin pori. Fisurile se vor propaga de la un por la altul până ce întregul material va fi secţionat.

Cercetările efectuate pe mai multe materiale sinterizate pe bază de pulbere de fier supuse la tracţiune şi la oboseală prin încovoiere plană, arătă că mecanismul de deformare şi de rupere a acestora este mult mai complex. Lucrarea îşi doreşte să prezinte fenomenul care precede ruperea statică şi dinamică a materialelor sinterizate şi mecanismul de rupere a acestora. Acesta arată cauzele care au condus la ruperea diferită a materialelor sinterizate în comparaţie cu cele compacte.

BIO-BASED PLASTICS AND COMPOSITES FOR SUSTAINABLE DEVELOPMENT

BY

INGRID BUCIŞCANU∗

"Gheorghe Asachi" Technical University of Iaşi,

Abstract. Depletion of fossil-fuel resources, the growing of the plastics waste issue and the increasing environmental awareness, determined the development of environmentally friendly or "green" alternatives to conventional plastics. Bio-based plastics and composites (BB-PC) are an innovative class of materials that are made up of biopolymers obtained from renewable resources, are biodegradable and, if properly designed andengineered, reach performance levels equivalent to conventional plastics. Bio-based plastics and composites are mainly used for packaging and automotive industry, but also have agricultural and biomedical applications. Arguments in favour and against bioplastics are put in terms of price, performances and environmental impact. This paper presents the main aspects of bio-based plastics and composites, regarding the raw materials, manufacturing technologies, application fields and contribution to the sustainable development goals.

Key words: sustainable development, renewable resources, bioplastics, biocomposites, natural fibers.

∗ Corresponding author e-mail: ibuciscanu@yahoo.com

1. Introduction

Development in the second half of the 20th century was significantly marked by the emergence of synthesis polymers and plastics, which have become ubiquitous and represent one of the foundations for the current level of living standards of mankind.

At present, two serious issues have arisen from extensive use of synthesis polymers and plastics:

► they accumulate in huge amounts in the environment and create a substantial solid waste disposal issue, due to their non- or low biodegradability;

► they are made up of non-renewable resources – petrol and gas- based raw materials, and their processing is energy-consuming and uses toxic additives.

Conventional plastics are in flagrant contradiction with the sustainable development concept. The need of reconciling convenient living with concern for environmental protection leaded to the emergence of a novel class of materials, called bioplastics and biocomposites. It is the aim of this paper to present the main aspects of bio-based plastics and composites, regarding the raw materials, manufacturing technologies, application fields and contribution to the sustainable development goals.

2. The Principle of Bio-Based Plastics and Composites

Bioplastics or green plastics can be defined as industrial products, except food and feed, whose components are derived entirely or almost entirely from renewable agroresources or from biomass feedstock, generally speaking from living matter; this is why they are also called "bio-based". They necessarily contain one or more biopolymers falling in the broader class of environmentally degradable polymers (EDPs). An EDP may be defined as one which degrades by any of the following mechanisms: oxidation, hydrolysis, photodegradation, biodegradation, to leave no harmful residues in the environment (Swift, 1993). It is obvious that only biodegradation has the ability to completely turn bioplastics into non harmful products and this accounts for the higher degree of attention that has been lately paid to the obtaining and processing of biodegradable polymers and plastics (BDPs).

Bioplastics must exhibit one or more of the following properties (see Fig.1):

1. they are bio-based
2. they are biodegradable;
3. they are made by environmentally friendly processing technologies.

Because different compounds can satisfy some or all of these criteria to different degrees, there are different "degrees of green" in green plastics.
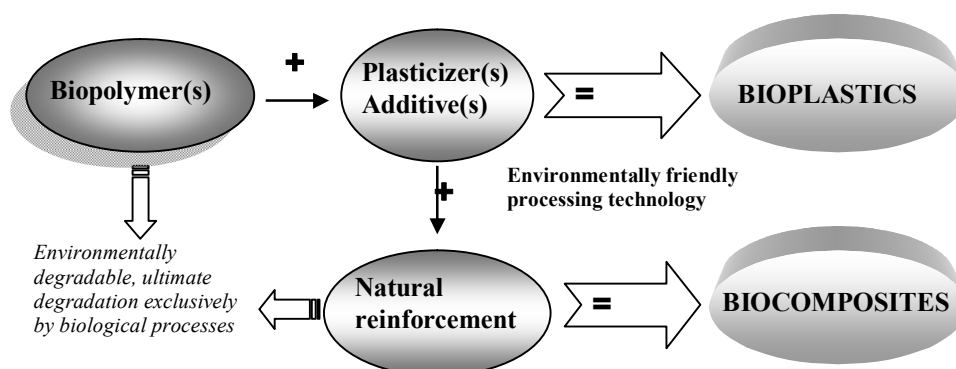
Fig. 1 – The principle of bio-based plastics and composites.

Fiber-reinforced plastics (FRPs) are composite materials with important applications as substitutes for steel and alloys, due to their outstanding properties: lightweight, tensile strength, fatigue endurance, toughness, corrosion resistance etc. The FRPs properties and behaviour are modulated by:

  ➢ the chemical nature of the polymer matrix;
  ➢ the fibers content, nature, fineness, length and orientation;
  ➢ the spatial configuration of the inserted fibrous structure.

Main fibrous   structure orientation and configurations in fiber-reinforced composites are presented in Fig. 2.

Aramide, kevlar and glass fibers are the classical reinforcement, but lately natural fibers have gained much attention both from ecological, economical and technical reasons. In the first place come the good mechanical, thermal and acoustic properties of most plant fibers, coupled with a low density. Therefore, plant fibers offer a high potential for reinforcement in lightweight structures with high impact strength and crash behaviour (Mueller & Krobjilowski, 2004), and excellent thermal and sound barrier effects (Büyükakinci *et al.*, 2011).

The use of bio-based polymers together with natural fibers reinforcement (NFR) results in *green or eco-friendly composites*, which, if properly designed and engineered, can compete with conventional FRPs and comply with the sustainable development requirements at the same time.

Several attempts to obtain such materials are signaled in the specialty literature. One feasible bio-based composite is polylactic acid (PLA) reinforced with kenaf fibres, developed by NEC Corporation for personal computer housings.With a 20% level of kenaf fibres, the main properties compete with glass fibre reinforced synthesis polymer, but the cost is 50% higher (Biron, 2007).
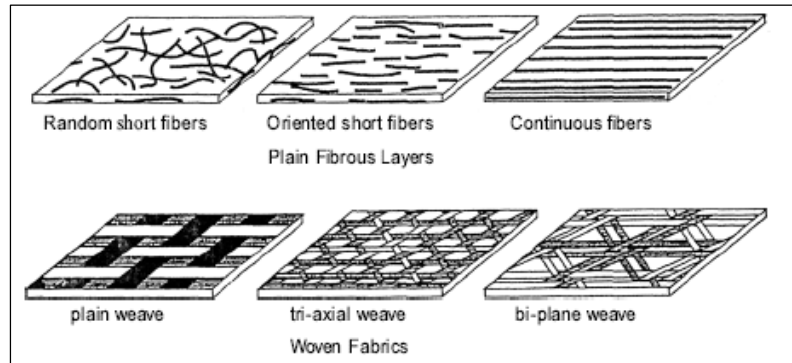
Fig. 2 – Main fibrous structure configurations in fiber-reinforced
composites (Gurdal *et al*., 1999).

3. Pathways for Obtaining Bio-based Polymers and Reinforcements

The main biopolymer constituents can be obtained from different
renewable starting sources, through several pathaways, as given in Fig. 3.
Detailed description of EDPs obtaining routes, chemical structures and
properties are beyond the scope of this paper and can be found in specialty
literature dedicated to this subject.
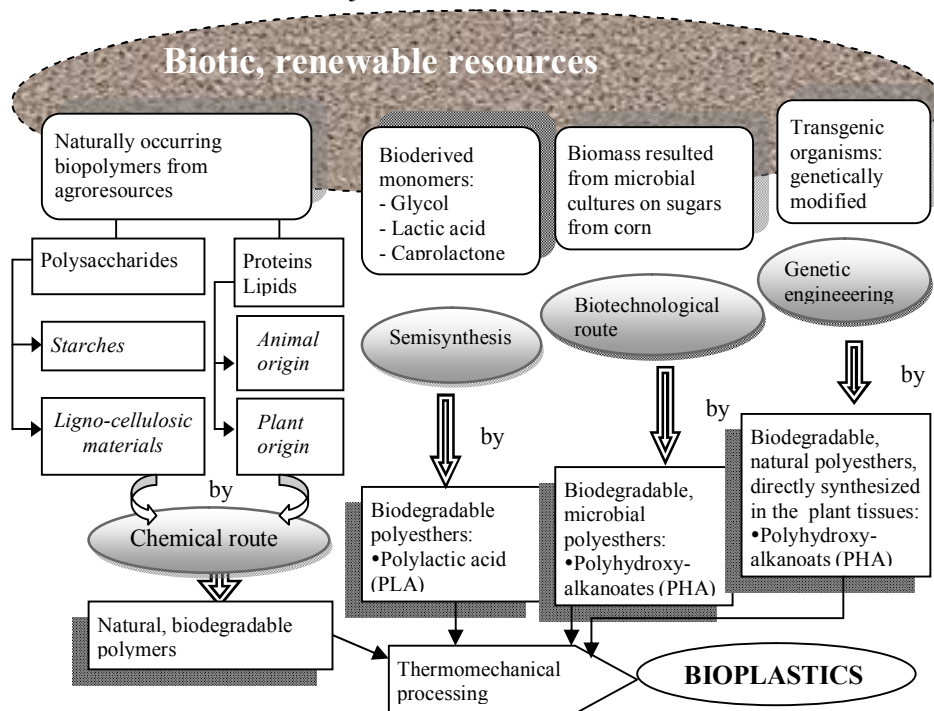
Fig. 3 – Main pathways for obtaining biodegradable polymers from renewable resources.

Biopolymers obtained as described above play the matrix role in green composites, where the reinforcement derives from natural sources as well (see Fig. 4).

To be used as reinforcements, natural fibers are subjected to different surface compatibilization treatments and processesd into different fibrous structures (yarns, slivers, woven and non-woven fabrics etc.)

At present, bio-based plastics and composites are only a niche market, but there are already more than 300 different bioplastic materials and blends on the market from around 60 European suppliers, making selection of the right grade a difficult task for plastic products designers and manufacturers.
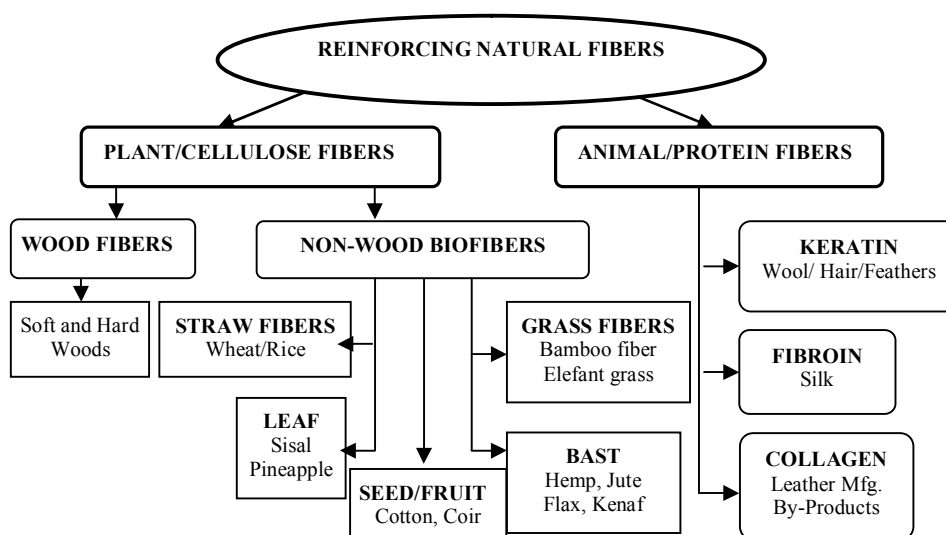
Fig. 4 – Natural resources for natural reinforcing fibers in composites (adapted From (Mohanty *et al*., 2002).

4. Technological Aspects Concerning Bio-Based Polymers Processing

A green plastic is entirely green as along as the manufacturing technology is environmentally friendly, *i.e.* is energetically efficient and uses non-toxic additives.

Most of the above-mentioned biopolymers fall in the class of thermoplastic materials, so the processing technologies must be similar to those used for syntesis polymers. Wet (casting and continuous spreading) and dry (extrusion and injection) methods are chosen depending on the physical form of the bio-based polymer (Biron, 2007).

The current problem in biopolymer processing is their low mechanical and chemical strength, high temperature sensitivity and low glass transition temperature. Moreover, the range between the melting temperature and the

decomposition point is very narrow – it does not exceed 20ºC. Biopolymers can be processed on conventional machines, provided special care is given to the values of the working parameters.

Natural fibers decompose at low temperatures; so, when the matrix is a synthesis polymer, a compromise must be found between the temperature needed to lower the polymer viscosity and the temperature threshold for the thermal damage of the fiber constituent.

There are three basic manufacturing techniques in producing composite structural products:

1) The pultrusion process;
2) The filament winding process;
3) The layup process.

One of the most performant and ecological technologies for composites obtaining is the Vacuum Assisted Resin Transfer Molding (VARTM) process (http://www.trianglepolymer.com).

5. Main Uses of Bio-Based Plastics and Composites

About 44 % of the plastic-made objects are of short-time use before they are discarded (disposable vessesls, utensiles, diapers, packaging bags, agricultural films, medical devices and disposables) so they do not require high stability (de Bragança & Fowler, 2007). Main uses of bioplastics and biocomposites are directed towards short-service, disposable products, mainly used in the food industry. A possible classification of BB-PCs after their uses is as follows:

- ***Food applications***:
✓ Food packaging, beverage and food containers
✓ Food wrapping and edible films with barrier properties
✓ Coatings of rigid fiber or greaseproof paper packaging materials
✓ Disposable food serving utensils: cups, cutlery, trays, plates, bags
✓ Service packaging for catering

- ***Non-food applications***
✓ Packaging: Shopping and biowaste bags, rigid foam for loose fills
✓ Personal hygiene products
✓ Agricultural: agricultural mulches, coverings of greenhouses, pots
✓ Pharmaceutical: drug capsules
✓ Biomedical: biomaterials

Biodegradable bioplastics used for food packaging and serving utensiles have attracted most of the bioplastics applications because they do not require separation from food waste and can be composted together with food residues. The food packaging, dishes and cutlery market is the single largest end use for bioplastics and will be the major growth driver in the future (http://www.sriconsulting.com).

The use of agroresources-based, biodegradable and environmentally benign plastics appears as a challenging, attractive alternative for supporting the sustainable and ecological agriculture concepts and practice

Lately, there is strong interest in using BB-PCs in the biomedical and pharmaceutical fields biodegradability, biocompatibility and bioresorbability make them attractive for producing fibres, sutures, clips, bone plates, tissue scaffolds, drug-delivery systems and implants.

Non-disposable applications such as cell phone housing, toys, pipes, structural engineering are acknowledged for using sustainable resources even if the final products are not easily biodegradable. One of the major field of application for natural fiber reinforced composites can be found in the automotive industry. In the medium-term time horizon, a total use of more than 100.000 tons can be expected in this area. Currently, an average of 5 to 10 kg of natural fibers is incorporated in every European passenger car with interiors parts such as door trim panels or trunk liner as the main fields of application (Mueller & Krobjilowski, 2004).

6. Sustainability of Bio-Based Plastics and Composites

Current plastics production from non-renewable resources and the existing plastic waste management practices are not sustainable. Bio-based polymers are considered promising candidates for sustainable development mainly because they contribute to the substitution of renewable resources for oil-based resources, they help to decrease greenhouse gas (GHG) emissions and, if used as biodegradable polymers, allow the closing of the loop of organic or biogenic carbon by composting.

Sustainability of BB-PCs must be included in the largest paradigm of sustainable development, which takes in account all the major factors that define the modern society, as given in Fig. 5. From the environmental point of view, sustainability is defined by several requirements where triggered biodegradability is defined as the ability of a bio-based material to be stable in its intended lifetime but to biodegrade after disposal in composting conditions (Mohanty *et al*. 2002). This property is important mainly for the plastic products with short service time, for which bioplastics found the main applications.

The Life Cycle Assessment (LCA) is the key measurement tool for assessing environmental sustainability of products or services. Through LCA it is possible to account for all the environmental impacts associated with a product, covering all the stages of its life, from the extraction of resources to ultimate disposal. Even if LCA is a vital tool, when using it as a basis for decision making it is necessary to keep in mind its limitations and partly subjective character; the decision itself remains to be made by the practitioners.

The sustainability of bioplastics is undergoing considerable debate in scientific literature, providing divergent views.
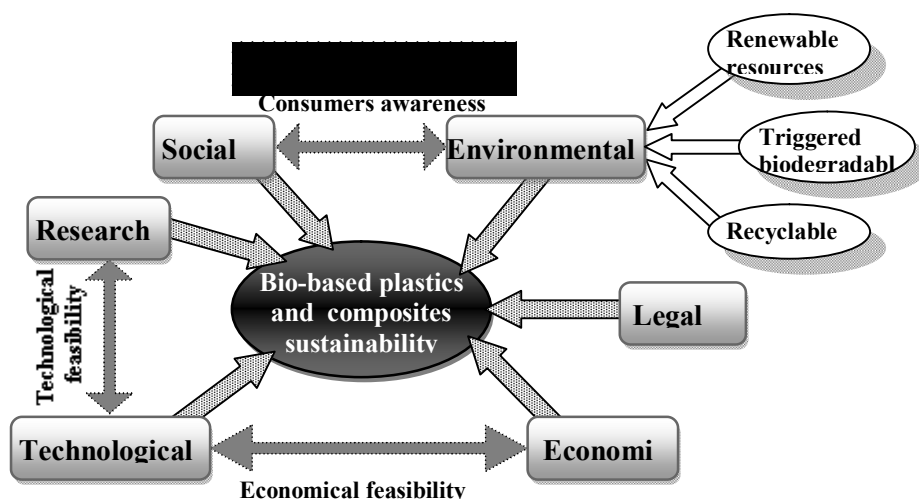
Fig. 5 – Factors that define the bio-based plastics and composites sustainability.

Questions have arisen on on the utility of EDPs, related to energy use and environmental impact, and serious doubts were expressed about wether they contribute to the reduction of fossil-base energy and GHG emission (Gerngross, 1999). This study was carried out on polyhydroxyalkanoates (PHA) and concluded that energy use and CO_2 emissions are often larger for these polymers than for synthetic polymers. At the time this article was published, these negative conclusions considerably hampered the development of reserach and production of bioplastics.

Other studies, extended to all environmental indicators and to other biobased polymers, show an updated, more optimistical picture. Thus, coroboration of more than twenty studies (Patel & Ramani, 2005) concluded that: (1) if the lyfe cycle is optimized for bio-based polymers, savings of ≈ 20 % for energy and GHG can be achieved, going up to 50 % for certain starch polymers and natural fibers composites, and (2) in the case of starch polymer pellets, energy requirements are mostly 25 -27 % below those for polyethylene (PE) and GHG emissions are 20 – 80% lower.

It must be noticed that bio-based materials are still in an early stage of research and development, compared to petrochemical plastics which have been optimized from decades and any comparative LCA study between young innovative products and mature products may be not carried out on an equal basis;

Table 1
Certification Labels for EDP-Based Products in EU States

Country	Organization	Standard compliance	Symbol/Logo
Germany	European Bioplastics	DIN V 54900 or EN 13432	
Belgium	AIB Vinçotte	EN 13432 and ISO 14851	

It is important to agree on common standards that distinguish degradable from non-degradable polymers and set univocal criteria for quantitative parameters of degradations. There are relatively few key players contributing to the development and issuing of EDPs. Based on the standards covering EDPs, a number of certification programs were developed in the EU. The purpose of certificates is to ensure the users of the nature of the material (*e.g.* if it can be composted, landfilled, buried or treated in aqueous media). Certificates are often accompanied by a label that may be placed on certified polymeric materials and related plastic items. Some of these labels, of which the European Bioplastic's "seedling" logo is well-known, are given in Table 1.

7. Conclusion

The bioplastics and biocomposites development is influenced by social, environmental, economic and technological factors, which ultimately define the sustainable development paradigm.

The main limitation of BB-PCs market is related to their high costs, compared with their conventional counterparts, even if they are regarded as a "green", innovative solution to environmental concerns like depletion of non-renewabale resources and the huge accumulation of nonbiodegradable wastes. Any green ideea is feasible only if it is economicaly efficient but one must have in mind that a clean environment has a price.

Bio-based materials will remain niche market materials with focused applications. The packaging sector has the greatest potential for bioplastics, but the most challenging one is those of biomaterials, where BB-PCs can find added-value advanced applications. Structural engineering is taking advantage of the unique properties that natural fibers impart to the composite materials.

Much research and technological advances are needed to make bio-based polymeric materials competitive and to narrow the price gap between bio-based plastics and conventional polymers.

REFERENCES

Biron M., *Thermoplastics and Thermoplastic Composites. Technical Information for Plastics Users.* Butterworth-Heinemann, Oxford, 2007.

Bolick R., *Composite Fabrication Via the VARTM Process.* http://www. trianglepolymer. com/resources/Intro+to+the+VARTM+process.pdf

Büyükakinci B.Y., Sökmen N., Küçük H., *Thermal Conductivity and Acoustic Properties of Natural Fiber Mixed Polyurethane Composites.* Tekstil ve Konfeksiyon, **21**, *2*, 124-132 (2011).

de Bragança R.M., Fowler P.A., *Handbook of Industrial Water Soluble Polymers.* Williams P.A (ed.), Blackwell Publishing Ltd, Oxford, 2007.

Gerngross, T.U., *Can Biotechnology Move us Toward a Sustainable Society?*. Nature Biotechnology, **17**, *6*, 541-544 (1999).

Gurdal Z., Haftka R.T., Hayela P., *Design and Optimization of Laminated Composite Materials.* Wiley & Sons, Inc., 1999.

Malveda M., Löchner U., Yokose K., *Biodegradable Polymers. SRIC Global Report.* 2010, http://www.sriconsulting.com/CEH/Public/Reports/580.0280/

Mohanty A.K., Misra M., Drzal L.T., *Sustainable Bio-Composites from Renewable Resources: Opportunities and Challenges in the Green Materials World.* Journal of Polymers and the Environment, **10**, *1-2*, 19-26 (2002).

Mueller D.H., Krobjilowski A., *Improving the Impact Strength of Natural Fiber Reinforced Composites by Specifically Designed Material and Process Parameters.* International Nonwovens Journal, **13**, *4*, 22-31 (2004).

Patel M., Ramani N. *Natural Fibers, Biopolymers and Biocomposites.* Mohanty A.K., Misra M., Drzal L.T. (Eds), Taylor & Francis Group, Boca Raton, 2005.

Swift G., *Directions for Environmentally Biodegradable Polymer Research.* Accounts of Chemical Research, **26**, *3*, 105–110 (1993).

MATERIALE BIOPLASTICE ŞI BIOCOMPOZITE PENTRU DEZVOLTARE DURABILĂ

(Rezumat)

Epuizarea combustibililor fosili, acutizarea problemelor ecologice legate de deşeurile din materiale plastice, necesitatea protecţiei mediului ca pilon al conceptului de dezvoltare durabilă, au determinat dezvoltarea de materiale prietenoase cu mediul, ca alternative "verzi" la plasticele convenţionale. Materialele bioplastice şi biocompozite sunt o clasă de materiale inovative fabricate din biopolimeri obţinuţi din resurse regenerabile, sunt biodegradabile şi au performanţe ajustate la cerinţe specifice. Bioplasticele şi biocompozitele sunt utilizate în special în industria ambalajelor şi a construcţiilor de maşini, dar au aplicaţii valoroase şi în agricultură şi în ingineria biomedicală. Argumentele pro sau contra acestor materiale se pun în termeni de costuri, performanţe şi impact asupra mediului. Lucrarea prezintă principalele aspecte privind bioplasticele şi biocompozitele, în ceea ce priveşte materia primă, tehnologiile de fabricaţie, domeniile de utilizare şi contribuţia la comandamentele dezvoltării durabile.

BEARING STEELS UNCONVENTIONAL THERMAL TREATED

BY

VASILE BULANCEA*, ANTONIA DIANA GHEORGHIU, MIHAI SUSAN, BOGDAN L.GAVRILĂ and GHEORGHE BULUC

"Gheorghe Asachi" Technical University of Iaşi

Abstract. Unconventional thermal treatments under 0°C and thermo-mechanical treatments have favorable influence on the structural and mechanical properties of the quenched steels. Cold treatment has as main effect the decrease of residual austenite amount of bearing steels with benefits on the bearing elements reliability.

Key words: cryogenic treatment, thermo-mechanical treatment, hardness, residual austenite.

1. Introduction

The usual technologies can be applied separately or together with the classic ones, in order to increase the reliability of bearings.

The thermal treatment under 0°C of bearing steels reduces the quantity of residual austenite, distributes more favorable the alloying elements between the matrix and carbides, reduces the internal stresses of second order, finishes the carbides size and distribution, increases the hardness and the durability of bearing elements (Alexandru & Bulancea, 2002; Bulancea, 2002).

---

* Corresponding author e-mail: vasile_bulancea@yahoo.com

The thermo-mechanical treatment‚ a combination of two technologies (plastic deformation and thermal treatment), applied to the bearing steels induces the refinement of the austenite grains.

By consequence the secondary phase, the hard martensitic structure becomes fine, too (Fiterău, 1976).One obtains mechanical properties, good plasticity and resistance and a reduced quantity of residual austenite (RA).

2. Experimental Researches

We investigated the bearing steels grades RUL 1 and RUL 2 (STAS 1456/1 – 89) with a chemical composition in the standard range, Table 1.

Table 1
Bearing Steels Compositions

Steel class	Steels	C	Mn	Cr	Ni	Mo	Other elements
Chrome steel	RUL1 (STAS) /100Cr6 (DIN)	0.95-1.10	0.20-0.45	1.30-1.65	Max. 0.30	Max. 0.08	Cu=max.0.25
Cr-Mn-Si steel	RUL2 (STAS) /100CrMn6 (DIN)	0.95-1.10	0.90-1.20	1.30-1.65	Max. 0.30	Max. 0.08	Si=0.40-0.65 Cu=max.0.25

The main stages of the thermal cycles – heat and cold treatments - are given in Table 2 (Alexandru & Bulancea, 2002; Ignat, 1980). Cooling at negative temperature must be achieved under a controlled regime.

The recommended values for different temperature ranges are: 2..5°C/min to −300C, with 3..5°C/min to −120°C and then immersion in liquid nitrogen at −196°C. The heating of the frozen samples occurs with 0,2… 0,3°C/min in N2 vapors till −120°C and in air after that. Heating the samples from temperatures higher than −196°C occurs in free air (Bulancea, 2002).

Table 2
Heat Treatment Cycles Variants

Heat treatment variants	The cyclic diagrams
A –classically HT	Hardening 840°C/30`/oil/25°C + 1 tempering 190°C/3h/air
B (cooling −30°C)	Hardening 840°C/oil + cooling −30°C/30`+1 tempering 170°C/1,5h/air
C (cooling − 60°C)	Hardening/oil + cooling − 60°C + 1 tempering 170°C
D (cooling − 90°C)	Hardening/oil + cooling − 90°C + 1 tempering 170°C
E (cooling −120°C)	Hardening/oil + cooling − 120°C + 1 tempering 170°C
F (cooling −196°C)	Hardening/oil + cooling − 196°C + 1 tempering 170°C

Bearing steels are usually thermo-mechanically treated, that is plastic deformation is conducted at high temperatures.

The variants of the thermo-mechanical treatments are given in Table 3, (Fiterău, 1976; Fiterău, 1976).

Table 3
Thermo-Mechanical Treatment Cycles

TTM Variants	TMT cyclic diagrams
TTM (1)	Heat plastic deformation / free cooling, air + baking to steeping + dimensional splintering + heating to austenitic + hardening + low tempering
TTM (2)	HATR / heat plastic deforming / suddenly hardening / low tempering
TTM (3)	HATR / heat plastic deforming / suddenly hardening / high tempering / HATR / secondary hardening / low tempering

Observations: Heating into austenite temperature range (HATR): TA = 850 - 1100°C/10, Plastic forming: TDef = 850…1100°C, εmax = 60%; Hardening: directly from TH in oil at 60...80°C; High tempering: TTemp. = 690°C/4…8h, cooling in the furnace; ReHATR: TA=850°C – RUL 1; TA=840°C – RUL 2; Secondary hardening: from TA in oil 60...80°C; Low tempering: TTemp.=160…200°C/3h.

3. Experimental Results

Hardness is an essential characteristic of bearing steels thermally and thermo-mechanically treated.

Fig. 1 depicts the dependence of HRC hardness on the residual austenite quantity (RA) that depends upon the final temperature of hardening process. The used cryogenic treatments indicate an increasing of HRC and a decreasing of RA when the final temperature reaches −196°C.
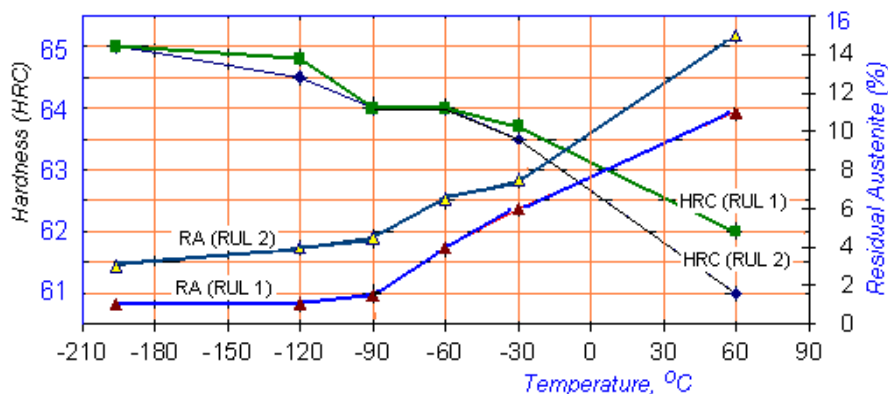
Fig. 1 − RA and HRC values versus hardening temperature
(measured after low tempering).

The small amounts of RA involve an increase in fatigue and wear resistance. The cooling under 0°C determines substructure changes, an increase of mean dimensions of the mosaic blocks, the decrease of the internal stresses of second order and the increase of dislocations density (Bulancea, 2002; Ignat, 1980).

The thermo-mechanical treatment in TTM (1) variant determines a structure with high RA amount (C-carbides, RA-residual austenite, M-martensite): RUL 1: 11,35%C; 16,9%RA; 73,75% M; RUL 2: 11,45%C; 14,8%RA; 73,75% M.

The second variant, TTM (2) has as effect a very high quantity of RA, between 19… 20% and 39… 41% for both steels.

Due the greater concentration of C into austenite and plastic deformation too, the RA (obtained after the hardening started at high temperatures, *e.g.* 1050… 1100°C) is strongly stressed. That explains the values of AR hardness, similar with these of martensite, and in consequences the high values of hardness at macroscopic level, even the temperatures are higher than usual hardening temperatures of usual bearing steels.

The TTM (3) variant indicated that the secondary Heating into austenite temperature range (that occurs upon a poor carbon matrix) increases Ms-Mf interval and stimulates the transition of austenite into martensite.
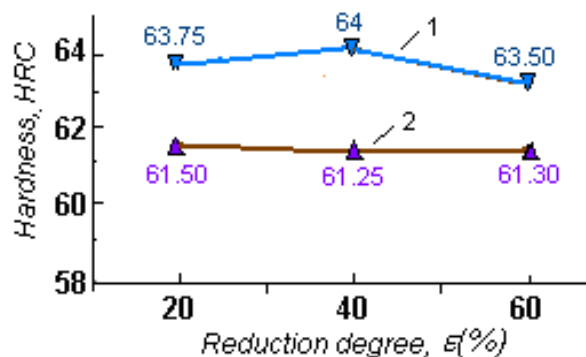
Fig. 2 – The hardness dependence on the reduction degree, ε,
after TTM(3), RUL 1, Plastic deformation: 1050℃,
low tempering at 160°C - curve 1 and at
200°C – curve 2, (Comăneci, 1999).

As result, the ratio martensite/RA is increased and RA diminished: 4… 6% (RUL 1) and 3.5… 5% (RUL 2). This variant conserves the substructure even after the secondary hardening and tempering (Comăneci, 1999). Hardness values after TTM (3) are presented in Figs. 2, 3 in correlation with plastic forming intensity and tempering temperature.

The low tempering at 160°C/3h determines high values of hardness: 64… 65.5 HRC for RUL 1 and 63... 64.33 HRC for RUL 2; if the tempering temperature increases at 200°C, the hardness decrease with 1… 2 HRC.
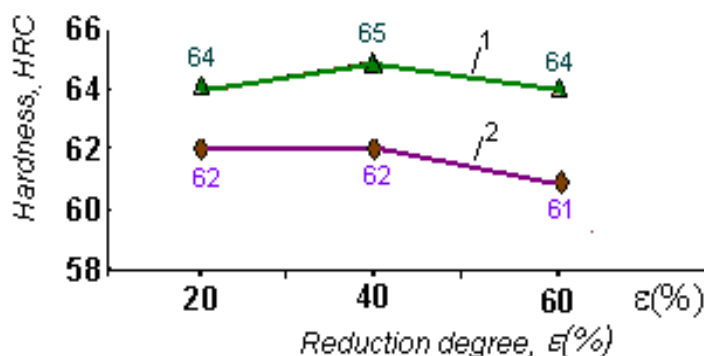
Fig. 3 – The hardness dependence on the reduction degree, ε, after TTM, RUL 2 steel, Plastic deformation: 850°C, low tempering at 160°C - curve 1 and at 200°C – curve 2, (Comăneci, 1999).

4. Conclusions

The unusual technologies exposed above represent possible variants for increased reliability of bearings.

i) Cryogenic variants that can be applied to bearing steels determine: very low percent of RA at –196°C; dimensional stability, especially for bearings to be used in aerospace; high resilience in arctic conditions; the experts suggest that the bearings that operate in normal conditions (0..120°C) contain 6… 8% RA; or a given and small quantity of RA, obtained in low cost process, can result only using thermal treatments under 0°C, (Fiterău, 1976);

ii) The examined variants of thermo-mechanical treatments have as results: high hardness in the range of standard; increasing of dimensional stability and of the security in work; plastic deformation of austenite at high temperature slows down the martensitic transition, resulting for TTM 2 in high quantities of RA; in those conditions, the carbide quantity decreases, due to the higher C content into austenite; this fact is confirmed by the tetragonality of martensite after the heat plastic deformation and hardening.

iii) The combination between the cryogenic treatment and thermo-mechanical treatment is an adequate one and has as result high hardness, fine structure, important reduction of RA and high resilience at low temperatures.

REFERENCES

Alexandru I., Bulancea V., *Handbook of Residual Stresses and Def. of Steel.* ASM Int®, March 2002.
Bulancea V., *The Role and the Importance of the Residual Austenite in the Constructive Elements of the Bearings.* Bull. of the Polytech. Inst. of Iaşi, **XLVIII (LII)**, *1-2*, Section: Mat. Sci. and Eng., 2002.
Comăneci R., Ph. D. Thessis, UTI, Iasi, 1999.
Fiterău V., *Thermal Treating Contribution on the Bearings Steels*, Rev. Met 1, 1976.
Ignat C., Ph. D. Thessis, IPI, Iasi, 1980.

OŢELURI DE RULMENŢI TRATATE TERMIC NECONVENŢIONAL

(Rezumat)

Tratamentele termice neconvenţionale sub 0°C şi tratamentele termomecanice influenţează pozitiv morfologia structurală şi proprietăţile mecanice ale oţelurilor tratate. Acestea reduc cantitatea de austenită reziduală a oţelurilor de rulmenţi, cu efecte benefice asupra fiabilităţii rulmenţilor.

DIMENSIONAL STABILITY OF BEARING ELEMENTS SUB-ZERO TREATED

BY

VASILE BULANCEA[*], ANTONIA DIANA GHEORGHIU, MIHAI SUSAN, BOGDAN L. GAVRILĂ and GHEORGHE BULUC

"Gheorghe Asachi" Technical University of Iaşi

Abstract. The thermal treatment under 0°C decreases the quantity of residual austenite and has a drastic influence on the dimensional stability of bearing elements too. The cooling at –60°C and at –90°C with 30 min standing, followed by a 1.5 hours standing at 170°C tempering induce a good dimensional stability.

Key words: heat treatment, sub-zero treatment, dimensional stability.

1. Introduction

Time variation of the dimensions of a metallic part is induced by modifications of metal structure and of stress spectra.

Neglecting the physical processes that occur during the thermal treatments, we have in the mind that the austenitizing followed by a quick cooling in the range of martensitic or bainitic quenching induces residual austenite in the bulk.

Residual austenite is a low temperature metastable compound with low specific volume. In time, residual austenite turns into other metastable phases,

---

[*] Corresponding author e-mail: vasile_bulancea@yahoo.com

martensite, bainite and so on, with an increased volume. Volume changes have as effect more residual stresses.

Austenite transition occurs slowly at ambient temperature and it is accentuated by the season's changes of temperatures.

Other special work conditions, as friction heating, cooling induced by special working conditions (flying on great altitudes, floating on polar seas) determines the same effects.

The accuracy of rotation and the functional state of bearing pieces require for them a good dimensional stability and high mechanical properties during working.

The paper presents some thermal treatments for some bearing steels, including cooling at negative temperatures, in order to increase their properties.

2. Experimental Procedures

Two bearing steel grades (RUL 1 and RUL 2) were studied; their chemical composition is given in the Table 1. First row of cells represents the values given by STAS 145611 – 89; the second indicates the results of spectral chemical analysis.

Modifying the known rules in order to obtain the optima tempering parameters that ensure high quality of structures, a good quenching effect and the desired hardness made the choice of thermal treatments.

We find that 800°C is an optimum globulizing tempering point for both steels; this temperature induces a uniform pearlitic structure with able mechanical working hardness.

Table 1
Chemical Composition of the Tested Steels

Steel	Chemical composition, %								
	C	Mn	Si	P Max	S Max	Cr	Ni Max	Cu Max	Mo Max
RUL 1-STAS 100Cr6 – DIN	0.95–1.10	0.2 – 0.45	0.17–0.37	0.027	0.02	1.3–1.65	0.3	0.25	0.08
	1.02	0.34	0.30	0.015	0.018	1.55	0.12	0.16	0.035
RUL 2 –STAS 100CrMn6-DIN	0.95–1.10	0.9 – 1.2	0.40–0.65	0.027	0.02	1.3–1.65	0.3	0.25	0.08
	1.01	1.08	0.60	0.020	0.015	1.60	0.18	0.11	0.055

The structure, the high quenching effect and the hardness values are optima after quenching from a temperature of 840°C.

As the heating temperature increases, the carbides are better solved, austenite is more homogenous, so the martensitic transition range decreases and the residual austenite amount increases.

The Table 2 gives the thermal treatments applied to the studied steels.

Table 2

Heat Treatments Cycles

Variants of heat treatment	The cycle diagram of thermal treatment
A	Quenching from 840°C/30 min /oil 60 … 80°C + 1 tempering at 170°C / 3 h/air
B	Quenching from 840°C/30 min /oil 60 … 80°C + 1 tempering at 190°C / 3 h/air
C	Quenching from 840°C/30 min /oil 60 … 80°C + 1 tempering at 210°C / 3 h/air
D	Quenching from 840°C/30 min /oil, 60 … 80°C + cooling at **–60°C**, 30 min + tempering at 170°C /1,5 h/air
E	Quenching from 840°C/30 min /oil 60 … 80°C + cooling at **–90°C**, 30 min + 1 tempering at 170°C /1,5 h/air
F	Quenching from 840°C/30 min /oil 60 … 80°C + 1 tempering 170°C / 8 h/air at RUL1 and 22 h at RUL2
G	Quenching from 840°C/30 min /oil 60 … 80°C + 3 tempering at RUL 1 (4 at RUL 2) 170°C /30 min/air

Time dependence of dimensional stability was investigated on French samples (Fig. 1).
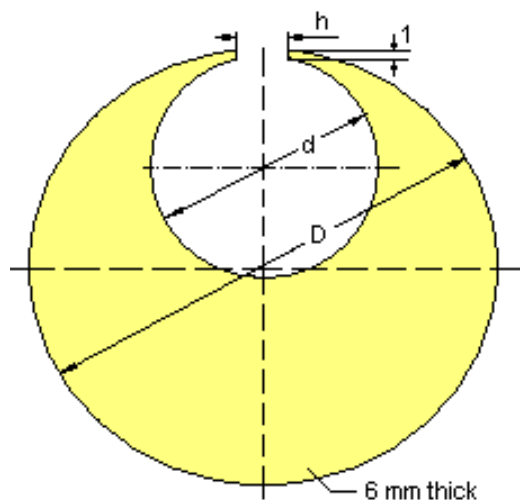
Fig. 1 – Schematic of a French specimen, with standard dimensions: D=50mm, d=25mm, h=6mm, (Alexandru & Bulancea, 2002).

3. Experimental Results

Thermally treated and rectified French samples were deposed in a thermostat box and periodically measured 3 months with a 10 days period in first month and monthly after.

The measurements have been performed with a universal device for lengths with 0.1 micrometers accuracy.

The results are given in the Table 3.

Table 3
Dimensional Variations of Steels Researches

HT Variant	Steel	Dimension	Relative variation $\Delta l/l$ (μm/mm)				
			After 10 days	After 20days	After 30 days	After 60 days	After 90 days
A	RUL 1	D	+2	+2… +3	+3	+3… +4	+4
		d	+1	+1… +2	+2	+2… +3	+3
	RUL 2	D	+3	+4… +5	+5	+5… +6	+6
		d	+2	+2… +3	+3	+3… +4	+4
B	RUL 1	D	+2	+2… +3	+3	+3… +4	+3… +4
		d	+1	+2	+2	+2… +3	+2… +3
	RUL 2	D	+3	+4	+4… +5	+5	+6
		d	+2	+2… +3	+2… +3	+3	+3… +4
C	RUL 1	D	+1	+1	+2	3	+3… +4
		d	0… +1	+1	+1	+1… +2	+2
	RUL 2	D	+2	+2… +3	+2… +3	+3… +4	+4
		d	+1	+1… +2	+1… +2	+2… +3	+3
D	RUL 1	D	0	0… -1	0… -1	-1	-1… -2
		d	0	0	0… -1	0… -1	0… -1
	RUL 2	D	0	-1	-1	-1… -2	-2
		d	0	0	0… -1	0… -1	0… -1
E	RUL 1	D	0	0… -1	0… -1	0	-1
		d	0	0… -1	0	0	0… -1
	RUL 2	D	0	0	-1	0… -1	0
		d	0	0	0… -1	0… -1	0… -1
F	RUL 1	D	0	0… +1	+1	+1	+1… +2
		d	0	0	0… +1	0… +1	0… +1
	RUL 2	D	0	0… +1	+1	+1	+1… +2
		d	0	0	0	0… +1	0… +1
G	RUL 1	D	+1	+1… +2	+2	+2… +3	+3
		d	0… +1	0… +1	+1	+1… +2	+1… +2
	RUL 2	D	+1	+2	+2	+3	+3
		d	0… +1	+1	+1… +2	+2	+2

The "h" interval is not given due to the parallel deviations in horizontal vertical flats. The tabulated values are too given in the Figs. 2,…,5, that presents the dimensional variations chart.
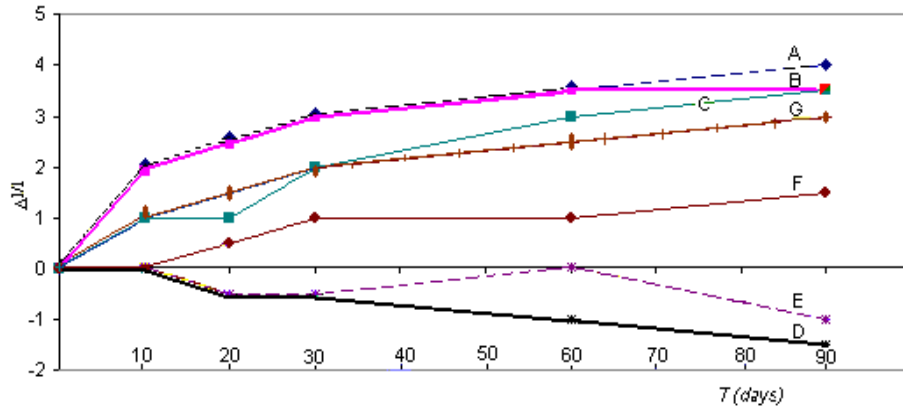
Fig. 2 – "D" dimension vs. deposed time dependence for steels RUL 1.
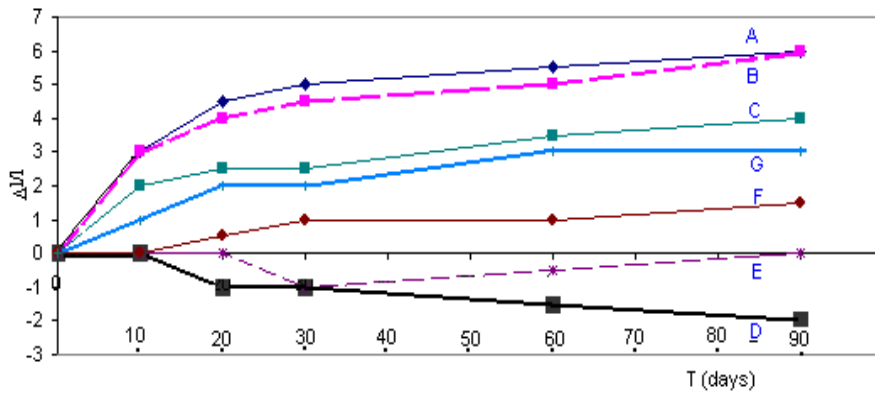
Fig. 3 – Variation of "D" dimension with the deposed time, RUL 2.
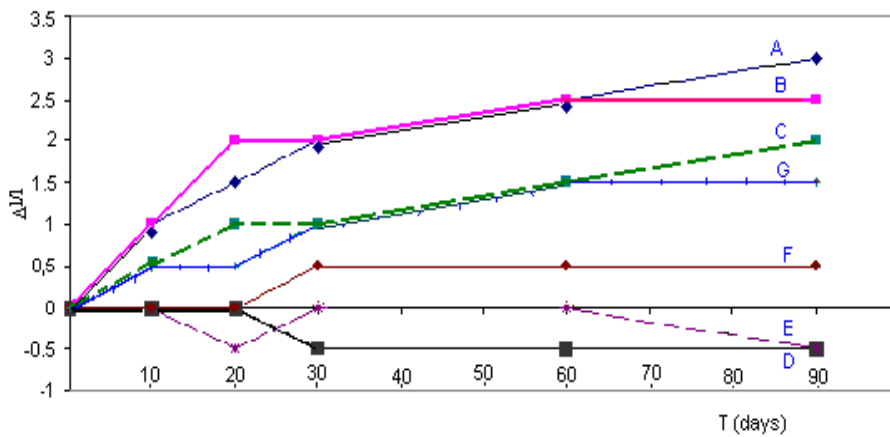
Fig. 4 – Variation of "d" dimension with the deposed time, RUL 1.
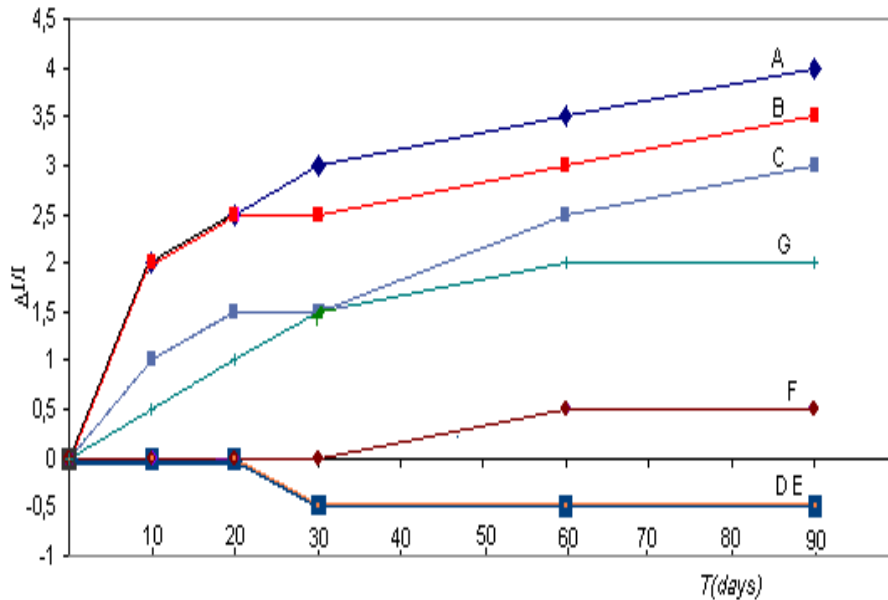
Fig. 5 – Variation of "d" dimension with the deposed time, RUL 2.

3. Conclusions

The experimental results as are concentrated in Table 3 and presented in Figs. 2 to 5 concerning the way heat treatment cycle influences the secondary variation of part dimensions as is reflected by the French samples leads to the following conclusions:

a) Classical heat treatment does not ensure an efficient dimensional stability, especially for RUL 2 steel. This can be observed on the graphs from Fig. 2 to Fig. 5 following curves A, B and C, corresponding to the as designated heat treatment cycles.

b) The same cycles proves that time dimensional stability slightly increases with increasing tempering temperature. It can be assumed that phase change at room temperature diminishes as result of a better equilibrium state due to increased tempering temperature.

c) Cooling at –60°C (cycle D with corresponding curves in figures) and at –90°C (cycle E) with 30 min keeping at the smallest temperature, followed by a 1.5 hours tempering at 170°C has as effect a better dimensional stability. This is secondary to almost a complete transformation of the residual austenite. One can observes a small decrease of the sample dimensions. The effect can be attributed to martensite dissociation and stresses relaxation too.

d) Tempering stage in treatment of steels is a way to impart a degree of plasticity, especially by reducing the high internal stresses associated with

quenching step. The final tempering after subzero thermal treatment can be assumed that allows a limited diffusion of the carbon and alloying element atoms, so more stress relief does occur during tempering step even for sub-zero treatment.

e) The above conclusion is confirmed by the effect long time tempering (cycle chart F) has on the samples that submit it. Cycle F ensures the best dimensional stability, but the hardness is decreased under the inferior permitted value. This is due to the intense coalescence of the carbides, so metallic matrix become too soft.

f) Under zero treated samples (D and E cycles) undergo the best dimensional stability with an appropriate hardness value.

The effect, not well explained until now, can be attributed to a complete residual austenite transformation, so the brittle structure is more uniform. At tempering temperatures, diffusion occurs in the structure with almost the same properties, carbide and equilibrium phase do form into a rather uniform structure, with little compositional variation.

g) Cyclical tempering (variant G) gives a higher dimensional stability than classical variants (A, B and C).

NU SE REGASESC IN TEXT TRIMITERILE BIBLIOGRAFICE
REFERENCES

[1]. Meng F., Tagashira K., Sohma H., *Wear Resistance and Microstructure of Cryogenic Treated Fe-1.4Cr-1C Bearing Steel*. Scripta Metall. Mater., **31**, *7*, 865-868 (1994).
[2]. Earl A. Carlson, *Cold Treating and Cryogenic Treatment of Steel*. ASM Handbook, **4**, Heat Treating, 1991.
[3]. Alexandru Ioan., .Bulancea Vasile, *Handbook of Residual Stresses and Deformation of Steel*. Ed. by G. Totten, M. Howes, T. Inoue, ASM International®, March 2002;
[4]. **** Cryogenic Processing and Wear Properties – Metal Progress, USA, **122**, *6*, 1972.

STABILITATEA DIMENSIONALĂ A ELEMENTELOR DE RULMENŢI
TRATATE SUB ZERO

(Rezumat)

Tratamentul criogenic scade cantitatea de austenită reziduală şi de asemenea are o influenţă drastică asupra stabilităţii dimensionale a elementelor de rulmenţi. Răcirea la -60°C şi la -90°C, urmată de 1,5 ore menţinere la temperatura 170°C induce o stabilitate dimensională bună.

ELECTROLESS Zn-Ni-P ALLOYS DEPOSITION ON STEEL FROM A CHLORIDE BATH

BY

MARIAN BURADA[1]*, VASILE SOARE[1], IONUŢ CONSTANTIN[1], FLORIN MINCULESCU[2], ANA MARIA POPESCU[3] and IOAN CARCEA[4]

[1] National R&D Institute for Nonferrous and Rare Metals – IMNR,
[2] Polytechnic University of Bucharest, BIOMAT,
[3] Institute of Physical Chemistry, Bucharest,
[4] "Gheorghe Asachi" Technical University of Iaşi

Abstract. Ternary Zn-Ni-P alloy thin films are considered a replacement for cadmium sacrificial coatings for anticorrosive protection of steel parts working in highly corrosive media. Zn-Ni-P thin films were autocatalytically deposited (electroless chemical plating) on carbon steel substrate from chloride alkaline baths. The effect of pH and process duration on physical-chemical and corrosion characteristics of the obtained films was investigated. Films were characterized by EDAX and SEM analysis techniques. Corrosion tests were done in 3.5% sodium chloride solution; corrosion current values were determined to be 4 - 10 A, comparative to 15 μA for the unplated steel sample.

Key words: corrosion, electroless deposition, thin films, Zn-Ni-P ternary alloys, chloride bath.

1. Introduction

Thanks to high corrosion resistance, cadmium is used intensively as an anticorrosive protection layer for steel parts used in energy systems,

---

* Corresponding author e-mail: ioan.carcea@yahoo.com

transportation, chemical equipment production, metallic constructions, etc. (Baldwin & Smith, 1996). In spite of that, cadmium plating presents major disadvantages due to the toxicity of the metal and its salts, as well as simultaneous discharge of hydrogen ions during the cadmiation process, making the steel substrate susceptible to hydrogen embrittlement failure (Safranek, 1997; Ashur *et al.*, 1996). These are the main reasons why, in the last decades alternate coatings to cadmium are being actively explored.

The most common sacrificial coatings replacements for Cd are zinc and its alloys. Zn presents a low electrode standard potential ($E_0 = -0.76$ V, measured vs. normal hydrogen electrode), thus being capable of acting as a sacrificial coating for plated steel parts (Swathirajan, 1986). The difference between the standard potentials of zinc and the substrate (iron) constitutes the corrosion force of the protection coating in corrosion conditions, and the high value of this difference leads to a rapid dissolution of zinc layer. The dissolution rate of the protective coating was considerably reduced by alloying zinc with other elements (Ni, Co, Fe, etc.) that shifted the standard electrode potential of the alloy to values closer to the substrate (Short *et al.*, 1996). Among these alloys, the best anticorrosive properties, similar to those of cadmium, are presented by the Zn-Ni alloys (Lin & Selman, 1993; Brenner, 1963).

Electrochemical deposition of Zn-Ni alloys is an anomalous process by nature. Although Ni is nobler than Zn, co-depositing these metals results in obtaining large quantities of Zn in the deposited alloy. As an effect of high Zn concentration, the alloy dissolution rate is also high in corrosive medium conditions.

Various studies and researches were performed for decreasing the anomalous effect of the codeposition and for increasing the Ni content in the alloy, thus decreasing the dissolution rate of the anticorrosive alloy coating. These researches were based mainly on the following directions: *1.* using inert species in the deposition bath, to inhibit zinc codeposition, and, *2.* developing ternary anticorrosive alloys: Zn-Ni-X (X= Cd, Co, P, Si, etc.) (Grigoryan *et al.*, 1989; Popov *et al.*, 1986). Among these, ternary Zn-Ni-P alloys suscitated special attention, an addition of 1-5% P considerably enhancing corrosion resistance (Zhou *et al.*, 1997; Valova *et al.*, 2001).

An alternative and attractive method for obtaining ternary Zn-Ni-P alloy coatings and for increasing Ni content in the deposited layer is the process of autocatalytic reduction of metals (chemical deposition, no current applied) in the presence of an oxidizing agent. This method was used for obtaining Zn-Ni-P coatings from sulphate and chloride solutions. Previous research work showed that the alloy deposition develops normally, obtaining coatings with high concentrations of nickel (80-90 wt%) and zinc concentrations of 10-15 wt% (Durairajan *et al.*, 2000; (Bouanani *et al.*, 1999). At these elemental concentrations, although the coatings film exhibits excellent anticorrosive properties, it cannot be used as a sacrificial coating for steel parts. The objective

of studies and researches done in the area is to enhance the zinc content in the alloy and thus the coatings to exhibit sacrificial properties.

Present work shows the experimental researches for autocatalytic obtaining of Zn-Ni-P thin films on steel substrate from chloride bath solutions. The effects of concentrations and pH of the bath and the duration of the process on physical-chemical and corrosion characteristics of the obtained coatings are studied.

2. Experimental

Zn-Ni-P thin films were deposited on mild carbon steel plates (C=0.28 % wt.) 40 x 20 mm in size, 0.6 mm in thickness. Before depositing, the surface of the steel samples was prepared. This is necessary because of the adherence between the substrate and the coating, with favorable consequences on anticorrosive protection efficiency, can be provided only by adequate preparation of the sample surface. The preparation process of the substrate for film deposition contained the following operations: 1. mechanically polished with successively finer grades of emery papers; 2. acetone degreasing and rinsing in double distilled water; 3. sample etching, for removing traces of surface adherent oxide, with 37% HCl solution at a temperature of 30-40°, for 1-2 minutes, followed by washing with double distilled water. The experimental installation for autocatalytic deposition consisted of a thermo resistant vessel of 600 cm^3 capacity and a magnetic heater-stirrer. The chemical composition of the autocatalytic deposition baths is given in Table 1.

Table 1
Composition of Autocatalytic Deposition Baths [g/l]

Deposition bath	Chemical composition				
	$ZnCl_2$	$NiCl_2*6H_2O$	$NaH_2PO_2*H_2O$	$C_6H_5Na_3O_7*2H_2O$	NH_4Cl
	10	47	45	10	100

Sodium hypophosphite was used as a reducing agent for the autocatalytic process, and also as a phosphorus source in the deposited alloy film. The deposition bath was prepared using analytical grade reagents and double distilled water.

The experimental values of the pH of the bath were set and maintained to the following values: 9, 9.5 and 10 respectively, with concentrated NaOH solution.

The deposition was carried out at a temperature of 85 ± 2°C. The time period of the deposition process was of 1 hour and 2 hours respectively, for each pH value. The deposition bath was stirred using a magnetic agitator, at a 30-40 rpm rate.

Electrochemical characterization of Zn-Ni-P coatings

For determining corrosion characteristics of the coatings, specific electrochemical analysis methods were used, which permitted the establishing of the corrosion potential (E_{cor}), determining polarization resistance and plotting Tafel polarization curves (Brânzoi *et al*., 2006; Zamfir *et al*.,1994).

Corrosion studies were performed using a PARSTAT 2273 potentiostat, the obtained data was processed using specialized „PowerCorr" software. The tests were executed in 3,5%, aqueous NaCl solution at a temperature of 25°C, in a three electrode electrochemical set up. Steel samples coated with the autocatalytic deposited thin film constituted the working electrode, and a platinum sheet the cell counter electrode. A saturated calomel electrode was used as reference electrode. The working electrode potential scanning rate was 0.166 mV/s.

The open circuit potential (E_{OPC}), (when no potential or current is being applied to the cell), was measured for analyzed samples for 30 minutes. During open circuit experiments, the free currents generated by the exposing the sample to the corrosive medium were measured vs. time.

The polarization resistance determination was effectuated by linear polarization with low potential applied. The analyzed sample was scanned at $\pm$ 20 mV vs. open circuit potential E_{OPC}. The determination time was of 30 minutes.

For determining Tafel polarization curves (with high potential applied), the potential was varied in steps, with a step size of 0,166 mV, in a $\pm$ 250 mV vs. E_{OCP} range, for 1-2 hours. The obtained data permitted the determination of kinetic parameters for the corrosion process of the studied coatings.

3. Results and Discutions

Deposited thin films analysis

The visual aspect of the obtained ternary Zn-Ni-P thin film deposits is uniform, bright gray and smooth. The obtained thin films were characterized using dispersive X ray microanalysis (EDAX) for determining the concentration and elemental distribution and scanning electron microscopy (SEM) for determining the morphology and microstructure. For increasing the accuracy degree of the elemental distribution, the EDAX analysis was performed in various points situated along a diagonal of the steel sample. The analyses were performed using a XL-30-ESEM TMP type electronic microscope, fitted with an EDAX detection device.

The thickness of the deposited films was measured with an optical microscope AxioImager A1m equipped with image capture system Canon Power Shot A 640 and image interpretation software AxioVision.

Table 2 contains the elemental chemical composition of the autocatalytic deposited thin films, determined by EDAX, as well as the measured thickness of the films.

Fig. 1 presents the EDAX specters recorded for the analyzed samples C 2, C 4 and C6 respectively.

Table 2
Elemental Chemical Composition of the Deposited Thin Films

Sample code	Bath pH	Deposition time [hour]	Thickness [m]	Chemical composition [% wt]		
				Ni	Zn	P
C 1	9,0	1	2,5	84,6	12,3	3,1
C 2		2	4,2	81,4	14,8	3,8
C 3	9,5	1	5,5	80,2	15,5	4,3
C 4		2	8,6	75,9	18,7	5,4
C 5	10	1	3,2	80,7	13,5	5,8
C 6		2	3,9	79,5	14,2	6,3

a

b

c
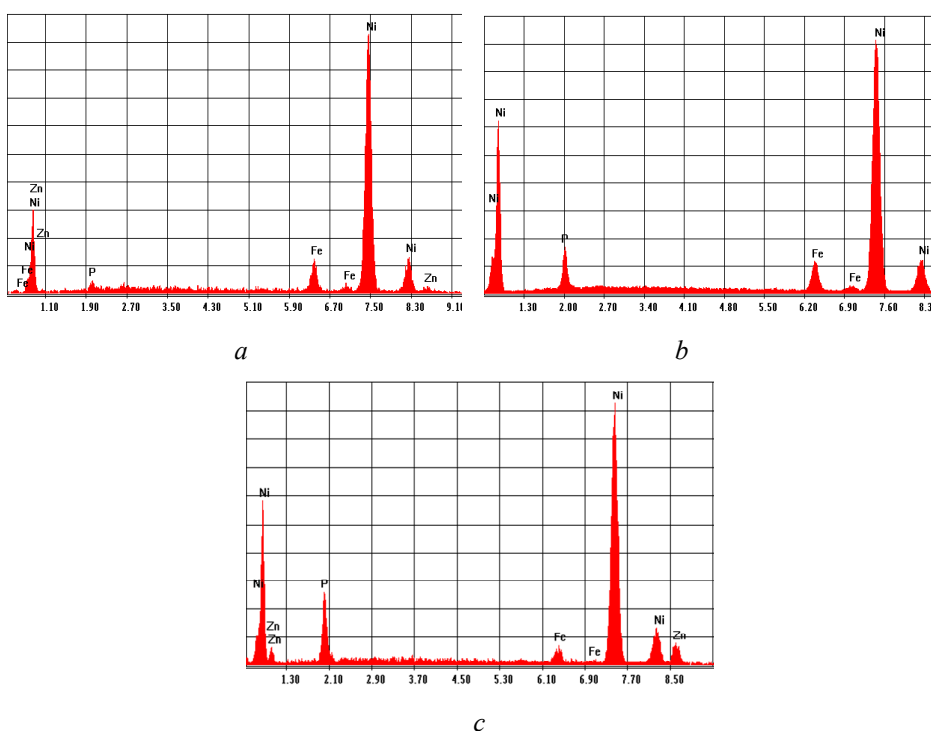
Fig. 1 – EDAX specters recorded for the samples C2 (*a*), C4 (*b*) and C6 (*c*).

Fig. 2 shows the SEM micrographs of the thin films obtained from baths with different values of pH.
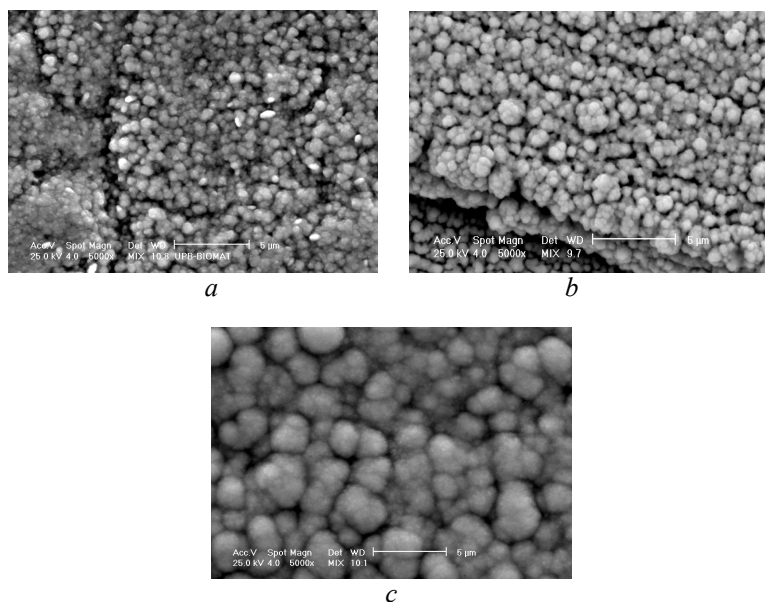
Fig. 3 – SEM micrographs (x5000) for samples C 2 (*a*), C 4 (*b*) and C 6 (*c*).

From the results obtained it could be concluded the following:

- The presence of a high Ni content in the obtained thin film; the concentration decreases with increasing of deposition time as well as pH value of the bath.

- The zinc concentration in the deposit increases dependant on deposition time as well as pH of the bath, the maximum value was obtained for a pH of 9.5 and 2 hours deposition time.

-The phosphorus concentration in the deposit increases with increasing of deposition time as well as pH value of the bath.

SEM micrographs reveal the fact that the autocatalytic deposited thin film is compact, polycrystalline and composed of fine grains covering the entire surface with a growth resembling a cauliflower pattern. It can be observed that the dimension of the crystallites increases with the increase of pH value of the deposition bath.

Determining corrosion characteristics

In Table 3 are presented the values of the open-circuit potential E_{OCP} for the coated samples as well as uncoated steel substrate (S).

In Table 4 are presented values for corrosion kinetic parameters determined by „PowerCorr" professional software for the samples.

The Tafel curves for the analyzed film samples and for the uncoated steel sample are presented in Fig. 4.

Table 3

E_{OCP} Potentials Measured in Open Circuit

Sample	S	C 1	C 2	C 3	C 4	C 5	C 6
E_{OCP} *vs.* SCE [mV]	- 595	-517	-512	-502	-494	-498	-483

Table 4

Kinetic Corrosion Parameters for the Steel Substrate and Studied Samples

Sample	I_{corr} [μA]	E_{corr} [V vs SCE]	$β_c$ [mV]	$β_a$ [mV]	R_p [Ω]	RC [mm/y]	E [%]
S	15.360	-0.574	378.58	43.92	3.774	0.378	0
C 1	4.122	-0.387	11.60	21.42	77.892	0.096	+ 79.86
C 2	4.630	-0.411	32.16	26.95	74.646	0.104	+ 79.42
C 3	7.194	-0.490	48.32	39.84	73.035	0.115	+ 76.36
C 4	9.875	-0.524	47.55	38.64	62.352	0.178	+ 69.07
C 5	8.163	-0.414	75.94	41.27	72.292	0.123	+ 75.73
C 6	8.547	-0.432	84.00	42.10	73.173	0.135	+ 74.27

where: I_{corr} = corrosion current

E_{corr} = corrosion potential

$β_c$ and $β_a$ = Tafel slopes (cathodic and anodic)

R_p = polarisation resistance

RC = corrosion rate

E   = corrosion protection efficiency
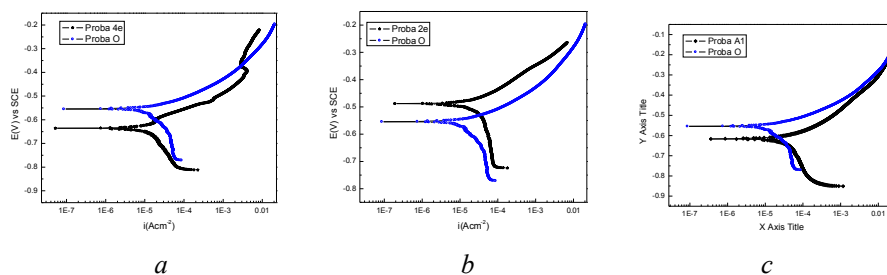
Fig. 4 – Tafel curves for samples C 2 (*a*), C 4 (*b*) and C 6 (*c*) (In blue, Tafel curves for witness sample-uncoated steel sample).

On the basis of the obtained test corrosion results it could be concluded the following: coated steel samples present values of the open circuit potentials (E_{OCP}) higher than the value for unplated steel sample; corrosion currents (I_{corr}) as well as the corrosion potentials (E_{corr}) measured for coated samples are lower than the values measured for the unplated sample; corrosion rate calculated

values, expressed in mm/year, are lower than the corrosion rate calculated for the unplated sample; corrosion protection efficiency values are higher (considering „0" the efficiency for the unplated sample).

C 1 and C 2 samples present the highest values for corrosion protection efficiency, samples also exhibit great nickel content in the autocatalytic deposited film.

4. Conclusion

The experimental results confirmed certain influences of the autocatalytic obtaining conditions (pH value and deposition time) on the composition, structure and corrosion resistance of Zn-Ni-P thin films deposited on mild carbon steel substrate from alkaline chloride bath.

The assessment of the autocatalytic deposition process has revealed the following technological aspects: the presence of a high Ni content in the film, which decreases with the increasing of the immersion time in the deposition bath; zinc and phosphorous content increasing with the increasing of the pH value of the bath as well as deposition time.

SEM analysis has shown that the autocatalytic deposited thin film is compact, polycrystalline and composed of fine grains covering the entire surface with a growth resembling a cauliflower pattern. It can be observed that the dimension of the crystallites increases with the increase of pH value of the deposition bath

Steel samples coated with Zn-Ni-P thin films exhibit greater corrosion resistance than the unplated steel sample. Determined values of I_{corr} corrosion currents ranged in a 4 - 10 µA interval, comparative to the corrosion current of the unplated sample of 15 µA. The highest values for electrokinetic parameters characterizing corrosion resistance were recorded for samples with high Ni content.

REFERENCES

Ashur A., Sharon J., Klein I.E., *Plat. Surf. Finish., 83, 58*, 1996.
Baldwin K.R., Smith C.J.E., *Trans. Inst. Met. Finish., 74, 202*, 1996.
Bouanani M.,Cherkaoui F., Fratesi R., *Microstructural Characterization and Corrosion Resistance of Ni–Zn–P Alloys Electrolessly Deposited from a Sulphate Bath. J. Appl. Electrochem., 29, 637* (1999).
Brânzoi I.V., Brânzoi F., Pilan L., *Caracteristici generale provind coroziunea şi protecţia anticorozivă a metalelor în diverse medii.* Ed. Printech, Bucureşti, 2006
Brenner A., *Electrodeposition of Alloys, Principles and Practice.* Academic Press, New York, 1963.

Durairajan A., Krishniyer A., Haran B.S., Popov B.N., *Characterization of Hydrogen Permeation Through a Corrosion-Resistant Zinc-Nickel-Phosphorus Alloy*. Corrosion (Houston), *56*, 283 (2000).

Grigoryan N.S., Kudryavtsev V.N., Zhdan P.A., *Zasch. Met.,* **25**, *288*, 1989.

Lin Y.P., Selman J.R., *Electrodeposition of Corrosion-Resistant Ni-Zn Alloy*. J. Electrochem. Soc*., 140*, 1299 (1993).

Popov B.N., Slavkov D., Grecv T., Lj. Arsov, *Kem. Ind.* **1**, 1986.

Safranek W.H., *Plat. Surf. Finish.* 85, 45, 1997.

Short N.R., Zhou S., Bennis J.K., *Electrochemical Studies on the Corrosion of a Range of Zinc Alloy Coated Steel in Alkaline Solutions*. Surf. Coat. Technol*., 79*, 218 (1996).

Swathirajan S., *Potentiodynamic and Galvanostatic Stripping Methods for Characterization of Alloy Electrodeposition Process and Product*. J. Electrochem. Soc., *133*, 671 (1986).

Valova E., Georgiev I., Armyanov S., Delplancke J.L., *Incorporation of Zinc in Electroless Deposited Nickel-Phosphorus Alloys I. A Comparative Study of Ni-P and Ni-Zn-P Coatings Deposition, Structure, and Composition*. J. Electrochem. Soc., **148**, *C266* , 2001.

Zamfir S., Vidu R., Brînzoi V., *Coroziunea materialelor metalice*. E.D.P., Bucureşti, 1994.

Zhou Z., O'Keefe T.J., *Modification of Anomalous Deposition of Zn-Ni Alloy by Using Tin Additions*. Surf. Coat. Technol*., 96*, 191 (1997).

DEPUNEREA FĂRĂ CURENT A ALIAJELOR Zn-Ni-P PE OŢEL DIN BĂI DE CLORURI

(Rezumat)

Filmele subţiri de aliaj Zn-Ni-P sunt considerate un înlocuitor pentru acoperirile de sacrificiu din cadmiu, pentru protecţia anticorozivă a pieselor de oţel. Filmele subţiri Zn-Ni-P au fost depuse autocatalitic (depunere chimică, fără aplicarea de curent) pe substrat de oţel carbon din băi alcaline de cloruri. A fost investigat efectul pH băii şi a timpului de depunere asupra caracteristicilor fizico-chimice şi de coroziune a filmelor subţiri obţinute. Filmele au fost analizate prin tehnici de analiză EDAX şi SEM. Testele de coroziune au fost realizate în soluţie apoasă de NaCl 3,5%; valorile măsurate ale curentului de coroziune pentru probele de oţel acoperite fiind situate în intervalul 4 – 10 A, faţă de un curent de coroziune de 15 µA măsurat pentru proba de

DYNAMIC AND STATIC CHARACTERISTICS OF THE LS HYDRAULIC DRIVE ON THE BASIS OF MULTIMODE DIRECTIONAL CONTROL VALVE

BY

Y. BURENNIKOV[*], L. KOZLOV and A. PETROV

Vinnitsa National Technical University

Abstract. The paper deals with the solution of a scientific task consisting in development and research of a new hydraulic drive circuit providing highly efficient operation of the hydraulic drive control system and the necessary dynamic and static. A circuit of the load-sensing (LS) hydraulic drive on the basis of multimode directional control valve for the mobile working machine has been developed. A non-linear mathematical model of the LS hydraulic drive on the basis of multimode directional control valve has been elaborated. Theoretical research was conducted on the basis of mathematical model using MATLAB 6.5 software package. It was determined that the design parameters of the pressure relief valve of the multimode directional control valve, realizing the feedback, influence dynamic and static characteristics of the LS hydraulic drive. Such values of the pressure relief valve parameters have been found which provide minimal values of stabilization error, regulation time and excessive control.

Key words: load-sensing hydraulic drive, directional control valve, mobile working machine, dynamic descriptions, static descriptions.

---

[*] Corresponding author e-mail: vadikkov@ukr.net

1. Introduction

Load-sensing (LS) hydraulic drives are widely used in modern mobile machines. Such hydraulic drives provide increased economic efficiency of the machine operation and higher quality of the work being performed (Jonson, 1995; SB 12 LS – Katalog ; RE 98071, 2001).

In LS hydraulic drives directional control valves of a special design are used and their characteristics, to a great extent, determine, the performance of the hydraulic drive as a whole. One of the characteristics of the directional control valve for LS hydraulic drives is control pressure difference on the spool of the pressure relief valve. The value of pressure difference Δp in the directional control valve of PVG type, manufactured by Danfoss, is 2,0 MPa, which reduces the efficiency of hydraulic drive operation (Catalogue HK.51. A1.02. Danfoss 11/91). Reduction of the control pressure difference without special compensating measures results in worsening of both static and dynamic characteristics of the hydraulic drive (Козлов, 2000; Burennikov, 2009). The authors of the given work set the task of designing the directional control valve for LS hydraulic drive with the reduced (compared to the analogs) value of the control pressure difference and of choosing such values of the design parameters which will provide values of static and dynamic characteristics depending on the requirements to LS hydraulic drive operation in the modes of pump unloading, adjusting of the flow rate, maximal flow rate and overload protection.

1.1. LS Hydraulic Drive Investigation

Proceeding from the analysis of the known circuits of hydraulic drives with a constant flow rate and LS hydraulic drives as well as the requirements to hydraulic drives of mobile working machines, LS hydraulic drive is developed on the basis of multimode directional control valve that operates in the modes of pump unloading, adjusting of the flow rate, maximal flow rate and overload protection. Fig. 1 shows the hydraulic drive circuit where directional control valve with the pressure relief section, designed in VNTU, is used.

The circuit comprises pump 1, directional control valve 25, hydraulic cylinder 3, pressure relief section 4 with pressure relief valve 5 having spool plunger 6, springs 8 and 9 as well as safety valve 10 with spring 11.

Parameters of the relief valve are included into the feedback transfer function and they have definite influence on the quality of the hydraulic drive operation. The stabilization error of flow through the directional control valve, the pressure regulation time and excessive correction value in the hydraulic drive are considered to be quality indicators of the hydraulic drive operation.
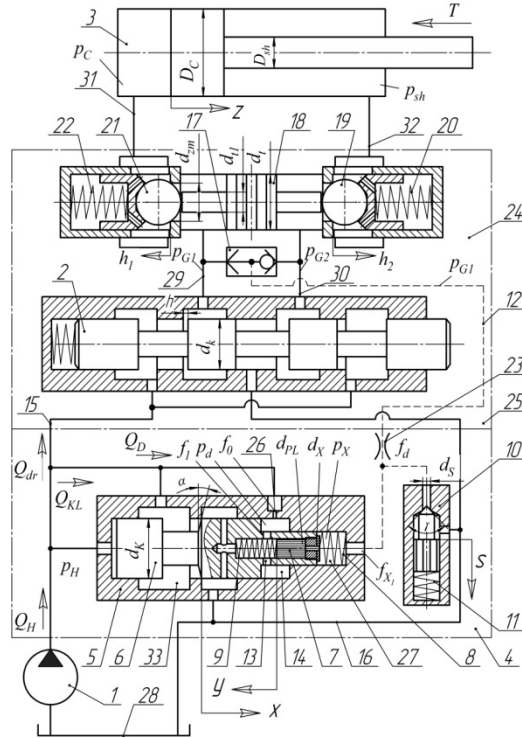
Fig. 1 − Basic circuit of the LS hydraulic drive.

The multimode directional control valve provides hydraulic drive operation in four modes: modes of pump unloading, adjusting of the flow rate, maximal flow rate and overload protection. In the mode of pump unloading directional control valve 25 is closed; control line 12 is connected with the tank and excessive pressure pG1 is equal to zero; plunger 7 under the action of the spring 9 will move to the right end position and open radial openings 13 connecting chamber 14 with the tank. In chamber 14 excessive pressure pD will be equal to the atmospheric pressure.

In this case the equation of forces acting on spool 6 (without taking into account friction forces and hydrodynamic force) will have the following form (1), and pump output pressure pH will be defined by the formula (2).

$$p_H \cdot \frac{\pi \cdot d_k^2}{4} = c \cdot H \tag{1}$$

$$p_H = \frac{4 \cdot c \cdot H}{\pi \cdot d_k^2} \tag{2}$$

The force of spring 8 is chosen so that the value of pressure p_H will be

$(0.3…0.4)$ MPa. Under the pressure p_H the total flow of pump 1 will pass to the tank through the work port of the pressure relief valve 5.

After switching of the directional control valve into the opening position fluid will be supplied to the hydraulic line 12 under the pressure p_{G1}, that depends on the load T value, and plunger 7 will move to the left end position, ovelapping radial openings 13. Pressure p_D in chamber 14 will be equal to pressure pH in the current mode and the equation of forces acting on spool 6 (without taking into account friction forces and hydrodynamic force) will have the form of (3).

$$p_H \cdot \frac{\pi \cdot d_k^2}{4} = p_H \cdot \left(\frac{\pi \cdot d_k^2}{4} - \frac{\pi \cdot d_X^2}{4} \right) + p_C \cdot \frac{\pi \cdot d_X^2}{4} + c \cdot H \qquad (3)$$

wherefrom

$$\Delta p = p_H - p_C = \frac{4 \cdot c \cdot H}{\pi \cdot d_X^2} \qquad (4)$$

where Δp – pressure difference at the work port of the directional control valve 2 which is also considered to be the pressure difference at the spool of the pressure relief valve will be $(0.7…0.8)$ MPa.

In this way spool 6 will maintain constant pressure difference value at the work port of the directional control valve 2, which makes it possible to change the value of flow Qdr to the hydraulic cylinder changing the size of work port. The difference of $Q_H -$ Qdr will be delivered from the pump to the tank through the work port of the pressure relief valve 5.

In the overload mode the rod of the hydraulic cylinder stops, pressure p_C increases considerably, valve 10 opens and part of the working fluid from cylinder 3 flows to the tank through the directional control valve 2. At its work port pressure difference Δp emerges, which keeps valve 5 in the open position and the whole pumping flow is delivered to the tank.

The advantage of the designed pressure relief section over the analogs is that working fluid from the pump is delivered to the tank not under pressure difference Δp (as in the analog (Catalogue HK.51. A1.02. Danfoss 11/91)) but under pressure pH = $(0.3…0.4)$ MPa and the value of the control pressure difference in the regulations mode is $\Delta p = (0.7…0.8)$ MPa, which reduces non-productive power losses in the hydraulic drive.

During one shift of a mobile working machine operation (*e. g.* of an excavator) thousands of switchings are performed. So the valve is constantly working in dynamic modes, which requires defining its dynamic characteristics and selecting the design parameters that provide the necessary dynamic characteristics of the valve. One of the requirements to the hydraulic drives of the mobile machines is also the stability of the actuator motion under changing load. This requirement is also taken into account at the design stage of the hydraulic drive in order to provide the necessary static characteristics.

In order to investigate the hydraulic drive operation and to determine its static and dynamic characteristics a non-linear mathematical model has been developed. The mathematical model has been developed under such assumptions: the hydraulic drive operation in the regulation mode; parameters of hydraulic drive elements are lumped ones; mass of plunger 7 is neglected; the fluid flows between the chambers of the valve, directional control valve, pump and hydraulic cylinder are neglected; coefficients of flow through the throttling and spool elements are constant; hydraulic drive operates in a non-cavitational mode; the hydraulic line 1 volume at the time of transient process remains unchanged; pressure losses in the hydraulic lines are neglected; the compliance coefficients of the gas-liquid mixture and of rubber-metal hoses were taken into account as the average values for the considered ranges of pressure change.

The mathematical model of the hydraulic drive includes flow continuity equations for the hydraulic lines between pump 1, directional control valve 2 and valve 5; between directional control valve 2 and hydraulic cylinder 3; between orifice 15 and radial openings in spool 6 and the equation of forces acting on spool 6, the piston of hydraulic cylinder and plunger 7. The mathematical model equations were written in Cochy form (5).

$$\frac{dp_{G1}}{dt} = \frac{1}{\beta \cdot W_{G1}} \cdot \left(0{,}43 \cdot h - \frac{6{,}3}{p_H - p_{G1}} - 6{,}9 \cdot 10^{-4} \right) - \frac{\mu \cdot f_{zm}}{\beta \cdot W_{G1}} \cdot \sqrt{\frac{2 \cdot (p_{G1} - p_C)}{\rho}} - \frac{\mu \cdot f_{dr}}{\beta \cdot W_{G1}} \cdot \sqrt{\frac{2 \cdot (p_{G1} - p_S)}{\rho}};$$

$$\frac{dp_H}{dt} = \frac{Q_H}{\beta \cdot W_H} - \frac{1}{\beta \cdot W_H} \cdot \left(0{,}43 \cdot h - \frac{6{,}3}{p_H - p_{G1}} - 6{,}9 \cdot 10^{-4} \right) - \frac{\mu \cdot \pi \cdot d_K \cdot x \cdot \sin\alpha}{\beta \cdot W_H} \cdot \sqrt{\frac{2 \cdot p_H}{\rho}} -$$

$$- \frac{\mu \cdot f_0}{\beta \cdot W_H} \cdot \sqrt{\frac{2 \cdot (p_H - p_D)}{\rho}};$$

$$\frac{dp_C}{dt} = \frac{dz}{dt} \cdot \frac{\pi \cdot D_C^2}{4 \cdot \beta \cdot W_C} - \frac{\mu \cdot f_{zm}}{\beta \cdot W_C} \cdot \sqrt{\frac{2 \cdot (p_{G1} - p_C)}{\rho}};$$

$$\frac{dp_{sh}}{dt} = \frac{\mu \cdot f_{zm}}{\beta \cdot W_{sh}} \cdot \sqrt{\frac{2 \cdot p_{sh}}{\rho}} - \frac{dz}{dt} \cdot \frac{\pi \cdot (D_C - D_{sh})^2}{4 \cdot \beta \cdot W_{sh}};$$

$$\frac{dp_D}{dt} = \frac{\mu \cdot f_0}{\beta \cdot W_D} \cdot \sqrt{\frac{2 \cdot (p_H - p_D)}{\rho}} - \frac{\mu \cdot f_1}{\beta \cdot W_D} \cdot \sqrt{\frac{2 p_D}{\rho}} - \frac{dx}{dt} \cdot \frac{\pi \cdot (d_K - d_X)^2}{4 \cdot \beta \cdot W_D} -$$

$$- \frac{\pi \cdot d_K \cdot \varepsilon_1^3 \cdot p_D}{48 \cdot v \cdot \rho \cdot (l_1 - x) \cdot \beta \cdot W_D} - \frac{\pi \cdot d_{PL} \cdot \varepsilon_2^3 \cdot p_D}{48 \cdot v \cdot \rho \cdot l_2 \cdot \beta \cdot W_D};$$

$$\frac{dp_S}{dt} = \frac{\mu \cdot f_{dr}}{\beta \cdot W_S} \cdot \sqrt{\frac{2 \cdot (p_{G1} - p_S)}{\rho}} - \frac{\mu \cdot f_S}{\beta \cdot W_S} \cdot \sqrt{\frac{2 p_S}{\rho}} - \frac{\mu \cdot f_X}{\beta \cdot W_S} \cdot \sqrt{\frac{2 \cdot (p_S - p_X)}{\rho}};$$

$$\frac{dV_C}{dt} = p_C \cdot \frac{\pi \cdot D_C^2}{4 \cdot m_C} - \frac{T}{m_C} + \frac{b_C}{m_C} \cdot \frac{dz}{dt} - p_{sh} \cdot \frac{\pi \cdot (D_C - D_{sh})^2}{4 \cdot m_C};$$

$$\frac{dV_{h1}}{dt} = \frac{2 \cdot d_{zm} \cdot h_1 \cdot (p_{G1} - p_C)}{m_{zm}} - \frac{c_{zm} \cdot (H_{zm} + h_1)}{m_{zm}}; \tag{5}$$

$$\frac{dV_{h2}}{dt} = p_{G1} \cdot \frac{\pi \cdot (d_{sh} - d_{sh1})^2}{4 \cdot m_{zm}} - \frac{p_{sh} \cdot 2 \cdot d_{zm} \cdot h_2}{m_{zm}} - \frac{c_{zm} \cdot (H_{zm} + h_2)}{m_{zm}};$$

$$\frac{dV_K}{dt} = p_H \cdot \frac{\pi \cdot d_K^2}{4 \cdot m_K} - p_X \cdot \frac{\pi \cdot d_X^2}{4 \cdot m_K} - p_D \cdot \frac{\pi \cdot (d_K - d_X)^2}{4 \cdot m_K} - \frac{c \cdot (H + x)}{m_K} -$$

$$- \frac{1}{m_K} \cdot \left(17 + 17{,}7 \cdot \mu \cdot \pi \cdot d_K \cdot x \cdot \sin\alpha \cdot \sqrt{\frac{2 \cdot p_H}{\rho}} - \frac{3{,}1 \cdot 10^5}{x} \right) - \frac{(\rho \cdot v \cdot \pi \cdot d_K \cdot (l_1 - x))}{m_K};$$

$$\frac{ds}{dt} = \frac{p_S \cdot \pi \cdot d_S \cdot s \cdot \sin(\gamma/2)}{b_S} - \frac{c_S \cdot (H_S + s)}{b_S};$$

$$\frac{dy}{dt} = p_X \cdot \frac{\pi \cdot d_{PL}^2}{4 \cdot b_1} - \frac{c_1 \cdot (H_1 + y)}{b_1},$$

where Q_H – the flow rate value of the pump 1, pH – pressure in the pumping line, p_C – pressure in the cylinder 3, p_D – pressure in the chamber 14, W_H – fluid volume in the pumping line, W_C – fluid volume in the piston chamber of the cylinder 3, W_D – fluid volume in the chamber 14, D_C – cylinder 3 piston diameter, dk, d_X – diameters of spool 6, m_C – cylinder 3 piston mass, m_K – spool 6 mass, V_C – speed of cylinder 3 piston motion, V_K – speed of spool 6 motion, f_0 – area of spool 6 orifice, f_{dr} – area of the directional valve working port, f_{PL} – plunger 7 area, x – coordinate of spool 6 position, y – coordinate of plunger 7 position, z – coordinate of cylinder 3 piston position, b – viscous damping coefficient of spool 6, b_C – viscous damping coefficient of cylinder 3 rod, β – coefficient taking into account the total deformation of gas-liquid mixture and rubber-metal hoses, α – the value of the working edge slope angle of the spool 6, ρ – working fluid density, c – spring 8 rate, c_1 – spring 9 rate, H – preset compression of the spring 8, H1 – preset compression of the spring 9. For computations and mathematical modeling of the processes and investigation of the system static and dynamic characteristics Simulink module of the MATLAB programming package has been used (Burennikov, 2009).

Mathematical model equations are solved under initial conditions pH (0) = 3•105 Pa, pC (0) = 0 Pa, pD (0) = 0 Pa, z (0) = 0 m, x (0) = 0.1•10-3 m, y (0) = 0 m, VC (0) = 0 m/sec, VK (0) = 0 m/sec with the value of load p = 160•105 Pa which simulated step change of the load. The dependences of state variables pH, pC, z, x, VC, VK versus time were found, which makes it possible to determine such dynamic characteristics as regulation time and excessive correction value.

The error of flow stabilization A in the hydraulic drive is calculated by the formula (6).

$$A = \frac{Q_{dr\,max} - Q_{dr\,min}}{Q_{dr\,min}} \cdot 100\% \tag{6}$$

where Q_{dr} – the values of flow to the hydraulic cylinder, Q_{drmax} its maximum and Q_{drmin} minimum values correspondingly. The possibility to minimize the stabilization error A, regulation time T_p and excessive correction value σ by means of choosing optimal values of the pressure relief valve design parameters is analyzed. Now we shall consider the influence of the relief valve main parameters – c, d_k, d_X and f_0 – on the values of excessive correction σ, regulation time Tp and stabilization error A of the hydraulic drive (Fig. 2).
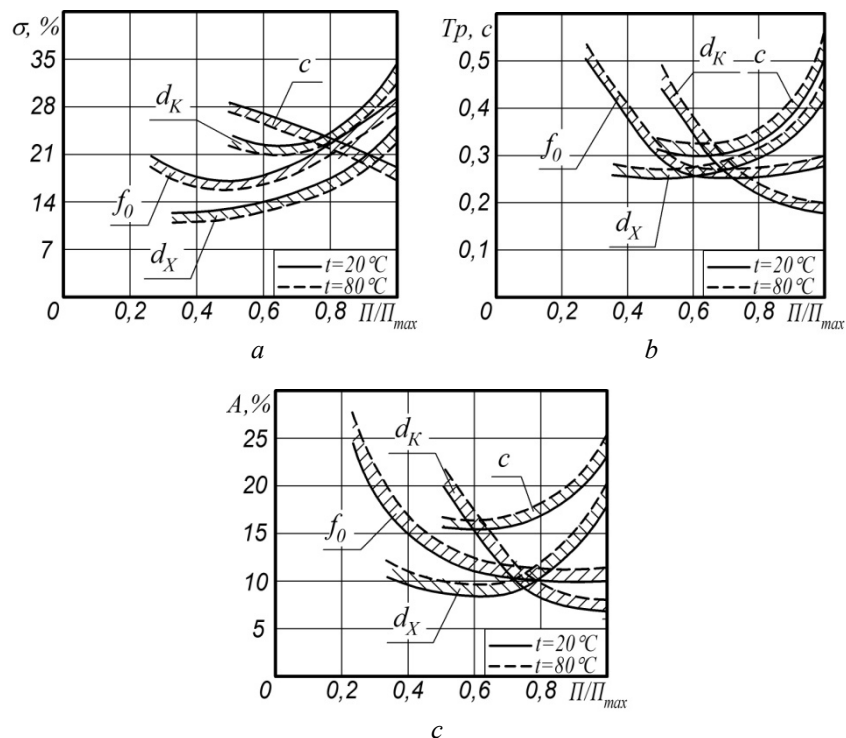
Fig. 2 – The influence of the valve parameters on the: a – excessive correction in the hydraulic drive; b – regulation time in the hydraulic drive; c – hydraulic drive stabilization error.

According to Fig. 2 the variation ranges of the design parameters were as follows: $d_k = (12...24) \cdot 10^{-3}$ m, $d_X = (6...16) \cdot 10^{-3}$ m, $c = (1,1...2,5) \cdot 10^4$ H/m and $f_0 = (0,4...1,6) \cdot 10^{-6}$ m^2.

3. Conclusion

1. The developed circuit of the LS hydraulic drive on the basis of multimode directional control valve, that works in the modes of pump unloading, adjusting of the flow rate, maximal flow rate and overload protection

and provides the hydraulic drive operation with the value of control pressure difference $\Delta p = 0.7...0.8$ MPa which is better than in the analog PVG of Danfoss (Denmark).

2. The minimal values of stabilization error A, regulation time Tp and excessive correction σ are provided under the following design parameters combination for the pressure relief valve of the multimode directional control valve: $d_k = (12...24) \cdot 10^{-3}$ m, $d_X = (6...16) \cdot 10^{-3}$ m, $c = (1,1...2,5) \cdot 10^4$ H/m and $f_0 = (0,4...1,6) \cdot 10^{-6}$ m^2.

REFERENCES

Jonson G., *Load-sensing systems control speed accurately.* Hydraulics & Pneumatics. – MARCH, 33 – 36 (1995).

* * SB 12 LS – Wegeventile von Bosch: Katalog, 198 p.

* * *Drive and Control Systems for Combine Harvesters and Forage Harvesters.* Bosch Rexroth AG. – 2001. – RE 98071.

* * *Load-Independent Proportional Valve.* Type PVG 120: Catalogue HK.51. A1.02. Danfoss 11/91.

Козлов Л. Г., Вдосконалення систем керування гідроприводів з LS-регулюванням. – Автореф. дис. канд. техн. наук: 05.02.03. – Вінниця, 2000. – 20 с.

Burennikov Yu.A., *Metrological Characteristic of the Test Rig with Automatic regestering of the Proportionally-Controlled Hydraulic Drive.* Yu.A. Burennikov, L.G. Kozlov, D.O. Lozinsky, O.V. Petrov and ect., Bul. Inst. Polit. Iasi, **LV (LIX)**, *1,*– 125-130 (2009).

PROPRIETĂŢILE DINAMICE ŞI STATICE ALE ACŢIONARILOR HIDRAULICE LS PE BAZA SUPAPEI DE CONTROL MULTIDIRECŢIONALE

(Rezumat)

Lucrarea se ocupă cu oferirea unei soluţii ştiinţifice ce constă în găsirea şi dezvoltarea unui circuit de acţionare hidraulic care să ofere o eficienţă ridicată a sistemului de control, de asemenea dinamica şi statica necesară. A fost dezvoltat un circuit de acţionare hidraulică sensibil la solicitare (L|S) pe baza unei supape de control multidirecţională pentru compomentele mobile de lucru. A fost alcătuit un model neliniar matematic a unei acţionări hidraulice (LS) pe baza unei supape de control multidirecţională. Cercetările teoretice au fost efectuate pe baza modelului matematic folosind pachetul software MATHLAB 6.5. S-a determinat faptul că parametrii de proiectare a supapei de presiune ce realizează feed-back-ul, influenţează dinamica şi proprietăţile statice ale acţionării hidraulice. Dintre aceste valori ai parametrilor supapei de presiune s-au determinat care dintre acestea oferă valori minime ale erorilor de stabilizare, timp de reglaj şi control minim.

OPTIMIZATION OF THE DESIGN PARAMETERS OF A COMBINED FLOW REGULATOR FOR THE VARIABLE AXIAL-PISTON PUMP

BY

Y. BURENNIKOV*, L. KOZLOV and S. REPINSKIY

Vinnitsa National Technical University

Abstract. The paper presents a control system for the axial-piston variable pump with a combined flow regulator having a profiled spool port. The regulator provides pump operation in the pump flow stabilization and constant power modes. Mathematical model is developed and control system investigation in static and dynamic modes is conducted using Simulink program of Matlab package. In the process of investigation the most influential parameters were revealed and the character of this influence was found to be an ambiguous one. Parameters change in order to improve certain characteristics can be accompanied with other characteristics becoming worse. The choice of parameter values that satisfy all the requirements to the axial-piston variable pump control system is a complicated task. The problem of parameter choice for the combined flow regulator can be solved by means of optimization methods. Optimization criterion indices are formulated, criteria constraints are chosen as well as optimization parameters and their variation ranges. On the basis of the improved optimization criterion that takes into account static and dynamic characteristics of the axial-piston variable pump control system in the flow stabilization and constant power modes by means of LP search optimal combination of the flow regulator design parameters has been found: $=8 \cdot 10\text{-}3$ m; $=8 \cdot 10\text{-}3$ m; $=1{,}5 \cdot 104$ N/m; $=6{,}7 \cdot 104$ N/m; $=1{,}0 \cdot 10\text{-}6$ m^2. This combination ensures stable control system operation in the flow stabilization mode with flow stabilization error $=3{,}2\%$, regulation time $=0{,}16$ sec, overshoot on pressure $=9{,}4\%$, and also stable control system operation in the constant power mode with $=0{,}21$ sec. and $=12{,}8\%$.

---

* Corresponding author e-mail: vadikkov@ukr.net

Key words: control system, axial-piston variable pump, combined regulator, profiled port, static characteristics, and dynamic characteristics.

1. Introduction

The tendency of wide application of variable axial-piston pumps (APP) is explained by the desire of hydraulic equipment consumers to extend functional capabilities, to implement energy-saving modes and to make optimal use of the engine power during operation processes. Technical characteristics and functional capabilities of a variable APP depend to a great extent, on the flow regulator that is included into the APP displacement control system (Свешников, 2005; Соболь, 1981; Попов, 1976; Бурєнніков, 2004). At the flow regulator design stage the influence of its design parameters on static, dynamic and power characteristics of the variable APP control system could be different in different operation modes. Parameter change for improving certain characteristics could be accompanied by other parameters becoming worse.

Therefore, the choice of parameter values that satisfy all the requirements to the variable APP control system is a rather complicated task.

Fig. 1 − Circuit of the variable APP control system with CFR.

In this case, the problem of choosing parameters for the combined regulator can be solved by the usage of optimization methods. LP search method (Соболь, 1981) was chosen among the wide range of optimization procedures as an effective method for finding optimal values in the multicondition problems. LP search method is also a universal tool as on its basis one's own optimization criterion can be created. The criterion can include several indices depending on the complexity of an applied problem.

Fig. 1 shows variable APP control system circuit with a combined flow regulator (CFR) that provides static characteristic of the axial-piston pump in the flow stabilization mode and statistic characteristic of a hyperbolic type in the constant-power mode through the form of a profiled port of the regulator spool.
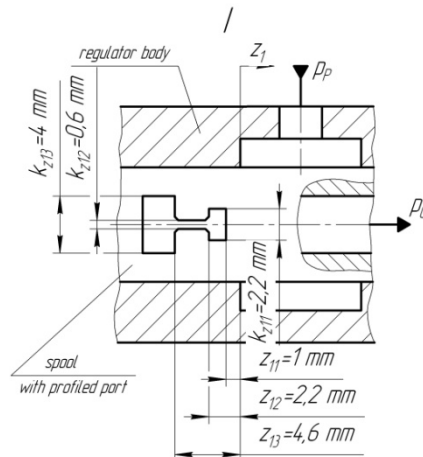
Fig. 2 – Profiled port of CFR spool.
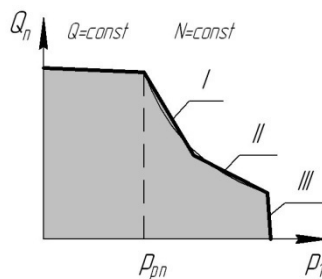
Fig. 3 – Variable APP static characteristic.

The circuit includes variable APP 1, proportional directional control valve *7* with the consumer load pressure monitoring device (LS signal), flow regulator *8* with spool *9* and spring *10* that is connected to hydraulic lines *3* and *15* and provides APP flow stabilization mode which controls the flow supplied

from hydraulic line *3* into control cylinder *4*. Faceplate *2* of the pump is under the influence of the action of cylinders *4*, *5* and spring *6*. At the discharge from cylinder *4* throttle *14* is installed. Power regulator *11* with spool *12* and spring *13* changes the pump displacement in accordance with working pressure so that APP constant-flow operation is ensured.

The control system functions in the following way. When consumers are disconnected, regulator control line *15* is communicated with the discharge line, pressure in it being practically absent. Flow, created by the pump, moves spool *9* to the right compressing spring *10* and is supplied to control cylinder *4*. Pressure p_C, created in the cylinder, will move the faceplate so that pump flow will be minimal and will compensate only for leakage in the control system and in the hydraulic drive.

Under steady-state operating conditions pressures p_P and p_1 as well as force of spring *10*, acting on spool *9*, determine such position of it wherein pressure p_C in cylinder *4* balances the moment at faceplate *2* that is created by pressure p_P in cylinder *5* together with spring *6*. Spring *10* is selected so that it could maintain a constant pressure drop $\Delta p_{LS} = p_P - p_1$ at the working port of the proportional directional control valve *7*. Any change in Δp_{LS} determines a corresponding change in inclination angle γ directed towards error reduction.

When pressure p_P grows considerably, power regulator *11* operates. Increase of pressure p_P acting on the left end of spool *12* moves the latter to the right, compresses spring *13* and opens the profiled working port of the spool (Fig. 2) that determines flow Q_{C1} to control cylinder *4* depending on coordinate of the spool motion. In control cylinder 4 pressure p_C is created that determines inclination angle γ of the pump faceplate *2* and changes the pump displacement in accordance with pressure so that constant product of the pump pressure and flow is provided and, therefore, stability of driving power is ensured.

The plot of static characteristic of APP with CFR is presented in Fig. 3. The profiled port of spool *12* of flow regulator *11* (Fig. 2) and corresponding variable gain of the port of spool k_{Z1} that depends on the shift of spool z_1 provides two areas on static characteristic that approximate to a hyperbolic curve that characterizes the pump operation in the constant power mode. Area I is provided by opening of the working port of the flow regulator spool with gain coefficient k_{Z11} for spool shift $z_{11} < z_1 \le z_{12}$. Area II for shift z_1 greater than z_{12} is provided by simultaneous opening of the working port $f_1(z_1) = (z_{12} - z_{11}) \cdot k_{Z11}$ and opening of the working port with gain coefficient

k_{Z12}. Maximal pressure restriction is achieved through k_{Z13} when shift z_1 exceeds z_{13} (area III).

For investigation of the processes in the variable APP control system a mathematical model was elaborated with certain assumptions. The model comprises: flow continuity equations; equation of the moments acting on the variable APP faceplate; equation of forces action on CFR spools as well as refined relationships between the variable pump faceplate resistance moment and flow rate through the profiled port of the spool (Burennikov, 2007; Буренніков, 2009). Solution of the mathematical model equation set was performed using MatLab Simulink software package.

Analysis of the requirements to the hydraulic drives of mobile working machines and APP flow regulators (Попов, 1976; Буренніков, 2004; Burennikov, 2007; Буренніков, 2009.) makes it possible to formulate the optimization criterion that includes, according to the rank level, the following indicators: in flow stabilization mode – stability; stabilization error δ of flow to the actuating hydraulic engine; regulation time t_r; overshooting σ; in constant power mode – stability; regulation time t_r; overshoot σ.

Stability of APP control system must be ensured both in the flow stabilization and constant power modes.

Conditions of performing some technological processes require the value of flow stabilization error δ to consumer to be minimal. Otherwise, if the pre-defined value is exceeded, error occur during control signal adjustment and accuracy of the machine operation is reduced. The permissible value of flow stabilization error δ under unfavorable conditions of APP control system operation should not exceed 6%.

Regulation time t_r must be minimal for unfavorable parameter combinations that characterize conditions of the APP control system operation. To provide the required response time, regulation time should not exceed 0,3 sec.

Overshoot σ in APP control system under unfavorable combination of parameters that characterize operating conditions should not be higher than 30% according to the value of p_P.

Criterial restrictions are used for excluding such optimization parameter sets from the obtained sequence of that caused excess of the values of the optimization criterion indices: unstable operation, $\delta > 6\%$, $t_r > 0,3$ sec and $\sigma > 30\%$.

Mathematical model of the processes in control system for flow stabilization and constant-power modes of the variable APP has made it possible to investigate the influence of CFR parameters on static, dynamic and power characteristics of the control system. In the process of research the most influential parameters were revealed and the character of this influence was

found to be an ambiguous one. The change of parameters for improving certain characteristics could be accompanied by other parameters becoming worse.

E. g. investigation of energy characteristics shows that hydraulic efficiency of the control system can be increased through the reduction of pressure drop Δp_{LS} at the flow regulator spool, which in its turn, is accompanied by the growth of stabilization error δ of the flow to hydraulic engine. It was found that the above-mentioned negative influence of Δp_{LS} reduction on δ could be compensated by the corresponding choice of the combined regulator design parameters (Fig. 4).

However, the required change of the combined regulator parameters (increase of the spool diameter d_r, spring strength c_r and gain coefficient of the working port k_z) has an ambiguous influence on the dynamic behavior of the control system. If d_r is increased, the stability is reduced as well as the indices of the transient process quality – regulation time t_r, oscillation k and overshoot σ (Table 1). Such worsening of dynamic characteristics could be compensated by the corresponding choice of the throttle conductance f_0 (reduction).
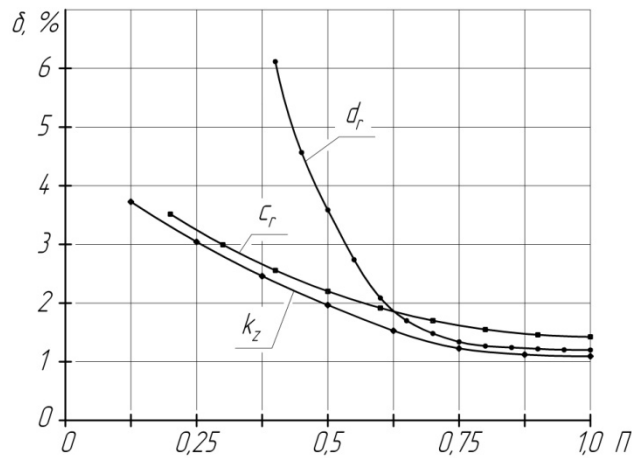
Fig. 4 – The influence of CFR design parameters on
flow stabilization error δ.

When APP operates in the constant-power mode, the combined regulator parameters d_{r1}, c_{r1}, k_{z1}, b_{r1} and f_0 have an ambiguous influence on the dynamic characteristics of the control system (Table 1).

Optimization parameters include such design parameters of the combined regulator that have the greatest influence on static and dynamic characteristics of the variable APP control system: d_r, c_r, d_{r1}, c_{r1} and f_0.

Optimization of the combined regulator design was performed proceeding from unfavorable combination of other parameters from Table 1 that do not belong to the optimization parameters.

If the optimization criterion is provided under unfavorable combination of the parameters that characterize the control system operating conditions in different APP operation modes, the optimization criterion can be also considered to be ensured under the rest of the above-mentioned parameter combinations.

Table 1

The Influence of the Main CFR Parameters on Static and Dynamic Characteristics of the Variable APP Control System

Combined regulator parameters		Values (variation range)	The unit of measurement	Influence on static characteristics δ	Influence on dynamic characteristics			
					stability	t_r	k	σ
d_r		$(4,0...10,0)\cdot10^{-3}$	m	↓	↓	↑	↑	↑
d_{r1}		$(4,0...10,0)\cdot10^{-3}$	m	−	↓	↑	↑	↑
c_r		$(0,8...4,0)\cdot10^{4}$	N/m	↓	−	↓	↓	↓
c_{r1}		$(3,0...10,0)\cdot10^{4}$	N/m	−	−	↓	↓	↓
k_z		$(0,5...4,0)\cdot10^{-3}$	m	↓	↑	↓	↓	↓
k_{z1}		$(0,25...4,0)\cdot10^{-3}$	m	−	↓	↑	↑	↑
b_r		5...500	N·c/m	0	↓	↑	↑	↑
b_{r1}		5...500	N·c/m	0	↑	0	0	↑
f_0	in flow stabilization mode	$(0,5...1,5)\cdot10^{-6}$	m²	0	↓	↑	↑	↑
	in constant-power mode			0	↑	↑	↑	↑

Note.   *„0" – no influence;*
       „−" – not investigated;
       „↑" – improves;
       „↓" – negative influence.

As variation ranges of the above parameters, that are given in Table 2, are rather narrow and their influence on static and dynamic characteristics has hyperbolic character (see Fig. 4), the number of probing tests in each of the parameter variation ranges could be small. Optimization was performed with the number of probing tests equal to three in each parameter range with uniform distribution of values in the range.

During the design optimization process of the APP combined flow regulator the sequence of 27 parameter combinations (d_r, c_r, f_0) was determined for APP flow stabilization mode and the sequence of 27 parameter combinations (d_{r1}, c_{r1}, f_{01}) for APP constant-power operation mode. For each combination of the above parameters the transient process of the state variables of the APP control system was calculated.

Table 2
The Range of Optimization Parameters Variations

Optimization parameter	Measurement unit	Variation range
d_r	m	$(6,0...10,0) \cdot 10^{-3}$
d_{r1}	m	$(6,0...10,0) \cdot 10^{-3}$
c_r	N/m	$(0,8...2,2) \cdot 10^4$
c_{r1}	N/m	$(3,4...10,0) \cdot 10^4$
f_0	m^2	$(0,5...1,5) \cdot 10^{-6}$

Indices that are included into optimization criterion were also determined for each combination of the combined regulator design parameters in APP flow stabilization mode and APP constant-power mode.
Search for the best parameters was confined to the following procedure: according to the first (in compliance with ranking) optimization criterion indicator combinations included into the criterial interval were found.

After choosing combinations in accordance with the first criterion the selection of combinations in accordance with the second criterion and then in accordance with the third and the forth criteria was conducted. As a result, one or several parameter combinations that could be considered optimal can be obtained.

Analysis of the results has shown that it is impossible to find the test which is characterized by the combination of d_r, c_r, f_0 for APP flow stabilization mode and provides the best values of all optimization criteria indicators because improvement of certain indicators causes worsening of other over. Taking into account the importance of optimization criterion indicators, the parameter combination $d_r = 8 \cdot 10^{-3}$ m, $c_r = 1,5 \cdot 10^4$ N/m, $f_0 = 1,0 \cdot 10^{-6}$ m^2 in test №11 could be considered to be a compromise with the following indicators being provided: stable operation of APP control system in APP flow stabilization mode, flow stabilization error $\delta = 3,2\%$, regulation time $t_r = 0,16$ sec and pressure overshoot $\sigma = 9,4\%$.

Similarly, parameter combination d_{r1}, c_{r1}, f_{01} cannot provide the best values of all optimization criterion indicators during APP constant power operation mode because while some of them improve others become worse. Taking into account the importance of optimization criterion, the parameter

combination d_{rl} =8•10^{-3} m, c_{rl} =6,7•10^4 N/m, f_{0l} =1,0•10^{-6} m2 in test №24 could be considered to be a compromise with the following values of the optimization criterion being provided (Table 3): stable operation of APP control system in the control-power mode, regulation time t_r =0,21 sec and pressure overshoot σ =12,8%.

Table 3
Results of Calculation of the Best Optimization Parameter Set

Optimization parameters			Optimization criterion indices				Test number
1			2				3
Flow stabilization mode							
d_r, m	c_r, H/m	f_0, m^2	stability	δ, %	t_r, c	σ, %	11
8·10^{-3}	1,5·10^4	1,0·10^{-6}	+	3,2	0,16	9,4	
Constant-power mode							
d_{rl}, m	c_{rl}, N/m	f_{0l}, m^2	stability	-	t_r, c	σ, %	24
8·10^{-3}	6,7·10^4	1,0·10^{-6}	+	-	0,21	12,8	

Note. "+" – system is stable, "-" – system unstable.

The combinations of parameters d_r, c_r, d_{rl}, c_{rl} and f_0, obtained as a result of optimization, can be used while designing a prototype of the combined flow regulator that is included into the variable APP control system.

3. Conclusion

On the basis of the improved optimization criterion that takes into account static and dynamic characteristics of the variable APP control system in flow-stabilization and constant-power modes the optimal design parameter set for the combined regulator was found by LP search method: d_r =8•10^{-3} m; c_r =8•10^{-3} m; d_{rl} =1,5•10^4 N/m; c_{rl} =6,7•10^4 N/m; f_0, =1,0•10^{-6} m^2 this combination ensures stable operation on the control system in flow stabilization error δ =3,2%, regulation time t_r =0,16 sec, pressure overshoot σ =9,4% as well as stable control system operation in the constant power mode with t_r =0,21 c, σ =12,8%.

REFERENCES

Burennikov Yu., *Dynamics of the Hydraulic Drive Control System With Variable-Displacement Pump*.Yu. Burennikov, L. Kozlov, S. Repinskiy, Bul. Inst. Polit. Iaşi, **LIII (LVII)**, *4*, 23–30 (2007).

Бурєнніков Ю.А., *Автоматична система керування регульованим насосом*. Ю. А. Бурєнніков, Л. Г. Козлов, С. В. Репінський, Вісник Тернопільського державного технічного університету, *3*, 134–141 (2009).

Бурєнніков Ю.А., Удосконалення схем регуляторів подачі насосів гідросистем, чутливих до навантаження, та їх статичні характеристики, Ю.А. Бурєнніков, Л.Г. Козлов, С.В. Репінський, Вісник Вінницького політехнічного інституту, *5*, 88–92 (2004).

Попов Д.Н., *Динамика и регулирование гидро- и пневмосистем*. Д. Н. Попов – М.: Машиностроение, 424 (1976).

Свешников В.К., *Аксиально-поршневые насосы в современных гидроприводах*. В. К. Свешников//Гидравлика и пневматика: Информационно-технический журнал. *18*, 8–12 (2005).

Соболь И.М., *Выбор оптимальных параметров в задачах со многими критеріями*. И.М. Соболь, Р. Б. Статников – М. : Наука, 110 (1981).

OPTIMIZAREA PARAMETRILOR DE PROIECTARE PENTRU UN REGULATOR DE DEBIT PENTRU O POMPĂ CU PISTON VARIABIL AXIAL

(Rezumat)

Această lucrare prezintă un sistem de control pentru o pompă cu piston variabil axial, cu regulator de debit cu intrare profil bobină. Acest regulator asigură funcționarea pompei în modul debit constant și putere constantă. A fost creat modelul matematic iar studiul sistemului în mod static și dinamic a fost efectuat folosind programul Simulink din pachetul Mathlab. În cadrul studiului au fost descoperiți cei mai influenți parametri, iar caracterul acestei influențe s-a dovedit a fi ambiguu. Modificarea unor parametri pentru a îmbunătăți anumite caracteristici poate fi însoțită de modificarea în rău a altor caracteristici. Alegerea valorilor parametrilor care satisfac toate cerințele pentru pompa cu piston variabil axial este o sarcină complicată. Problema alegerii parametrilor pentru regulatorul de debit se poate rezolva prin metoda optimizării. Sunt prezentați indicii criteriilor de optimizare, sunt alese limitele, parametrii de optimizare și plaja de variație. S-au determinat parametrii de proiectare ai regulatorului de debit pe baza criteriilor de îmbunătățire a optimizării care iau în calcul caracteristicile statice și dinamice ale pompei cu piston variabil axial ce asigură funcționarea pompei în modul debit constant și putere constantă prin găsirea variantei optime LP: $=8 \cdot 10\text{-}3$ m; $=8 \cdot 10\text{-}3$ m; $=1{,}5 \cdot 104$ N/m; $=6{,}7 \cdot 104$ N/m; $=1{,}0 \cdot 10\text{-}6$ m^2. Această combinație asigură stabilitatea operațională în modul de debit constant cu o eroare de stabilizare a debitului $= 3{,}2\%$, timp de reglaj $= 0{,}16$ sec, depășirea presiunii $= 9{,}4\%$ și de asemenea stabilitatea operațională a sistemului în mod de putere constantă $= 0{,}12$ sec. și $12{,}8\%$.

METAL PLASTICITY UNDER NON-MONOTONIC LOADING

BY

YU. BURENNIKOV[1*], I. RUSU[2] and N. LOZAN[3]

[1] Vinnitsa National Technical University,
[2] "Gheorghe Asachi" Technical University of Iaşi,

Abstract. The paper presents further development of the tensor model of the failure accumulation process, which is used for evaluation of metal plasticity under non-monotonic loading. A notion of the second-rank failure is introduced. Its components depend on the invariants of the deformation rate guide tensor and physico-mechanical properties of the deformed metal. A hypothesis is adopted that metal failure occurs when function of the tensor main invariants has a corresponding value. Procedure for the failure function construction is elaborated and its approximation is proposed. On the basis of the tensor model of failure accumulation process deformability criterion is elaborated, which makes it possible to estimate the value of the utilized plasticity margin depending on the non-monotonic loading history and initial anisotropy of the ultimate strain. Besides, the paper presents a procedure for calculation of the stress deviator components, which takes into account deformational strengthening anisotropy. This has made it possible to achieve considerable increase of the accuracy in stress tensor components estimation.

The proposed method for evaluation of metal plasticity under non-Monotonic loading makes it possible to extend considerably the possibilities of the plastic metal forming processes by the development of new technologies that take advantage of non-monotonic loading distinguishing features.

Key words: plastic deformation, plasticity of metals, non-monotonous loading, damage accumulation, tensor models, stressed state, stress intensity, stress deviator, failure, destruction, boundary deformations, tensile impulse, hardening, load trajectories, strengthening.

---

* Corresponding author e-mail: vadikkov@ukr.net

1. Introduction

A lot of research works are dedicated to the problem of the plasticity of metals under non-monotonous loading, the main ones being (Огородніков, *et al*., 2005; Михалевич, 1998; Дель, 1983; Сивак & Сивак 2010). However, at present there is no common opinion concerning modeling of damage accumulation and evaluation, on this basis, the plasticity of metals under non-monotonous plastic forming. In research (Огородніков, *et al*., 2005; Михалевич, 1998; Дель, 1983) tensor models of damage accumulation process are considered, in which the non-monotony of deformation is described by an indirect deformation increment tensor

$$\beta_{ij} = \sqrt{\frac{2}{3}} \frac{d\varepsilon_{ij}}{de_u} \tag{1}$$

$$e_u = \int_0^t \dot{\varepsilon}_u d\tau \tag{2}$$

where $d\varepsilon_{ij}$ - is an increment of plastic deformation,

$\dot{\varepsilon}_u$ - the intensity of deformation rates,

e_u - the degree of deformation,

t - the time of deformation.

According to *g. a*. Smirnov-Aliyev (1968), deformation can be considered non-monotonic if Nadai-Lode parameter changes in the forming process, such approach to non-monotony evaluation was adopted in (Сивак & Сивак 2010), the damage accumulation model got its further development in this research.

To quantify the intensity of damage accumulation process we'll use the damage tensor (Дель, 1983), the components of which are determined by the formula:

$$\psi_{ij} = \int_0^{e_u} F(e_u^*, \eta, \mu_\sigma)\beta_{ij} de_u \tag{3}$$

$$\eta = \frac{3\sigma}{\sigma_u} \tag{4}$$

$$\mu_v = \frac{2\sigma_2 - \sigma_1 - \sigma_3}{\sigma_1 - \sigma_3} \tag{5}$$

where $F(e_u^*, \eta, \mu_\sigma)$ is a function that describes sensitivity of the material to the scheme of stressed state and the regularities of its change,
η - index of the stressed state stiffness,

μ_σ - Nadai-Lode parameter,

$\sigma = \dfrac{1}{3}\delta_{ij}\sigma_{ij}$ - average stress,

σ_u - stress intensity.

Let us use the proportion of the plastic flow theory:

$$d\varepsilon_{ij} = \frac{3}{2}\frac{de_u}{\sigma_u}S_{ij} \tag{6}$$

where S_{ij} – components of the stress deviator.

From (1) and (5) it follows that:

$$\frac{d\varepsilon_{ij}}{de_u} = \sqrt{\frac{3}{2}}\beta_{ij} = \frac{3}{2}\frac{S_{ij}}{\sigma_u} \tag{7}$$

or

$$\beta_{ij} = \sqrt{\frac{3}{2}}\frac{S_{ij}}{\sigma_u} \tag{8}$$

where $S_{ij}^0 = \sqrt{\dfrac{3}{2}}\dfrac{S_{ij}}{\sigma_u}$ are the guide tensor components.

As:

$$S_{ij}^0 = 0 \ , \ S_{ij}^0 S_{ij}^0 = 1 \tag{9}$$

after the solution of equations (9) taking into account (5), we find:

$$S_1^0 = \mp\frac{\mu_\sigma - 3}{v_b\sqrt{\mu_\sigma^2 + 3}} \ , \ \ S_2^0 = \pm\frac{2\mu_\sigma}{v_b\sqrt{\mu_\sigma^2 + 3}} \ , \ \ S_3^0 = \mp\frac{\mu_\sigma - 3}{v_b\sqrt{\mu_\sigma^2 + 3}} \tag{10}$$

where S_1^0, S_2^0, S_3^0 are main components of the guide tensor.

Taking into account (8), formula (3) for finding damage tensor components takes the form:

$$\psi_{ij} = \int\limits_0^{e_u} F(e_u, \eta, \mu_\sigma)S_{ij}^0 de_u \tag{11}$$

From (11) it follows the tensor ψ_{ij} is the deviator. Let us assume that failure occurs under the condition that a certain function of tensor ψ_{ij} invariants reaches a definite value. First invariant of this tensor is zero. Disregarding the influence of the third invariant we write the failure condition in the form (Дель, 1983)

$$\psi_{ij}\psi_{ij} = const \tag{12}$$

Subintegral function in (11) can be chosen so that:

$$\psi_{ij}\psi_{ij} = 1 \tag{13}$$

To determine the form of the function $F(e_u, \eta, \mu_\sigma)$ let us consider simple loading under which S_{ij}^0, η, μ_σ remain constant. Then

$$\psi_{ij} = S_{ij}^0 \int_0^{e_u^*} F(e_u, \eta, \mu_\sigma) de_u = S_{ij}^0 \varphi(e_u, \eta, \mu_\sigma) \tag{14}$$

where $\varphi(e_u, \eta, \mu_\sigma) = \int_0^{e_u^*} F(e_u, \eta, \mu_\sigma) de_u$

As $S_{ij}^0 S_{ij}^0 = 1$, from (13) it follows that in the process of destruction, when $e_u = e_p$, $\varphi(e_u, \eta, \mu_\sigma) = 1$. Besides,

$$\varphi(0, \eta, \mu_\sigma) = 0 \tag{15}$$

Satisfying these conditions let us choose the dependence

$$\varphi = \sum_{k=1}^m b_k \left(\frac{e_u}{e_p(\eta, \mu_\sigma)} \right)^{n_k}, \quad \sum_{k=1}^m b_k = 1, \quad n_k > 0 \tag{16}$$

to determine function φ,

where $e_p(\eta, \mu_\sigma)$ is the surface of boundary deformations.

Further the dependence:

$$\varphi = (1-a) \frac{e_u}{e_p(\eta, \mu_\sigma)} + a \frac{e_u^2}{e_p^2(\eta, \mu_\sigma)} \tag{17}$$

is adopted for function φ,

where a is a constant which depends on the mechanical properties of materials.

To determine the magnitude of plasticity resource used under non-monotonous loading, the failure condition (13) we rewrite as

$$\psi = \psi_{ij}\psi_{ij}. \tag{18}$$

We use formula (18) to estimate the magnitude of the used resource of plasticity in the surface layer of wire under surface plastic deformation, which is caused by the blows of hardened steel balls. The blows are caused by joint of the vibrations imposed on the chamber and movements which are transferred to the working medium from the balls and wires that are processed.

In this process the non-monotony of plastic deformation is caused by intermediate unloading. In addition, the impulse of compression, which occurs when a ball hits, propagates in a continuous elastic medium and reaches the wire surface, free from tension stresses, and, while reflecting from it, creates a tensile impulse which has the same shape as the compression impulse but propagates in the opposite direction.

The resultant stress on the free surface is always zero, but in the layers, adjacent to the free surface, tensile stresses emerge that under non-favourable conditions can lead to destruction (Кольский & Рейдер, 1973). That is why for evaluation of the plasticity of the metal surface layer under impact surface plastic deformation tensile stresses should be also taken into account, i.e. the plastic deformation process must be considered as a non-monotonous one. Non-monotony of the load, in this case, is caused by the change in the direction of stresses.

The surface plastic deformation allows obtaining a surface layer of metal with the necessary physical and mechanical properties and optimal relief. However, the degree of deformation in the metal surface layer is limited.

This is caused by damage accumulation processes that take place under plastic deformation together with simultaneous hardening of the surface layer. With growing degree of plastic deformation the intensity of hardening decreases and the intensity of damage accumulation increases.

Then comes the moment when the intensity of damage accumulation considerably exceeds the intensity of hardening. The degree of deformation, under which intensive plastic loosening starts, depends on the mechanical properties of the material of the part to be processed and on the loading history determined by the parameters of the process.

In (Богатов, *et al.,* 1984) it is shown that the accumulated plastic strain should be such that the used plasticity resource of the deformed metal does not exceed values $\psi \le 0,3...0,4$. For higher values of the used plasticity resource stable thermodynamic defects occur.

In this work the permissible values of the used plasticity resource were calculated by the formula (18). Besides the loading path was set by a curve in the three-dimensional space with the following coordinates: the degree of deformation e_u, stiffness index of stressed state η, Nadai-Lode parameter μ_σ.

We performed investigation of the plastic deformation in the surface layer of the wire made from steel 20.

Dependence of the plasticity of steel 20 on the diagram of stressed state is described by the surface of boundary deformations that was approximated by the dependence (19) obtained in (Сивак, *et* al., 2000).

$$e_p(\eta, \mu_\sigma) = 0.68 \exp(0.43\mu_\sigma - 0.91\eta). \tag{19}$$

To construct the load trajectories $\eta(e_p)$, $\mu_\sigma(e_p)$ it is necessary to have information about the state of strain and the regularities of its change throughout the process of plastic deformation.

To calculate these trajectories, the solution of the problem obtained in (Смирнов-Аляев, 1968) was used, where the solution of the boundary problem of the plasticity theory is given for the case of pressing the ball into the elastoplastic medium. It is assumed that the stress tensor components depend only on the coordinates ρ and φ (Fig. 1) and the equality $\sigma_u = \sigma_\theta$ is satisfied.
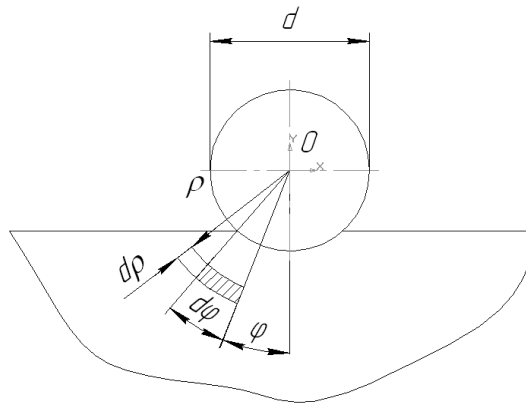
Fig. 1 – Calculation scheme.

Then the equilibrium equations in spherical coordinate system take the form (Смирнов-Аляев, 1968)

$$\frac{\partial \sigma_\rho}{\partial \rho} + \frac{1}{\rho}\frac{\partial \tau}{\partial \varphi} + \frac{2}{\rho}(\sigma_\rho - \sigma_\varphi) + \frac{1}{\rho}\tau \cdot ctg\varphi = 0, \tag{20}$$

$$\frac{\partial \tau}{\partial \rho} + \frac{1}{\rho}\frac{\partial \sigma_\varphi}{\partial \varphi} + \frac{3}{\rho}\tau = 0 . \tag{21}$$

The plasticity condition under the adopted assumptions has the form:

$$\sigma_\rho - \sigma_\varphi = \sigma_u \sqrt{1 - 3\left(\frac{\tau}{\sigma_u}\right)^2} \tag{22}$$

In the system of equations (20), (21), (22) the number of unknown quantities equals the number of equations. But it is impossible to solve these equations without additional conditions.

Therefore, in (Смирнов-Аляев, 1968) the intensity of stress σ_u and the degree of deformation e_u are assumed to depend only on the coordinate ρ .

Under the assumptions adopted in (Смирнов-Аляев, 1968) the solution of the system (20)-(22) was obtained, which was used in calculating the value of the used plasticity resource on criterion (18). To take into account strengthening of the metal surface layer, caused by multiple blows of the balls, the flow curve of steel 10 was used (Сивак, *et* al., 2000).

Analysis of the results of the used plasticity resource calculation has shown that the maximum permissible value of the deformation degree e_p and thus, the optimal value of hardening, is achieved on the condition that the residual depth of the wells after strikes is equal to $\delta = 0,004d$, the average number of strikes of the balls does not exceed 15-20. These results are obtained on the condition that the used resource of plasticity $\psi \le 0,4$.

The results of calculations satisfactorily agree with the experimental results obtained by measuring the hardness of the metal surface layer using graphic etalon $HV - \sigma_u - e_u$ for steel 10.

REFERENCES

Богатов А.А., Мижирицкий О.И., Смирнов С.В., *Ресурс пластичності металлов при обработке давлением*. М.: Металлургия, 144 (1984).

Дель Г.Д. Пластичность деформированного металла // Физика и техника высоких давлений, *11*, 28-32 (1983).

Кольский Г., Рейдер Д., *Волны напряжений и разрушение*. Разрушение, Т. 1. – М.: Мир, 570-608 (1973).

Михалевич В.М., Тензорні моделі накопичення пошкоджень. – Вінниця: Універсум – Вінниця, 195 (1998).

Огородніков В.А., Киселёв В.Б., Сивак И.О. Энергия. Деформации. разрушение (Задачи автотехнической экспертизы). – Винница: Універсум – Вінниця, 204 (2005).

Сивак И.О., Сивак Р.И., Алиев И.С., *Деформируемость заготовок при радиальном выдавливании с контурной осадкой*. Механика Твёрдого Деформируемого Тела и Обработка Металлов Давлением. – Тула: Тул Гу., 278-284 (2000).

Сивак Р.И., Сивак И.О., *Пластичность металлов при сложном нагружении*. Вісник Національного Технічного Університету України «Київський Політехнічний Інститут». Серія Машинобудування, *60*, 129-132 (2010).

Смирнов-Аляев Г.А., *Механические основы пластической обработки металлов.* – Л.: Машиностроение, 272 (1968).

PLASTICITATEA METALELOR SUB ACŢIUNEA UNEI SOLICITĂRI NON-MONOTONE

(Rezumat)

Lucrarea prezintă continuarea cercetării modelului tensorului procesului de rupere prin acumulare, care este folosit pentru evaluarea plasticităţii metalelor sub solicitare non-monotonă. S-a introdus noţiunea de ruptură de gradul doi. Componentele sale depind de invarianţii tensorului gradului de deformare a metalului. Este adoptată ipoteza că ruptura apare când funcţia invariantului tensorului principal are o valoare corespondentă. Este elaborată procedura de alcătuire a funcţiei de rupere şi sunt propuse aproximări. Pe baza modelului tensorului de rupere prin acumulare s-a elaborat un criteriu de deformabilitate, ceea ce face posibil să se estimeze valoarea utilizată pentru limita de plasticitate în funcţie de solicitarea non-monotonă anterioară şi de anizotropia iniţială a tensiunii de rupere. Totodată, lucrarea prezintă o procedură de calcul pentru componentele tensiunii deviatoare, cere iau în calcul anizotropia tensiunii de deformare. Aceasta a făcut posibil să se obţină o creştere considerabilă a acurateţei estimării componentelor tensiunii.

Metoda propusă pentru evaluarea plasticităţii metalului la solicitarea non-monotonă face posibilă extinderea considerabilă a posibilităţilor de prelucrare plastică a metalelor prin dezvoltarea unor noi tehnologii ce folosesc avantajul caracteristicilor distinctive de solicitare non-monotonă.

BUSINESS PROCESSES PERFECTION OF SMALL MOTOR TRANSPORT ENTERPRISES

BY

YU. BURENNIKOV*, **YU. JR. BURENNIKOV, A. DOBROVOLSKY**
and S. KRIVA

Vinnytsia National Technical University

Abstract. The paper investigates basic factors of perfecting vehicles technical maintenance being the primary among the main business-processes at auto dealers service stations. Enhancing of logistic and innovative development of the business processes is provided.

Key words: business-processes, service stations, logistic, innovative development

1. Introduction

The aims of change management in auto business, based on permanent perfection and reengineering business processes, are substantial cut of spending (productive, financial, operation, temporal and others), upgrading due to passing to the new technological level of customers service, expansion of scales and increase of business competitiveness by means of providing business processes flexibility, realization of advantages set by the selected strategy.

Thus, such perfection is related to reorganization of the activity, so that considerable attention is paid to the increase of profits, cost cutting, improvement of quality and meeting clients demands.

---

* Corresponding author e-mail: vadikkov@ukr.net

Approach to the changes due to perfection (improvement) of the business process is based on the evolutional increase of activity effectiveness, which involves not cardinal change of technologies, but permanent optimization of logistic chain of operations done by subdivisions of an organization.

Planning measures concerning improvement and reengineering of business processes should be guided by the following principles:

• strive to promote efficiency of the process, results of the activity for strengthening and creation of competitive advantages;

• maximization of resources loading and increase of the productivity;

• multi-variant approach and alternativeness of implementation of tasks, flexibility of technology for better choice of the most effective way to the process realization;

• delegation of responsibilities, stimulation of decision making by performers at all levels of management of a transport company;

• priority implementation of works, at places where they can be executed with the least expenses or the best result;

• strengthening of control together with deburocratization;

• reduction of amount of actions after concordances, intermediate control, verification.

For realization of changes in the business processes the following data are necessary: results of actual implementation analysis of performance indicators, data about expenses, profits and quality of work; competition investigation the business process organization, the quality and satisfaction of clients in other companies; about the requirements of car manufacturer to organization implementing particular works (Ivanov & Bogachenko, 2007).

The comparative analysis of such information allows the enterprise to find ways to increase efficiency and make decision about perfecting the corresponding business process or separate operation by correcting regulations, and instructions of a company or about the cardinal change of activity up to the transmission of part of the works into outsourcing.

Change management on the basis of permanent improvement of business processes can be shown by the example of grating service in realization of an automobile routine maintenance (Evans, 2000).

As a research object a small transport enterprise of «Vinnytsia Vinmotors» LTD official auto dealer of Toyota in Vinnytsia, was taken. Logistic of the investigated business process in Fig 1.

Descriptions of process of «Vinnytsia Vinmotors » LTD :

– total time of the business process – 81 min.;

– the number of personnel involved – 12 workers.

Problems exposed during the research:

– long queue and time spent for waiting near the dispatcher's room while the order is prepared;

– impossibility to predict the loading volumes at the stations and, as a

result, their uneven loading;

– long processing of the documents on paper carriers.

On arrival in a service center a client applies with a request to get some service for his car. The manager meets a visitor, listens to him and examines the car, confirms the willingness of the service station to render the necessary service to him. Then in dispatchers service room a specialist on registration of work orders (a dispatcher shown in Fig. 1) enters data about the client and his car into registration base, prepares a corresponding order. After printing and configuration the work order in a paper-form is directed to the workshop to the manager for implementation. The manager, planning the loading of repair zone posts, manages implementation of works. On their completion the mechanic adds to the work order data about the actually executed services and materials spent.
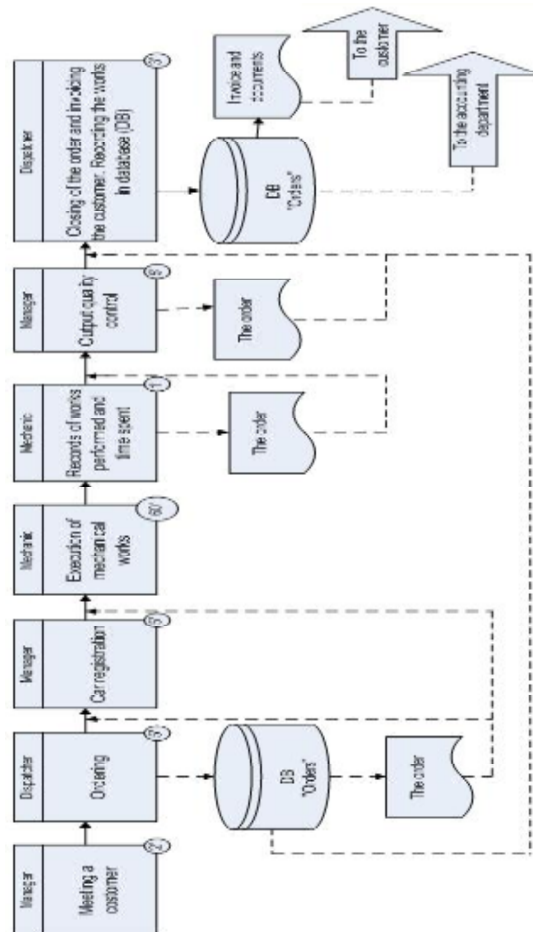
Fig. 1 – Diagram of the routine maintenance process by
«Vinnytsia Vinmotors» (before improvement).

Descriptions of the process:
• Total time of the business process – 81 min.;
• The number of personnel involved – 12 workers.
Problems:
• Long queue and time spent for waiting near the dispatcher's room while the order is prepared;
• Impossibility to predict the loading volumes at the stations and, as a result, their uneven loading;
• Long processing of the documents on paper carriers.

A mark is there made about realization of output quality control. Whereupon the work order is directed to the dispatchers service for closing and invoicing the client. In dispatchers service they enter the information into database, print, sign and give invoice to the client. As the analysis of the given process duration has shown (see Fig. 1), a customer has to wait for 81 min. an average (without taking into account the queue and assuming that the order preparation and works started immediately).The same analysis shows that 12 employees are needs to implement the annual production program for this process.

Thus, the results of analysis showed the presence of the following problems:
• servicing time is 81 min, while for competitors the index equals 68 min;
• clients are not content with the service and complaint about the long expectation in a queue while the order is processed, as at this time the same specialists are busy with registration of other services.

At first glance, the terms can be reduced due to organization of planning time of works implementation and more professional management of orders. Let us conduct the revision of technology of measures implementation. The improved business process is presented in Fig. 2.

Descriptions of process at the «Vinnytsia Vinmotors» LTD after the improvement:
– total time sped of the business process – 71 min (12 % reduction);
– the number of personnel involved – 10 workers (2 dispatchers less, 17 % reduction);
Distinguishing features:
– ordering, queuing for servicing, order preparation, records of time spent, works performed and their quality is done electronically in the on-line mode;
– in parallel with registration, the order is prepared after receiving confirmation from the receptionist about readiness to service the customer car.

Changes concerned the following issues. A client, arriving at the service station, by means of touch panel of data input (touch screen) and noncontact card of client for a car with the corresponding ID code chooses the necessary service (in our case, the car maintenance). These data are transmitted to the

dispatcher and the workshop manager online. Touch screen automatically prints to the client a receipt with through index numeration of his turn, in which he, oriented by informative board, forecasts the time and invitation and waits to be invited for servicing.
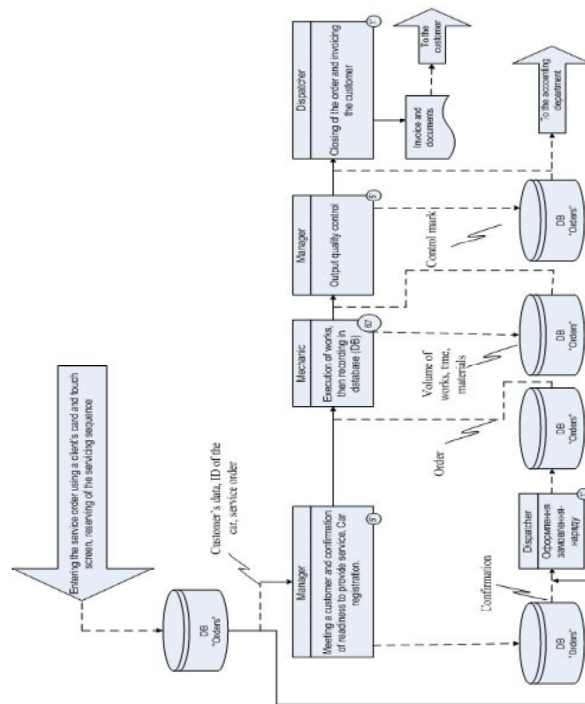
Fig. 2 – Diagram of the "Routine maintenance" process of its operations (after an improvement).

When his turn comes, the manager, before accepting the car (to sign the act of reception-handing transport vehicle), confirms in real-time the ID code of the car and data marked through by the client's touchscreen card. It allows the dispatcher in parallel with an acceptance to prepare for order the services chosen by a client. After receiving all the data required to prepare the order in electronic form, the dispatcher's service prepares it in the electronic system and directs to the workshop manager. The manager, using the automated time recoding system, estimates the priority of works in the workshop, manages the process. Thus, the mechanic confirms implementing the amount of work and time spent on them real-time, and, if necessary, brings in additional work to the electronic form of order. In the same way the account of quality of the produced work is built on the results of output control. The electronic form of order with the actually done work is directed real-time to the dispatcher's service for forming the invoice. With necessary additions the invoice is printed, signed by a headmaster and passed to the client to be paid.

Descriptions of the process:
• Total time of the business process – 71 min (12 % reduction);
• The number of personnel involved – 10 workers (2 dispatchers less, 17 % reduction);
Distinguishing features:
• Ordering, queuing for servicing, order preparation, records of time spent, works performed and their quality is done electronically in the on-line mode;
• In parallel with registration, the order is prepared after receiving confirmation from the receptionist about readiness to service the customer car.

3. Conclusion

An the whole, due to such optimization and transferring the part of planned procedures from «off-line» to «on-line» environment duration of implementing the business process has been decreased by 12% — from 81 to 71 min (Figs. 1-2), and amount of the involved personnel for providing the annual volume of work for cars maintenance services decreased by 17% — from 12 to 10 persons due to two regular staff units in dispatching office.

Such improvement of the business process of providing service on regular automobile maintenance makes it possible not only to save time and costs due to the structural changes of the personnel at the investigated enterprise, but, eventually, to increase the capacity of the corresponding working lines.

REFERENCES

Evans K., *The Remaining Need for Localization of Logistics Practices and Services in Europe*. Internat. J. of Physic. Distrib. T Logistics Management, **30**, *5*, 443-453 (2000).
Howard Smith, Peter Fingar *Business Process Management. The Third Wave*, MK Press, 2003.
Ivanov V.V., Bogachenko P.V., *Automobile management.* Infra-M, 2007.

PERFECȚIONAREA PROCESELOR DE AFACERI A REPREZENTANTELOR
AUTO CU MOTOARE DE MICĂ CAPACITATE

(Rezumat)

Lucrarea investighează factorii de bază a perfecționării întreținerii tehnice a vehiculelor, fiind primul printre principalele procese de afaceri în stațiile de service a dealerilor auto. Este prevăzută consolidarea dezvoltării logistice și inovatoare a proceselor de afaceri.

POTENTIAL USE IN MEDICAL APPLICATIONS OF MAGNESIUM NANOCRISTALLINE ALLOY

BY

A. BUZAIANU[1*], S. RUSU[2], ROXANA TRUSCA[1], E. VASILE[1], I. RUSU[2] and P. MOTOIU[3]

[1]METAV-R&D S.A., Bucharest
[2]"Gheorghe Asachi" Technical University of Iaşi,
[3]Romanian Ministry of Education, Research, Youth and Sports

Abstract. The nanocrystalline structures of metal materials offer radical improvements of properties or new functions. One the actual technology in the development of engineering materials is the production of the ultrarapid solidified Mg-base alloys. The aspects favorable results from these $Mg_{98,45}Nd_{0,64}Ag_{0,41}Zn_{0,5}$ alloy as regards the grain size modification and the homogeneity shown interesting phenomena: an improvement in room-temperature of ductility and strength, and an improvement in corrosion and degradation resistance compared to currently available Mg alloys. The micro structural, mechanical and electrochemical characteristics of the newly developed alloy should systematically be analyzed using scanning electron microscopy (SEM), transmission electron microscopy (TEM).The corrosion behavior was evaluated by immersion test and potentiodynamic polarization analysis in order to select these alloys to be suitable for alternative solution to vascular implant applications.

Key words: nanocrystalline structure, ultrarapid solidification Mg-base alloy, biomedical application.

---

* Corresponding author e-mail: aurelianbuzaianu@yahoo.fr

1. Introduction

The advantages of the ultrarapid solidification are reflected by the favorable modification of the properties of material. The characteristics of the magnesium alloys to serve as a structural metals and possible applications for biodegradable implants, for use in orthopedic and cardiovascular is already documented in the literature. According to (Verbrugge, 1933; Heublein, 2003; Staiger, 2006) the relase of specifically combination, can lead to premature loss of mechanical integrity of the implant and limit the formation of excessive hydrogen gas than can cause separation of tissues (Erbel *et al.*, 2007). There are several parameters to consider in the selection of a biomaterials and biodegradable for stents constructions. These include, but are not limited to: the strength of the material to avoid potential immediate recoil, the rate of degradation, electrochemical potential corrosion, biocompatibility with the vessel wall and lack of toxicity. Magnesium bioasorbable stents are attractive since they have the potential to perform similarly to stainless steel metal stents. Radiological advantages of magnesium include compatibility with magnetic resonance imaging, magnetic resonance angiography and computedtomograpy. Vascular stents comprising magnesium alloys are less thrombogenic then other metals uses for stents. Magnesium is abundant in tissues of animal and is the fourth most abundant metal ion in cells, the most abundant free divalent ion and the fore is deeply and intrinsically woven into cellular metabolism

The aim of the present study is to evaluate the effect of rapid solidification in vitro corrosion performance (Hänzi *et al.*, 2010) of biodegradable $Mg_{98,45}Nd_{0,64}Ag_{0,41}Zn_{0,5}$ alloy. The selected alloy was chosen due to the adequate biocompatibility of Ag and Nd and their beneficiary effect on the corrosion behavior, end good mechanical properties and potential capability to serve for a biodegradable implant having adequate degradation kinetics. Degradable implant materials are advantageous to the patient and the health system because a second surgery for removing of the implant is avoided.

2. Methods and Equipment to Evaluation of Materials

The range of the specific cooling rate in ultrarapid solidification - capable to produce really new constitutional and structural modifications (sometimes at the limit of amorphous structures) - is given by the ultrahigh rates, approaching 10^6 K/s.

The cooling range of 10^5 K/s can be considered as a limit, non-equilibrium being obtained beyond it. This makes the ultrarapid solidification a means to create absolutely new metallic materials. One of the simpler methods to obtain the ultrarapid layers is the "chill block melt spinning process".
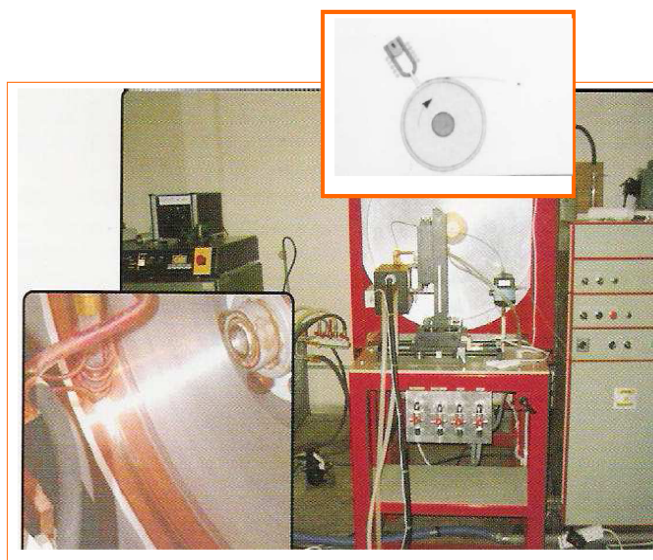
Fig. 1 – The presentation of the ultrarapid
solidification process of magnesium ribbons.

The apparatus we have used in experiments required to design a system enabling reproducible properties of the melt to be obtained. The equipment assures the magnesium melt argon productive atmosphere control as well as the control of the alloy jet ejection through the bottom hole of the crucible. The main elements of the equipment are: a melt heating induction coil, a melting crucible having an ejection gauged hole and the argon pressure systems. The presentation of the ultrarapid solidification process used is illustrated in Fig.1.

Ribbon samples about 35-40 m thick were prepared by a single-roller melt spinning apparatus. As a main investigation device a Transmission Electron Microscope (TEM) type Philips CM-30, equipped with EDS system was used. TEM offers a wide field for research of the fine structures as well as of the nanostructures and nanoprecipitates formed in the ultrarapidly solidified magnesium ribbon.

3. Results and Discussion

The solidification of the ultrarapidly cooled complex magnesium alloys leads to the formation of the quasi-isotropic nanocrystalline structures. The low anisotropy is mainly due to the temperature gradients which are inducing homogeneous nucleation. The rapid solidification pattern we followed uses the interface temperature computation. According to the pattern the liquid is highly under cooled, the conditions to nucleate the heterogeneous structures being replaced.

<center>a   b</center>
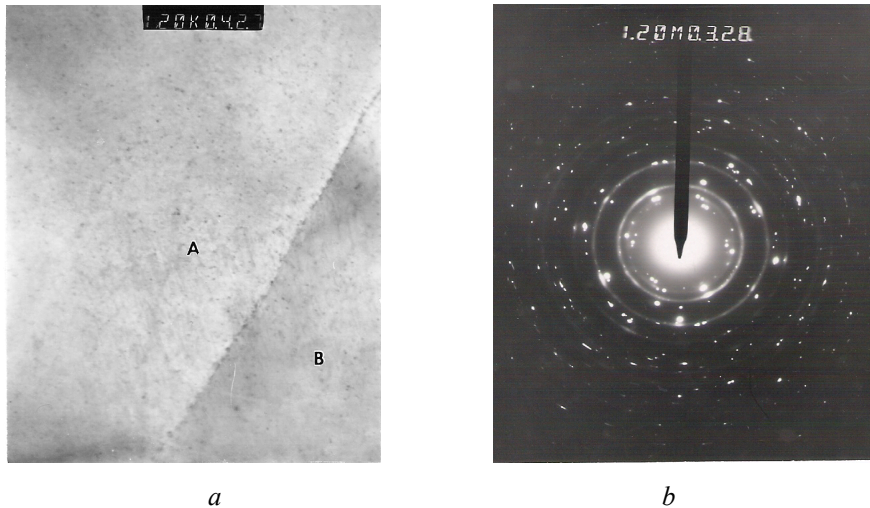
Fig. 2 – TEM analysis of nanocrystalline structure in the ribbon magnesium alloy:
a − Nano-precipitate formation into the matrix in first stage of solidification;
b − Electron diffraction pattern on the selected area (SAED image).

From the point of view of the possibilities to obtain metastable intermediate phases by ultrarapid solidification, these can result only when a large interval of the kinetically condition exist, between the inferior limit, when amorphous alloys result, and the superior limit, over which the equilibrium micro structural phases occur.

The ultrarapid solidification of $Mg_{98,45}Nd_{0,64}Ag_{0,41}Zn_{0,5}$ alloy ribbons is associated to a germination and a growth of nanocrystalline structure, on the direction of the temperature gradient (Fig. 2). The samples are constituted of a nanocrystalline structure primary phase showing a textured aspect, created by the directionalization of the solidification from the cooling surface toward the ribbon a free surface.

The first crystallization stage of the as obtained Mg-ribbons could not be analysed, as the particles are not enough for being identified and described morphologically (under 5nm). The structural identified on the area chosen by the electron diffraction (SAED) evidence phases which area similar to those of the matrix. It is significant to note that for these Mg-base alloys, with variable content of Ag and Nd, the ribbon can be bent 180°C, without appearance of cracks. This indicates a good ductility of the alloys obtained. The specific tensile σ_r and density ρ defined as being to ratio σ_r/ρ is of more then 26; which is more then the value of 20 obtained for the standard alloys.The general advantages of the ultrarapid solidification are reflected by favourable modification of the material properties. The degree of ductility was determined by measuring the radius of curvature at which the fracture occurred in a simple bending test.
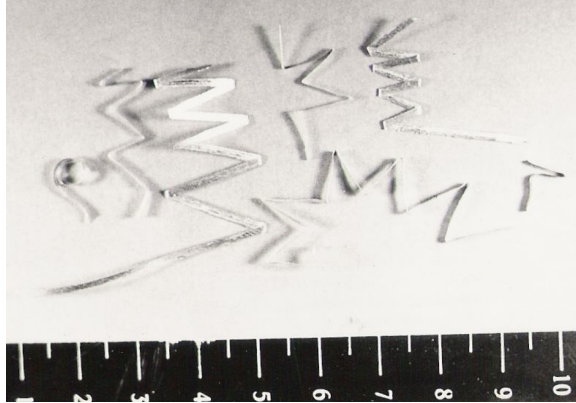
Fig. 3 – Ductility of the Mg $_{98,45}$ Nd $_{0,64}$ Ag $_{0,41}$ Zn $_{0,5}$ ultrarapid solidification ribbons.

The use of Mg-alloy to produce biodegradable implants is known (Staiger, *et al.*, 2006; Hänzi *et al*., 2009; Zberg *et al*., 2009) due to the Mg electrode potential and to its specific degradable capabilities. The classical alloys have the disadvantage of non-homogeneity, unavoidable with materials produced by conventional metallurgical operations, which also exhibit incontrollable low corrosive resistance. The chemical composition of the magnesium alloys tested by the present investigation is shown in Table 1.

Table 1

The Chemical Composition of the Mg-alloy

Mg-System Alloys			Chemical composition [%]			
			Mg	Nd	Ag	Zn
Mg $_{98,45}$ Nd $_{0,64}$ Ag $_{0,41}$ Zn $_{0,5}$	[%at]	(atomic %)	98.45	0.64	0.41	0.50
Mg 93Nd3,5Ag1,8Zn0,5	[%wt]	(mass %)	93.30	3.58	1.74	0.50

Table 2

The Mechanical Properties of Nanocristaline Alloy At Ambient Temperature

Mg- Alloys (% at)	Mechanical properties	
Mg $_{98,45}$ Nd $_{0,64}$ Ag $_{0,41}$ Zn $_{0,5}$	Modulus of elasticity (E) 50,50 GPa	Medium tensile fracture strength (R_m) 350 MPa

For corrosion resistance, instead of attempts being made in Hank's Balanced Salt Solution / simulated body fluid (SBF) to the normal salinity of 0.9% Na Cl in his attempt to acceleration of corrosion of the alloy by testing the solutions aqueous much more corrosive than 3% NaCl (ASTM-B-117).

Unlike Mg alloys produced by conventional technologies, for which the corrosion can be done on the basis of micropila formation, if solidification of alloys is ultrarapid (Zberg *et al*., 2009), this theory is no longer valid, because

the resulting materials have a high degree of homogeneity. The corosion of ultrarapid solidification alloys is primarily due to the thermodynamic phase instability, results in relation to its oxidized form.

And in case of solidified alloys, there may be a few local areas which may constitute areas of anode and cathode processes. These are the atomic distances apart, and the reaction takes place can be considered in its entirety to the same potential. It was found experimentally that an ultrarapid solidified magnesium alloy immersed in an electrolyte solution test, taken by itself quasiconstant electronic potential in and at the same time, the entire area. By measuring the takes potential value can be confirmed in fact, better corrosion and stability that this types of alloys have, compared to those established *by conventional technologies* (Gunde *et al*., 2010; Yuncag, 2010).

Measurements were made using a classic type microvoltmeter EO 30 and an electrochemical cell with calomel. The ion symbolized Mg^+ is not observed experimentally because of its instability and rapid transition in Mg^{2+}. The existence of Mg^+ was determined indirectly based on valence active research area, due to ionization of magnesium. In this case, the ionization process steps involve one electron to form the Mg ion. Its further oxidation occurs in solution after the ionization process.

Actual valence is determined by comparing the amount of dissolved metal and the current passing through the solution of NaCl. By calculation, based on power failure, you can set the speed of anodic dissolution of alloys (corrosion rate) for ultrarapid solidified magnesium; stationary potential moves to positive areas reaching a maximum of -1.64V. The ultrarapid solidified ribbons have thickness between 35-40 μm and mixed electrode potential between -1630 mV_{esc} and -1640 mV_{esc}, values determined in aqueous solutions of 3 wt % NaCl, at 30°C.

To study the corrosion mechanism we conducted a study of scanning electron microscopy (SEM). The ultrarapidly solidified magnesium samples found that corrosion initiation zones focus on included of argon bubbles on the solidification of bands. This was exemplified in the following micrographs Fig. 4 and Fig. 5.
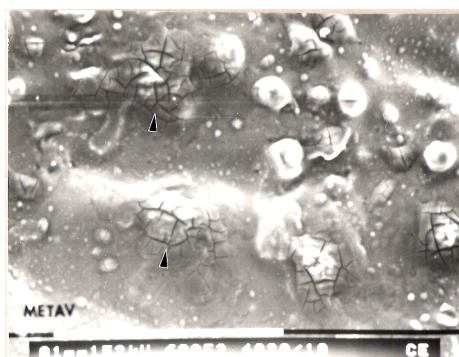
Fig. 4 – SEM microstructure. It highlighted the inclusions should initiate corrosion in the ultrarapidly solidified ribbons with a nanocrystalline structure.

We can say that there is a link between the dissolution kinetics of magnesium alloys, phase composition and texture of the surface ribbons resulting on ultrarapid solidified. The study on the influence of metallic impurities showed stable values over time of power failure (corrosion rate) if the alloys have values: 0.035% Fe, 0.005% Cu and 0.001% Ni, the value for which the corrosion rate remains acceptable for the classic produced alloys. For ultra rapid solidified alloys, over 300% increase in the levels of contaminants above have not led to lower corrosion resistance characteristics.

In case of corrosion tests performed in 3% NaCl aqueous solution, for classically obtained alloys tests, occurring of "pitting" phenomena. Solubility of magnesium anode to the destruction of oxide film content is determined by reaching the surface of a magnesium alloy a critical value of the concentration of chloride ions. Moving to the negative value indicates the potential destruction of protective oxide film continuity. After the destruction of the locally protective film, magnesium leaching is determined by the phenomenon of pitting corrosion. Once increasing concentration of chloride ions in the solution takes place a growth of the potential rate and magnesium solubilization.

Fig. 5 – SEM microstructure revealed that "centers of corrosion" bands formed on the surface of ultrarapidly solidified alloy of nanocrystalline structure.

To view the pitting areas, the conventional magnesium alloys Mg-3.5 Nd-1.5Ag-0.5Zn were placed in a solution feroxil K Fe (CN) 61% mixed with phenolphthalein in alcohol solution (1:1 solution). As a result, areas with "pitting" spots appeared which can be observed in Fig.6.
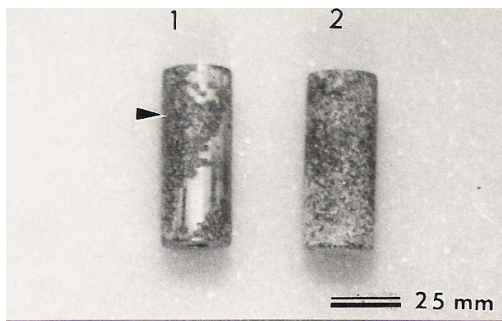
Fig. 6 – Pitting corrosion tests performed to the conventional magnesium alloy technology.

The morphology of ultrarapidly solidified magnesium ribbos strip of the corrosion test subject, is a typical and specific relief generally copies that cooling of cooper disk surface.
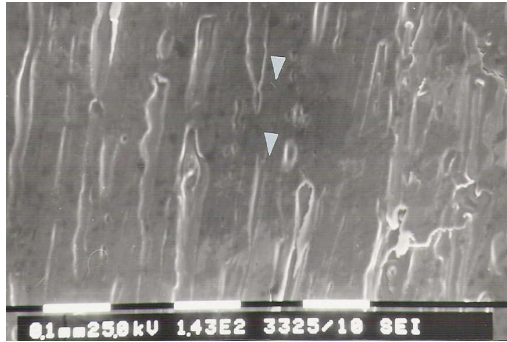
Fig. 7 – SEM microstructure. Micro relief of
ribbons may constitute evidence
of initiate area of corrosion.

For tests in saline solution, the absorption capacity of the Cl^- anion is greater and primarily affects the phenomenon activity. Film is formed as a reaction type:

$$Mg+2H_2O \rightarrow Mg(OH)_2 +2H^+ +2e^-$$ (1)
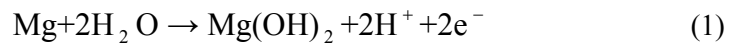
The kinetics process of the alloy corrosion and passivation tendency was assessed by the volume of hydrogen removed that is inversely proportional to the thickness of the oxide film and can be explained by the following equation:

$$V= k\, t^{0,66}$$ (2)
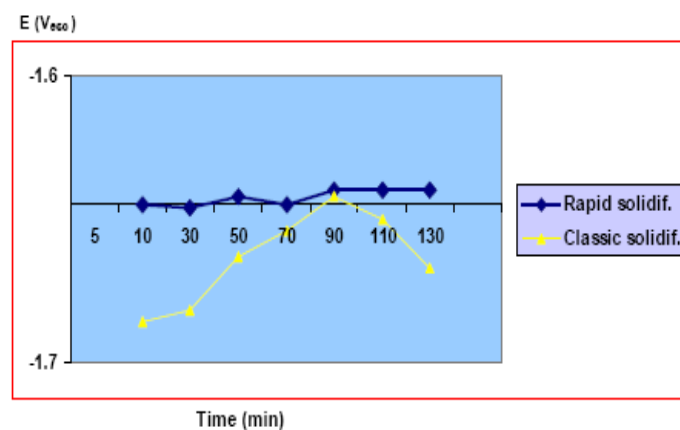
Fig. 8 – Variation of electrode potential test in 3% NaCl
solution at 37°C for rapid and classic solidification Mg alloy.

The increasing of thickness (t) in time, determines the potential displacement of magnesium ribbons alloys for positive values (Fig.8).
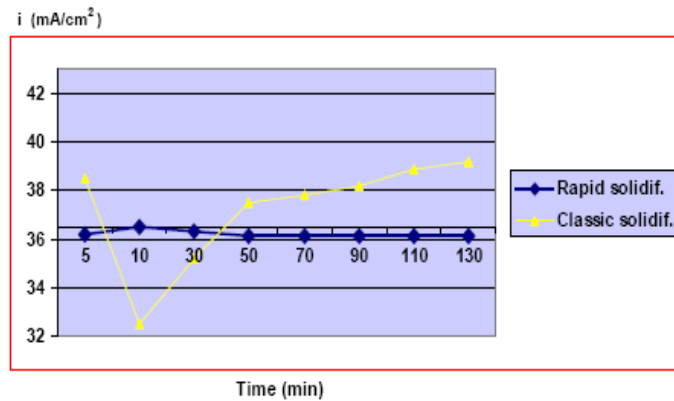
Fig. 9 – Variation of current density test in 3% NaCl
solution at 37°C for rapid and classic solidification Mg alloy.

For ultrarapidly solidified alloys tested, a decrease of the pH solution is more pronounced. Papers more pronounced in comparison with the obtained classical solidification alloys. This may mean that the corrosion rate gradually decreases in NaCl solution.

EDAX and X-ray diffraction analysis revealed the presence of a majority of MgO and Mg(OH). The thickness of oxide and hydroxide surfaces lies around 100nm.
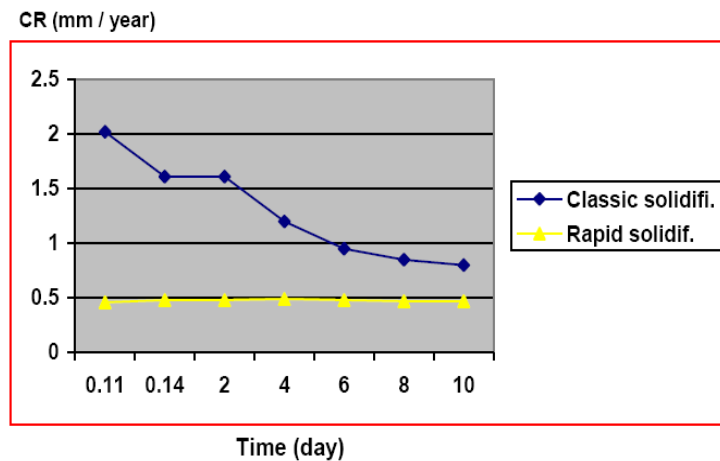
Fig. 10 – Corrosion rate (CR) calculated from hydrogen
evolution obtained during immersion testes in 3% NaCl
solution at 37°C for rapid and classic solidification Mg alloy.

Evolution of corrosion products, the purpose of increasing the amount of hydroxide, can be highlighted with the increasing volume of hydrogen released and its measurement (Fig. 10). The carbonate structures that are formed due to dissolution of CO_2 in the solution that's free Mg^{+2} ions (Salman *et al.*, 2010).

MgOH bruscit appearance is not the result of contamination of the magnesium melt, before ultrarapid solidification, but is the result of hydrolysis oxide crystallizes in the monoclinic system. That opens the volume changes of parameters and some form of structure defects in bruscit sudden with microporosity created I bay argon, a mixture of the crystals and inclusion of H_2O, leading to migration to interfaces and epitaxial growth (metal-oxide-hydroxide) aspect was revealed by electronic microscopy images.

TEM images show that the bands formed on the surface of a crystalline structure consisting of a variety of polyhedral and triclinic and monoclinic type structures as shown in Fig.11.

By association, it appears are some complex macle, more evident as the intermingling macles on the position 7 and 8. Macles seem to be formed by parallel hemitropy (to which the rotation was performed around an axis contained in the plan of macle).

a   b
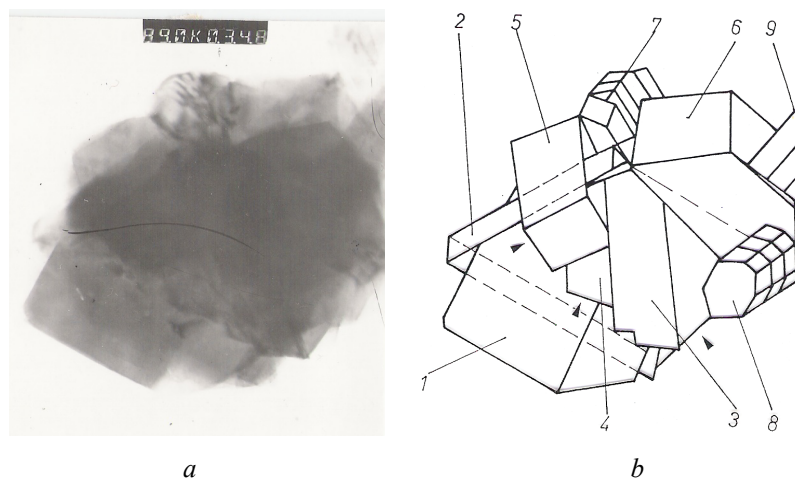
Fig. 11 – *a*) TEM analysis of the corrosion products formed on the ultrapidly solidified alloy (moclinic and triclinic structures), 0,11 m; *b*) The model of TEM image of the crystalline edifice.

TEM image reveals a typical epitaxial growth, created by the combination of two different kinds of crystals. Development of epitaxial hydroxides and magnesium oxide (heading 1 or 2 and 3) are based on growth opportunity associated contact surfaces due to matching of two species of crystal symmetry (default interatomic distances based structures).

Contrary to the known products of corrosion of the ultrarapyd magnesiun solidification, together with two compounds with periclase (MgO) and bruscita (Mg (OH)) of dimmension about 20-50 nm in size, there are other compounds such as hydroxides and halides; this compounds that are stopped in growth by Mg_9Nd from to the strip surface.

The chloride ions are less electronegative than fluoride ions, but are similar to the hydroxyl ions. TEM analysis demonstrated that chloride ions are "placed" in fact the structural defects of the type of corrosion products types bruscit or periclase.

4. Conclusion

Ultrarapyd solidification of magnesium alloys with a variable content of 1.5-2% Ag and 3-3.5% Nd, leads to a significant increase of mechanical properties and increased the corrosion resistance. This reduces or even cancels the effect they may have higher levels of contamination and the method leads to a homogeneous distribution of impurities.

Lack of flux inclusions, the uniformity and smoothness of the structure in ultrarapyd solidified magnesium alloys, which are the main factors that give them a high and controllable resistance to corrosion with a convenient subdivision of the corrosion products.

It has been demonstrated that the use of elements such as Ag and Nd in a Mg-based nanostructured alloy, creates favorable conditions to request these alloys both in terms of electrochemical and mechanical properties of strength and ductility with good prospects for use in the stands manufacture.

REFERENCES

* * Magnesium Tehnology. EDT Nyberg Eric, Publication of TMS. The Minerals, Metals and Materials Society, 2009.

Aghion E., Levy G., The effect of Ca on the in Vitro Corrosion Performance of Biodegradable Mg-Nd_Y-Zr Alloy. Journal of Materials Science, DOI 10.1007/s10853-010-4317-7, 2010.

Erbel R. et al., Temporary Scaffolding of Coronary Arteries With Bioabsorbable Magnesium Stents: a Prospective, Non-Randomized Multicentre Trial. The Lancet 369, 1869-1875 (2007).

Gunde P., Hänzi A., Furrer C., A., Schmutz P., Uggowitzer P. J., The influence of heat treatment and plastic deformation on the biodegradation of a Mg-Y-RE alloy, Journal Biomed Mater Res. A 92, 2, 409-418 (2010).

Hänzi A.C., Gerber I., Schinhammer M., Löffler J.F., Uggowitzer P. J., On the in Vitro And in Vivo Degradation Performance and Biological Response of new Biodegradable Mg–Y–Zn Alloys. Acta Biomater. 6, 1824 – 1833 (2010).

Hänzi A.C., Gunde P., Schinhammer M., Uggowitzer P.J., *On the Bio-Degradation Performance of a Mg–Y–RE Alloy With Various Surface Conditions in Simulated Body Fluid*. Acta Biomater. **5**, 162 – 171 (2009).

Heublein B., *Biocorrosion of Magnesium Alloys: a new Principal in cardiovascular Implant Technology.* Heart **89**, 651-656 (2003).

Kainer K.U., *Wiley-VCH*, Editors of Magnesium**,** Weinheim, Germany, 2010.

Salman S.A., Ichino R., Okido M., *A Comparative Electrochemical Study of AZ31 and AZ91 Magnesium Alloy.* International Journal of Corrosion; DOI:10.1155/2010/412129, 2010.

Staiger M.P., Pietak A.M., Huadmai J., Dias G., *Biomaterials* 27:1728, 2006.

Staiger M.P., Pietak A.M., Huadmai J., Dias G., *Magnesium an Dits Alloys as Orthopedic Biomaterials*. Biomaterials, **27**, 1728-1734 (2006).

Verbrugge J., *La tolerance du tissue osseux vis-à-vis du magnesium métallique*, Presse Med., **55**,1112-1114, (1933).

Yuncag Li, *The Effects of Calcium and Yttrium Additions on the Microstructure, Mechanical Properties and Biocompatibility of Biodegradable Magnesium Alloys*. Journal of Materials Science*, **45**, 20211, 3096-3110 (2010).

Zberg B., Arata E. R., Uggowitzer P. J., Löffler J. F., *Fabrication and Mechanical Properties of Glassy MgZnCa Wires and Reliability Analysis by Weibull Statistics*. Acta Mater. **57**, 3223 – 3231 (2009).

Zberg B., Uggowitzer P.J., Löffler J.F., *MgZnCa glasses Without Clinically Observable Hydrogen Evolution for Biodegradable Implants*. Nature. Mater. **8** (2009), 887 – 891. (Highlighted as "No gas from glass", *Nature* **461**, 701 (2009).

POTENŢIALUL DE UTILIZARE PENTRU APLICAŢII MEDICALE AL UNUI ALIAJ DE MAGNEZIU NANOCRISTALIN

(Rezumat)

Stucturile nanocristaline ale materialelor metalice oferă importante creşteri ale proprietăţilor acestora precum şi noi funcţionalităţi. Una din direcţiile importante de dezvoltare este aceea de realizare a unor aliaje pe bază de magneziu solidificate ultrarapid. Au fost înregistrate unele aspecte favorabile la un aliaj de tipul $Mg_{98,45}Nd_{0,64}Ag_{0,41}Zn_{0,5}$ în ceea ce priveşte: fineţea mărimii de grăunte, omogenitatea structurală a aliajului, creşterea ductilităţii, a limitei de rupere şi a coroziunii prin comparaţie cu aliajele cunoscute pe bază de Mg. Aceste modificări de proprietăţi face din noul aliaj prezentat un potenţial material de realizare a implanturilor metalice biodegradabile.

NONFERROUS METALS RECOVERY FROM OXIDIC SUBPRODUCTS OBTAINED FROM WASTE ELECTRICAL EQUIPMENT

BY

TRAIAN BUZATU* and IONELA POENIŢA BÎRLOAGĂ

University POLITEHNICA of Bucharest,
Department of Engineering and Management for Elaboration of Metallic Materials

Abstract. In this study, we proposed a new feasible hydrometallurgical process for recovering lead from lead-acid battery paste passing through the following steps: desulphurization, leaching Pb (OH) 2 solutions with acetate ions, iron cement to obtain lead cement that can be used to obtain new batteries, with an observed efficiency up to 99.5%. The best working conditions for leaching of lead-acid paste, using a solution of acetic acid and urea for obtain high concentrations of ion acetate and cement of metallic lead on iron span are present below.

Key words: lead-acid batteries, leaching, desulphurization

1. Introduction

Lead components have attracted scientific interest not only because of the coordination properties and stereochemistry, but also because of the toxic effect on the human body. In other news, a lead-acid battery is the largest consumer of lead, using more than 70% of Pb, (Dutrizac *et al*., 2000; Buzatu &

---

* Corresponding author; e-mail: traian1983@yahoo.com

Roman, 2008). Taking into account the most advertised toxic properties of Pb, efficient recycling or recovery of waste is an stringent need for environmental reasons and economic.

For treatment of waste battery paste were used as thermal methods, as well as hydrometallurgical (Habashi, 1997; Gong *et al*., 1992b; Prengman, 2005). Although thermal methods still represent more than 90% of recovery technologies, they are under severe critical, mainly due SO_2 emissions resulting from $PbSO_4$ decomposition at high temperatures, higher 1000°C and evaporative emissions of lead from these high temperatures. Hydrometallurgical methods have been used to remove sulfur from the Na_2SO_4 soluble paste (aq) or (NH4) $_2SO_4$ (aq) using Na_2CO_3 (aq), NaOH (aq) or $(NH_4)_2CO_3$ (aq) (Prengaman *et al*., 2001; Buzatu *et al*., 2009). Na_2SO_4 is then crystallized from the remainder solution and can then be sold. Insoluble product of $PbCO_3$ or Pb $(OH)_2$ form a collected or filtered sludge will be recirculated to the smelter.

High content of PbO_2 in sludge is a major problem in the leaching process. While the majority of PbO is easily dissolved by most of leaching electrolytes, PbO_2 require before leaching Pb (IV) reducing to Pb (II). A number of researchers (Ferracin, *et al*., 2002) have succeeded to completely solubilized sludge samples by using ascorbic acid solutions but undesirable were obtained solid residue after 24 h. The recovery of lead using lead-acid battery paste exhausted with high metallic contain of lead and antimony (about 13%) and has been reported the by other researchers (Maja, *et al*., 1990).

Other versions of the hydrometallurgical / electro-deposition method, both of PbO_2 $PbCO_3$ are converted to PbO by calcinations / reduction. PbO is then soluble in H_2SiF_2 (aq) where Pb is electro deposited (Prengman, 1995).

In this study, we proposed a new hydrometallurgical process for recovering lead from feasible industrial lead-acid battery paste via the following steps: desulphurization, leaching $Pb(OH)_2$ solutions with acetate ions, making the cement with cement fier lead to can be used to obtain new batteries, with an observed efficiency up to 99.5%.

2. Experimental

Waste has been subjected to a desulphurization process and obtains a product consisting of lead hydroxide, Pb $(OH)_2$. This is a hydrometallurgical procedures (process Plinth), based on leaching of pasta in weak acid H_2SO_4 solutions in the presence of chloride (CaCl or NaCI). The general scheme for the recovery of lead from spent batteries include combined operations mechanical, pyro and hydrometallurgical.

The spent batteries after crushing in the mills and classification screens and dense medium are obtained these classes of materials: metal

fraction represented by grids, battery terminals and connectors, light fraction represented by the plastic housing and separators, the fine fraction represented by sulphated paste and the acid solution represented by the depleted electrolyte and by the washing water from the classifying operation. Metal fraction is subject to melting in short revolving furnaces at temperatures of 450...500°C in the presence of charcoal and soda as flux for the retention of residual sulfur for pasts involved in grids. Sulfated or dryed pastes without prior desulphurization, held together with dust by filters bags from dedusting gas and the resulted slag from melting operations, are subject to solubilization in dilute solutions of hydrochloric acid and sulfuric acid or sodium chloride and calcium chloride. In this case leaching of PbSO4, PbO. PbSO4, PbO and PbO2 lead compounds from the paste is made according to the reaction:

$PbSO_4 + 2CaCl_2 \rightarrow CaPbCl_4 + CaSO_4$

$PbOPbSO_4 + 4CaCl_2 + H_2SO_4 \rightarrow 2CaPbCl_4 + 2CaSO_4 + H_2O$

$PbO + 2CaCl_2 + H_2SO_4 \rightarrow CaPbCl_4 + CaSO_4 + H_2O$

$PbO_2 + Pb + 2H_2SO_4 + 4CaCl_2 \rightarrow 2CaPbCl_4 + 2CaSO_4 + 2H_2O$
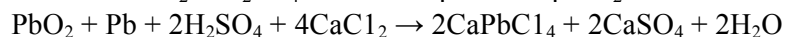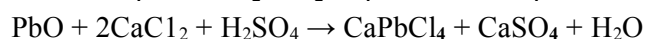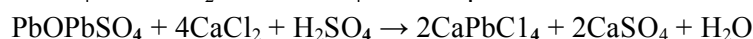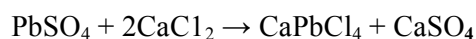
Lead hydroxide, Pb (OH)₂, used in preliminary investigations to establish the best working conditions were obtained by preparing the paste. Samples of paste industrial lead-acid batteries were obtained by dismantling the batteries removed from service. Before any use, the paste was spread thin and dry (about 12% wt) in an oven at 105°C for at least 4 h.

The high content of CaSO4 in the acid battery paste was due to the addition of CaCO3 for neutralizing the excess sulfuric acid from the battery crushing unit. Table 1 show the phase composition of lead compounds, usually found in industrial sludge. The paste was processed for desulphurization and obtaining of lead hydroxide and lead hydroxide was subjected to acetic acid leaching process.

$Pb(OH)_2 + 2CH_3COOH \rightarrow Pb(CH_3COO)_2 + 2H_2O$ $\Delta Gr = -15,127 \text{ kJ}$

Table 1
Chemical Composition of Industrial Pastes Lead Acid Battery Batteries Removed from Service, After Neutralization

Compound	Composition of paste (%wt)
$PbSO_4$	53,70
PbO	13,40
PbO_2	22,40
$CaSO_4$	8,50
Unidentified	2,00

After a series of preliminary tests, was set the working temperature at 60°C and were obtained a passing efficiency of lead in solution of 95% after a period of 20 hours. After the experimental data processing with Jandel Scientific program result the following equation that describes the leaching of lead oxide in acetic acid under mentioned conditions.

3. Result and Discussion

Experimental data are shown in Table 2 and Fig. 1.

Table 2
Experimental Data for Solubilization of Lead Hydroxide with Acetic Acid

No.	$t \cdot 10^{-3}$, [s]	Pb, [g/l]	Pb acetate, mol/l	Acetic acid, mol/l	Reacted acetic acid, mol/l	Efficiency, %
1	0	0	0	0.3333	0	
2	1.8	4.9473	0.01195	0.3094	0.0239	7.1696
3	3.6	9.522	0.023	0.2873	0.046	13.7993
4	7.2	17.7399	0.04285	0.2476	0.0857	25.7087
5	14.4	30.9258	0.0747	0.1839	0.1494	44.8178
6	21.6	40.7169	0.09835	0.1366	0.1967	59.0070
7	28.8	47.9826	0.1159	0.1015	0.2318	69.5365
8	43.2	57.4011	0.13865	0.056	0.2773	83.1858
9	57.6	62.5968	0.1512	0.0309	0.3024	90.7155
10	68.4	64.8945	0.15675	0.0198	0.3135	94.0453
11	72	65.5155	0.15825	0.0168	0.3165	94.9453
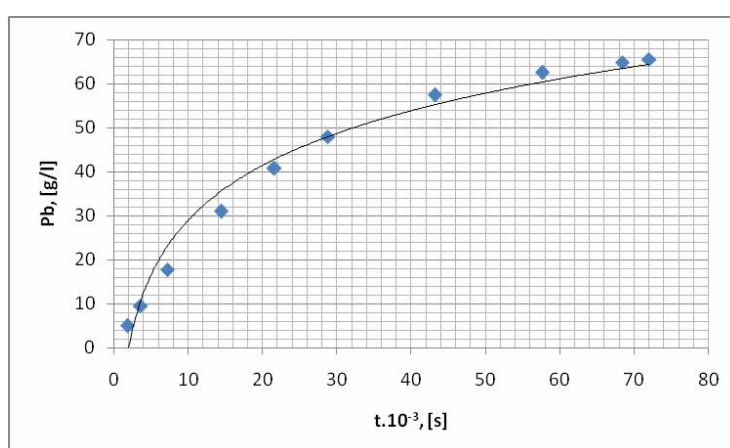
Fig. 1 – Variation of Pb concentration in solution.
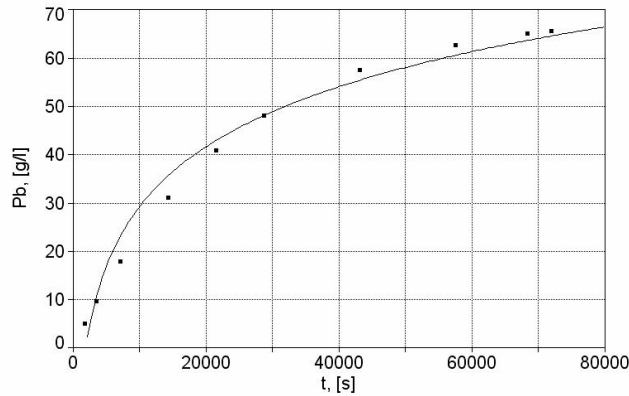
Fig. 2 – Experimental data for concentration variation of Pb in solution.

$$\text{Rank 13   Eqn 13   } y = a + b\ln x \qquad (1)$$

where: y is the concentration of lead in solution, [g/l]; x - reaction time, [s].

Parm	Value	Std Error	t-value	95% Confidence	Limits
a	-136.050497	9.683862615	-14.0491973	-158.459488	-113.641506
b	17.92465492	0.977240074	18.34212021	15.66326763	20.18604222

$$\text{Rank 13   Eqn 13   } y = a + b\ln x$$

Removing	Error @Xmin	Error @Xmean	Error @Xmax
a	-80.24238999	2.73127074905	2.1117197734
b	79.242389990	-3.731270749	-3.111719773

Fig. 3 shows concentration variations of acetic acid over time, these data were processed to determine the mathematical model which best describe the leaching and determination of reaction kinetics.

$$\text{Rank 2   Eqn 22   } \ln y = a + bx \qquad (2)$$

where: y is the concentration of lead in solution, [g/l]; x - reaction time, [s].

Parm	Value	Std Error	t-value	95% Confidence	Limits
a	-1.09863318	0.000212597	-5167.67103	-1.09912514	-1.09814121
b	-4.1301e-05	1.8369e-08	-2248.39941	-4.1343e-05	-4.1258e-05

Removing	Error @Xmin	Error @Xmean	Error @Xmax
a	2.0000626628	2.0000626628	2.0000626628
b	0.0771744324	2.7278879225	18.563270598
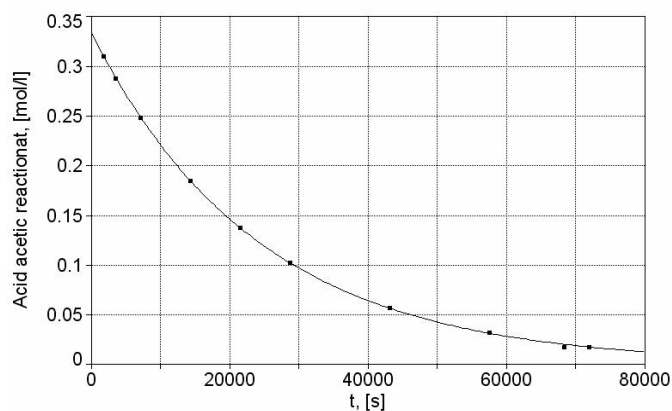
Fig. 3 – Concentration variation of acetic acid in time.
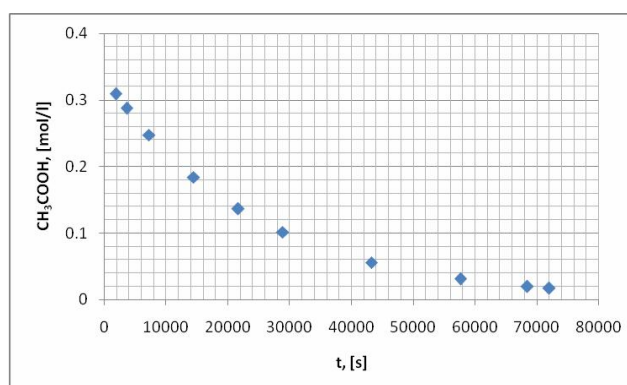
Fig. 4 – Experimental data for concentration variation of acetic acid.

The equation which describes the leaching of lead hydroxide, lny = a + bx, corresponds to a kinetic form:

$$\frac{dx}{dt} = k_n (\propto - x)^n \tag{3}$$

in integral form being:

$$k_n = \frac{1}{(n-1)t} \left[\frac{1}{(\propto - x)^{n-1}} - \frac{1}{\propto^{(n-1)}} \right] \tag{4}$$

or, for n = 1, we have:

$$k = \frac{1}{t} ln \frac{\propto}{\propto - x} , \text{ or:} \tag{5}$$

equation determined by comparison with experimental data:

$$lny = -1.0986 - 4.1301.10^{-5} \ x \qquad (7)$$

we have: $\alpha = 0.3358$[mol/l], and the reaction rate constant, $k = -4.1301.10^{-5}[s^{-1}]$.

Representing graphic equation (4) and introducing the experimental data from Table 2, from slope of the line (4), Fig. 5, can be determined the reaction rate constant and can be comparable with the value obtained from equation (5):

Table 3
Rate Constant Determinate From Experimental Data with the Theoretical Equation

Nr.crt	$t.10^{-3}$, [s]	$ln[\alpha/(\alpha-x)]$	Δt	$\Delta[ln\alpha/(\alpha-x)]$	$\Delta[ln\alpha/(\alpha-x) /\Delta t]$
1	1.8	0.0744			
2	3.6	0.1485	1800	0.0741	4.11667E-05
3	7.2	0.2972	3600	0.1487	4.13056E-05
4	14.4	0.5946	7200	0.2974	4.13056E-05
5	21.6	0.8919	7200	0.2973	4.12917E-05
6	28.8	1.1889	7200	0.297	4.125E-05
7	43.2	1.7837	14400	0.5948	4.13056E-05
8	57.6	2.3783	14400	0.5946	4.12917E-05
9	68.4	2.8233	10800	0.445	4.12037E-05
10	72	2.9877	3600	0.1644	4.56667E-05
				Average	4.17541E-05

It notes that there is a very good agreement between theoretical equation (first order kinetics) and the equation determined from experimental data.

4. Conclusion

The process of leaching lead hydroxide, $Pb(OH)_2$, in acetic acid is a slow process, corresponding to a first-order kinetics, under the circumstances, due to the very low dissociation of acetic acid, about 4%.

Solubility study of $Pb(OH)_2$ paste obtained from acetic acid and urea solution was performed in order to determine the best working conditions for leaching and cementation of lead where the sludge was used as industrial raw material.

Preliminary studies have shown that the use of acetate solution of urea is the best compromise between leaching kinds of lead compounds (II) and pH of the reaction solution maintaining an appropriate ratio water / acetic acid. To increase the speed of solubilization, further attempts will be made to increase the concentration of ions in solution using ion acetate complex.

REFERENCES

Dutrizac D.M., Gonzales J.A., Henke D.M., James S.E., Siegmund J.A., (Eds.), Lead–Zinc,The Minerals, Metals & Materials Society (TMS), Pennsylvania, 17–22 (2000).

Buzatu T., Roman R., *Reciclarea şi regenerarea deşeurilor neferoase*. Printech, Bucureşti, 2008.

Habashi F., *Part Three, Primary Metals: 9 Lead. Handbook of Extractive Metallurgy*. Volume II: Primary Metals, Secondary Metals, Light Metals. Wiley VCH, Weinhelm, 581–640 (1997).

Gong Y., Dutrizac J.E., Chen T.T., *The Reaction of Anglesite (PbSO4) with Sodium Carbonate Solutions*. Hydrometallurgy, **31**, 175–199 (1992b).

Prengman R.D., 2005, *Recovering Lead from Batteries*. JOM, **47**, *1*, 31–33.

Prengaman, R.D.,Morgan, C.,Hine, E.,Homer, P., Griffin,G.M., 2001, US Patent, No: 6177056.

Buzatu T., *et al*, *Tehnologii ecologice de reciclare a acumulatorilor uzaţi*. Bucureşti, Gepropol, 2009.

Ferracin L.C., Chàcon-Sanhueza A.E., Davoglio R.A., Rocha L.O.,Caffeu D.J., Fontanetti A.R., Rocha-Filho R.C., Biaggio S.R., *Lead Recovery from a Typical Brazilian Sludge of Exhausted Lead-Acid Batteries Using an Electrohydrometallurgical Process*. Hydrometallurgy, **65**, 137–144 (2002).

Maja M., Penazzi N., Baudino M., Ginatta M.V., *Recycling of the Lead-Acid Batteries: the Ginatta Process*. Journal of Power Sources, **31**, 287–294 (1990).

Prengman R.D., *Recovering Lead from Batteries*. JOM, **47**, *1*, 31–33 (1995).

RECUPERAREA METALELOR NEFEROASE DIN SUBPRODUSELE OXIDICE
OBŢINUTE DIN DEŞEURILE ECHIPAMENTELOR ELECTRICE

(Rezumat)

În acest studiu, am propus un nou proces hidrometalurgic fezabil industrial pentru recuperarea plumbului din pasta bateriilor plumb-acid trecând prin următoarele etape: desulfurare, solubilizarea $Pb(OH)_2$ cu soluţii cu ioni acetat, cementare cu fier cu obţinerea unui cement de plumb ce poate fi folosit la obţinerea noilor acumulatori, cu o eficienţă observată de până la 99,5%. Cele mai bune condiţii de lucru pentru solubilizarea pastei plumb-acid, folosind o soluţie de acid acetic şi uree pentru obţinerea unei concentraţii mari de ioni acetat şi cementarea plumbului metalic pe şpan de fier, sunt prezentate în studiul ce urmează.

RESEARCHES CONCERNING THE PROCUREMENT AND CHARACTERIZATION OF SOME PERMEABLE POROUS SINTERED MATERIALS OF BRONZE POWDERS FOR FILTERING ELEMENTS BY 25% POROSITY
I. OBTAINING MATERIALS AND DETERMINATION OF SOME CHARACTERISTICS

BY

OVIDIU CALANCIA*, VASILE CAŢARSCHI and ŞTEFAN LUCIAN TOMA

"Gheorghe Asachi" Technical University of Iaşi,

Abstract. The present paper discusses the selection, preparation and properties of bronze powder CuSn10P1 used to obtain porous permeable materials designed to achieve of some filter elements by 25% porosity. Experiments were carried out shaping and sintering using different working arrangements and have determined some characteristics of these materials (density and hardness after sintering) looking at how they change.

Key words: permeable porous material, porosity, apparent density, grain size, sifting, plus mesh, shaping, sintering, sintering density, hardness.

1. Introduction

Permeable porous sintered materials is characterized by a greater than 25% porosity, pore structure containing open and communicated, which

---

* Correspondind author e-mail: calacea_ovidiu_is@yahoo.com

enable them to carry out different fluid filtration. These materials are used for making products such as: filter elements, heat exchangers, fluid dispensers, electrodes, fluid mixers, liquid or gas separators, etc., with applications in chemistry, aerospace, engineering, agriculture, medicine, etc. (Vida-Simiti & Magyarosy 1992).

This class of materials, porosity should be associated with good permeability, adequate mechanical strength at static and dynamic appear during their use and resistance to corrosion caused by the environments in / with which they work. The great variety of porous materials is determined by the broad spectrum of implementation of specific areas and the variety of raw materials and manufacturing technologies used.

These materials are complex functionality that, in addition to outstanding filter characteristics, they are taxed and others, such as resistance to corrosion resistant, high mechanical properties, good electrical and thermal conductivity, good absorbency, etc.

For combination of such properties, one of the important factors is the material consisting of powder particles used in the manufacture of sintered material. Currently, the diversity of materials for production of sintered porous permeable include: bronze, stainless steel, copper, iron, nickel and nickel-based alloys, silver, titanium, metal carbides, etc.

Following studies and data from literature was found for a filter element, optimum powdery material which is fuel filters meet the bronze powder spherical (Vida-Simiti, 1998), with an average grain dimension (calculated at 50% passing), d_g, 92 m. Optimum average pore dimension, $D_{pore} = 2Pd_g / 3 (1-P)$, is 20 m for a 25% porosity (P) of the material.

2. Experiments and Results

Preliminary researches on porous permeable sintered materials obtained consisted of carrying out tests, using as raw material spherical bronze powder CuSn10P1. Stages of experiments on porous sintered porous materials obtained were: - determination the characteristics of powder used; - shaping experiments; - sintering experiments.

2.1. Determination the Characteristics of the Powder Used

For spherical bronze powder to be used to achieve a porous permeable material to determine density (ρ_a) using a device consisting of a conical funnel mounted on a base and a cylindrical receptacle (Fig. 1) (Vida-Simiti, 1994).
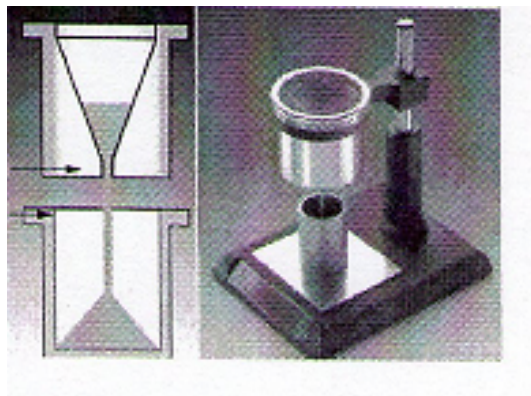
Fig. 1 – Device for determining the apparent density (ρ_a), (installation and working scheme of the device).

There have been three determinations, using the relationship:

$$\rho_a = (m_2 - m_1) / V_u$$

where:

    m_1 - mass of the receptacle ($m_1 = 129.2$ g);
    m_2 - mass of the powder receptacle;
    V_u - volume of the receptacle ($V_u = 25$ cm^3).
    The results are recorded in Table 1.

Table 1
Apparent Density Spherical Bronze Powder CuSn10P1

No.	Mass of the receptacle, m_1 [g]	Mass of the powder receptacle, m_2 [g]	Volume of the receptacle, V_u [cm^3]	Apparent density, ρ_a [g/cm^3]
1		251,2		4,88
2	129,2	249,7	25	4,82
3		250,5		4,85
Average values	129,2	250,26	25	4,85

By using a vibrating sieve analyzer to determine the composition of the powder size proposed for testing (Table 2).

Determination of average apparent density value resulting from measurements performed CuSn10P1 bronze spherical powder is $\rho_a = 4.85$ g/cm^3 > 1.5 g/cm^3 for which to determine the composition grading will use a portion of 100 g powder.

Table 2

Analysis of the Granulometric Composition of Spherical Bronze Powder

No.	Grain size	Mass of the grain-size fraction, m_{fi}	Ratio of fraction, x_i	Sifting, S_i	Plus mesh, P_i
	[m]	[g]	[%]	[%]	[%]
1	> 200	2,2	2,2	97,8	2,2
2	200÷120	28,5	28,5	69,3	28,5
3	120÷90	27,0	27,0	42,3	27,0
4	90÷71	22,3	22,3	20,0	22,3
5	71÷63	2,8	2,8	17,2	2,8
6	63÷56	2,5	2,5	14,7	2,5
7	56÷45	5,2	5,2	9,5	5,2
8	< 45	7,7	7,7	0,0	7,7

Figs. 2 and 3 are the results of the powder particle size analysis a sifting based and as a histogram.

For each dust particle size fractions belonging presented in Table 2 and apparent densityes were determined using the same device as the determinations made in preparing Table 1.

The results are presented in Table 3.
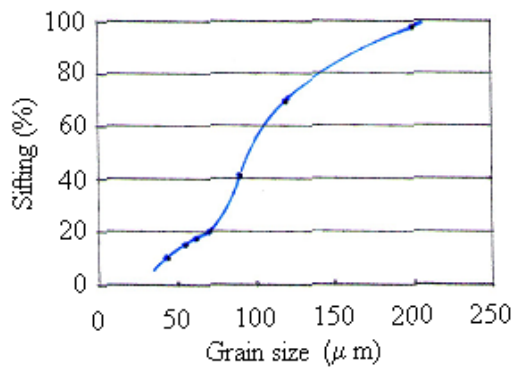
Fig. 2 – Variation of the sifting a the grain size powder CuSn10P1 based.
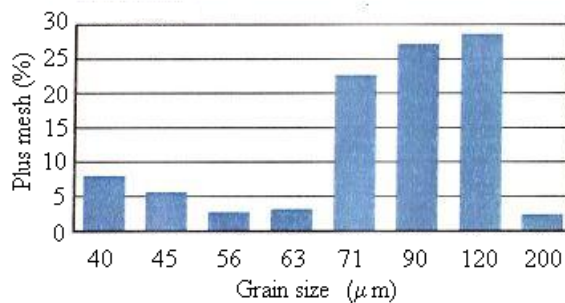
Fig. 3 – Resulting histogram analysis of the plus mesh a the grain size powder CuSn10P1 based

Table 3
Composition and Size Fractions of Apparent Densities of Spherical Bronze Powder
CuSn10P1

No.	Grain size [μm]	Ratio of fraction, x_i, [%]	Apparent density of grain size, ρ_{ai} [g/cm^3]
1	> 200	2,2	5,12
2	- 200 +120	28,5	4,99
3	- 120 +90	27,0	4,84
4	- 90 +71	22,3	4,83
5	- 71 +63	2,8	4,82
6	- 63 +56	2,5	4,80
7	- 56 +45	5,2	4,79
8	< 45	7,7	4,58

We can say that if fine particle size fractions, apparent density is lower, which is explained by the higher capacity due to gas adsorption surface area larger. Economic reasons proposes fractions using permeable porous sintering materials resources in the composition of the powder particle size, *i.e.* 200 ÷ 120, 120 ÷ 90 and 90 ÷ 71 μm fractions.

The choice of these fractions is favored by higher apparent densities, involving an arrangement of particles in the powder mass, more compact, without cover large amounts of gas.

2.2. Shaping Experiments

Was chosen shaping technology by casting free of particulate forms. For the most compact arrangement of particles in the form of subsidence have been made by vibrating. The length of vibration was 30 minutes.

Categories bronze powder samples in the training were coded according to fraction size and duration of vibration used is presented in Table 4.

Table 4
Types of Powder Samples Made at Shaping

Cod sample powder	Grain size, [μm]	Time shaking, [min]
FBz1	200÷120	0
FBz1.1		30
FBz2	120÷90	0
FBz2.1		30
FBz3	90÷71	0
FBz3.1		30

To prevent the powder to form the membership were made during the sintering, the forms have been coated with a protective layer consisting of a graphite-based solution, ammonia, carpenters glue and water (Dima *et. al.*, 2007).

Applying the coating was heated form as before.

Pour the powder forms are cylindrical with a diameter of 25.5 mm, height 5 mm, the material was made as a stainless steel. Application of vibration was made with equipment vibration.

2.3. Sintering Experiments

Sintering experiments were conducted in a furnace controlled atmosphere type tunnel oven using the following schemes ENDOGAZ sintering:

- R1 regime: temperature of sintering, T_{sint} = 830°C and speed of the conveyor belt, v_b = 2 m / h;

- R2 regime: temperature of sintering, T_{sint} = 860°C and speed of the conveyor belt, v_b = 3 m / h.

Sintering regimes were chosen in order to lower sintering temperature, sintering time is higher and higher sintering temperature during sintering is lower. Sintering temperature was chosen so as not to occur during liquid phase sintering.

Permeable porous materials obtained after sintering were coded according to the schemes of work used (sintering regime R1 and R2 sintering regime). Codification, density and hardness of materials obtained from different fractions of spherical particles freely cast bronze CuSn10P1 forms without vibrating and vibrated, sintered to those established (R1 and R2) are presented in Table 5.

As shown in Table 5 both sintered density and hardness of materials increases with decreasing grain produced and used with increasing sintering temperature.

Table 5
Results of Experiments on the Sintering

Cod of material	Time shaking $t_{shaking}$ [min]	Temperature of sintering T_{sint} [°C]	Speed belt v_b [m/h]	Density of sintering ρ_{sint} [g/cm³]	Hardness of sintering HB_{sint}
R1FBz1	0	830	2	5,68	11,2
R1FBz2	0	830	2	5,71	11,7
R1FBz3	0	830	2	5,92	11,9
R1FBz1.1	30	830	2	5,73	15,0
R1FBz2.1	30	830	2	5,95	15,1
R1FBz3.1	30	830	2	6,16	17,5
R2FBz1	0	860	3	6,19	14,0
R2FBz2	0	860	3	6,19	17,6
R2FBz3	0	860	3	6,48	18,7
R2FBz1.1	30	860	3	6,33	17,4
R2FBz2.1	30	860	3	6,36	19,6
R2FBz3.1	30	860	3	6,53	20,6

Also, if the material has been used by vibration compaction, density and hardness of both materials increased.

Fig. 4 is shown the density variation of materials obtained by particle size fraction used for both shaping and sintering regimes.

Fig. 5 is depicted by changes in grain hardness powder materials used for both forming and sintering regimes.
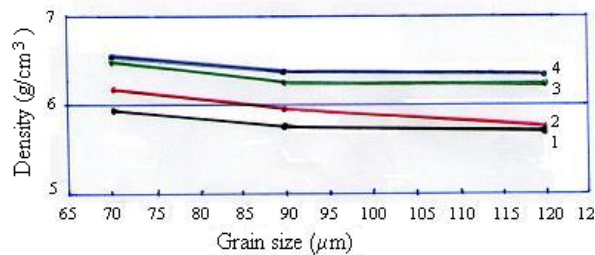
Fig. 4 – Changes in density of materials sintered at 830°C (R1) and 860°C (R2) of the spherical bronze powders CuSn10P1by granulation: 1 - loosely, R1; 2 - with compaction, R1; 3 – loosely, R2; 4 - with compaction, R2.
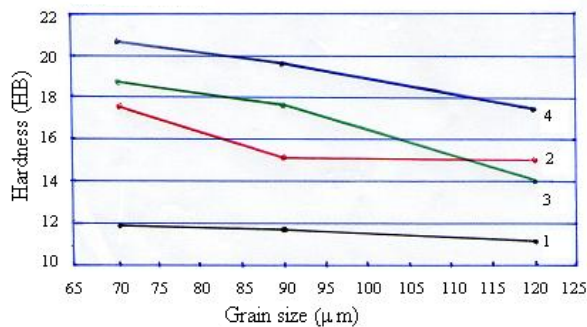
Fig. 5 – Changes in material hardness sintered at 830°C (R1) and 86°C (R2) of the spherical bronze powders by granulation CuSn10P1: 1 - loosely, R1; 2 - with compaction, R1; 3 - loosely, R2; 4 - with compaction, R2.

3. Conclusion

Following research for obtaining a sintered filter material that meets the requirements initially, as raw material should be made of spherical particles with smooth surfaces, with a grain size fraction in a range of values restricted and in which the ratio of large particle size and the smallest should be in the range $0.5 \div 0.1$.

Shaping method chosen should be such as to ensure a degree of arrangement of particles as evenly as to be able to control the porosity of the material. In this regard shaping by the free shedding of powder in the form, followed by its vibration, is most effective and economic method.

Sintering material is done in conjunction with the shaping mold, the atmosphere and temperature to ensure that only the achievement gaps between particles without spheroidization and closing pore.

Increasing sintering temperature to 830°C to 860°C of condos in obtaining material density and hardness greater. For the same degree of sintering, the density and hardness increases with decreasing particle size fraction. In this case the particle size fraction is that which dictates the degree of sintering of the material. If fractions are finer particle size, density and hardness values are higher. For sintered materials the shaping is conducted without vibration, density and hardness are lower than its use with vibration shaping.

REFERENCES

Dima A., *et. al*., *Experimental Researches Concerning the Procurement and Characterization of Some Sintered Metallic Materials Based On Copper*. Tehnologii şi Materiale Avansate, **2**, Galaţi, 2007.

Vida-Simiti I., Magyarosy I., *Materiale poroase permeabile sinterizate*. Editura "OID – ICM", Bucureşti, 1992.

Vida-Simiti I., *Materiale permeabile sinterizate*. Editura Casa Cărţii de Ştiinţă, Cluj-Napoca, 1998.

Vida-Simiti I., *Proprietăţi tehnologice în metalurgia pulberilor*. Editura Enciclopedică, Bucureşti, 1994.

CERCETĂRI PRIVIND OBŢINEREA ŞI CARACTERIZAREA UNOR MATERIALE POROASE PERMEABILE SINTERIZATE DIN PULBERI DE BRONZ PENTRU ELEMENTE FILTRANTE CU POROZITATE DE 25%

I. OBŢINEREA MATERIALELOR ŞI DETERMINAREA UNOR CARACTERISTICI

(Rezumat)

Articolul abordează aspecte privind alegerea, pregătirea şi proprietăţile pulberilor de bronz CuSn10P1 utilizate la obţinerea de materiale poroase permeabile destinate realizării unor elemente filtrante cu porozitate de 25%. Au fost efectuate experimentări de formare şi sinterizare utilizând regimuri de lucru diferite şi s-au determinat unele caracteristici ale acestor materiale (densitatea şi duritatea după sinterizare) analizându-se modul lor de variaţie.

RESEARCHES CONCERNING THE PROCUREMENT AND CHARACTERIZATION OF SOME PERMEABLE POROUS SINTERED MATERIALS OF BRONZE POWDERS FOR FILTERING ELEMENTS BY 25% POROSITY

II: DETERMINATION POROSITY AND CHARACTERIZATION MICROSTRUCTURES MATERIALS

BY

OVIDIU CALANCIA* and VASILE CAŢARSCHI

"Gheorghe Asachi" Technical University of Iaşi

Abstract. This article continues research on permeable porous materials sintered bronze spherical powder CuSn10P1 obtained in Part I of the paper. Was used to determine the values of average pore size and porosity, and microscopic examination of these materials.

Key words: filtering material, porosity, average pore dimension, microstructure.

1. Introduction

In paper (Calancia *et al.*, 2011) were made permeable porous sintered material samples which were used three types of spherical bronze powder fractions (CuSn10P1): $200 \div 120$ m fraction FBz1 codified, $120 \div 90$ m

---

* Correspondind author e-mail: calacea_ovidiu_is@yahoo.com

fraction codified FBz2 and fraction 90 ÷ 71 m FBz3 codified. Operation of powders formation in these fractions was performed by free pouring in forms without vibrating (coding samples made in this case was: FBz1, FBz2 and FBz3) and vibrating for 30 minutes (the encoding used was: FBz1.1, FBz2.1 and FBz3.1). Powders these granulometric fractions formed with and without vibration were the raw material for sintered porous permeable materials that were used two variants of these working conditions.

So were a number of materials obtained by sintering at a temperature of 830°C with a tape speed of 2 m/h (encoding material was: 1FBz1, 1FBz2, 1FBz3, 1FBz1.1, 1FBz2.1 and 1FBz3.1) and a second series of the sintering temperature of 860°C with a tape speed of 3 m/h (encoding material was: 2FBz1, 2FBz2, 2FBz3, 2FBz1.1, 2FBz2.1 and 2FBz3.1). For all these types of densities and hardness were determined after sintering (Calancia *et al*., 2011).

2. Determinations, Analysis and Results

Samples of porous materials obtained by sintering porous bronze spherical powder (CuSn10P1) were used for determination of values of characteristics and microscopic analysis necessary porosity characterization and structure. To this end were made:
      - determinations of average pore dimension and porosity;
      - microscopic examinations for structural analysis.

2.1. Determinations of Porosity and Average Pore Dimension

Porosity determination by calculation was made, but also visually by micrographic examination. To determine the porosity relationship was used:

$$P = (1 - \rho_{sint} / \rho_m) \ (\%)$$

that:

ρ_{sint} - density porous material;
ρ_m - density compact material (ρ_m = 8.79 g/cm^3) (Vida-Simiti, 1997).

For each type of material were measured by a micrographic field 100 pores. Average pore dimension of the arithmetic mean of 100 measurements.
The values of these features are presented in Table 1.

Table 1
Physico-Mechanical Properties of Sintered Materials

Cod of material	Density sintered material, ρ_{sint} [g/cm³]	Hardness sintered material, HB_{sint}	Porosity sintered material, P [%]	Average pore dimension, D_{pore} [m]	Remarks
R1FBz1 R1FBz2 R1FBz3	5,68 5,71 5,92	11,2 11,7 11,9	35,41 35,07 32,68	50,3 39,3 17,0	Without vibration shaping and sintering at 830°C
R1FBz1.1 R1FBz2.1 R1FBz31	5,73 5,95 6,16	15,0 15,1 17,5	34,84 32,50 29,95	45,0 29,0 16,5	With vibration shaping and sintering at 830°C
R2FBz1 R2FBz2 R2FBz3	6,19 6,19 6,48	14,0 17,6 18,7	29,61 29,61 26,31	50,0 32,0 15,0	Without vibration shaping and sintering at 860°C
R2FBz1.1 R2FBz2.1 R2FBz3.1	6,33 6,36 6,53	17,4 19,6 20,6	28,02 27,68 25,75	42,0 27,0 13,5	With vibration shaping and sintering at 860°C

2.2. Microscopic Examinations for Characterization Microstructure

Microstructural characterization of materials was done by examining scanning electron microscope (Dima *et. al*., 2007.

Fig. 1 presents R1FBz1 picture (free shed in shape and sintered at temperature of 830°C), which highlights the arrangement of granule powder. There is a random arrangement of grains, which led to obtain, after sintering of large pores (D_{pore} = 50 m), intercommunicate and unevenly distributed. This is because the arrangement of particles in the direction of more stable employment places the powder mass, is made as a result of the free flow of powder in the form under the influence of weight and the fact that powders particles do not have 100% of spherical particles.

Fig. 2 represents R1FBz2 picture material, obtained in the shaping and sintering (open shed in the form and sintered at temperature of 830°C).

There is a more uniform distribution of particles due to particle size fraction is used in a range closer to the first case and the same arrangement of randomly shaped grains. Lower porosity of this material is also due to better sintering.
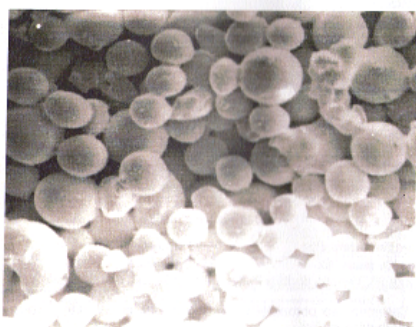
Fig. 1 – R1FBz1 picture material, x100.   Fig. 2 – R1FBz2 picture material, x100.

R1FBz3 material obtained from the formation and sintering of the finer fraction, present in the structure (Fig. 3) a higher degree of ordering of the granules from other materials. In terms of porosity, there is a decrease of total porosity, which is due to the intense sintering.

Figs. 4, 5 and 6 are presented pictures of the materials obtained from the three types of particle size fractions under conditions of free pouring in forms and vibrating tamped 30 minutes.

Fig. 3 − R1FBz3 picture material, x100.   Fig. 4 − R1FBz1.1 picture material, x100.
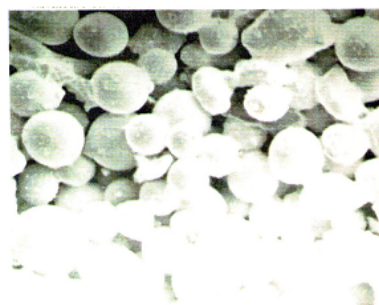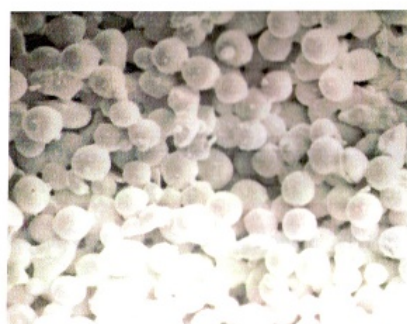
Fig. 5 − R1FBz2.1 picture material, x100.   Fig. 6 − R1FBz3.1 picture material, x100.
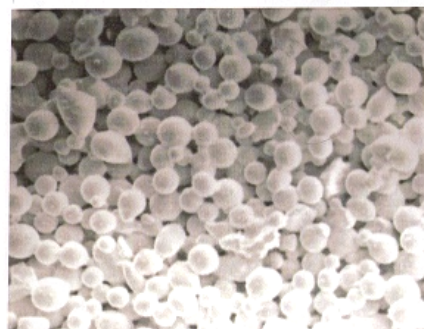
Analysis of these images reveals that stratification on dimensions is obtained by vibrating, which depends on the size fraction range of particle size and particle size distribution during this range.

There is not much difference between the porosity of the material in a state that paid tamped free vibration, because there was an actual movement of particles due to wave vibrator, it will only contribute to the emergence of a vibration around the equilibrium, which favored only the finest grain segregation. To enable the movement of particles so that they ultimately provide a potential energy minimum, with their orderly arrangement requires that the vibratory wave energy is high enough.

Increasing the sintering temperature of 830°C to 860°C led, as shown in Figs. 7,...,9 at a higher sintering material to obtain higher densities and smaller porositys. Also observed the appearance of pores is closed and isolated, in fact undesirable for obtaining porous filters.

Fig. 7 – R2FBz1 picture
material, x100.

Fig. 8 – R2FBz2 picture
material, x100.
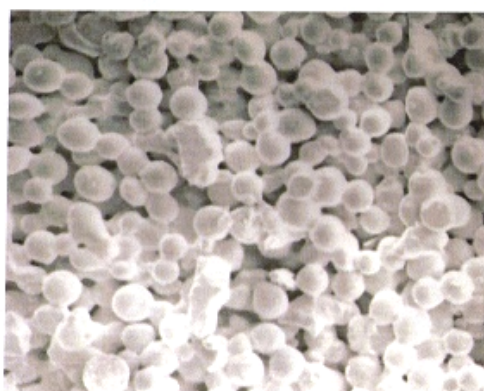
Fig. 9 – R2FBz3 picture material, x100.

Figs. 10,…,12 are presented pictures of the three types of shaping materials under vibration and sintering temperatures of 860°C.
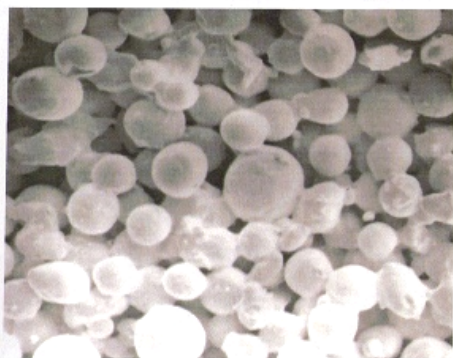
Fig. 10 – R2FBz1.1 picture
material, x100.
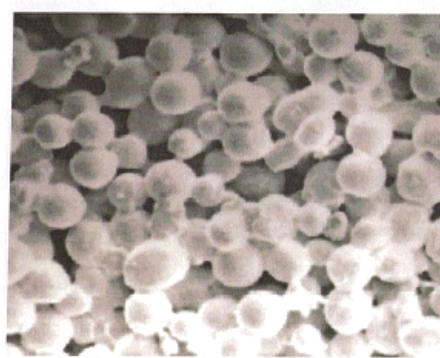
Fig. 11 – R2FBz2.1 picture
material, x100.
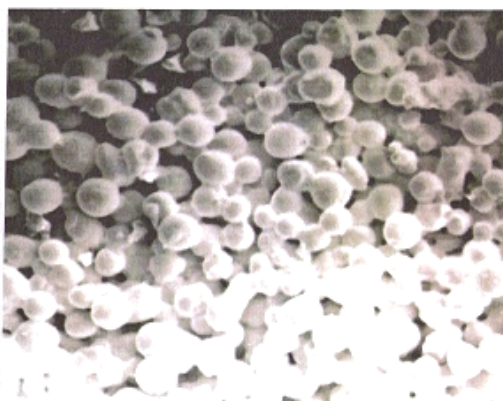
Fig. 12 – R2FBz3.1 picture material, x100.

He found a greater degree of sintering average pore dimension decreases with development in the more confined and isolated pores and total porosity of the material decreases.

3. Conclusion

To adjust the porosity of permeable porous sintered materials is necessary choosing the right shaping method to achieve an overall arrangement as uniform. In this shaping through free shedding of powder in the form, followed by its vibration is most effective method.

The materials obtained by sintering at a temperature of 830°C powders formed without vibrating structure presents a random arrangement of granules (where the largest fraction) whose degree of ordering improves the increasing fineness fractions. The pores are unevenly distributed and intercommunicate. Lower average pore dimensions from 50 m to 17 m, and porosity ranges from 35.4 m to 32.7 m with increasing fineness fractions.

For the same sintering temperature of 830°C formed with vibrating particulate materials are produced and stacked on particle size is found not much difference between them and the porosity of the materials formed without vibration.

Increasing sintering temperature to 830°C to 860°C led to a higher sintering materials to obtain higher densities and smaller pores (with the same differences of values depending on how the shaping formation).

Using permeable porous sintered metal filter is recommended for fine filter (filter fineness should be less than 25 m) and filters that use thin filter elements.

REFERENCES

Calancia Ov., Caţarschi V., Toma Şt. L.: *Researches Concerning the Procurement and Characterization of Some Permeable Porous Sintered Materials of Bronze Powders for Filtering Elements by 25% Porosity. Part I: Obtaining Materials and Determination of Some Characteristics.* Bul. Inst. Politehnic Iaşi, s. Secţia Ştiinţa şi Ingineria Materialelor, **LVII (LXI)**, 2011.

Dima A., *et. al.*, *Experimental Researches Concerning the Procurement and Characterization of Some Sintered Metallic Materials Based on Copper.* Tehnologii şi Materiale Avansate, **2**, Galaţi, 2007.

Vida-Simiti I., *Cercetări asupra unor caracteristici ale structurilor permeabile poroase din pulberi sinterizate.* Construcţia de Maşini, Bucureşti, 1997.

CERCETĂRI PRIVIND OBŢINEREA UNOR MATERIALE POROASE PERMEABILE PRIN SINTERIZAREA PULBERILOR DE BRONZ PENTRU ELEMENTE FILTRANTE CU POROZITATE DE 25%

II: DETERMINAREA POROZITĂŢII ŞI CARACTERIZAREA MICROSTRUCTURALĂ A MATERIALELOR

(Rezumat)

Prezentul articol continuă cercetările asupra materialelor permeabile poroase sinterizate din pulberi sferice de bronz CuSn10P1 obţinute în partea I a lucrării. Au fost

efectuate determinări ale valorilor porozităţilor şi dimensiunilor medii ale porilor, precum şi examinări microscopice ale acestor materiale.

INFLUENCE OF NONFERROUS ALLOY THERMAL RECYCLING ON WORK ENVIRONMENT

BY

GABRIELA CĂLDĂRESCU and **GEORGE TANASIEVICI**

Territorial Labour Inspectorate of Iaşi,

Abstract. Within the current context, when the decreased raw material consumption represents a global issue, the recycling concept has registered an emphasized development, and nonferrous alloys, especially the copper and aluminium ones, occupy an important part. This paper includes several positive aspects, characteristic to this concept, as well as the negative influence of their thermal recycling on work environment.

Key words: thermal recycling, nonferrous alloys, work environment quality.

1. Introduction

Current studies worldwide show that the progress achieved in science and technique, from all economic branches, has generated the use of important quantities of raw material and energy, resources that are limited. Nonferrous metal materials, especially copper, aluminium and their alloys, are raw materials which are the most frequently used, and researches are developed worldwide, based on economic efficiency criteria, in order to increase these quantities of raw materials, which are necessary for technological development.

---

* Corresponding author e-mail: gabriela.caldarescu@expertssm.ro

Researches accomplished all around the world show that this raw material increase is achievable by means of a modern concept named RECYCLING.

Recycling is a waste management concept and it generally prevents the loss of some potentially useful materials, reduces the raw material consumption, and reduces the energy consumption.

The causes that have generated the practice of material recycling have been mainly of economic nature, including the following recyclable materials worldwide: glass, paper, ferrous metal materials, nonferrous metal materials (copper and aluminium alloys, etc.), textiles, plastics, etc., and they may come from a wide range of industrial or domestic sources.

There is an irregular and constantly decreasing distribution of global reserves of copper and bauxite ores, which makes the recycling of copper and aluminium alloys, in view of their valorisation, even more important.

Copper is the most recyclable metal used in engineering applications, copper and copper-based alloys being reused for hundreds of years. Due to its aspect, copper is known as the "red metal", but it may equally be defined as a "green metal", being a lasting, easily remeltable or refinable metal, economically recyclable by means of non-polluting technologies (Applying and Valorizing Technologies of Metal Wastes, 2008).

Beside copper, the extended use, for the last 25 years, of aluminium and its alloy in the fields of machine manufacturing, civil and industrial engineering, packing, electricity, low-voltage technical equipment, has generated an increased quantity of aluminium and aluminium-based wastes.

A special branch of metallurgy and industry has thus been developed, named the secondary aluminium industry or the aluminium waste recycling industry.

2. Observations on Thermal Recycling of Copper and Copper-Based Alloys

Copper may be considered a 100% recyclable element and, theoretically, all products made of copper and copper-based alloys maybe recycled an operation that implies no loss or transformation of chemical and physical properties.

Approximately 40% of the global production of copper and copper-based products is obtained of wastes, and, for some products, the percentage exceeds 90%.

Wastes of copper and copper alloys (brass, bronze, etc.) are collected in various forms, from various sources and they may be classified as follows:

a. by their copper content (copper, brass, bronze wastes);

b. by their aspect (bars, threads, mixtures of massive and light wastes);

c. by their creation process (casting, lamination, forging, metal cutting etc.);

d. by their sources (electronic and electric wastes, car industry wastes, building wastes etc.);

e. by their destination (refining, melting);

f. by the service time of the material or of the product that generates or turns into wastes (old wastes, new wastes).

An important part in wastes classification is played by the chemical structure too, as copper wastes are divided in two main categories:

I.   highly pure, unalloyed, uncovered copper wastes;

II.   oxidized or covered wastes.

According to the criteria established at Davenport in 1986, according to their processing method and their quality, copper wastes may be classified in four groups:

1. *wastes of inferior category, with a variable chemical structure (between 10 - 95% Cu).*

These wastes are melted in furnaces with shafts or floors and then thermally or electrolytically refined. They may also be introduced in Peirce Smith converters after primary elaboration;

2. *wastes of alloys consisting mainly of brasses, bronzes, Cu-Ni alloys, deriving from new or old wastes.*

They may not be processed by refining in order to obtain pure copper, being directly melted in furnaces with reverberation or induction and then cast as half-finished or unfinished parts. Sometimes, they are subject to oxidizing refining operations, for the removal of aluminium, silicon and iron from the scale. In this case, the oxidizing process must be controlled very well since there is the tendency of oxidizing the copper and other useful elements at the same time (Zn from brasses and Sn from bronzes);

3. *most wastes, new or old, are mainly made of copper, but which is unpurified by other elements (such as some metals used for plating, welding, bonding).*

These wastes are melted in Pierce-Smith converters since primary elaboration or in furnaces for anodes, specific to primary or secondary refinery, when significant quantities of impurities (Al, Fe, Zn, Si, Sn) are eliminated by oxidizing. The obtained metal is afterwards cast as anodes for electrolytic refinery. It may be delivered as thermally refined copper, used to obtain alloys;

4. *wastes having the quality of cathode copper, which is merely melted and cast.* These wastes are mainly generated from processing operations (scraps of bars, wires, cast parts). They are melted and cast as blocks of copper or alloys and cast and brasses or bronzes.

In Romania, copper wastes are characterized according to standard SR EN 12861 from September 2001, which is identical to the European standard EN 12861:1999 adopted by ECS (European Committee for Standardization).

According to this standard, secondary materials and nonferrous wastes are classified by categories, groups and sorts:

Categories (established based on the chemical structure):

➢ secondary materials and wastes of copper, briefly Cu;

➤ secondary materials and wastes of copper-zinc, CuZn;
➤ secondary materials and wastes of copper alloys with tin, CuSn;
➤ secondary materials and wastes of copper alloys with aluminium, CuAl;
➤ secondary materials and wastes of copper alloys with lead, CuPb;
➤ secondary materials and wastes of copper-nickel-zinc alloys, CuNiZn;

Groups (established by forms and sizes):
➤ group B, secondary materials and wastes in pieces;
➤ group S, facings;
➤ group Ox, oxides, ashes, breezes, grounds and slams;
➤ group C, cables leads with insulation;
➤ group D, other old nonferrous wastes and metals.

Copper wires

Matrix wastes

Eends of flat half-finished goods

Copper/brass radiators

Coppers pipes

Big scraps and processing wastes

Copper plate ends

Massive copper pieces

Fittings

Cuttings, stamping, cutting, perforating scraps

Fig. 1 – Examples of copper and copper alloys wastes.

Copper wastes (secondary copper) valorisation is achieved based on the contamination degree, included in various quality groups, and it requires specific processing operations. The secondary copper obtaining flows consists in the succession of the following stages:

- preparation of wastes;
- actual elaboration (melting, converting, refining, alloying);
- processing by casting, deformation etc.

The smelting and refining techniques of copper wastes differ according to their content or the lack of accompanying elements. Recycling is achieved in various flows that may include only one processing operation (for example: simple melting) or they may include a series of complex metallurgic operations.

Technologies consisting of several operations are based on physical and chemical processes which are developed successively or simultaneously. The latter, as well as the aggregates specific to copper waste processing must be correlated to the type of materials used as bulk, especially to the chemical structure of wastes (copper content, impurity degree or alloying degree) and the destination of the elaborated metal or alloy.

The elaboration stages for secondary copper and copper-based alloys, as well as the specific thermal aggregates which form a waste recycling flow are dictated by the quality and the quantity of wastes.

The melting operation and the thermal refinery require specific melting equipment's of great capacity or furnaces with shafts (the cupola furnace type). They are completely different from the ones used for the direct melting of wastes.

Stationary furnaces are the most frequently used because they have big processing capacities, but rotary furnaces are more flexible.

Crucible furnaces, stationary or swinging, electric or gas fuelled, are used to obtain small quantities of special alloys.

Induced electric furnaces are more widely spread in foundries of special alloy parts or blocks.

Reverberated or rotary furnaces for thermal refinery may be used to melt wastes belonging to quality classes No. 1 and No. 2, following stages that are similar to the process in the furnaces making anodes for primary copper metallurgy (Buzatu M. & Buzatu R., 1994).

3. Observations on Thermal Recycling of Aluminium and Aluminium-Based Alloys

Beside copper, aluminium belongs to the category of 100% recyclable nonferrous metal materials and its recycling is preferred to the production of primary aluminium, from both an economic and an ecologic perspective. Statistics and analyses worldwide show that, annually, the total consumption of aluminium registered an average increase by 3% as follows: 2.7% of the

primary aluminium production and 4% of the secondary aluminium one, and, as the aluminium recycling rate is progressively increasing, an approximate 25% increase may be noticed by 2005.

The recycling capacity depends on the service time of aluminium products, which may vary: from several months for the packing and printing segments, 10–12 years for cast car parts, to more than 30-40 years for buildings and electric power.
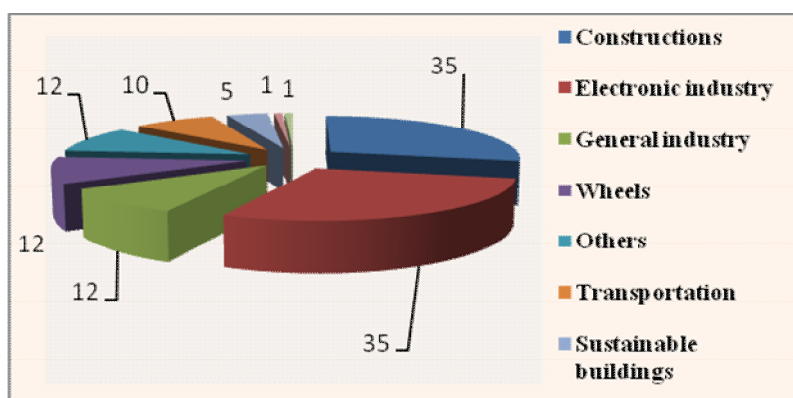
Fig. 2 – Service time assessment for aluminium products by categories at the level of year 2005.

Waste source	1996		2010	
	Collecting capacity	Recycling capacity	(Estimated) Collecting capacity	(Estimated) Recycling capacity
Transport	92	74	98	78
Wheels	81	65	98	78
Constructions	70	56	86	69
Packages	33	28	49	42
Printing	95	85	95	85
General engineering	30	26	42	36
Electric engineering	60	54	64	58
Sustainable consumptions	26	22	37	31
Others	25	21	40	34
Average	57	48	68	57

The combination of the two parameters, the service time and the recycling capacity, expresses the aluminium recycling rate, which is estimated to have a substantial annual increase. Therefore, at the level of year 2010, the

recycled aluminium quantity reached approximately 3.2 million, compared to the level of year 1996, when it was of about 1.7 millions.

In Europe, collecting and recycling capacities for aluminium wastes, expressed in %, reach a high recycling degree, of approximately: 41% for beverage packages, 85% in constructions and 95% in transport.

Just as the wastes containing copper, the aluminium ones are classified according to certain classifying criteria:

I.   by the source of origin:
- transports (aluminium components for cars, trains, planes etc.);
- constructions (window carpentry, wall frames, facades etc.);
- packages (sheets, beverage packages, aerosols, drugs etc.);
- mechanical engineering (aluminium components for cars and equipment's);
- electric engineering, (aluminium wires etc.);
- domestic devices (aluminium cups, dishes, cooking pans etc.).

II.   by their structure and processing method:
- pure aluminium;
- deformed alloys;
- cast alloys.

III.   By the degree of combination with other materials:
- Without combination (pure aluminium);
- With poor combination (aluminium may be easily separated from wastes by dismantling and very slight crushing);
- With medium combination;
- With strong combination (aluminium is difficult to separate from wastes, the separation is achieved only following intense crumbling or thermal processing);
- With total combination (aluminium cannot be separated from mixtures of materials).

IV.   By size and shape of wastes:
- Dense, massive wastes;
- Thin, small wastes.

In the case of cast alloys, the main alloying elements are: silicon, copper and magnesium, which reach a concentration of approximately 12%.

The main alloying elements of deformed alloys are magnesium, manganese and silicon, their concentration varying between 2–2.5%. According to ASTM specifications, the most frequently used aluminium (Al6061) includes the following elements: copper (0.15–0.6%), magnesium (0.8–1.2%), silicon (0.4–0.8%), zinc (<0.25%) and iron (<0.7%) (Buzatu M. & Buzatu R., 1994).

The aluminium meant for recycling may be separated in two categories, as follows:

I. new wastes;

II. old wastes.

According to the Romanian standard, the aluminium wastes classification includes several categories, groups and sorts. Based on the chemical structure, the following categories have been established:

a. category of technical aluminium wastes;

category of aluminium alloy wastes (AlA).

Each category includes 4 (four) groups:

1. groups of wastes in lumps, with the symbol of <u>letter B</u>, which includes laminated or extruded aluminium wastes, cast aluminium and mixed wastes;

2. group of wastes as chips, facings, scrapings, symbolized by the <u>letter S</u>;

3. groups of wastes in the form of cables and conductors, symbolized by the <u>letter C</u> (for technical aluminium wastes);

4. group of wastes in the form of ashes and breezes, symbolized by the <u>letter Ox</u> (for aluminium alloy wastes).

4. Observations on the Influence of Thermal Recycling on the Work Environment

The <u>work environment</u> is a crucial element of the work system and it represents the result of the interferences among its other 3 elements – working means, working assignment and executor.

Air pollution is an issue for both the outside and the inside of buildings, which forms the work environment, the ambient where the executor performs his activity. this may directly or indirectly influence, on the one hand, the physical environment of the work place, the lightning, the microclimate (temperature, humidity, air currents), noise, vibrations, radiations, air purity, and, on the other hand, the social environment by the induction of certain indirect psychosocial risks.

The negative effects on the work environment are manifested by the accumulation of toxic substances, and the contamination with hazardous chemical substances takes place due to: air emissions (dust, smoke, frog, vapours etc.), their inappropriate discharge or the incorrect storage of wastes.

The choice of optimal technological solutions must consider the fact that they are themselves raw-material and energy consuming, they generate wastes and they have negative effects on the environment.

Moreover, the valorisation of aluminium wastes presents a set of technical and economic barriers, especially in the case of wastes coming from mixed flows, since it implies supplementary preparing operations for the removal of contaminants. The increased quantity of recycled aluminium is due to the separating skills of the aluminium components existing in waste mixtures.

5. Conclusion

The evaluation of the impact that the thermal recycling of nonferrous metal materials has on the work environment is important for the protection of human security and health, and the permanent improvement of working methods, of technological processes may render this complex process more accessible, more effective and more efficient.

The set of relations and exchanging rates established between a man and his work environments, as well as their interdependence influence the equilibrium at work, generate the working conditions, as well as the perspectives for society development as a whole.

International authorities with competences in the protection of labour security and health are concerned with the increased pollution in the work environment and therefore sanction, by means of laws and directives; but we believe that an important part is played by engineers and technologists who may find, by studies and analyses, technical solutions to issues related to the negative influences that thermal recycling of nonferrous metal alloys has on the work environment.

NU SE REGASESTE IN TEXT TOATA BIBLIOGRAFIA

REFERENCES

[1]. * * Tehnologii de aplicare şi valorificare a deşeurilor metalice (*Applying and valorizing technologies of metal wastes*) Editura Didactică şi pedagogică, Bucharest, 2008.
[2]. Buzatu M., Buzatu R., *Metale şi materiale secundare.* (*Metals and secondary materials*), Editura Universităţii Politehnica, Bucharest, 1994.
[3]. * * *A Strategy for Developing Recycling Markets in Ireland. Market development 2001.* www.epa-ie/r-d/Products/Aluminium.pdf
[4] * * *European Aluminium Association Aluminium the Material: Recycled Aluminium 2001*, www.eaa.net
[5]. Chandler R., *Metal Bulletin's 9th International Secondary Conference.* 7-9 November 2001, Prague.
[6]. * * *Aluminium in February 2002.* Mineral Industry Surveys, April 2002.
[7]. Hobert H., Wolf S., *Recycling of Aluminium and the Effect on Sustainable Development.*
[8]. Wernick I., Themelis N.J., *Annual Reviews Energy and Environment.* **23**, 1998.
[9]. Bumbu I., *Reciclarea, tratarea şi depozitarea deşeurilor solide.* (*Recycling, Treatment and Storage of Solid Wastes*), Technological Univ. of Moldova. Faculty of Urbanism and Architecture. Department of Ecotechnics, Ecologic Management and Water Engineering, Chişinău, 2007.

INFUIENŢA RECICLĂRII TERMICE A ALIAJELOR NEFEROASE ASUPRA MEDIULUI DE MUNCĂ

(Rezumat)

În contextul actual când reducerea consumului de materii prime constituie o problemă mondială, conceptul de reciclare a cunoscut o dezvoltare puternică, iar aliajele neferoase, cu precădere cele din cupru şi aluminiu, ocupă un rol important. În această lucrare sunt prezentate câteva aspecte pozitive, caracteristice acestui concept, dar şi influenţa negativă a reciclării termice a acestora asupra mediului de muncă.

[1]. (Applying and Valorizing Technologies of Metal Wastes, 2008)
[2]. (Buzatu & Buzatu, 1994)
[3]. (www.epa-ie/r-d)
[4] (www.eaa.net)
[5]. (Chandler, 2001)
[6]. (Aluminium in February 2002)
[7]. (Hobert & Wolf)
[8]. (Wernick & Themelis, 1998)
[9]. (Bumbu, 2007)

THE INTELLIGENT FLEXIBLE SYSTEM FOR THERMAL PROCESSING OF STEELS SUSCEPTIBLE TO CRACKING (I)

BY

**VASILE CAŢARSCHI[1]*, OVIDIU CALANCIA[1]
and SMARANDA CAŢARSCHI[2]**

[1] "Gheorghe Asachi" Technical University of Iaşi,
[2] "Anghel Saligny" Vocational Group of Iassy

Abstract. The work with the theme The intelligent flexible system for thermal processing (IFSTP) of steels susceptible to cracking has in view the development of the knowledge in the metallurgic field of research, like that of the plastic deformations and heat treatments. The intelligent flexible systems for thermal processing of metallic materials belong to the sistem of assisted and controlled controlling of the thermal processes from the plastic deformation and heat treatment sector. This represents an important branch of the systems with artificial intelligence that are used in both controlling the production processes and operations of prediction for the physical and mechanical properties of the materials, depending on necessities.

From the applicative point of view, the original contributions of the researches aim: 1) the development of certain intelligent fexible systems of thermal processing of steels, which can play role both of control (detection and adjustment of certain prescribed accuate) and execution (drive, by means of automation hardware modules), able to interupt/start, for instance complex thermal-electrical systems and installations, in view ofachieving certain thermal processes etc. and 2) of accomplishing industrial thermal processes with a superior quality and with 30% less energetical consumptions in improved ecological conditions.

Key words: flexible system, echo technologies, software instruments, thermal processing.

---

* Corresponding author e-mail: vcatar@yahoo.com

1. Theoretical Issues

The Intelligent Flexible Systems for Thermal Processing (IFSTP) of Steels Susceptible to Cracking in stationary/nonstationary system allow the study of steels subject to various thermal systems in view to modify their shape by plastic deformations and their properties by thermal treatments, based on three major components (Fig. 1):

- (1) study of the thermal processing technology and range of steels to be used;

- (2) modelling of the thermal processing technology and issue of related software with proper informatics equipment;

- (3) implementation of the software on the equipment of techological execution and quality check of the products achieved.

The research chart of an *intelligent flexible system for the thermal processing of steels* (SFIPT) can be represented as follows:
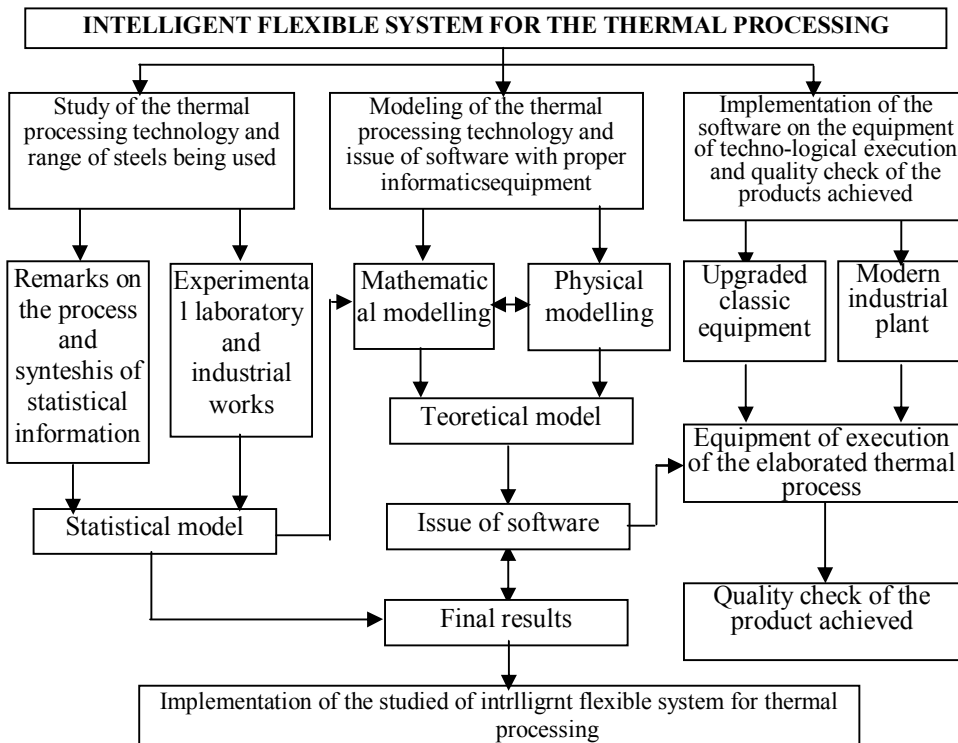
Fig. 1 – The research chart of an intelligent flexible system
for the thermal processing of steels.

Concerning component (1), the thermal processing techology needs the engineering for the metal heating, holding and cooling.

In first stage, the steels are heated either for plastic deformation or for heat treatments. Heating can be applied to blanks having as initial state: (1*) cold, (2*) warm and (3*) hot (between the forging operations). The definition of the initial and final temperatures, conditions of thermal transfer and conditions of final checking is a must.

Within component (2), the mathematic modelling of the heating process of a steel blank in an industrial furnace, it is based on the variation of the temperature with time, by the Fourier's thermal conductivity differential (including time and Maxwell's thermal conductivity coefficient), particularized in relation with the geometrical shape of the metal and expressed in spherical, cyllindrical or carthesian coordinates. In Europe, the methodology given by Heiligenstaedt which introduces strings of infinite sums of certain trigonometric functions to resolve the problem has been very much extended *(the case of flat plates)*. In case of the *infinite length cyllinder*, Bessel functions are used, which acts asperiodical trigonometric functions with decreasing amplitude (J_0, J_1, J_2). The temperatures of the material are expressed by strings of infinite sums of Bessel-Fourier functions and Biot criterion, taking into consideration the thermal and physical characteristics of the metal and coefficient of heat exchange. Equations for the surface and core temperature are established as well as for any other curve within the thermal field located between the surface and core of the blank. The survey and limitation of the thermal stresses exclude the risk of cracking when heating for forging or distortion during the heat treatment. In accordance with the modeling achieved, the software through which all parameters of the flexible system are established is issued. Such aspects are being detailed in the referential papers.

Within component (3) equipment of technological execution are included (furnaces, installations etc) which must be flexible, provide good leveling of the temperature within all working area of the furnace, provide most efficient use of the heat, minimal heat losses etc. Such equipment must be able to achieve both technically and quality wise the implementation of the software resulted from the study of the two first components. This is done either by controlling the heating equipment by means of a process computer or computerized modules or inserting the heating charts needed to the technological process in the modernized programmer of the thermal equipment.

World wide, the development *of the intelligent flexible systems for thermal processing* (technology-software/hardware-production equipment), started from the Pacific area (USA, Japan, China, Taiwan) has gradually extended all over the world, both in the research laboratories of the trans-

national companies (General Electrics, Boeing, Texas Instruments or General Motors) and in the national research laboratories (for instance National Institute of Materials Science in Japan, Bariloche Atomic Center in Argentina, Institute for Materials in London, Chinese Society for metals in Beijing, National Institute of Technology in India) or affiliated to certain universities (such as Department of Metal Engineering from the Swansea University in Wales). At the time being, the indisputable of the research in *intelligent flexible systems for thermal processing* is *the Special Research Center for Steels* in Japan, within the National Institute of Materials Science, where blanks of various sizes are heat treated and castings can reach 200, 400 even 600 tons. In the related literature various *intelligent flexible systems for thermal transfer* (or some components of them) can be found, developed by:

- *Massachusetts Institute of Technology* – U.S.A. within the Institute of New and Advanced Materials;

- *California Institute of Technology*- U.S.A. within the Department of Materials Science – *Boeing Concern*

- *Organisme National de Recherches en Aéronautique* (ONERA) – France; *Aerospatiale concern* – France

- *Eurocopter Concern* – European Union etc.

In Romania, together with the development of the investigation, control and automation methods for thermal processes, methods of computer designed and computer assisted control have been also developed for technologies of heating and heat treatment for various steel products. Thus, components (1), (2) and (3) above mentioned, of certain *intelligent flexible systems for thermal processing,* have been generally treated separately in many specialty papers and less as an unitary system.

Within the last five years, the interest of introducing in the Romanian industry of certain *intelligent flexible systems for thermal processing, of steel blanks* is first of all of scientific nature and then of experimental and applicable character. Theoretical and experimental research in this field has been completed by researchers from the Bucharest Polytechnic University, Timisoara Technical University (with departments of Hunedoara), Low Danube University of Galati and Technical University of Cluj Napoca. At the Gheorghe Asachi Technical University of Iasi, the research based on analytic calculations and experimental tests of heating of solid steel blanks, got extended within the last five years, with applications at S.C. FORTUS S.A. Iasi and got continuously improved as they have significant effect on the economic state of the company and on the stability of the labor force.

Further, the condition of the hot processing *intelligent flexible systems* within the last ten years both in Romania and advanced countries, with concrete reference to some periodicals from the attached reference list is

presented:

In paper (Altan *et al.*, 2004), there are presented elements of the *intelligent flexible systems* of thermal transfer used within certain advanced forging technologies. There are analyzed the basic elements where modeling of the thermal processes in steel starts from, using several simplifying hypotheses. There are analyzed the plasticity properties of carbon and alloy steels and the thermal and physical characteristics are regarded as constant with temperature. The heating curves are particularized on steel grades. The paperwork can be used in *designing the advanced intelligent flexible systems*. In similar circumstances are determined the IFSTP components, for the steel bloks in heating conditions for forjing, in paper (Catarschi, 2003).

In (Ramsay, 1995), *the intelligent flexible systems being approached* are totally integrated (heat treatment installations controlled by computerized modules). The transformations occurring in steels at ferrite and perlite level for heat treatments of full quenching and annealing are studied. There are presented the ranges of the heating temperatures as per the Fe-C diagram, the importance of the heat treatments, structures obtained by researches conducted at Iron and Steel Society, University of Missouri – Rolla. There are mentioned the thermal stresses being present as well the importance of their reduction and elimination.

Paper (Roman, 1991) is a monograph of the *intelligent flexible systems* concerning the first two components and includes the issues regarding the conversion of the mathematical models in software in various programming languages, out of which C language is largely discussed. Specialists with informatics skills can use the paper. Various ways of resolving linear and non-linear equations are presented as well as for the Bessel functions of rank zero (J_o), one (J_1) and (J_2) etc. out of the numerical methods of resolving, both the method of finished differences (MDF) and of finished elements (MEF) are presented.

In paper (Ilegbusi Olisegun Jensen *et al.*, 1999), the problems of the *intelligent flexible systems* for the heat and mass transfer in metals and metal alloys are designed for mathematicians, physicists, mechanical and metallurgical engineers. For thermal transfers, the following are used as numerical techniques: linear and non-linear equations, approximate functions, numerical integration's, ordinary differentials, partial differentials, method of finished differences, method of finished elements, method of Boundary integration etc. also, there are presented the methods of implementation and verification of the processes modeled by hardware, software, artificial intelligence etc. The thermal and physical properties of steels are regarded as constant (with average values) in case of linear and variable equations under certain restricting conditions for non-linear equations. It is a representative

work in the field of the *intelligent flexible systems for heat transfer.* The software products convert into various programming languages the mathematical models of the designed thermal processes, out of which most used are C++, Borland C and more recently C# (Roman, 1991; Ilegbusi Olisegun Jensen *et al.*, 1999; Catarschi, 2003).

In paper (Oprescu *et al.*, 2002), elements of the (3) component of the *intelligent flexible systems for heat treatments* which include heat producing equipment, controlled atmosphere producing installations, optimal and complex control of the heat treatment installations etc. are presented. Also, there are presented certain specific elements of thermal calculation, which can be used within the mathematical modelling of specific to component (2) of the *intelligent flexible systems for heat treatments* chart.

In paper (Alexandru, 2003), it is treated component (2) of the *intelligent flexible systems* where, for the mathematical modelling of the cooling (as process opposite to heating), the equation of thermal conductivity is used with initial and limit conditions specific to cooling, where the heat transfer takes place from metal to the work environment. It is necessary to be known the heat transfer coefficient from the metal surface to the environment; this coefficient is component of the Biot criterion. The cooling rate must be controlled in order to control also the evolution of the thermal stresses, especially at temperatures below 550°C.

Paper (Prejban *et al.*, 2003) presents the influence of heat treatments on certain physical and mechanical characteristics of the steel 15VMoCr14X. Both investigation methods and experimental results are presented.

In paper (Catarschi, 2003), the author presents a monograph of the *intelligent flexible systems for the thermal transfer in metallic materials designed for plastic deformation* where all three components are studied. Within component (1), various technologies of thermal processing and a quite largerange of steels are studied. Within component (2) of the intelligent flexible systems, mathematical modeling of thermal processing deals with seven technological variants of combination of certain thermal regimes. Each technological variant includes specific initial and final conditions. Out of them, three variants present the cases of blanks with initial condition as cold and other four variants are for blanks with hot initial condition. In case of blanks with cold initial condition, the requirements of checking against cracks are set for the period when the steel is within the elastic temperature range (0-550°C). Together with the definition of the size and type of equipment to produce the thermal transfer in metal, it is assumed that the technologic execution can be also achieved, within component (3) of the *intelligent flexible systems,* by implementing the necessary software.

The seven technological variants are graphically shown in the paper (Catarschi, 2003), depending on the initial condition of the steel before heating (similar to the hereby chart completed (Fig. 2) for five heating periods for: 2 ingots of average diameter of 1587 mm of steel grade 55MoCrNi15 susceptible to cracking, with cold initial condition, in bogie hearth furnace, in view of forging, from which resulted the heating curves for the furnace, temperature, ingot surface and core as well as the thermal gradient between core and surface). The input data include: furnace initial temperature, metal initial temperature, furnace type, grade of the steel being heated, average diameter of the blank, number blanks on batch and further, furnace heating rate (to be optimized) is to be considered. The paper can be regarded as a basic contribution in achieving the *intelligent flexible systems for thermal transfer in steels.*

In paper (Catarschi, 2003), the author presents the theoretical and experimental researches conducted throughout six years, within a doctorate thesis, with applications for solid steel blanks.

2. Experimental Researches

The applications of heating/cooling of steel parts designed to plastic deformations or heat treatments are very numerous but solid parts and some steel grades are the cause of troubles quite hard to resolve. Thus, out of the 17 steel grades studied, several grades required by industry (*i.e.* at S.C. FORTUS S.A. Iaşi, S.C. ASAM S.A. Iaşi etc.) are here below presented whose properties have been established by both theoretical and experimental research (Fig. 2 and Fig. 3):

Quenching and tempering alloy steel 42MoCr11 (turbine rotors, internal ignition engine shafts, gears etc);

- *Ditto* 65MnCr15 (mill rolls, shafts, rollers, cylinder sleeves etc.);

- *Ditto* 34MoCrNi15 (big gears, shafts, locomotive axles, tie rods, connection rods);

- *Ditto* 34MoCr11 (internal ignition engine shafts, gears, crane forged hooks etc.);

- *Ditto* 40Cr10 (shafts, driving wheels, piston rods, friction disks);

- *Low alloy steel for plastic deformation tools* 55MoCrNi15 (moulds, big anvils, mill rolls etc);

- *Ditto* 90VMoCr18 (hot plastic deformation tools: mill rolls, shaped anvils etc.);

- *Carburizing low alloy steel* 16CrMo4 (pistons, heat resisting fasteners);

- *Ditto* Wb36 (0,12-0,17%C; 0,8-1,2%Mn; 0,25-0,5%Si; 0,5-0,8%Cr; 1,0-1,3%Ni; 0,25-0,4%Mo, wear resisting fasteners);

- Carburizing alloy steel: 21MoMnCr12 (gears for heavy machines, shafts, cam shafts etc.);

- *Ditto* 12MoCr50 (wear resisting fasteners etc.);
- *Ditto* 13CrNi30 (heat treated parts with high strength: gears etc.);
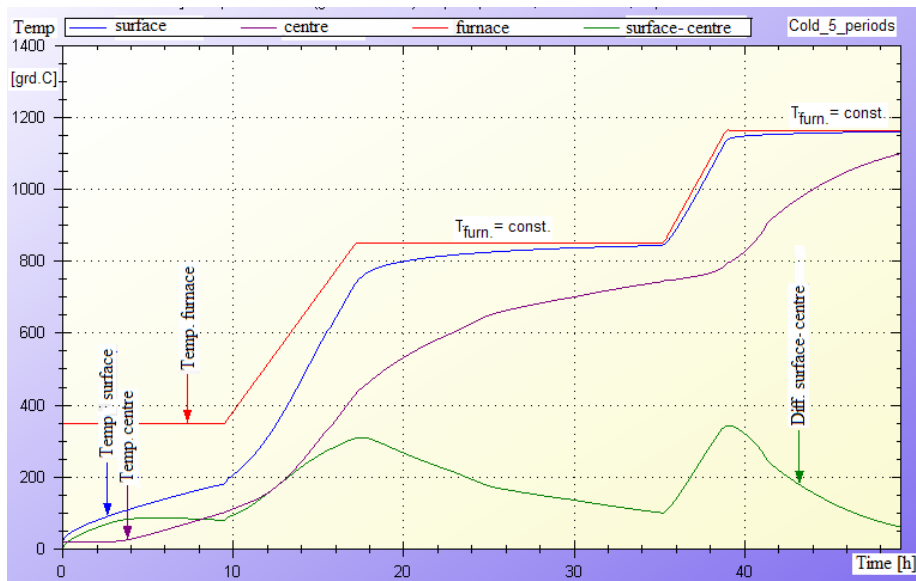
Fig. 2 – Heating of cold ingots in 5 periods, steel mark 55MoCrNi15; 60 tons/ingot.
Initial temperatures: surface = 20°C; centre = 20°C; furnace = 350°C; c_{entre} = 0 mm;
Final temperatures: surface = 1180°C; centre = 1110°C; furnace = 1172°C;
Heating time [hours]: t_1 = 9.60; t_2 = 7.48; t_3 = 17.94; t_4 = 3.85; t_5 = 10.55; Total time = 49.42; Heating speeds [°C/h]: w_1 = 60; w_2 = 90; - r_{furn} = 3.87; medium diameter = 1587 mm; ingot length = 4810 mm; ingots number = 2; furnace CI = 40.0 m^2.

In case of heat treatments, the thermal stresses have acceptable limits much lower than in case of plastic deformations. Such elements are used within the *intelligent flexible systems for thermal treatment of steels susceptible to cracking in stationary/nonstationary system, using new software products.*

The five heating periods are achieved as follows :
- periods I, III and IV with the regime Tfurn. = const.
- periods II and IV with the regime Tfurn.2 = Tfurn.1 + wΣ τ_i. with n=1, 2, 3,…..,∞.

The checking at cracking of the steel half-product is necessary in the temperatures interval 0….600°C.
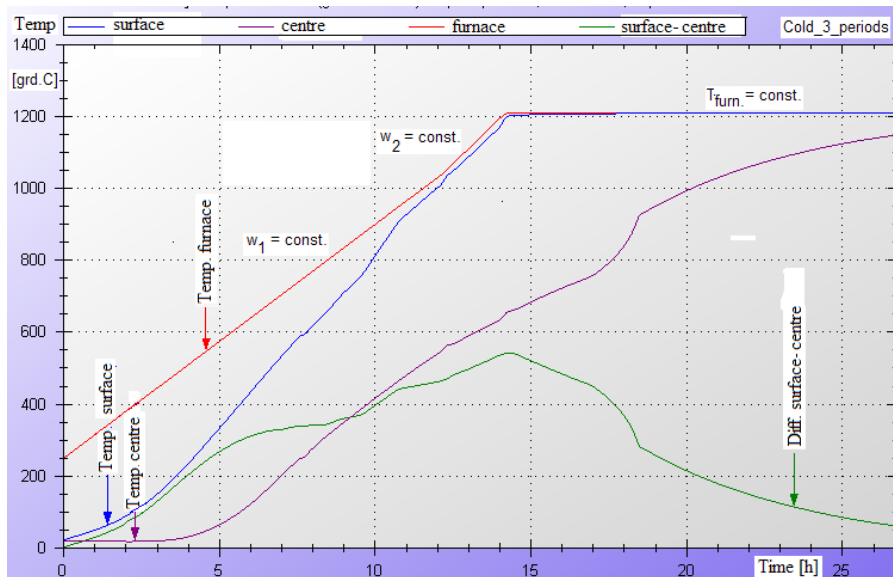
Fig. 3 −Heating of cold ingots in 3 periods, steel mark 34MoCr11; 44,9 tons/ingot.
Initial temperatures: surface = 20°C; centre = 20°C; furnace = 300°C; r_{centre} = 0 mm;
Final temperatures: surface = 1197°C; centre = 1136°C; furnace = 1201°C;
Heating time [hours]: t_1 = 18.58; t_2 = 6.23; t3 = 15.34; Total time = 40.15;
Heating speeds [°C/h]: w_1 = 84; w_2 = 100; - r_{furn} = 3.99; medium diameter = 1631 mm;
ingot length = 3605 mm; ingots number = 4; furnace CI = 40 m^2.

The three heating periods are achieved as follows:
- periods I and II with the regime $T_{furn.2} = T_{furn.1} + w\Sigma \tau_i$. with n=1, 2, 3,…..,∞
- period III with the regime $T_{furn.fin.}$ = const.
The checking at cracking of the steel half-product is necessary in the temperatures interval 0….600°C.

3. Conclusion

The software product utilized is formed by computer software related to the heating regimes designed in C# language. Heating diagrams obtained can be used both for the simulation of the heating technological processes and for their application at industrial scale in the production workshops of hot sectors.

The new technologies ensure the compliance with the European environmental norms creating this way optimum work conditions to the operators, which serve the heating and heat treatment installations.

REFERENCES

Alexandru P., *Modelarea numerica a racirii pieselor cilindrice din otel*. Metalurgia, **5**, 20-24 (2003).

Altan T., Ngaile G., Shen G., *Cold and Hot Forging: Fundamentals and Applications*. Published ASM International, 2004.

Catarschi V., *Heating of Solid Steel Blanks*. Cermi Technical, Scientific and Didactic Publishing House, Iasi, 324 (2003).

Ilegbusi Olisegun Jensen, Iguchi Manabu, Walter E. Wahnsiedler, *Mathematical and Physical Modeling of Materials Processing Operations*. Publisher: CRC Press, 512 (1999).

Oprescu I., *et al*., *Instalatii pentru tratamente termice ale materialelor metalice*. Ed. Universitatii Politehnica Bucuresti, 2002.

Prejban I., Heput T., Mihut G., Vilceanu L., *The Influence of the Thermals Treatments Ovet the Physical and Mechanical Characteristics of Steel Type 15VMoCr14X*. Metalurgia International, *3*, 11-16 (2003).

Ramsay C., *Full Annealing & Normalizing*. Advanced Materials & Processes, **147**, *3*, Publisher ASM International, 40-43 (1995).

Roman E.M., *Programming in Mathematica*. Addison Wesley Publishing Company, Redwood City, California, 1991.

SISTEM FLEXIBIL INTELIGENT PENTRU PRELUCRĂRI TERMICE A OŢELURILOR SUSCEPTIBILE LA FISURARE (I)

(Rezumat)

Lucrarea cu tema Sistemele flexibile inteligente pentru prelucrările termice a oţelurilor susceptibile la fisurare urmăreşte dezvoltarea cunoaşterii în domeniul de cercetare metalurgic, cum este cel al deformărilor plastice şi al tratamentelor termice. Sistemele flexibile inteligente pentru prelucrările termice a materialelor metalice fac parte din sistemele de conducere asistată şi controlată a proceselor termice din sectoarele de deformări plastice şi tratamente termice. Acestea reprezintă o ramură importantă a sistemelor cu inteligenţă artificială care se folosesc atât în comanda şi controlul proceselor de producţie cât şi în operaţiile de predicţie a proprietăţilor fizico-mecanice a materialelor în funcţie de necesităţi.

Din punct de vedere aplicativ, contribuţiile originale ale cercetărilor sunt: 1) de a dezvolta sisteme flexibile inteligente de prelucrare termică a oţelurilor, care pot avea rol atât de comandă (detecţie şi reglare a unor temperaturi prescrise) cât şi de execuţie (acţionare, prin intermediul unor module hard de automatizare), capabile să întrerupă/pornească de exemplu, sisteme şi instalaţii termo-electrice complexe, în scopul realizării unor procese termice etc. şi 2) de a realiza procese termice industriale superioare calitativ şi cu consumuri energetice reduse cu până la 30%, în condiţii ecologice îmbunătăţite.

THE INTELLIGENT FLEXIBLE SYSTEM FOR THERMAL PROCESSING OF STEELS SUSCEPTIBLE TO CRACKING (II)

BY

**VASILE CAŢARSCHI[1*], OVIDIU CALANCIA[1], ŞTEFAN LUCIAN TOMA[1]
and SMARANDA CAŢARSCHI[2]**

[1] "Gheorghe Asachi" Technical University of Iaşi,
[2] "Anghel Saligny" Vocational Group of Iaşi

Abstract. The purpose of the work with the theme The Intelligent Flexible Systems for thermal processing of steels susceptible to cracking (II) in stationary/no stationary system is to achieve a theoretical and applicative research based on the multi-disciplinary approach in mathematics, physics, informatics and metallurgy and to elaborate intelligent flexible systems of thermal processing of steels, with applications in metallurgy and mechanics.

Key words: flexible system, echo technologies, software instruments, thermal processing.

1. Introduction

The work with the theme Intelligent Flexible Systems for Thermal Processing (ISFTP) of Steels Susceptible to Cracking (II) in stationary/no stationary system has as main objectives:

---

* Corresponding author e-mail: vcatar@yahoo.com

(1) development of certain *intelligent flexible systems of thermal processing of steels*, and study of certain steels susceptible to cracking;

(2) development of new technologies of thermal processing of steels for an intelligent industry by using informatics technologies (mathematical modelling and software in C# language),

(3) reduction of the scrap rate of the heat treated blanks;

(4) increase of the operational safety of the products completed by using *intelligent flexible systems;*

(5) increase of the operational safety of the industrial thermal machinery and plants;

(6) increase of the scientific performance by stimulating the formation of research teams involving students, master and doctorate candidates.

The results of the researches have as applications the thermal processes in plastic deformations and heat treatments, with the acquirement of certain optimal properties of the studied materials (tool steels, Mo-Cr-Ni, Mn-Cr, Mo-Cr alloy steels etc). Within the mathematical modelling, the starting point is the thermal conductivity Fourier's differential, with various initial and limit (surface) conditions, using sums of Bessel-Fourier infinite series, Biot and Fourier non-dimensional criteria and r/R, x/X simplexes. Together with obtaining the solutions of Bessel-Fourier equations, there are also achieved the solutions of the graphic points for drawing up the temperature curves of the environment (furnace) and thermal field from the metal. Thermal and physical properties of the metal are used, as well as certain laboratory and industrial experiments.

The intelligent flexible systems for thermal processing of metallic materials belong to the system of assisted and controlled controlling of the thermal processes from the plastic deformation and heat treatment sector. This represents an important branch of the systems with artificial intelligence that are used in both controlling the production processes and operations of prediction for the physical and mechanical properties of the materials, depending on necessities.

The functions that can be fulfilled by the intelligent flexible systems are:

(a) generation of modern thermal technologies based on the most recent achievements in the plastic deformations and heat treatment field;

(b) implementation of such modern technologies in related sectors on equipment competitive with the related technologies and

(c) verification and control of the quality of the processed products.

The function of generation of certain modern technologies (a) necessitates the use on large scale of the possibilities offered by the computer equipment (computer networks, software, data bases, data use and acquisition boards etc), having as basis the mathematical and physical modelling of the thermal phenomena and processes which compose the said technologies as well

as the software resulting from their use. Each steel grade, shape of blank and type of equipment can be distinctly considered when a new technology of thermal processing is generated, based on initial and limit conditions pre-established.

By (b), implementation of these modern technologies, it is aimed that new technologies would replace the old technologies of the thermal processes (based on obsolete norms, causes 30% higher energetic consumption and still produce scrap). Where necessary, modernization or replacements of machinery can be conducted, to fulfil the control requirements needed.

The (c) function of verification and control for the quality of the processed products requires the necessity to verify how the designed technological norms, permanent control of the prescribed temperatures of the thermal processes (thermocouples, radiation pyrometers) and quality control of the processed products (hardness control, US test etc) (Richard L. Houghton, 2004).

By achieving the objectives within the complex research in mathematic sis obtained, by solving the Fourier's non-linear equation of thermal conductivity. The non-linearity of the equation is given by the variation with temperature of the thermal conductivity coefficient and specific heat of the material. Thus, several forms of expression this equation appears. For the solution of these equations specific initial and limit conditions are set, depending on the zone of the isotopic material that will be croosedby the thermal flux, from surface to the material core (heating) or oppositely (cooling). Finally, by establishing the general solution of the thermal conductivity differential, the general form of the thermal field in material is obtained. By particularizing depending on the initial condition of the material, the solutions of the thermal field in the material are obtained (Catarschi, 2003). The mathematical modelling for the steel cooling starts up also from the thermal conductivity differential, terms are introduced depending on material and temperature (Kelvin's coefficient of thermal diffusivity and specific heat). To resolve the non-linear equation of thermal conductivity several simplifying hypotheses are introduced (Catarschi, 2003).

The mathematical modelling of each thermal system requires to be transposed in software – program for which C# language will be adopted (due to its degree of compactness). Every soft-program of a thermal system requires the use of a large number of files containing all input data and some sub-programs to achieve the executables to finally work with, within the new designed technologies. The input data needed to obtain the charts of the furnace and metal temperature evolution, for the list of steel grades that can be appealed include the following:

- variation with temperature of the thermal conductivity and specific heat of the steels;
- variation of the final thermal gradient in steel depending on the

characteristic dimension (i.e. radius) of the material;

• variation with temperature of the yield point, tensile strength, elasticity modulus, Poisson's coefficient, coefficient of thermal linear expansion of steels etc.

Beside these files containing data, certain sub-programs are also needed, representing: heat exchange between metal and the furnace shell; roots of rank 0, 1 and 2 of Bessel's functions; types of furnaces etc.

Fig. 1 The simplified architecture of data processing for a *intelligent flexible system for thermal processing of steels in stationary/no stationary system,* can be that of the hereby Fig. 1 with the following components: (entry block, data, rules, processing unit, rules assessment, exit block, conclusions, approvals, actions, knowledge base, user interface, actions).
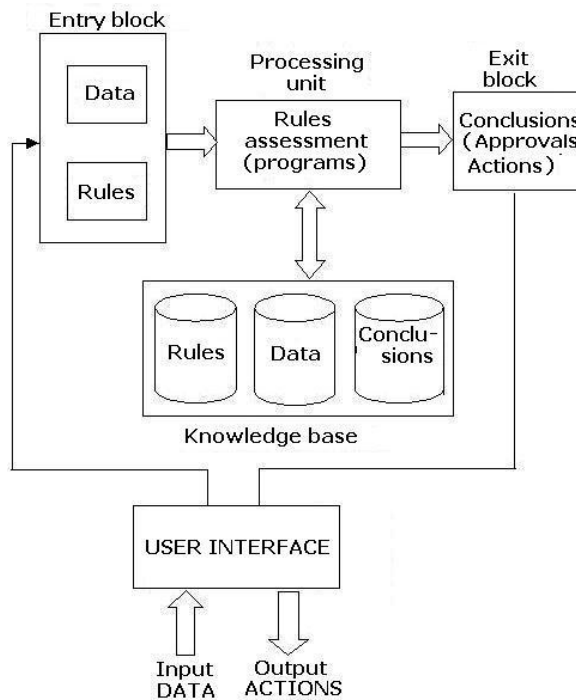
Fig . 1 – Block scheme.

The sub-programs for the heating systems completed by the method of finished differences require the calculation of a time step which defines a certain temperature step and a certain move step of the heat flux inside the metal. All above mentioned files and sub-programs must be unified within a software package (software products) to produce new optimized technologies, with various thermal systems of the metal. For heating systems within the

elastic range of temperatures (0 - 550°C), additional condition of verification against cracking are added, required for the limitation of the metal heating rate. This is completed in view of eliminating the risk of cracking at heating for plastic deformation and of distortion during the heat treatment. The thermal systems can be modelled and converted into soft-wares for each type of initial condition of the blanks: (1*) cold, (2*) warm and (3*) hot (Catarschi, 2003).

2. Experimental Researches

The above mentioned mathematical and informatics researches must cover, by the objectives whose activities are mentioned here-above, the thematic area of the new production processes and procedures which also includes *the intelligent flexible systems of thermal processing of steels in stationary/no stationary system* (for plastic deformations and heat treatments) (Gaba, 1998; Dulamita *et al.,* 1991; Catarschi, 2003).

A. From the basic point of view, the researches aim the elaboration of new approaches and theories in the area related to the theme, by achieving a thorough study of the complex thermal and physical phenomena which are governing the internal transformations specific to metallic materials. The research manner introduces certain most modern methods of implementation of the thermal processes by *intelligent flexible systems of thermal processing of steels and transformations inside the metallic materials at nanometric level,* following the applied heat treatments.

The original contributions of the fundamental researches of the present project refer to:

1) The conception and the developments of mathematical modellations and software for thermal manufacture in ISFTP;

2) Study of the effects of the transformations thermally induced in the metallic material, studied at level:

- a - *micro structural* (interaction between the phases of the metallic layers being under different expansions/contractions);

- b – *sub-micro structural* (interaction between layers being in twin crystal relation with elements of the inside rigid layers);

- c - *nanostructural* (modification of the elementary cells of outer layers, as a consequence of the variation of the system of arrangement of the compact atomic planes during the eutectoid transformations of the inner metallic grid, such as the martensitic transformation etc.).

B. From the applicative point of view, the original contributions of the researches aim:

1) the development of certain *intelligent flexible systems of thermal processing of steels*, which can play role both of control (detection and adjustment of certain prescribed accurate) and execution (drive, by means of automation hardware modules), able to interrupt/start, for instance complex

thermal-electrical systems and installations, in view of achieving certain thermal processes etc. (Richard L. Houghton, 2004; Catarschi, 2003). Therefore, *the intelligent flexible system of thermal processing* must be able to perform the *training* of the neural, neuro-fuzzy or genetic algorithms - based networks, in view of optimal establishment of the parameters of the physical models which are too complex for a simple modelling.

2) of accomplishing industrial thermal processes with a superior quality and with 30% less energetically consumptions in improved ecological conditions (Catarschi, 2003) (Fig. 2 and Fig. 3). From here on it results the relevance and the practical importance of the mention contributions

The data can be introduced in the system from key boarder from measuring devices connected with the computer: thermocouples, thermo resistors, tensiometric bridges, data acquisition board etc. On this purpose, a *friendly* user interface was provided. The entry block will store and manage the data and rules. The rules will be of IF – THEN type. The entry block together with the processing unit actually makes a neural system of neuro-fuzzy type, with hidden layers having neurons for the establishment of the rules.
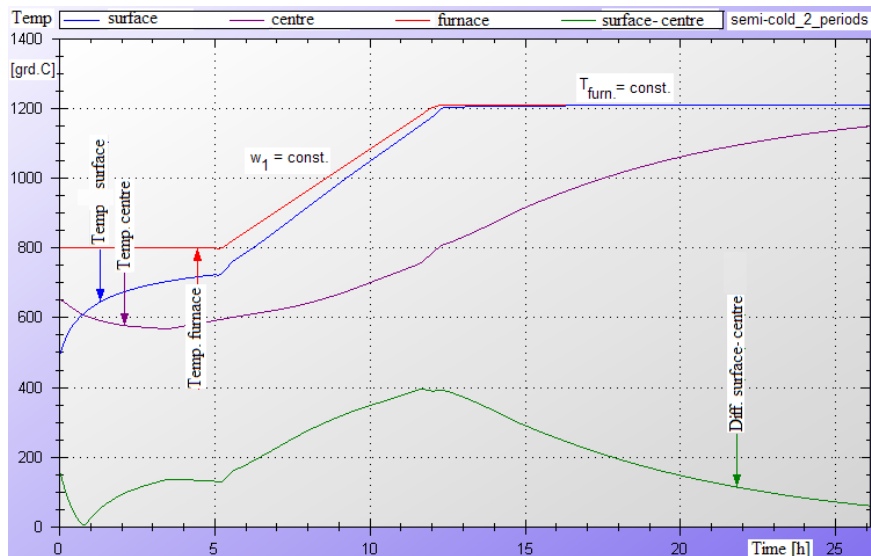
Fig. 2 – Heating of half-cold ingots in 3 periods, steel mark 65MnCr15; 44,9 tons/ingot. Initial temperatures: surface = 500°C; centre = 655°C; furnace = 800°C; c_{entre} = 0 mm; Final temperatures: surface = 1200°C; centre = 1139°C; furnace = 1205°C; ingots number = 4, Heating time [hours]: t_1 = 6.33; t_2 = 6.92; t_3 = 11.24; Total time = 24.49; furnace CI = 40.0 m^2, Heating speeds [°C/h]: w_1 = 59; r_{furn} = 2.77; medium diameter =1631 mm; ingot length = 3605 mm.

The three heating periods (Fig.2) are achieved as follows :
-   periods I and III with the regime Tfurn. = const.

- periods II with the regime Tfurn.2 = Tfurn.1 + wΣ τ$_i$. with n=1, 2, 3,…..,∞

The two heating periods (Fig.3) are achieved as follows :

- periods I with the regime Tfurn.2 = Tfurn.1 + wΣ τ$_i$. with n=1, 2, 3,…..,∞

- periods II with the regime Tfurn. = const.

In this system, the fuzzy interface is of MIN-MAX type and de-fuzzing is completed in the exit block of CENTROID type. On purpose to define accurately the rules and coefficients of the network, training operations will be conducted on simulated data. The test base will be made up both of simulated data and experimental measurements. The training base should on one hand be enough large to provide the convergence of the solutions and, on the other hand, the *overtraining* situation must be avoided because it is leading to high discrepancies. To be operational, the system will be achieved on a Pentium IV computer with 2.7 GHz tact and 1024 M RAM.
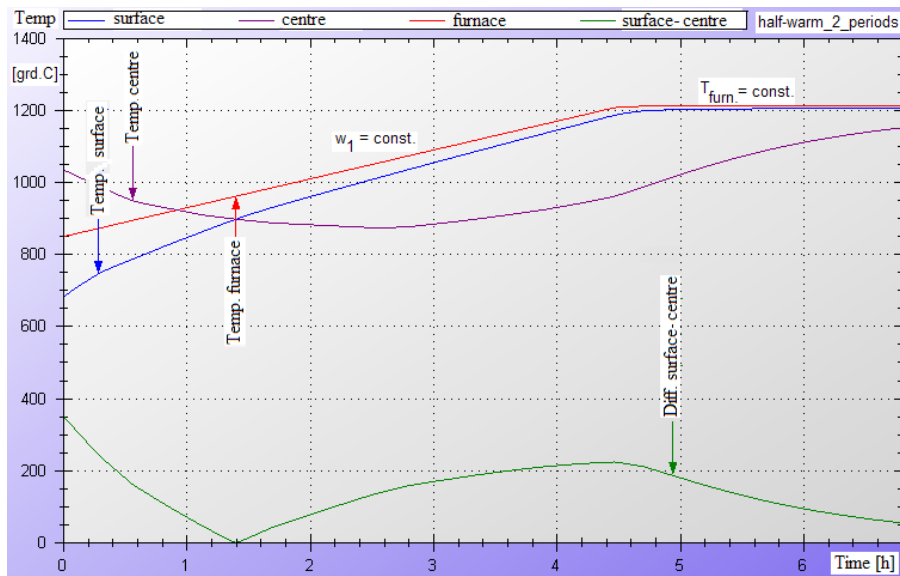
Fig. 3 – Heating of half-warm ingots in 2 periods, steel mark 42MoCr11; 23,5 tons/ingot.
Initial temperatures: surface = 650°C; centre = 1020°C; furnace = 850°C; c$_{entre}$ = 0 mm;
Final temperatures: surface = 1202°C; centre = 1150°C; furnace = 1205°C;
furnace CI = 16 m^2, Heating time [hours]: t$_1$ = 5.92; t$_2$ = 3.25; Total time = 9.17;
Heating speeds [°C/h]: w$_1$ = 59; r$_{furn}$ = 2.77; medium diameter = 1100 mm;
ingot length = 3640 mm; ingots number = 2;

The experimental data will be acquired by means of a data acquisition board of National Texas Instrument type. For testing, the *intelligent flexible*

system for thermal processing and software for the acquisition board will be programmed in C#.

During the operations of research of the steels, material flaws can be induced such as: non-homogeneities, holes, inclusions, anisotropies etc. In view of revealing detecting their location and sizes it is provided the use of two main methods of non-destructive tests:

- method of the circular currents using sensors suitable to the geometry of the product when the product being tested is metallic and good electricity conductor;

- ultra-sons method using Lambda waves in case of materials showing electric isolation properties or in case of thin plates.

Related testing equipment is existing for both methods. Such equipment is connected to computers, so that the readings of the test could be introduced as input data. Also, both methods allow the non-destructive determination of certain mechanical parameters such as: elasticity modulus, shearing modulus, Poisson coefficient, residual stresses, and phase modifications.

It is to mention that various options of *intelligent flexible systems for thermal processing of metallic materials* built on this purpose are presently used by companies such as Boening USA, Aerospatiale France, Eurocopter –UE.

Using programming in C# language the existing software of the research team will be completed with other original software for thermal transfers, at the level of the modern related software, by collaboration between specialized engineers, physicists and informatics staff. The verification of the software within certain industrial experiments allows the diversification, development and capitalization of the same on the international and Romanian market, directly or via INTERNET.

We consider that by the above mentioned, the present theme has multiple reasons to improve the level of the scientific knowledge in a priority field such as nano-sciences, nano-technologies, materials and new production technologies.

In paper (Richard L. Houghton, 2004) there are presented processes, materials and applications of certain *intelligent flexible systems for heat treatments,* methods and equipment of completing heat treatments. They are regarded as new and modern elements in this field and are used in USA.

Paper (ASM Handbook – Heat Treating, 1991) is a monograph for heat treatments applied to stainless steels, high alloy steels and heat resisting steels with applications within the certain *intelligent flexible systems for heat treatments*. There are presented the influences of the alloy elements and transformations being produced in the heated material as well as its properties before and after the applied heat treatment. It is a paper useful to designing new *intelligent flexible systems for heat treatments in steels.*

In paper (Soren O.S. *et al*., 2004) there are presented computerized methods of verification and control that must be performed after various heat

treatments as well as the testing and assessment methods to be used. The study of the heat treated products is conducted on surface and in their cross section in order to establish various properties, structures and sub-structures.

Papers (Gaba, 1998; Dulamita *et al.,* 1991) also deal with component (2) of the *intelligent flexible systems for thermal transfer*, where, for mathematical modelling of the heat the thermal conductivity equation is used, with initial and limit conditions specific to heating. They are papers that can be used in view of designing the *intelligent flexible systems for heat treatments* provided in this work.

3. Conclusion

In conclusion, one can assume that the theme of the project belongs to a priority domain and the fundamental and applicative researches and that will be conducted within the work aim to deepen, enlarge and spread the deep scientific knowledge of the *intelligent flexible systems for thermal processing*, within the Romanian education and research system, opening the way of capitalization of their huge applicative potential, by developing new technologies superior to those that are being currently used according to norms.

REFERENCES

* * ASM Handbook – Heat Treating**. -** *Heat Treating of Stainsless Steels and Heat Resistant Alloys – Includes Super Alloys and Refractory Metals and Alloys.* 1991.

Catarschi V., *Heating of Solid Steel Blanks.* Technical, Scientific and Didactic Publishing House CERMI, Iasi, 324 (2003).

Dulamita T., Cojocaru M., Toma V., Suciu V., Gherghescu I., Mot M., *Mathematical Modelling at the Designing and Control of the Technological Processes of Heat Treatment.* Metalurgia *8,* 23-28 (1991).

Gaba A., *Mathematical Model of Calculation of the Heat Transfer in Heating Furnaces.* Metalurgia, *4,* 194-198 (1998).

Richard L. Houghton – *The Process & Materials Technology Section of the U.S. Heat Treating Industry's Recently Revised Technology Roadmap is Focusing on New and Improved Heat Treating Processes, Materials, and Application Knowledge***.** Advanced Materials & Processes, Publisher ASM International, *6,* 36-37 (2004).

Soren O. Segerberg, Ian L. Bodin, Imre Felde, *Computerized, Wireless Instrumentation Has Been Developed for Testing and Evaluating Quench Ants and Quenching Systems.* Heat Treating Progress: Process & Quality Control, Publisher ASM International, *6,* 2004.

SISTEM FLEXIBIL INTELIGENT PENTRU PRELUCRARI TERMICE ALE OŢELURILOR SUSCEPTIBILE LA FISURARE (II)

(Rezumat)

Scopul lucrării Sisteme flexibile inteligente pentru prelucrări termice a oţelurilor susceptibile la fisurare în regim staţionar /nestaţionar folosind noi produse software este de a realiza o cercetare teoretică şi aplicativă bazată pe abordarea multidisciplinară in matematică, fizică, informatică şi metalurgie şi de a elabora sisteme flexibile inteligente pentru prelucrări termice ale oţelurilor, cu aplicaţii în metalurgie şi mecanică.

SOFTWARE FOR PRIORITIZING THE FUNCTIONS IN FUNCTIONAL ANALYSIS

BY

FLORIN CHICHERNEA[∗] **and ALEXANDRU CHICHERNEA**

University Transilvania, Braşov

Abstract. Value Analysis is a method that provides an operating technique using a creative and organized approach. It is managed by a group, each of them selected by their expertise in specific subjects and coordinated by a Value Analysis expert.

The paper presents a complete study of Value Analysis applied specifically to one equipment, and the software for prioritizing of the functions in value and cost. The software includes 9 computer programs and can be used for 2 to 10 functions. Introducing a single time the value for calculation, the software outputs are the diagrams of the functions value weighting, the diagram of the functions cost weighting and the diagram of Value and cost weightings of the functions.

Key words: value analysis, optimum variant, software, prioritizing the functions.

1. Value Analysis

Value Analysis is a method that provides an operating technique utilizing a creative and organized approach. It is managed by a group, each of

---

[∗] Corresponding author e-mail: chichernea.f@unitbv.ro

them selected by their expertise in specific subjects and coordinated by a Value Analysis expert.

The Value Analysis group activity is managed in seven stages:
1. formation and functional analysis,
2. creativeness,
3. evaluation and selection of the proposals,
4. the creative phase,
5. development of the selected proposals,
6. presentation of the selected proposals, set in order by priority,
7. implementation phase.

An example of *the software for prioritizing of the functions in value and cost* is presented integrated in a study of Value Analysis, applied to the re-design of a jaw crusher used for primary crushing of a wide variety of materials in the mining, iron and steel and pit and quarry industries (Chichernea, 2002).

Next the establishing mode of the optimum constructive solution is presented from the technical and economic viewpoint for *two parts participating in two functions with a high cost:1. the Flywheel who contribute at the function F7 (ensure uniformity of the movement) and; 2. the Bearing who contribute at the function F4 (supports the assembly)*.

2. Establishing the List of Functions and Dimensions

Table 1 presents the list of functions of the jaw crusher.

Table 1
List of Functions

Symbol	Function	Type of function	Technical dimension of function		
			Name	UM	Value
F1	Ensure milling	FS*	blast degree	-	3 - 10
...					
F3	Ensures adjustment	FC**	length	mm	15 - 30
F4	*Supports the assembly*	*FS*	*weight*	*daN*	*20000*
F5	Aesthetics	FE***	colour, form	-	-
...					
F7	*Ensure uniformity of the movement*	*FS*	*revolution*	*rpm*	

*FS – Service function **FC – Constraint function ***FE – Estimation function

3. Establishing the Levels of Importance of the Functions

Table 2 presents the value weighting of the functions (Chichernea, 2008; Chichernea, 2009; Chichernea Fl. & Chichernea Al., 2010a; Chichernea Fl., Chichernea Al., 2010b).

Table 2

Value Weighting of the Functions (*X Coordinate)

Functions	F1	F4	F3	F7	F5	F6	F2	F10	Total
F4	1	1	0	0	0	0	0	0	
...									
F7	1	1	1	1	0	0	0	0	
No. of points	8	7	6	5	4	3	2	1	36
Ratio	0,222	0,194	0,167	0,139	0,111	0,083	0,056	0,028	1
*Percentage %	22,2	19,4	16,7	13,9	11,1	8,33	5,56	2,78	100

The percentage of values of the functions value weighting result in the last row of the Table 2. The print screen 1 shows the part of the software that calculates the value weighting of the functions, in Table 2.
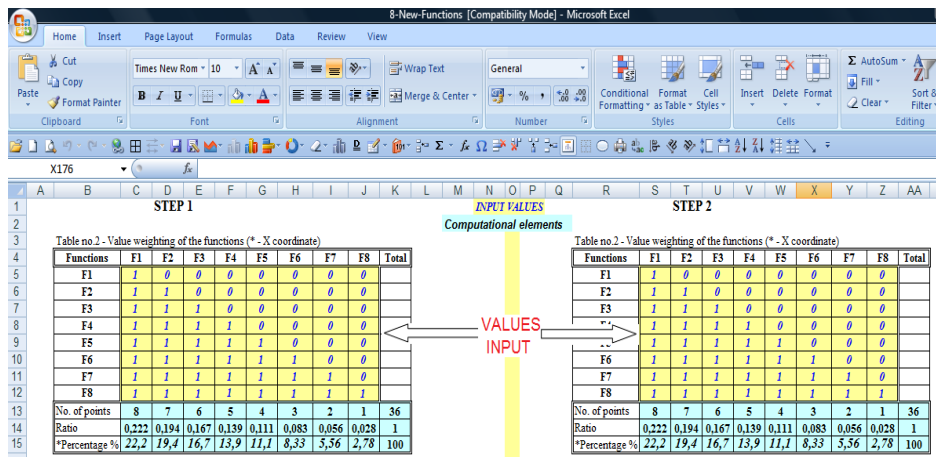
Fig. 1 – Print screen 1.

4. Economic Dimensioning of the Functions

Costs were assigned to the various functions by means of the functions-costs matrix shown in Table 3 in the print screen 2.

5. Diagrams

The construction of the diagrams is presented below.

Based on the values for coordinates x_i and y_i presented in Table 4 in the print screen 3 the diagrams of Figs. 2,…,4 are plotted in the print screen 4, the print screen 5 and in the print screen 6.
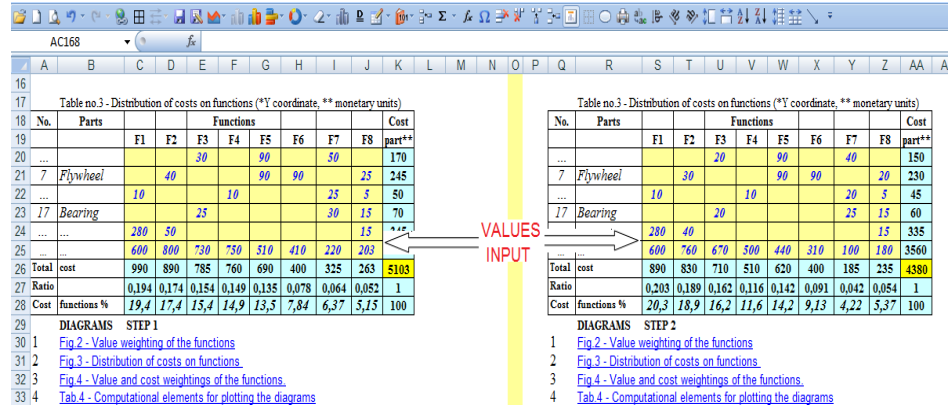
Table no.3 - Distribution of costs on functions (*Y coordinate, ** monetary units) — STEP 1

No.	Parts	F1	F2	F3	F4	F5	F6	F7	F8	Cost part**
...				30		90		50		170
7	Flywheel		40			90	90		25	245
...		10			10			25	5	50
17	Bearing			25				30	15	70
...	...	280	50						15	*15
...	...	600	800	730	750	510	410	220	203	
Total cost		990	890	785	760	690	400	325	263	5103
Ratio		0,194	0,174	0,154	0,149	0,135	0,078	0,064	0,052	1
Cost functions %		19,4	17,4	15,4	14,9	13,5	7,84	6,37	5,15	100

DIAGRAMS STEP 1
1 Fig.2 - Value weighting of the functions
2 Fig.3 - Distribution of costs on functions
3 Fig.4 - Value and cost weightings of the functions.
4 Tab.4 - Computational elements for plotting the diagrams

VALUES INPUT

Table no.3 - Distribution of costs on functions (*Y coordinate, ** monetary units) — STEP 2

No.	Parts	F1	F2	F3	F4	F5	F6	F7	F8	Cost part**
...				20		90		40		150
7	Flywheel		30			90	90		20	230
...		10			10			20	5	45
17	Bearing			20				25	15	60
...	...	280	40						15	335
...	...	600	760	670	500	440	310	100	180	3560
Total cost		890	830	710	510	620	400	185	235	4380
Ratio		0,203	0,189	0,162	0,116	0,142	0,091	0,042	0,054	1
Cost functions %		20,3	18,9	16,2	11,6	14,2	9,13	4,22	5,37	100

DIAGRAMS STEP 2
1 Fig.2 - Value weighting of the functions
2 Fig.3 - Distribution of costs on functions
3 Fig.4 - Value and cost weightings of the functions.
4 Tab.4 - Computational elements for plotting the diagrams

Fig. 2 – Print screen 2.

The parameters have the following computed values: a = 0.95, 43.6°, S = 23.39, S' = 0.

Table 4 provides the necessary values for constructing the following types of diagrams:

1. Fig. 4, in the print screen 4, the diagram of the value weighting of functions,

2. Fig. 5, in the print screen 5, the diagram of the cost weighting of functions, Fig. 6, in the print screen 6, the diagram of the value and cost weighting of functions.

13 Lucrarea 13-New-Functions [Compatibility Mode] - Microsoft Excel

STEP 1 — Table no.4 - Computational elements for plotting the diagrams.

No.	Computational elements	F1	F2	F3	F4	F5	F6	F7	F8		Total value
1	X_i	22,2	19,4	16,7	13,9	11,1	8,33	5,56	2,78	0	100
2	Y_i	19,4	17,4	15,4	14,9	13,5	7,84	6,37	5,15	0	100
	y = x	22,2									0
3	$(X_i)^2$	493,8	378,1	277,8	192,9	123,5	69,444	30,864	7,716		1574
4	X_i*Y_i	431,1	339,1	256,4	206,9	150,2	65,321	35,382	14,32		1499
5	$(Y_i - a*X_i)^2$	3,092	1,152	0,236	2,786	8,656	0,0092	1,1645	6,295		23,39
6	$S'*$	78,15	41,73	16,2	-46,36	-65,38	1,5994	-11,99	-13,94		2E-13

Parameters are the values:
a = 0,95   S = 23,39
α = 43,6   S' = 2E-13

STEP 2 — Table no.4 - Computational elements for plotting the diagrams.

No.	Computational elements	F1	F2	F3	F4	F5	F6	F7	F8		Total value
1	X_i	22,2	19,4	16,7	13,9	11,1	8,33	5,56	2,78	0	100
2	Y_i	20,3	18,9	16,2	11,6	14,2	9,13	4,22	5,37	0	100
	y = x	22,2									0
3	$(X_i)^2$	493,8	378,1	277,8	192,9	123,5	69,444	30,864	7,716		1574,1
4	X_i*Y_i	451,5	368,5	270,2	161,7	157,3	76,104	23,465	14,9		1523,7
5	$(Y_i - a*X_i)^2$	1,418	0,016	0,006	3,241	11,56	1,1364	1,3314	7,164		25,873
6	$S'*$	52,92	-4,983	-2,574	50,01	-75,56	-17,767	12,821	-14,87		4E-13

Parameters are the values:
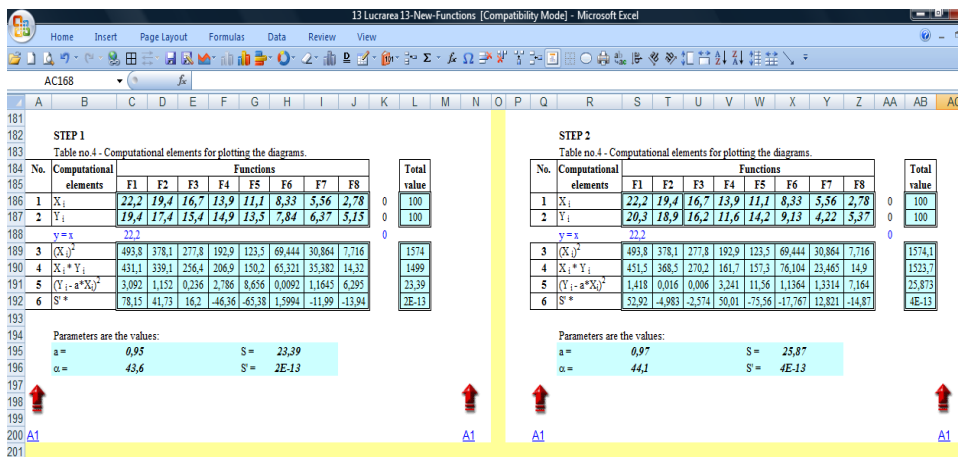a = 0,97   S = 25,87
α = 44,1   S' = 4E-13

Fig. 3 – Print screen 3.

The print screen 4 shows the part of the software that present the Fig. 2 with the diagram of the value weighting of functions.
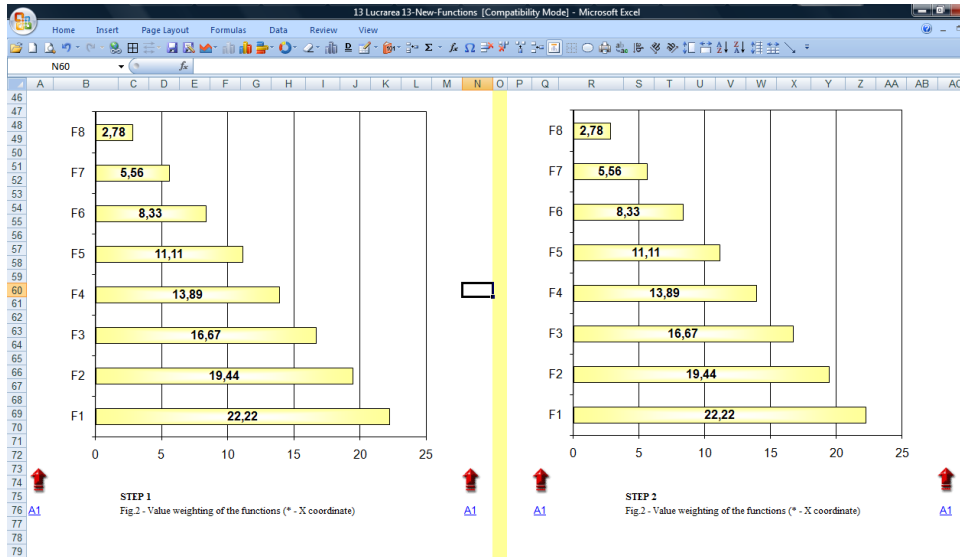
Fig. 4 – Print screen 4.

The print screen 5 shows the part of the software that present the Fig. 3 with the diagram of the cost weighting of functions.
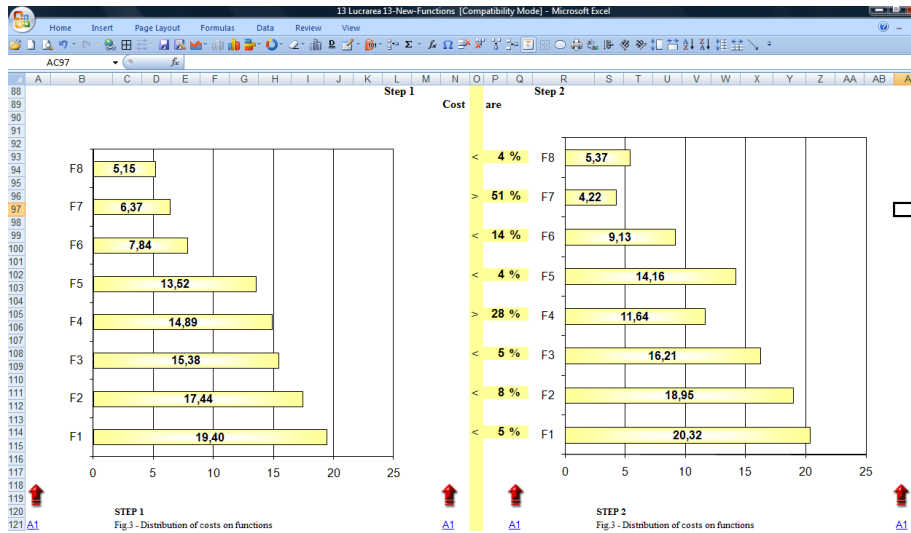

Fig. 5 – Print screen 5.

The print screen 6 shows the part of the software that present the Fig. 4 with the diagram of the value and cost weightings of functions.
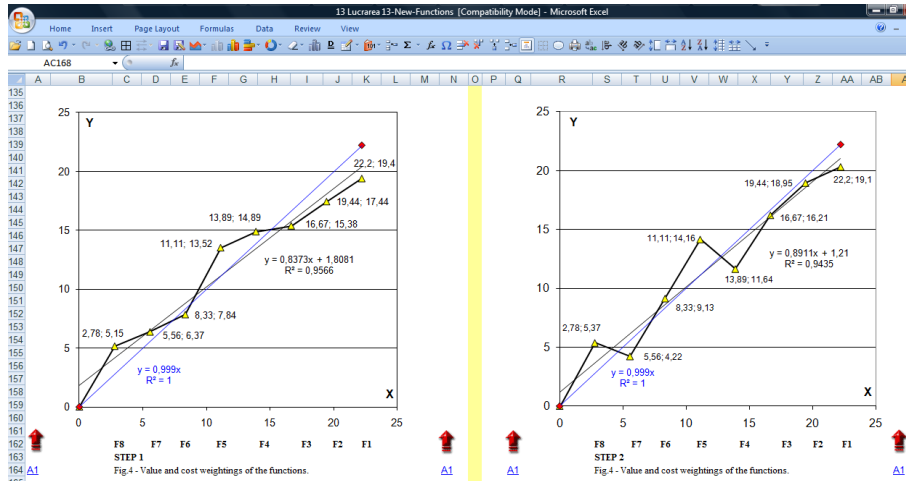
Fig. 6 – Print screen 6.

In the approach of Value Analysis following the chapters:

a – Establishig the functional-technological form of the parts in view of cost reduction for the flywheel and for the bearing. In this section be made an analysis for more constructive variants for the flywheel and for the bearing;

b – Comparison of the variants for the flywheel and for the bearing. In this section be made an analysis from the technical and economic viewpoint for the flywheel and for the bearing and will be carried out in order to select a technically optimum variant for the flywheel and for the bearing.

c – Establishing the levels of importance of the functions, step 2. The problems of a, b and c have been treated extensively in the work presented in the bibliography (Chichernea, 2008; Chichernea, 2009; Chichernea Fl. & Chichernea Al., 2010a; Chichernea Fl., Chichernea Al., 2010b; Chichernea Fl., 2010a; Chichernea Fl., 2010b). For the step 2 the calculation is performed on the right side of the software, as can be seen in print screens 1, 2, 3, 4, 5 and 6.

In Fig. 6 (print screen 6), which presents a value analysis modeling approach, shows the steps to optimize the value analysis product. In the softwares can obtain additional one diagrame with the cost weightings of the functions, in step 1 and in step 2, for comparing the costs in two steps. In the print screen 7 shows the Fig. 7 with the value and cost weightings of the functions, in step 1 and in step 2. Value system remains the same, but the cost has different values, one exampel shows in Fig. 7 in print screen 7.
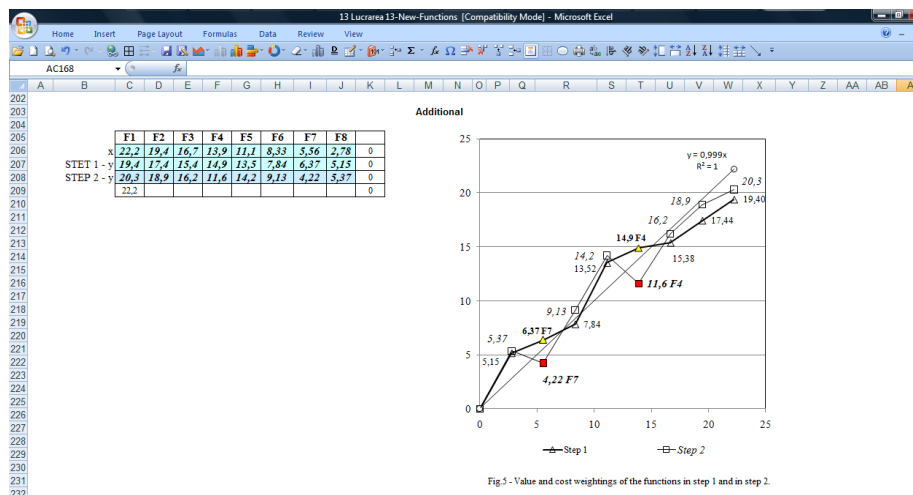
Fig. 7 – Print screen 7.

Only the costs are represented in order to not overload the diagram and to observe the decrease of the value of cost of function F4 and for function F7: 1. for the function F4 and 2, for the function F7.

6. Conclusion

In two steps of Value Analysis study two component of jaw crusher, the flywheel who contribute at the function F7 (*ensure uniformity of the movement*) and the bearing who contribute at the function F4 (*supports the assembly*) was redesign and optimized:

1. from engineering viewpoint (Figs. 8, 9),

2. from the economic viewpoint: a. the cost of function F7 (Fig. 7, print screen 7) decrease from 6,37 %, in the first step of Value Analysis study to 4,22 % in the second step of Value Analysis study (decrease with 51 %); b. the cost of function F4 (Fig. 7, print screen 7) decrease from 14,9 %, in the first step of Value Analysis study to 11,6 % in the second step of Value Analysis study (decrease with 28 %).

3. in the third step of Value Analysis study are analyzed other functions above the regression straight line (for example F5) and their costs reduced, then the regression line is re-plotted and the functions relocated above it are noted; these functions too are analyzed in view of reducing their costs, followed by the re-plotting of the regression line, etc.

4. in the fourth step of Value Analysis study are analyzed other function above the regression straight line and their costs reduced, then the regression line is re-plotted and the functions relocated above it are noted; these functions too are analyzed in view of reducing their costs, followed by the re-plotting of the regression line etc.

At the end of the Value Analysis study the points are aligned as perfectly as possible along the straight line y = a * x, with a tilt of 45°, this is the optimal situation, the values weighting of functions and the functions cost weighting are equal.
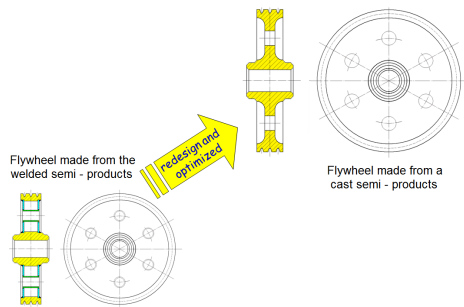

Fig. 8 – Flywheel redesign and optimized from engineering viewpoint.
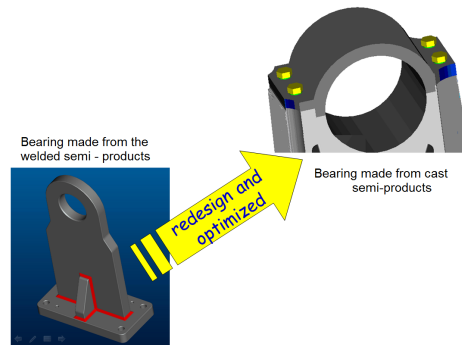
Fig. 9 – Bearing redesign and optimized from engineering viewpoint.

The advantages of this software are:

1 - after entering data, calculating and drawing diagrams is very fast, compared to a manual calculation,

2 - the calculation is done in parallel to step 1 and step 2,

3 - values and diagrams for the two iterations are always visible,

4 - reduce data entry time with each of the four separate charts by entering data once in the input area,

5 - changes can be made very quickly,

6 - changing the calculations and diagrams being made automatically and quickly,

7 - observations and conclusions can be made with the results of two iterations always in front,

8 - the software can run for 2 to 10 functions,

9 - the software is very simple and not create problems for use even by those not familiar with computer programming.

REFERENCES

Chichernea Fl., *Analiza Valorii*. Editura Universităţii Transilvania din Braşov, 2002.
Chichernea Fl., *Value Analysis*. Part I., Rev. Metalurgia International, 9, 62 (2008)
Chichernea Fl., *Value Analysis*. Part II, Rev. Metalurgia International, 3, 5 (2009).
Chichernea Fl., Chichernea Al., *Value Analysis*. Part III, Rev. Metalurgia International, 2, 22 (2010).

Chichernea Fl., Chichernea Al., *Value Analysis*. Part IV, Rev. Metalurgia International, *3*, 20 (2010).

Chichernea Fl., *Creating a Functional Model of Jaw Crusher Using the Value Analysis*. Part I, Proceedings of The 14th International Conference, Modern Technologies, Quality and Innovation, New face of TCMR, Iaşi, Chişinău, Belgrad, ModTech, Slănic Moldova, România, 171 (2010).

Chichernea Fl., *Optimisation of the Constructive Solution of Jaw Crusher an Iterative Process in Value Analysis Method*. Part II, Proceedings of The 14th International Conference, Modern Technologies, Quality and Innovation, New face of TCMR, Iaşi, Chişinău, Belgrad, ModTech, Slănic Moldova, România, 175 (2010).

SOFTWARE PENTRU PRIORITIZAREA FUNCŢIILOR ÎN ANALIZA FUNCŢIONALĂ

(Rezumat)

Analiza Valorii este o metodă care oferă o tehnică de operare folosind o abordare creativă şi organizată. Aceasta este gestionată de un grup, fiecare dintre membri fiind selectaţi în funcţie de expertiza lor în subiecte specifice şi coordonată de către un expert în Analiza Valorii.

Lucrarea prezintă un studiu complet de Analiza Valorii aplicat în mod specific la unui echipament şi software-ul pentru prioritizarea funcţiilor în valoare şi de cost. Software-ul include 9 programe de calculator şi pot fi utilizate pentru 2-10 funcţii. Introducând o singură dată valorile de calcul, rezultatele software-ului sunt diagrame cu ponderea funcţiilor în valoare, diagrama cu ponderea funcţiilor în cost şi diagrama cu ponderea funcţiilor în valoare şi cost.

SYNTHESIS, CHARACTERIZATION AND DYEING BEHAVIOUR ON WOOL FIBERS OF A NEW PREMETALLISED DYES BASED ON Cu(II)

BY

LAURA CHIRILĂ[1]*, ROMEN BUTNARU[1], SANDA CREŢU[2] and ANDREI VICTOR SANDU[2]

"Gheorghe Asachi" Technical University of Iaşi,
[1] Faculty of Textile Leather & Industrial Management
[2] Faculty of Materials Science & Engineering

Abstract. In this paper, are described the synthesis conditions and characterization of a new complexed compound, as a result of complexation reaction between a new acid dye with salt. The formation, stability and molar ratio combination of new complexed species were studied and carried out in liquid phase. In order to mark out the dyeability of a new compound, the dyeing process was achieved comparatively in different procedure: with preformation of premetallised dye in solid phase and with the complex formation directly on the wool fibers. The characterization of premetallised dye was performed by following methods: chemical elemental analysis, FTIR, SEM and thermal analysis. As a result of the mentioned methods the proposed structural formula were established. In addition the tinctorial resistance of dyed samples on wet treatments (wash and friction) and uniformity of color expressed by K/S constant were evaluated.

Key words: acid dye, premetallised dye, wash fastness.

---

* Corresponding author; e-mail: chirila_laura@yahoo.com

1. Introduction

As raw material of a major importance for textile industry, determined by the particularly proprieties of the fiber, wool comes from a series of mammals, so its properties depending on the breed and individuality of the biological source. The important supplier of textile fiber is the family of sheep and collateral related species .The qualities of wool, marked by a high hydrophilic, tinctorial capacity and remarkable chemical reactivity, thermo-insulation and good workability, highlight both the value and economic importance (Radu, 2003; Ifrim, 2006).

Azo dyes and their metal complexes are comonly used in textile industry, especially in dyeing wool fibers. In scientifical researches many metalic ions were been used with excellent improuvements of the dyed material such as: higher strenghts to washings and to the light (Dixit, *et al.*, 2009; Kocaokutgen & Ozkinali, 2004).

Chromium complexes derived from acid dyes have been widely tested on the wool fibers but the recently studies have showed that they are causing many environmental problems, due to the content of chromium salts overflowed into the resulted waste waters. The aim of this work was to investigate the possibility of the replacement of chromium ion, used in textile dyeing by the other metals ions, based on a new developed acid dye, those synthesis being designated to the using in dyeing wool fibers.

2. Experimental

2.1. Materials

The following chemicals were used for this study: for the synthesis of the premetallised dyes a new acid dye respectively sodium (E)-2 –((1-amino-4-sulfonatonaphthalen-2-yl)diazenyl) - 6-methoxybenzo [d] thiazole - 5 or 7 - sulfonate has been used, denominated HL and copper chloride from Merck Company (Târlea, *et al.*, 2007a; Târlea, *et al.*, 2007b).
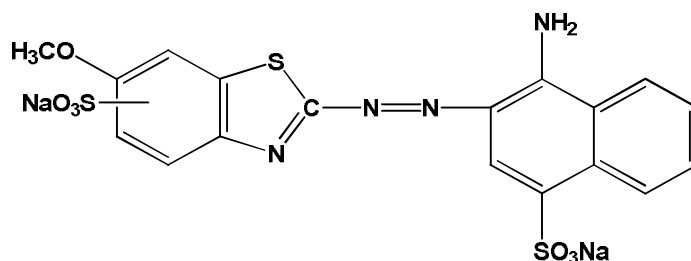
The structure of acid dye is shown in Fig. 1.

Fig. 1 – Chemical structure of HL.

Sodium sulphonate 10% as electrolyte reagent and CH_3COOH, 5M in order to obtain different values of acidic medium in the dyeing process were used.

2.2. Methods

The molar combination ratio, and the stability constants for new obtained compounds were determined using "molar ratio method" (J.H. Yoe and A.L. Jones), and Harvey-Manning method by applying pH-metry, conductometry, spectrophotometry in visible domain (Sibiescu, 2005).

The quantitative amount of each constitutive element from new synthesized premetallised dyes was achieved by chemical elemental analysis. The new synthesized premetallised dyes were examined in KBr pellets and the FT-IR spectrophotometer was FT-IR-Spektrometer "Nexus 470" (Fa. Thermo Nicolet, Offenbach), and the spectra were recorded in the range of 4000-450 cm^{-1} wavenumbers. The morphological changes appeared in the structure of acid dyes, were pointed out by electronic images, using a scanning electronic microscope S-3000 N of HITACHI with 15 UV. Using Thermo gravimetric Analysis TG, in dynamic conditions, the thermal behavior was studied in the presence of NETZSCH TG 209C, the study being conducted comparatively on the uncomplexed dyes and complexed dyes. 5.0 mg of sample was heat-treated at room temperature (RT) to 500°C with rate 10°C/min. Weight loss and residual mass in each stage of thermal decomposition were evaluated by Netzch Program. Dyeing wool fibers was performed in two applying methods using Mathis „Polycolor P4702" equipment. The color fastness of dyed wool samples with synthesized premetallised dyes to washing and rubbing were evaluated according with SR EN ISO 105-C06 and respectively with SR EN ISO 105-X12. The color intensity was expressed by K/S parameter using Spectroflash 300® spectrophotometer Data color Company.

2.3. Synthesis of Premetallised Dye

100 mL, 10^{-2} M·L^{-1} of HL were mixed together with 50 mL for the same concentration, and stirred during 90 minutes, until the mass of reaction are completely homogenous. The solid product has been obtaining by drying of the resulted compounds after a several centrifugations and washings of this mixture.

2.4. Dyeing Procedure

The above prepared premetallised dyes have been applying in following conditions: dyes material was wool fibers; concentration of premetallised dyes

in the bath process was 3%, Hm 1:100. The dyeing took place at 100°C during 60 minutes, according with the following dyeing diagram.
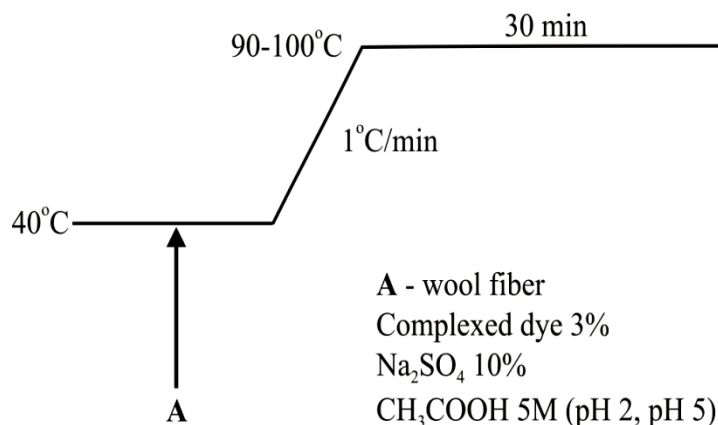

A - wool fiber
Complexed dye 3%
Na_2SO_4 10%
CH_3COOH 5M (pH 2, pH 5)

Fig. 2 – Dyeing diagram used in the dyeing process.

3. Results and Discussions

Experimental measurements for the study in liqiud phase were made in solutions of $0.5 \cdot 10^{-3}$ mol/L concentration. The registered values for each applyied method are graphical reperesented depending on the combination ratios, and the summarized obtained values are given in Table 1.

Table 1
The registered Values for each Applyied Methods

Compound	Molar ratio	pH	Conductivity [mS]	λ_{max}	Absorbance	Stability constant
CuL$_2$	1:1	5.56	195	550	0.393	$\beta= 9,36 \cdot 10^{14}$
	2:1	5.75	180	560	0.412	$\beta= 17,53 \cdot 10^{21}$

From Table 1 can be concluded that between the interaction between Cu^{2+} and ligand HL, two complex compounds have been forming in molar ratios: 1:1, 1:2. Also the values of the stability constants prouved a higher stability of resulted compounds, both methods highlighting those formation. The molecular structure of the premetallised dyes was confirmed by the following methods:

Elemental chemical analysis, expressed by the experimental and calculated values of the constitutive elements is in agreement with the proposed molecular formula. The experimental results and theoretical being showed in Table 2.

Table 2

Chemical Elemental Analysis for Sythesized Premetallised Dye

Compound	CuL$_2$	
Element	Calculated	Experimental
C %	34.38	34.23
H%	1.91	1.80
N%	6.68	6.56
S%	15.28	15.14
Cu%	5.05	4.92

Thermal analysis-the heat stability has been evaluated comparatively for the uncomplexed and premetallised dyes. The results show that the new synthesized premetallised dyes have a higher stability than the acid dye form wich they derived.

The *IR spectra* in infrared domain achieved on KBr pellets, show the presence of peaks assigned to the coordinative Cu←N, and covalent Cu—O bonds, whose presence explain the premetallised dyes formation. These bonds appear as bands with low intensity and can be observed at in a range of 600-400 cm^{-1}.

Table 3

The thermal Behavior for the Studied Compounds

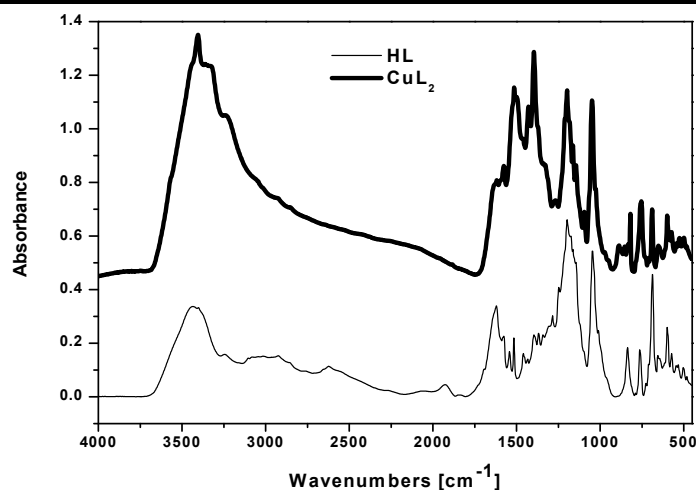| Compound	Stage	Mass change, [%]	Onset, [°C]	Rezidual mass, [%]
HL	I	13.68	136.9	50.39
	II	10.27	283.5	
	III	21.08	455.2	
CuL$_2$	I	12.06	231.8	68.98
	II	15.62	312.7	
	III	6.48	415.0	

Fig. 3 – FTIR spectra for the studied compunnds.

The **SEM** images show that after the complexation process the microsctructure of HL is slightly modified.

As can be seen from the Table 4, all the samples dyed with premetallised dye gives the shade which are changing a little beat according with the used metallic ion. Comparing the obtained result by both methods can be observed that, when premetallised dyes have been used, deep shades were obtained. Can be noted, as well, that pH value has a significant role in obtaining higher results; lower values of pH lead to record the improved fastness in all cases.

The fastness strenghts values to washing and rubbing of dyed samples in both methods are given in Table 4. Disregarding of the tested methods, the samples dyed with premetallised dye have good washings and rubbing fastness in comparing with the case when uncomplexed dye was used.
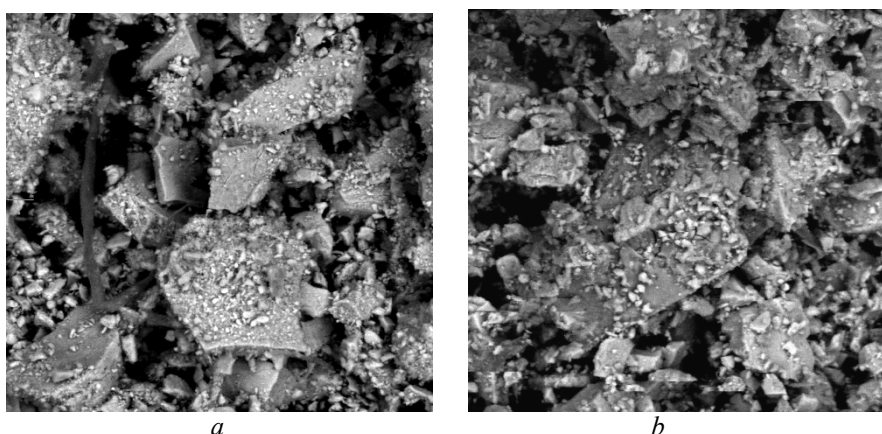

Fig. 4 – SEM images (1000X): *a* – HL; *b* – CuL2.

Table 4
The Properties of Dyed Wool Fibers with Studied Compounds

Sample	Method	pH	K/S	λ_{max}	Tinctorial strenghts		
					Washing	Rubbing	
						Wet	Dry
HL	-	2	9.47	560	3-4	3	3
		5	14.31	540	4	3-4	3
CuL$_2$	Concomitent	2	12.66	540	3-4	3	3
		5	4.39	550	3	3	2-3
	Preformation	2	14.42	550	4-5	4-5	4
		5	6.26	550	4	4	4

4. Conclusion

A new complexed dye, starting from a new acid dyes with copper ion was prepared. The formation, stability and molar ratio combination of new complexed dyes were studied and carried out in liquid phase. Also the syntheses in solid phase have been performed, followed by the characterization of those compounds. In order to mark out the dye ability of a new compound, the dyeing process was achieved in comparing with the complex formation directly on the wool fibers. The characterization of premetallised dye was performed by following methods: chemical elemental analysis, FTIR, SEM and thermal analysis. As a result of the mentioned methods the proposed structural formula were established. In addition, were evaluated the resistance of dyed samples on wet treatments (wash and friction) and uniformity of color expressed by K/S constant.

REFERENCES

Dixit C., Patel H. M., Desai D.J., Dixit R.B., *E-J. Chem.,* **6**, 315, (2009).

Ifrim S., *Chimia lânii*, Ed. Performantica, 2006, Iaşi.

Kocaokutgen H., Ozkinali S., *Characterisation and Applications of Some o,o'-Dihydroxyazo dyes Containing a 7-Hydroxy Group and their Chromium Complexes On Nylon and Wool*. Textile Research Journal, **74**, *1*, 78 – 82 (2004).

Radu C.D., *Fizico-chimia cheratinelor*. Ed. Performantica, 2003, Iaşi.

Sibiescu D., *Coordinate Compounds Chemistry*. Ed. Pim, (2005), Iaşi.

Târlea M.M., Cincu C., Marton G., Draghici C., Tarko L., *New Sulphonic Acid Derivates Obtained by Sulphonation 2-Aminobenzothiazoles -6 –Substituted*, Rev. Chem., **58**, *2*, 218-223(2007).

Târlea M. M., Cincu C., Marton G., Tomas S., Silvestro L., *Acid Benzothiazolic Dyes for Dyeing Protein Substrates*. Rev. Chem., **58**, *10*, 972-977 (2007).

SINTEZA, CARACTERIZAREA ŞI COMPORTAMENTUL LA VOPSIRE PE FIBRELE DE LÂNĂ A UNOR COLORANŢI PREMETALAŢI PE BAZĂ DE Cu(II)

(Rezumat)

În acest studiu, sunt descrise sinteza şi caracterizarea unor noi compuşi complexaţi, ca rezultat al reacţiei de complexare dintre un nou colorant acid şi clorura cuprică. Formarea, stabilitatea şi raportul de combinare au fost studiate şi evidenţiate în

fază lichidă. În scopul evidenţierii capacităţii de vopsire a noului compus, procesul de vopsire a fost realizat comparativ prin două procedee: cu preformarea coloranţilor premetalaţi în fază solidă şi respectiv cu formarea coloranţilor complecşi direct pe fibra de lână. Caracterizarea coloranţilor premetalaţi a fost realizată prin aplicare următoarelor metode: analiză chimică elementală, FTIR, SEM şi analiză termică. De asemeni pentru fibrele de lână vopsite au fost evaluate rezistenţele tinctoriale (la spălare şi frecare) precum şi uniformitatea culorii exprimată prin indicele K/S.

SYNTHESIS, CHARACTERIZATION AND DYEING BEHAVIOUR ON WOOL FIBERS OF A NEW PREMETALLISED DYES BASED ON Ni(II) AND Zn(II)

BY

**LAURA CHIRILĂ[1]*, ROMEN BUTNARU[1], ANDREI VICTOR SANDU[2]
and SANDA CREŢU[2]**

"Gheorghe Asachi" Technical University of Iaşi,
[1]Faculty of Textile Leather & Industrial Management
[2]Faculty of Materials Science & Engineering

Abstract. Two premetallised dyes based on a new acid azo dye as ligand and Ni(II), Zn(II) ions at 1:2 molar ratio were synthesized and characterized by chemical elemental analysis, FTIR, SEM-EDX and thermal analysis in dynamic conditions. The synthesized premetallised dyes have been applied on wool fibers in order to highlight the dyeing behaviour. The dyed wool fibers were achieved at different two values of acidic medium, pH 2 and respectively pH 5, the dyes exhibiting a good affinity toward wool fibers. Also, the chromatic parameters in CIELab system, wash fastness and rubbing strengths (wet and dry) have been investigated.

Key words: premetallised dyes, characterization, dyeing behavior.

1. Introduction

Metal complexes for wool fibers are obtained by complexation reaction of the acid dyes. Also, they are a very important class of the metal complex highlighting by the highest fastness to light and wet treatments (Lewis, 1992).

---

* Corresponding author; e-mail: chirila_laura@yahoo.com

The most successful metals used in wool dyeing is by far widely chrome, but in the last period was proving that this can affect the environment and the human health.

The aim of this study is to change this metals ion with the other ions of the transitionals metals, in order to obtain new premetallised dyes. The acid dye from which premetallised dyes derived was complexed by the authors using others metallic ions (Chirila *et al*., 2011; Sibiescu *et al*., 2010; Kamellia *et al*., 2009; Moustafa, 1995).

2. Experimental

2.1. Materials

For highlighting the purpose of this investigation, two new premetallised dyes were used, they were obtained through complexation reaction between a new acid dyesodium(*E*) -2- ((2-hydroxy-6-sulfonatonaphtalen-1-yl) diazenyl) -6- methoxybenzo [*d*] thiazole- 5 or 7-sulfonate and Ni(II), Zn(II) ions (Tarlea *et al*., 2007a; Tarlea *et al*., 2007b). The complexation reagent was supplied from Merk Company. A pure woolen fabric with 128 g/m^2 was used for this study. Na$_2$SO4 10% as surfactant reagent was added in the bath process. CH$_3$COOH 5M was used in order to adjust the pH in the dyeing process.
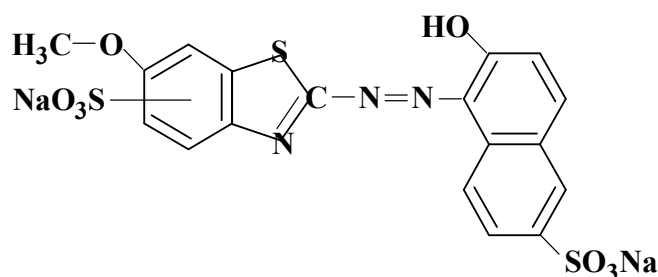

Fig. 1 – Chemical structure of HL.

2.2. Synthesis of the Premetallised Dyes

A mixture of 50 mL solution copper and respectively nickel chloride 10^{-2} M·L^{-1} and 100 mL solution of HL for the same concentration was subjected to stirring conditions, at room temperature, for 90 minutes until the mixture became homogeneous. The repeated centrifugations and washings with ethylic alcohol and water were used in order to separate the resulted micro disperse system and after the obtained products were dried in an oven at 105ºC until constant mass. All the reagents were prepared with bidistilated water.

2.3. Methods

The absorption spectra were measured using FT-IR Infrared spectroscopy was recorded with FT-IR-Spektrometer "Nexus 470" (Fa. Thermo Nicolet, Offenbach), and thermal behavior was investigated on a NETZSCH TG 209C equipment. Elemental analysis was carried out based on the destructive methods. The morphological structure of the compound, before and after the complexation reaction was examined by a scanning electronic microscope S-3000 N of HITACHI with 15 UV. The color values, expressed by the L *, a*, b* parameters were performed using Spectroflash 300® spectrophotometer Data color Company. The tinctorial fastnesses were evaluated according with SR EN ISO 105-C06 for washings tests and respectively with SR EN ISO 105-X12 for the rubbing tests. The chromatic parameters were achieved using a D65/10 as source of illumination.

2.4. Dyeing Process

The wool samples were dyed with Mathis „Polycolor P4702"equipment. Both types of dyes (complexed and uncomplexed) were applied at 3% owf at 100:1 liquor ratio. 10% sodium sulphate was added as electrolyte agent and the pH was adjusted to 2 and 5 with CH_3COOH, 5M. The wool samples were added to the bath, process under continuous stirring at 40ºC for 60 minutes, and after the bath was heated with 1ºC/min until 100ºC, when the dyeing process has been continuing for more than 30 minutes.

3. Results and Discussions

The calculated and experimental content of constitutive elements from each synthesized premetallised dye are shown in Table 1.

Table 1
The Chemical Elemental Analysis for the Studied Compounds

Compound	NiL_2		ZnL_2	
Element	Calculated	Experimental	Calculated	Experimental
C %	33.72	33.65	33.56	33.44
H%	1.87	1.74	1.84	1.75
N%	6.55	6.49	6.52	6.44
S%	14.98	14.81	14.91	14.87
M%	4.69	4.60	5.05	4.97

A conclusion witch can be drawn is that exists a good concordance between both values (calculated and obtained experimental) of all the compounds.

Table 2
The Thermal Behavior for the Studied Compounds

Compound	Stage	Mass change [%]	Onset [°C]	Rezidual mass [%]
HL	I	3.37	86.30	93.92
	II	1.95	404.10	
NiL$_2$	I	6.39	92.90	68.98
	II	11.09	312.30	
	III	8.46	482.20	
ZnL$_2$	I	1.32	96.00	71.51
	II	6.58	192.40	
	III	7.38	420.80	

Effects of metallic ions treatment were also analyzed form thermal point of view. The thermo grams of uncomplexed and premetallised dyes are depicted in Fig. 2. Differences in percent residual mass have shown that the thermal stability of the premetallised dyes was improved.
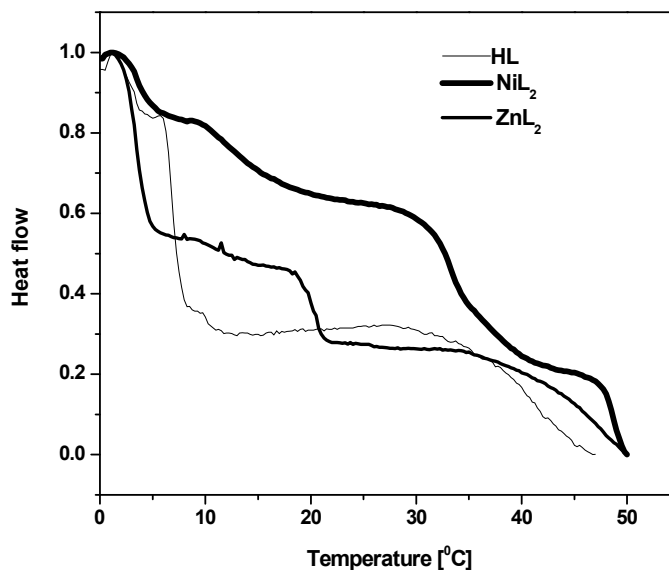

Fig. 2 – The thermograms for the studied compounds.

The SEM micrographs of dyes before and after the complexation reaction are shown in the Fig. 3. The images obtained from SEM provide information about the premetallised dyes microstructure.
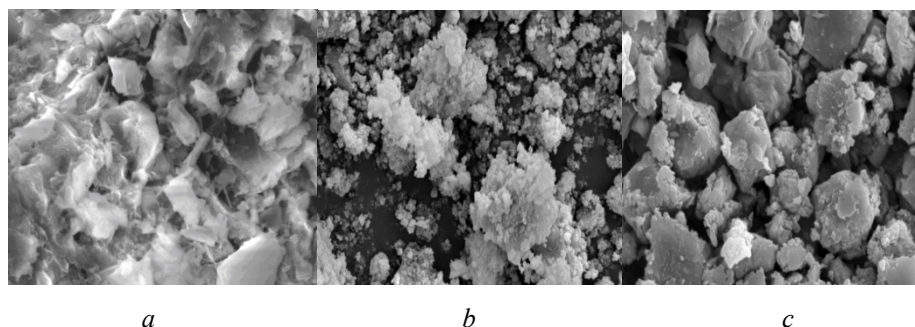

a   *b*   *c*

Fig. 3 – SEM images at 5000X for the obtained compounds:
a) –HL; *b*)- NiL$_2$; *c*) -ZnL$_2$.

The micrographs demonstrate that complexation process leads to change in the morphological structure, as a result of chemical structure changing. It is obvious that the microstructure of uncomplexed dyes is changed by the modifications provided, after being treated with metallic ions. Initially the morphological structure of acid dye was amorphous–crystalline with irregular shapes and different size, and in the end became crystalline with an ordered structure.

The spectra of premetallised dyes before and after complexation process were illustrated in comparison, in Fig. 4.
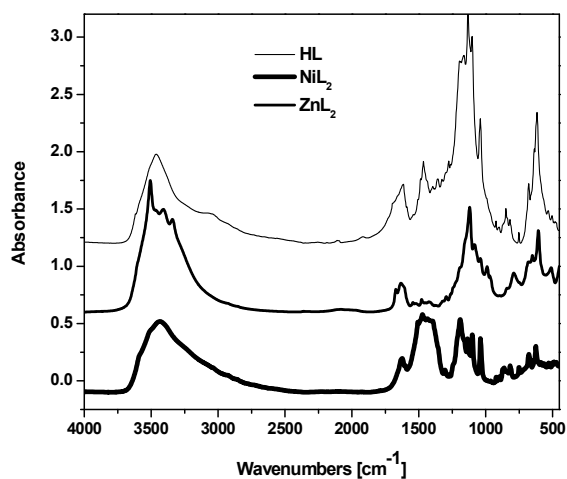

Fig. 4 – IR spectra for analyzed compounds.

It could be seen that the vibrations of the ligand are slightly modified by the premetallised dyes formation.

The complexation of the acid dyes lead to M←N and respectively M-O bonds formation. This bonds show by the absorption bands, with low intensity witch can be observed in the range of 600-400 cm^{-1}. The attributed bonds of different types of waters and —OH groups were identified as large overlapped bands in the range of 3400-3200 cm^{-1} wave numbers. The absorption spectra in infrared domain of the premetallised dyes give important information about the formation of coordinative bonds, and default about the premetallised dyes. The tinctorial strengths to washing and rubbing are summarized in Table 3.

Table 3

The Tinctorial Strenghts for the Samples Dyed with Studied Compounds

Sample	pH	Tinctorial strengths		
		Washing	Rubbing	
			Wet	Dry
HL	2	3	3	3
	5	2-3	3	2-3
NiL$_2$	2	3-4	3-4	4
	5	3	3	3
ZnL$_2$	2	4	4-5	4-5
	5	3-4	4	4

It could be found that the fastness to rubbing tests was grade up to 5 for ZnL$_2$. The smallest values can be observed for samples dyed with uncomplexed dyes. The chromatic parameters recorded from samples dyed in both conditions, with uncomplexed and premetallised dyes can be seen in Table 4.

Table 4

The Chromatic Parameters for Dyed Samples with Studied Compounds

Sample	pH	L*	a*	b*
HL	2	41.12	30.82	13.70
	5	41.60	23.77	8.90
NiL$_2$	2	38.79	26.07	11.41
	5	33.65	-1.64	-6.75
ZnL$_2$	2	32.63	22.93	1.09
	5	40.26	0.62	-14.73

The results indicated that the application of premetallised dyes conduct to obtaining a large wide of colors, after the complexation process. The addition of metallic ions in the structure of acid dye could reduce the dyes amounts from the waste waters, due to increased exhaustion.

4. Conclusion

In this study, were evaluated the complexation process effects on the formation and stability of the premetallised dyes and their dyeing behavior. The formation of these premetallised dyes was performed by chemical elemental analysis, SEM spectra, spectroscopy in infrared domain and thermal analysis in dynamic conditions. The dyeing ability of these synthesized dyes was achieved for wool fibers in acid medium, in comparison with uncomplexed dyes. The evaluation of samples dyed with premetallised dyes highlights that this dye conducts to slightly increased values for chromatic parameters and tinctorial strengths, with less dye migration and higher uniformity on the surface and dyed fibers.

REFERENCES

Chirila L., Butnaru R., Sandu I., Vasilache V., Sandu A.V., *Rev. Chem.*, **62**, *3*, 265-271 (2011).
Kamellia N., Zolfaghar R., Masoud S., *Dyes and Pigments.* **83**, 304 (2009).
Lewis D.M., *Wool Dyeing, Society of Dyers and Colourists.* 196 (1992).
Moustafa M.M., Journal of the Society of Dyers and Colourists, **111**, *11*, 349 (1995).
Sibiescu D., Chirila L., Rosca I., Butnaru R., Vizitiu M., Carja G., *Environmental Engineering and Management Journal.* **9**, *1*, 119 (2010).
Tarlea M.M., Cincu C., Marton G., Tomas S., Silvestro L., *Acid Benzothiazolic Dyes for Dyeing Protein Substrates.* Rev. Chem., **58**, *10*, 972-977 (2007a).
Tarlea M.M., Cincu C., Marton, G., Draghici C., Tarko L., *New Sulphonic Acid Derivates Obtained by Sulphonation 2-Aminobenzothiazoles -6 –Substituted.* Rev. Chem., **58**, *2*, 218-223, (2007b).

SINTEZA, CARACTERIZAREA ŞI COMPORTAMENTUL LA VOPSIRE PE FIBRELE DE LÂNĂ A UNOR COLORANŢI PREMETALAŢI PE BAZĂ DE Ni(II) ŞI Zn(II)

(Rezumat)

Au fost sintetizaţi şi caracterizaţi prin analiză chimică elementală, FTIR, SEM-EDX şi analiză termică în regim dinamic, doi coloranţi premetalaţi la raportul de

combinare de 1:2, derivaţi de la un nou colorant acid ca ligand şi ionii Ni(II), Zn(II).
Coloranţii premetalaţi sintetizaţi au fost aplicaţi pe fibrele de lână în scopul testării
comportării la vopsire a acestora. Fibrele de lână au fost vopsite la două valori diferite
ale pH-ului acid, pH 2 şi respectiv pH 5, coloranţii manifestând o bună afinitate faţă de
fibrele de lână. De asemeni, au fost investigate rezistenţele tinctoriale la spălare şi
frecare (umedă şi uscată), precum şi parametri cromatici în sistemul CIELab.